Neuroprotective adjuncts in Thoracic Endovascular Aortic Repair

Lydia Hanna MBBS BSc (Anat) MRCS

Department of Surgery & Cancer, Imperial College London

Imperial Vascular Unit at St Mary's Hospital, London, UK

2022

A thesis submitted to Imperial College London for the degree of Doctorate of Philosophy

Supervisors

Professor Richard Gibbs MD FRCS

Mr Colin Bicknell MD FRCS

Professor Mohammad Hamady FRCR

Declaration of originality

I hearby declare that the work in this thesis is my own, any individuals who have collaborated are credited and all else is appropriately referenced

Signed: Dated: 24/10/2024

Copyright declaration

The copyright of this thesis rests with the author. Unless otherwise indicated, its contents are licensed under a Creative Commons Attribution-Non-Commercial 4.0 International Licence (CC BY-NC). Under this licence, you may copy and redistribute the material in any medium or format. You may also create and distribute modified versions of the work. This is on the condition that: you credit the author and do not use it, or any derivative works, for a commercial purpose. When reusing or sharing this work, ensure you make the licence terms clear to others by naming the licence and linking to the licence text. Where a work has been adapted, you should indicate that the work has been changed and describe those changes. Please seek permission from the copyright holder for uses of this work that are not included in this licence or permitted under UK Copyright Law.'

This work is dedicated to all the patients and their families/carers who have so kindly and patiently contributed to this research, without whom this thesis would not have been possible.

Acknowledgements

First and foremost, I would like to thank my family (**John, Lucy, Julie, Lyzette, Taz, Gabby and Bella**) and my partner (**Dan**) all of whom continue to be my biggest supporters in this career and re-direct my compass when I am lost. I cannot express how grateful I am to have such a strong and encouraging support system who never let me quit.

I am beyond grateful to my three supervisors, whose skills and personalities perfectly complemented each other and whose supervision and guidance have ultimately led to the success of this research.

I would like to thank **Professor Richard Gibbs,** my primary supervisor and mentor. I am very grateful that you welcomed me into the research team, despite being two hours late to the interview(!). I am indebted to you for the unwavering academic, professional, and personal support you have given me over the years and continue to provide. It goes without saying you have been instrumental in this research (and my surgical career), providing constant inspiration, enthusiasm, pragmatic advice, and guidance for me to keep going, firing off emails to 'get things done' when I encountered obstacles. Thank you for always being available for me and providing calmness and assurance when I was sinking and propping me up when things were difficult with your wise words and (unique) sense of humour. Thank you for introducing me to research and encouraging me to continue in it and making my time a fun 3 and a half years!

I would also like to thank **Mr Colin Bicknell** for diligently teaching me research methodology when I had absolutely no clue about academia, and for being the sounding board when I was stuck. I am also very grateful for your understanding when the cleaner recycled our very expensive model, despite my best efforts to rescue it from the hospital's compactor bin, and for buying me a new thoracic model without hesitation.

I also want to thank **Professor Mohammad Hamady**, who has the patience of a saint (!), taught me an immense amount regarding endovascular surgery, and listened to and championed on all my ideas and endeavours. Thank you for being a constant source of support and encouragement both professionally and personally and gifting me with some unforgettable catch phrases that were a constant source of laughter. I

am indebted to **Dr Abhinav Singh** for giving up his time to report all the MRI scans, and to the **MRI radiographers** who worked tirelessly to ensure the patients were scanned. Without them, this research would have been impossible. I would also like to thank **Dr Chris Tighe** and **Artur Andrade** who welcomed me into their research lab, taught me about mass spectroscopy and gave up their time to help me conduct these experiments. To **Nate** and all the **kind gentleman** at Telford Enterprise, thank you for teaching me everything there is to know about CO_2, industrial gases, pressure regulators and a lot of other physics, and rescuing me when I blew up the tank!

To my 'research buddy' **Ammar**, I could not have gotten through the three and a half years without you. We have had many research triumphs and disasters (followed by trips to AE) that I will cherish! Thank you for being a good friend to me, helping me in many sticky situations and providing sound advice when I was about to combust. To my dear friend **Vik**, I am so very grateful for all your academic and personal support and for ensuring I took care of myself towards the end. To **William Montgomery,** thank you for coming alongside me and supporting me in all stent-graft related things at the drop of a text. My research was made a lot easier with you involved, and I came to understand stent-graft technology because of the many insightful discussions we had over the three years.

I would also like to thank **Professor Modarai**, **Mr Said Abisi** and the wider clinical team at St Thomas' Hospital, London for welcoming me into their department and all the support they provided towards patient recruitment. Lastly, I would also like to thank the wider clinical team at the Imperial Vascular unit (in particular, **Mr Mike Jenkins, Miss Celia Riga, Dr Sadie Syed, Dr Ganan Sritharan, Sumi, Sangeeta, Bon**), who in addition to my supervisors, really are a unique and fantastic bunch of people, from whom I learnt a huge amount regarding vascular surgery, and who ultimately made my time at St Marys full of laughter and memorable moments that I will always look back on with a smile.

Table of Contents

Abstract **16**

Study funding **18**

Publications and Presentations **19**

List of Figures **21**

List of Tables **28**

Abbreviations **32**

Chapter 1: Introduction **35**

1.1 Anatomy of the thoracic aorta **35**

1.2 Thoracic aortic disease **37**

1.2.1 Thoracic and thoracoabdominal aortic aneurysm 37

1.2.2 Acute aortic syndromes 38

1.2.3 Blunt traumatic thoracic aortic injury 41

1.3 Presentation of thoracic aortic diseases **41**

1.4 Management of thoracic aortic disease **42**

1.4.1 Open surgical repair 43

1.4.2 Thoracic endovascular aortic repair (TEVAR) 43

1.5 Neurological brain injury following TEVAR **46**

1.5.1 Characterising stroke following TEVAR....47
1.5.2 Characterising 'silent' brain infarcts following TEVAR....48
1.5.3 Cognitive impairment following TEVAR....51
1.6 Mechanism of neurological brain injury in TEVAR....52
1.6.1 Periprocedural cerebral embolization and its significance to neurological brain injury....52
1.6.2 The aetiology of peri-procedural emboli....55
1.6.3 The harmful effects of solid versus gaseous emboli....59
1.7 Neuroprotective adjuncts against neurological brain injury....62
1.7.1 Solid protection: Cerebral embolic filter devices....62
1.7.2 Solid protection: Carotid clamping and flow reversal....67
1.7.3 Solid protection: Robotic navigation....68
1.7.4 Gaseous protection: TEVAR delivery system flushing techniques....68
1.7.5 Gaseous protection: Gaseous filter devices....69
1.8 Summary....70
1.9 Hypothesis....71
1.10 Aims....71
1.11 Study outcomes....72
Chapter 2: Pathology specific incidence and trends in stroke following thoracic endovascular aortic repair (TEVAR) for descending thoracic aortic pathology: a systematic review and meta-analysis.....73
2.1 Aim....73
2.2 Methods....73

2.2.1 Search strategy 73
2.2.2 Selection criteria 74
2.2.3 Data extraction and analysis 75
2.2.4 Risk of bias 76
2.3 Results 76
2.3.1 Atherosclerotic aneurysms 78
2.3.2 Acute type B dissection 89
2.3.3 Chronic type B dissection 107
2.3.4 Blunt traumatic injury 118
2.4 Meta-regression analysis 137
2.5 Sensitivity analysis 137
2.6 Risk of bias and quality of the evidence 142
2.7 Discussion 143
2.7.1 Summary of findings 143
2.7.2 Overall completeness, applicability, and quality of the evidence 143
2.7.3 Clinical interpretation of the data 144
2.7.4 Implications for research and wider clinical practice 145
2.8 Conclusion 146
Chapter 3: Methods 147
3.1 Ethical approval 148
3.2 CO_2 Study 149
3.2.1 Study design and setting 149

3.2.2 Study objectives 149
3.2.3 Participants 150
3.2.4 Study procedures: TEVAR 151
3.2.5 Study procedures: CO_2 flushing technique 151
3.2.6 Study procedures: Clinical pre-operative evaluation 156
3.2.7 Study procedures Research pre-operative CTA evaluation 156
3.2.8 Study procedures: Intra-operative Transcranial doppler monitoring 158
3.2.9 Study procedures: Diffusion-weighted Magnetic Resonance Imaging 161
3.2.10 Study procedures: Stroke assessment 162
3.2.11 Study procedures: Neuropsychological assessment 162
3.2.12 Study endpoints 165
3.2.13 Sample size calculation 165

3.3 Sentinel dual-filter CEPD study 165

3.3.1 Study design 165
3.3.2 Study Objectives 166
3.3.3 Participants 166
3.3.4 Study procedures: TEVAR 166
3.3.5 Study procedures: Sentinel CEPD insertion 167
3.3.6 Study procedures: Clinical pre-operative evaluation 168
3.3.7 Study procedures: Research pre-operative CTA evaluation 168
3.3.8 Study procedures: Intra-operative Transcranial doppler monitoring 168
3.3.9 Study procedures: Diffusion-weighted magnetic resonance imaging 169
3.3.10 Study procedures: Stroke Assessment 169
3.3.11 Study procedures: Neuropsychological assessment 169
3.3.12 Histological filter assessment 169

3.3.13 Study endpoints....169
3.3.14 Sample size calculation....170
3.4 Statistical analysis for clinical studies....170
3.5 Benchtop Study....171
3.5.1 Time quantification....175
3.5.2 Composition ascertainment....176
3.5.3 Volume quantification....179
3.5.4 Gas distribution quantification....180
3.5.5 Anatomy of the model....181
3.5.6 Physiology of the model....183
3.5.7 Quantification of air bubbles and emboli....184
3.6 Statistical analysis for benchtop work....185
Chapter 4: CO_2 Study....186
4.1 Aim....186
4.2 Results....186
4.2.1 Study population....186
4.2.2 Clinical outcomes....189
4.2.3 Intra-operative TCD-detected cerebral embolisation....191
4.2.4 Clinical stroke, DW-MRI and TCD outcomes....212
4.2.5 Predictors of TCD-detected HITS....227
4.2.6 Predictors of Stroke and DW-MRI infarcts....227
4.2.7 Neurocognitive outcomes....228
4.2.8 Neurocognitive outcomes in relation to DW-MRI outcomes....229

4.2.9 Neurocognitive outcomes in relation to TCD data 239
4.2.10 Predictors of neurocognitive outcomes 240
4.3 Discussion 241
4.4 Limitations 249
4.5 Conclusion 250
Chapter 5: Comparative analysis between CO_2 flushed endografts and standard saline flushed endografts: DW-MRI and stroke outcome 251
5.1 Aim 251
5.2 Results 251
5.2.1 Study population 251
5.2.2 Clinical outcomes 253
5.2.3 DW-MRI outcomes 254
5.2.4 Univariate and multivariate analyses for DWM-MRI and stroke outcomes 267
5.3 Discussion 269
5.4 Limitations 273
5.5 Conclusion 274
Chapter 6: Benchtop experimental studies 275
6.1 Aim 275
6.2 Results 275
6.2.1 Time needed to flush endografts 275
6.2.2 Gas volumetric analysis 277

6.2.3 Gas composition analysis....278
6.2.4 Gas distribution....280
6.3 Discussion....285
6.4 Limitations....290
6.5 Conclusion....290
Chapter 7: Cerebral Embolic Filter Study....291
7.1 Aim....291
7.2 Results....291
7.2.1 Study population....291
7.2.2 Clinical outcomes....292
7.2.3 DW-MRI outcomes....295
7.2.4 Neurocognitive outcomes....297
7.2.5 Histological analysis....299
7.3 Discussion....300
7.4 Limitations....303
7.5 Conclusion....304
Chapter 8: Conclusions and future work....305
8.1 General discussion and conclusion....305
8.2 Future work....309
8.2.1 Gaseous embolisation....309
8.2.2 Solid embolisation....310

8.2.3 Complete embolic protection in TEVAR 312

Appendix list 313

References 335

Abstract

Brain injury, in the form of overt stroke and covert stroke affects up to 70% of people undergoing thoracic endovascular aortic repair (TEVAR). While covert stroke remains an under investigated complication from TEVAR, a systematic review, meta-analysis and meta-regression of the literature has demonstrated that the stroke rate has not improved over time.

This body of work aimed to investigate the efficacy of neuroprotective adjuncts against TEVAR related peri-procedural solid and gaseous emboli, to reduce diffusion-weighted magnetic resonance imaging cerebral infarcts (DW-MRI infarcts), cognitive impairment, and stroke.

Flushing TEVAR grafts with CO_2 to reduce cerebral air embolisation was associated with a 43% incidence of DW-MRI infarcts. Patients who had fewer or no cerebral infarcts were less likely to experience neurocognitive decline during 6-week follow-up, compared to patients with procedure-related infarcts.

The incidence of DW-MRI infarcts with standard saline flushing of TEVAER grafts was 74% compared to 43% with CO_2 flushing ($p<0.001$). The median total infarct surface area with CO_2 flushing was $0mm^2$ (range, 0-1679) compared to $10mm^2$ (0-2912) with standard saline flushing ($p=0.007$). There was no significant difference in the stroke rate (13% saline vs 7% CO_2, $p=0.196$).

Bench-top experiments using mass spectrometry demonstrated that CO_2 at 2litres, 4bar pressure for 1 minute provided the optimal 'flush time' to de-air the devices.

No difference was observed in the incidence of DW-MRI infarcts patients who underwent TEVAR under cerebral embolic protection ((CEPD) to prevent solid embolisation, compared to controls (71% CEPD vs 65% control, p=0.71). The median total infarct surface area with CEPD was 5mm^2 (0-16mm^2) versus 15mm^2 (0-36mm^2) in controls (p=0.42), representing a 67% reduction. At 6-week follow-up, 10% (1/10) CEPD patients experienced less neurocognitive impairment on the composite score compared to 33% (4/12) of control patients (p=0.32).

Study funding

Infrastructure for all studies in this research was provided by the NIHR Imperial Biomedical research centre (BRC).

The carbon-dioxide studies were funded by the Imperial Healthcare NHS charity (Grant award number 1181910).

The cerebral embolic filter protection studies were funded by the Stroke association (Grant award number TSA 2016/0).

Publications and Presentations

Peer-reviewed publications

Hanna L, Gibbs R. Brain Protection in the Endo-Management of Proximal Aortic Aneurysms. Hearts. 2020 Jul 1;1(2):5.

Hanna L, Grover G, Perera A, Chaudhery M, Abdullah A, Singh A, Bicknell C, Modarai B, Hamady M, Gibbs R. Carbon-dioxide versus saline flushing of thoracic aortic stents-grafts to reduce vascular brain infarcts: An observational study. European Journal of Vascular and Endovascular Surgery. 2020 May 1;59(5):e32.

Hanna L, Abdullah A, Gibbs R, Jenkins M, Hamady M. Left Subclavian Artery Scallop Endografts to Facilitate a Proximal Landing Zone and Upper Extremity Access for Branched Endovascular Aortic Repair of Type II Thoracoabdominal Aortic Aneurysms. CardioVascular and Interventional Radiology. 2021 Oct;44(10):1657-62.

Hanna L, Abdullah A, Kashef E, Riga C, Jenkins M, Bicknell C, Gibbs R, Hamady M. Four-year results of the Bolton relay proximal scallop endograft in the management of thoracic and thoracoabdominal aortic pathology with unfavorable proximal landing zone. Journal of Vascular Surgery. 2021 Nov 1;74(5):1447-55.

Abdallah N, Mouchati C, Crowley C, Hanna L, Goodall R, Salciccioli JD, Marshall DC, Gibbs RG, Shalhoub J. Trends in mortality from aortic dissection analyzed from the World Health Organization mortality database from 2000 to 2017. International Journal of Cardiology. 2022 May 21.

Hanna L, Sounderajah V, Abdullah AA, Marshall DC, Salciccioli JD, Shalhoub J, Gibbs RG. Trends in thoracic aortic aneurysm hospital admissions, interventions and mortality in England between 1998 to 2020: An observational study. European Journal of Vascular and Endovascular Surgery. 2022 Jul 13.

Book chapters

Hanna L, R Gibbs, M Hamady. How to Prevent Stroke During Thoracic Endovascular Aortic Repair in Current Technologies and Adjuvants in Endovascular Aortic Repair. Minerva.

Armour CH, Menichini C, Hanna L, Gibbs RG, Xu XY. Computational Modelling of Flow and Thrombus Formation in Type B Aortic Dissection: The Influence of False Lumen Perfused Side Branches. In Solid (Bio) mechanics: Challenges of the Next Decade 2022 (pp. 53-72). Springer, Cham.

Oral presentations

Carbon-dioxide flushed stent-grafts versus standard saline flushing to prevent cerebral embolic injury during TEVAR.
Hanna L, Grover G, Perera A, A Abdullah, Riga C, Jenkins M, Bicknell C, Hamady M, Gibbs R. European Society of Cardiovascular Surgery. Groningen, Netherlands (March 2019.)

Carbon-dioxide flushed stent-grafts prevent cerebral embolic injury during TEVAR.
Hanna L, Grover G, Perera A, A Abdullah, Riga C, Jenkins M, Bicknell C, Hamady M, Gibbs R. British Society of Endovascular Therapy (BSET), Warwickshire, UK (June 2020).

Carbon-dioxide flushed stent-grafts versus standard saline flushing to prevent cerebral embolic injury during TEVAR.
Hanna L, Grover G, Perera A, A Abdullah, Riga C, Jenkins M, Bicknell C, Hamady M, Gibbs R. Vascular Society AGM Scientific Prize Session. Manchester, UK (November 2020).

Prizes

1st prize European Society of Cardiovascular Surgery. Groningen, Netherlands (March 2019).
Runner up Norman Tanner Prize, Royal Society of Medicine. London, UK (May 2021).

List of Figures

Chapter 1:

1.1 Anatomy of the thoracic aorta

1.2 Ascending, arch, descending and type 1-IV thoracoabdominal aneurysms

1.3 Aortic Dissection Stanford Type A and B dissection and De Bakey classification

1.4 Non-A-non-B aortic dissection with entry tear within the arch

1.5 Ishimaru proximal landing zone classification. Zone 4 is >20mm distal to the left subclavian artery; Zone 3 within 20mm of the left subclavian artery; Zone 2 is proximal to the left subclavian artery; Zone 1 is proximal to the left common carotid artery; Zone 0 is proximal to the innominate artery

1.6 Arch debranching and extra-anatomical bypass procedures used in TEVAR.

1.7 Scallop, fenestrated and arch branch TEVAR devices procedures

1.8 Cerebral embolic protection devices currently available for use with transcatheter based procedures; (A) Sentinel™, (B)TriGuard, (C) Embrella, (D)Protemb, (E) Emblok, (F), Emboline, (G) Embol-X, (H) Point-guard, (I) Filterlex, (J), Embolisher

Chapter 2:

2.1 PRISMA flow chart

2.2 Forrest plot for pooled incidence of stroke following TEVAR for atherosclerotic aneurysms.

2.3 Scatter plot of the relationship between year of publication and stroke as a weighted proportion for atherosclerotic aneurysms

2.4 Funnel Plot for atherosclerotic aneurysm

2.5 Forrest plot for pooled incidence of stroke following TEVAR for acute type b dissection

2.6 Scatter plot of the relationship between year of publication and stroke as a weighted proportion for acute type b dissection

2.7 Funnel Plot for acute type b dissection

2.8 Trim and Fill plot for acute type b dissection

2.9 Forrest plot for pooled incidence of stroke following TEVAR for chronic type B dissection

2.10 Scatter plot of the relationship between year of publication and stroke as a weighted proportion for chronic type b dissection

2.11 Funnel Plot for chronic type b dissection

2.12 Forrest plot for pooled incidence of stroke following TEVAR for blunt aortic injury

2.13 Scatter plot of the relationship between year of publication and stroke as a weighted proportion for blunt aortic injury

2.14 Funnel Plot for blunt aortic injury

2.15 Trim and Fill plot for blunt aortic injury

2.16 Forrest plot of pooled incidence or stroke rate following TEVAR for atherosclerotic aneurysms by geographical region

2.17 Forrest plot of pooled incidence or stroke rate following TEVAR for acute type b dissection by geographical region

2.18 Forrest plot of pooled incidence or stroke rate following TEVAR for chronic type b dissection by geographical region

2.19 Forrest plot of pooled incidence or stroke rate following TEVAR for blunt aortic injury by geographical region

Chapter 3:

3.1 Flushing of Cook device

3.2 Flushing of CTAG device

3.3 Pressure regulator and Purple Medical laparoscopic tubing with in-line filter, 0.02um pores.

3.4 Classification of aortic arch type I to III

3.5 Quantitative grading of atheroma I-V; I, normal; II, intimal thickening; III, atheroma < 5mm; IV, atheroma > 5mm; V, mobile lesion

3.6 Transcranial doppler monitoring of the middle cerebral artery through the temporal bone

3.7 Solid (A) and Gas (B) embolus

3.8 Shower of emboli released during procedural step

3.9 Grooved pegboard

3.10 Sentinel cerebral embolic protection system with two filters; one in the innominate artery and one in the left common carotid artery. The left subclavian remains unprotected

3.11 Cerebral territories protected by the Sentinel dual-filter system

3.12 Flow/pressure regulator specific to CO_2 gases used within the European Union

3.13 Deployment chamber (plastic tube) for all deployments for collection of gas bubbles for composition and volume analysis (A); with endograft deployed (B); three-way tap and line that was connected onto another three-way tap allowing gas to be aspirated in a 20mls syringe and then transferred to a 2.5, 5 or 10ml syringe for volumetric analysis and compositional analysis(C)

3.14 Schematic of the setup used to continuously measure a stream's composition

3.15 Schematic of the setup used to individually analyse a sample composition

3.16 Endograft inserted into stainless steel tube that was then connected to the mass spectrometer

3.17 Schematic drawing of model

3.18 Dimensions of the arch of the thoracoabdominal model

3.19 Thoracoabdominal model in its entirety

3.20 Harvard pulsatile pump

3.21 GAMPT bubble detector

Chapter 4:

4.1a TCD-detected HITS by procedural step for **undifferentiated data**

4.1b TCD-detected HITS by procedural step and differentiated into **solid and gas**

4.1c TCD-detected HITS according to **left and right cerebral arteries**

4.1d TCD-detected HITS according to **atheroma grade**

4.1e Differentiated TCD-detected HITS according to **atheroma grade**

4.1f TCD-detected HITS according to **arch grade**

4.1g Differentiated TCD-detected HITS according to **arch grade**

4.1h TCD-detected HITS according to Fazekas **periventricular white matter (PVWM) disease**

4.1i TCD-detected HITS according to Fazekas **deep white matter (DWM) disease**

4.1j TCD-detected HITS according to **proximal landing zone**

4.1k Differentiated TCD-detected HITS according to **proximal landing zone**

4.1l TCD-detected HITS according to **pathology**

4.1m Differentiated TCD-detected HITS according to **pathology**

4.2a Distribution of number of DW-MRI infarcts according to **proximal landing zone**

4.2b Distribution of DW-MRI infarct surface area according to **proximal landing zone**

4.2c Distribution of number of DW-MRI infarcts according to **pathology**

4.2d Distribution of DW-MRI infarct surface area according to **pathology**

4.3a TCD-detected HITS according to **clinical outcome**

4.3b Differentiated TCD-detected HITS according to **clinical outcome**

4.4a Correlation between number of TCD-detected HITs, solid and gaseous TCD-detected HITS, and number of new DW-MRI infarcts

4.4b Correlation between number of TCD-detected HITs, solid and gaseous TCD-detected HITS, and surface area of new DW-MRI infarcts

4.5a Percentage change score for each neurocognitive test according to the presence of a DW-MRI infarct and no DW-MRI infarct

4.5b Percentage change in FAS score according to number of infarcts

4.5c Percentage change in REY auditory verbal learning according to number of infarcts

4.5d Percentage change in REY delayed recall according to number of infarcts

4.5e Percentage change in Trail making test A according to number of infarcts

4.5f Percentage change in Trail making test B according to number of infarcts

4.5g Percentage change in Grooved peg board (dominant hand) according to number of infarcts

4.5h Percentage change in Grooved peg board (non-dominant hand) according to number of infarcts

4.6a TCD-detected HITS in patients with and without a 20% decline in at least one neurocognitive test

4.6b Differentiated TCD-detected HITS in patients with and without a 20% decline in at least one neurocognitive test

Chapter 5:

5.1a Comparison of the proportion of patients (incidence) with new DW-MRI infarcts according to zone for saline and CO_2 group.

5.1b Number of new DW-MRI infarcts according to **proximal landing zone**

5.1c Surface area of new DW-MRI infarcts according to **proximal landing zone**

5.2a Comparison of the proportion of patients (incidence) with new DW-MRI infarcts according to pathology for saline and CO_2 group.

5.2b Number of new DW-MRI infarcts according to **pathology**

5.2c Surface area of new DW-MRI infarcts according to **pathology**

Chapter 6:

6.1 Mass spectrometry plot for CO_2 flushing through the metal tube (A and through the endograft (B) showing stepwise pattern indicating plug flow through the tube and endograft.

6.2 Arterial waveform produced at the ascending aorta

6.3 Neat and organised pattern of CO_2 bubbles released at 2L (A) compared to disorganised pattern of CO_2 bubbles released with 6L(B)

Chapter 7:

7.1 Histological analysis

Chapter 8:

8.1 Fluoroscopy image showing three vessel filter protection using two Sentinel^{TM} CEPDs. The proximal and distal filters in the brachiocephalic (blue arrow) and left common carotid (green arrow), respectively, and the proximal filter in the left subclavian (red arrow)

List of Tables

Chapter 1:

1.1 Commercially available cerebral embolic protection devices

1.2 Evidence base for cerebral embolic protection devices

Chapter 2:

2.1 Study/patient characteristics (a), TEVAR characteristic(b), stroke and mortality (c) for atherosclerotic aneurysms

2.2 Risk of bias assessment of studies reporting stroke following TEVAR for atherosclerotic aneurysms

2.3 Justifications for risk of bias assessment for studies reporting stroke following TEVAR for atherosclerotic aneurysms

2.4 Study/patient characteristics (a), TEVAR characteristic(b), stroke and mortality (c) for acute type b dissection

2.5 Risk of bias assessment of studies reporting stroke following TEVAR for acute type b dissection

2.6 Justifications for risk of bias assessment for studies reporting stroke following TEVAR for acute type b dissection

2.7 Study/patient characteristics(a), TEVAR characteristics(b), and stroke and mortality outcomes(c) for chronic type b dissection

2.8 Risk of bias assessment of studies reporting stroke following TEVAR for chronic type b dissection

2.9 Justifications for risk of bias assessment for studies reporting stroke following TEVAR for chronic type b dissection

2.10 Study/patient characteristics(a), TEVAR characteristics(b), and stroke and mortality outcomes(c) for blunt aortic injury

2.11 Risk of bias assessment of studies reporting stroke following TEVAR for blunt aortic injury

2.12 Justifications for risk of bias assessment for studies reporting stroke following TEVAR for blunt aortic injury

2.13 GRADE assessment of studies reporting stroke following TEVAR for aneurysm, acute type b dissection, chronic type b dissection and blunt aortic injury

Chapter 3:

3.1 Endograft conditions

Chapter 4:

4.1 Demographic characteristics of the study population

4.2 Procedural characteristics for 75 patients

4.3 Clinical outcomes for 75 patients

4.4 MRI features of the 28 patients with an infarct

4.5 Predictors of TCD-detected HITS on univariate linear regression analysis

4.6 Predictors of Stroke infarct on univariate logistic regression analysis

4.7 Predictors of new DW-MRI infarct on univariate logistic regression

Chapter 5:

5.1 Demographic characteristics of the study population

5.2 Procedural characteristics of the study population

5.3 Clinical outcomes of the study population

5.4 DW-MRI characteristics

5.5 Characteristics of DW-MRI infarcts according to proximal landing zone

5.6 Characteristics of DW-MRI infarcts according to pathology

Chapter 6:

6.1 Time taken for CO_2 to purge the endograft at various flow rates

6.2 Bubbles released under various flush techniques

6.3 Composition of gas release using mass spectroscopy

6.4 Haemodynamic measures from the model under various systolic/diastolic ratios (SD), stroke volume (SV), heart rate (HR), blood pressure (BP), mean arterial pressure (MAP)

6.5 Bubble detector results under various flushing conditions

Chapter 7:

7.1 Demographic characteristics of the study population

7.2 Procedural characteristics of the study population

7.3 Clinical outcomes

7.4 DW-MRI infarcts according to cerebrovascular territory

7.5 Neurocognitive outcomes

Abbreviations

AAA Abdominal aortic aneurysm

ACT Activated clotting time

ADC Apparent diffusion coefficient

AF Atrial fibrillation

AVR Aortic valve replacement

CABG Coronary artery bypass graft

CAS Carotid artery stenting

CCA Common carotid artery

CEA Carotid endarterectomy

CFA Common femoral artery

CI Confidence interval

COWAT Controlled oral word association test

CEPD Cerebral embolic protection device

CSF Cerebrospinal fluid

CTA Computed tomography angiogram

DBT Dynamic bubble trap

DHCA Deep hypothermic circulatory arrest

DW-MRI Diffusion weighted magnetic resonance imaging

EDD Embolic deflection device

EPD Embolic protection device

EQ EuroQol

EQ-VAS EuroQol visual analogue scale

EQ5D EuroQol 5 dimension

EVAR Endovascular aortic repair

FEVAR Fenestrated endovascular aortic repair

FLAIR Fluid-attenuated inversion recovery

GA General Anaesthesia

HADS Hospital anxiety and depression scale

HDU High dependency unit

HITS High-intensity transient signals

HRQOL Health-related quality of life

IMH Intramural haematoma

INR International normalised ratio

IQR Interquartile range

LSA Left subclavian artery

MAP Mean arterial pressure

MCA Middle cerebral artery

MCS Mental composite score

MEP Motor evoked potential

MES micro embolic signals

MRI Magnetic resonance imaging

N/A Non-applicable

NART National adult reading test

NHS National Health Service

NIAS Neurological Injury associated with Aortic Stenting

NRES National Research Ethics Service

OPA Outpatient appointment

OR Odds ratio

PAU Penetrating aortic ulcer

PCI Percutaneous coronary intervention

PCS Physical composite score

PFO Patent foramen ovale

POCD Post-operative cognitive dysfunction

PRISMA Preferred Reporting Items for Systematic reviews and Meta-analyses

PROMs Patient reported outcome measures

RCT Randomised controlled trial

SCI Silent cerebral infarction

SF-36 Short Form-36

TAA Thoracic aortic aneurysm

TAAA Thoracoabdominal aortic aneurysm

TAVI Transcatheter aortic valve implantation

TCD Transcranial Doppler

TEVAR Thoracic endovascular aortic repair

TIA Transient ischaemic attack

UK United Kingdom

USA United States of America

Chapter 1: Introduction

1.1 Anatomy of the thoracic aorta

The thoracic aorta (TA) is the largest blood vessel in the body. It originates from the left ventricle of the heart as the ascending aorta at the level of the inferior border of the 3rd costal cartilage to the left of the sternum (Figure 1.1). Thereafter it becomes the aortic arch at the level of the upper border of the 2nd right sternocostal junction.[1] The aortic arch initially lies anterior to the trachea and gives rise to the 'great vessels' or the supra-aortic trunks (SAT) that supply the head, neck and upper limbs. The SAT include the innominate (IA, also known as the brachiocephalic artery (BA)), the left common carotid artery (LCCA), and the left subclavian artery (LSA). They are important landmarks in determining the 5 proximal landing zones (PLZ) for thoracic aortic endovascular aortic repair (TEVAR) according to the Ishimaru classification.[2] The IA gives rise to the right common carotid artery (RCCA) and the right subclavian artery (RSA). These vessels supply the right side of the brain and right upper limb respectively. The LCCA supplies the left side of the brain, while the LSA supplies the left upper extremity and the left hindbrain through the vertebral artery (VA).[3]

There is great variation in the branching patterns of the SAT; the most common branch pattern (96% of humans) consists of the three origins as described above. The second common branch pattern is defined as a 'bovine' arch. This occurs in up to 15% of humans when the IA and LCCA have a common origin from the aortic arch.[4] The aortic arch becomes the descending thoracic aorta (DTA) at the LSA/level of the 4th thoracic vertebral body. The DTA runs in the left para-spinal area alongside the 5th-12th thoracic vertebral bodies. The DTA provides several important branches to structures in the thorax including the bronchial, intercostal and spinal arteries.[3] The DTA ends at the level of the aortic hiatus at the diaphragm to become the abdominal aorta (AA).

As with all arterial blood vessels, the thoracic aortic is comprised of three layers; (1) the tunica adventitia (outer most layer) containing collagen, vasa vasorum and lymphatics that contribute to the health of the arterial wall, (2) the tunic media (second inner layer) that is made up of elastin and collagen fibres and smooth muscle cells, that are responsible for the aortic haemodynamics, (3) the tunica media (inner most layer) that contains the endothelial cells that are in direct contact with flowing blood and possess antithrombotic and anti-atherosclerotic properties.[1]

The diameter of the thoracic aorta varies throughout its course from the heart to the diaphragm and according to age, sex, and body habitus[5]. The ascending aorta is approximately 5cm in length and the normal diameter averages 3.09 ± 0.41cm.[6] The aortic arch diameter averages 2.94 ±0.42cm to the IA, 2.77± 0.37cm at the proximal transverse arch, 2.61 ± 0.41 at the distal transverse arch, 2.47 ± 0.40 at the isthmus and 2.43 ± 0.35 at the diapghram.[6]

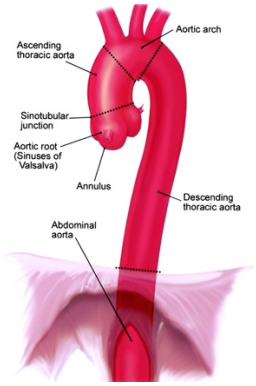


Figure 1.1 Anatomy of the thoracic aorta.

1.2 Thoracic aortic disease

The thoracic aorta is subject to the development of a variety of pathologies that may include aneurysmal disease, dissecting disease, and trauma, all of which are potentially life-threatening disorders unless managed promptly and in centres of aortic excellence.

1.2.1 Thoracic and thoracoabdominal aortic aneurysm

An aortic aneurysm is defined as a focal and pathological dilatation of more than 50% of the normal diameter of the aortic wall or an aortic diameter over 3cm. Aortic aneurysms are described in terms of their size, location, aetiology, and morphology. Thus, they may occur at any segment of the thoracic aorta and may be quite extensive to involve the abdominal aorta (thoracoabdominal aneurysm, TAAA, Figure 1.2).

The most common segment to be involved in the aortic root and/or the ascending aorta (60%), followed by the descending aorta (40%). The arch is involved in 10% of cases and 10% involve the thoracoabdominal aorta.[7] The incidence of both thoracic and thoracoabdominal aneurysms remains unclear, but is estimated to be 6-10.4 per 100,000 person years and is probably rising due to the ageing general population and with widespread availability of imaging.[8]

The aetiology is multi-factorial and more diverse to aneurysms affecting the abdominal aorta only. This may include degenerative processes such as atherosclerosis (most common for descending thoracic aortic aneurysms (DTAA) and TAAAs), connective tissue disorders (most common for ascending aortic aneurysms), following cardiac abnormalities such as bicuspid aortic valve (BAV), following medical management of acute aortic dissection that dilates over time in the chronic phase, acute infections such as

syphilis and staphylococcus, chronic inflammatory conditions (eg Takayasu's arteritis), traumatic transection managed conservatively that may develop into pseudoaneurysm, and genetic conditions such as Turner Syndrome.[7] Aneurysms are most commonly fusiform but can be saccular when due to infection or the result of trauma.

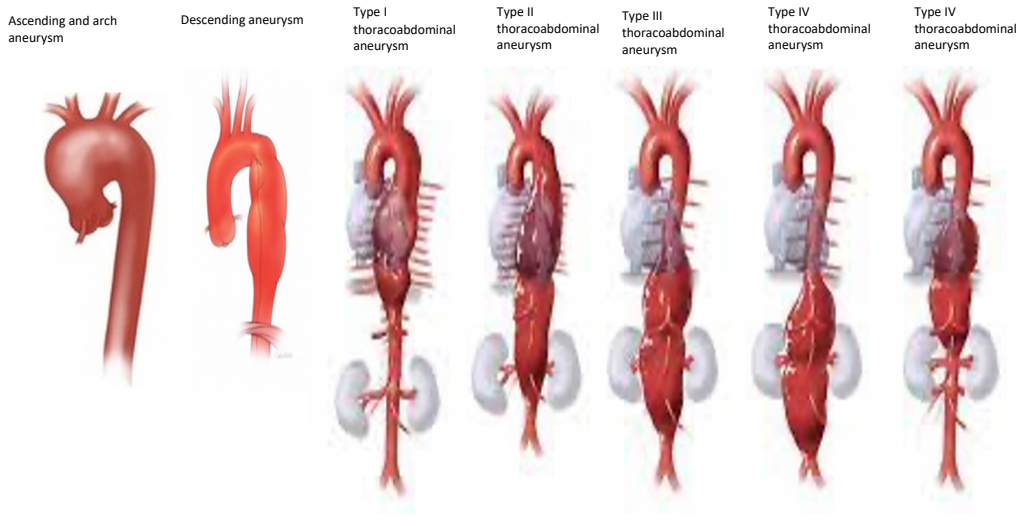


Figure 1.2 Ascending, arch, descending and type 1-IV thoracoabdominal aneurysms

1.2.2 Acute aortic syndromes

Acute aortic syndromes (AAS) include aortic dissection (AD), intramural haematoma (IMH) and penetrating aortic ulcer (PAU). The term 'acute' signifies symptoms within a 14-day period. Population-based studies also suggest a rise in the incidence of these conditions.[9] Histologically, this heterogenous syndrome is underpinned by disruption of the tunica media of the aorta whereby a tear develops in the intima that allows blood to flow between the layers of the aorta (AD) thereby creating a true and false lumen. With respect to IMH, there is no intimal tear or identifiable entry point however blood is apparent within the wall (IMH). Rupture of the vasa vasorum in the medial layer of the aortic wall is thought to

explain IMH.[10] PAU is thought to result from erosion of atheromatous plaque with penetration of the elastic lamina. PAU may degenerate into an aneurysm, dissection or rupture.[11]

These conditions can progress to another one of the same groups as the disease process progresses/evolves. It is also not uncommon for these pathologies to coexist in one patient. The aetiology for AAS is thought to be due to high and uncontrolled hypertension. High blood pressures increase the shear stress force on the arterial wall, weakening its ability to function as a compliant and elastic conduit.[11] Other important risk factors include age, atherosclerosis,[12] congenital bicuspid or uni-commissural aortic valves,[13] cocaine abuse,[14] pregnancy,[15] vigorous and strenuous activity.[16]

AAS may involve any segment of the aorta. An intimal tear involving the ascending aorta is characterised as a Type A dissection, whereas one that is distal to the LSA is characterised as a Type B dissection (Stanford Classification).[17] The De Bakey classification is an extension of this and characterises the dissection further into the thoracoabdominal aorta[18] (Figure 1.3). A European surgical consensus document also recognises dissections of the arch without involvement of the ascending aorta as a distinct group, termed non-A-non-B dissection (Figure 1.4).[19]

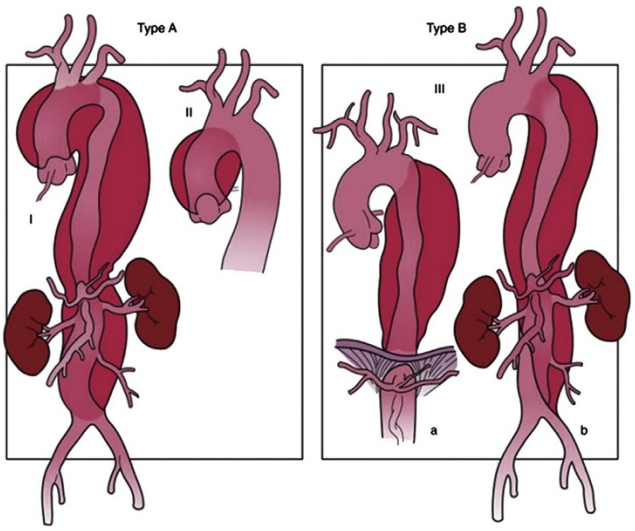


Figure 1.3 Aortic Dissection Stanford Type A and B dissection and De Bakey classification.

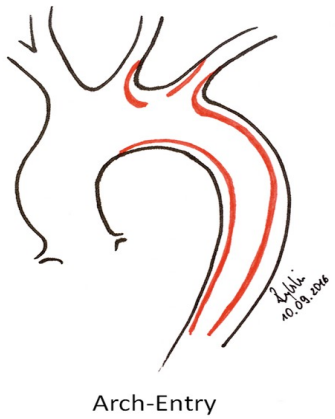


Figure 1.4 Non-A-non-B aortic dissection with entry tear within the arch.[20]

Distinction between IMH and AD with a thrombosed false lumen can be challenging without proper imaging. Unenhanced computed tomography of the aorta (CTA) is key to making a diagnosis of IMH. IMH are also more often localised in comparison to AD that may progress to involve the entire thoracoabdominal

segment.[21] There is no formal anatomical classification for IMH or PAU beyond characterising the aortic segment involved.

1.2.3 Blunt traumatic thoracic aortic injury

Blunt traumatic thoracic aortic injury (BTAI) occurs because of sudden deceleration from a forceful impact and/or collision usually within a trauma setting. The most common location for injury is at the aortic isthmus just distal to the level of LSA as this part of the thoracic aorta is fixed and tethered compared to the mobile aortic arch. It is a lethal condition with a mortality of 86.2% and is the second commonest cause of death following blunt trauma.[22] As mentioned earlier, if managed conservatively, there is a risk of pseudoaneurysm formation and aortic rupture.

1.3 Presentation of thoracic aortic diseases

The broad spectrum of thoracic aortic disease makes accurate diagnosis a challenge. Patients with thoracic aortic diseases are most often asymptomatic with the diagnosis made only during an imaging examination undertaken for another reason. The most common symptom among thoracic aortic disease is chest pain, making these conditions difficult to differentiate from other conditions such as myocardial infarction, pulmonary embolism, musculoskeletal pain, and gastrointestinal reflux. Other rarer symptoms include upper respiratory symptoms such as cough and dysphagia due to mass compression on the trachea and oesophagus, respectively from mass compression by a large aneurysm, or compression of the laryngeal nerves causing a hoarse voice, abdominal pain, and acute limb ischaemia from visceral and extremity malperfusion in AAS. Patients may acutely present with hypotension and limb and visceral malperfusion from aortic rupture.

1.4 **Management of thoracic aortic disease**

Broadly speaking, thoracic aortic disease may be managed conservatively, open surgical repair (OSR) or thoracic endovascular aortic repair (TEVAR). At this current time, there is no medication therapy that can protect against the development of thoracic aortic disease or prevent aortic growth and/or rupture once the pathological process has started. Given that hypertension is a significant risk factor for the development of many thoracic aortic diseases, optimal blood pressure control and best medical therapy for the management of cardiovascular disease is crucial for all patients to improve outcomes.

At this present time, OSR or TEVAR (with or without adjunctive procedures) remains the only definitive treatment options for thoracic aortic diseases. Patients in extremis (aortic rupture, organ malperfusion) are offered intervention immediately. However, the optimal timing of surgery outside of these clinical scenarios has not been well defined. Many thoracic aortic diseases have a quiescent phase whereby patients enter life-long surveillance. Patients are offered surgical intervention when the morphological appearances of the aorta risk aortic rupture. Typically, this is based on the diameter of the aorta; there is a 7% risk of rupture at >6cm in diameter and this is metric is used in current clinical practice.[23] Pragmatically intervention should be calculated on a risk benefit basis; if the risk of intervention is greater than the risk of rupture then intervention should be deferred until the aneurysm has reached a larger size with a concomitant greater rupture risk.

The following discussion is based on surgical intervention of thoracic aortic diseases of the arch and descending thoracic aorta given these segments of the thoracic aorta are within the remit of vascular and/or cardiac surgeons, whereas ascending aortic pathology requires management under a cardiothoracic team.

1.4.1 Open surgical repair

The aim of open surgical repair (OSR) is to replace the diseased thoracic aorta with a synthetic graft that is hand-sewn directly onto healthy aortic tissue. While outcomes from OSR have considerably improved over the last 20-years in high-volume centres and with better patient selection, OSR remains a significant undertaking for patients because of the surgical insult sustained from thoracolaparotomy, aortic cross clamping, and need for extracorporeal circulation (left heart bypass or full cardiopulmonary bypass) in more extensive diseases such as in the repair of type III and type II TAAAs. Complications from OSR include mortality (10% in elective cases, rising to 45% in emergency cases), cardiac (26%), respiratory (35.8%), acute kidney injury (12.3%), and spinal cord ischaemia (9.6%).[24,25] Stroke has been reported to occur in 2% to 8% of patients.[24-29] Based neurological assessment and neuroradiological evaluation on CT or magnetic resonance imaging, the majority of strokes from OSR are due to cerebral embolization of atherosclerotic debris or thrombus during clamping and manipulation of the aortic arch.[29]

1.4.2 Thoracic endovascular aortic repair (TEVAR)

Thoracic endovascular aortic repair (TEVAR) is a minimally invasive technique that involves endograft insertion through the femoral artery. The endograft is manoeuvred into the correct location within the thoracic aorta under x-ray guidance. Once in the desired position, the endograft is deployed and relines the diseased aorta from the inside. TEVAR is dependent on an adequate (>20mm) and healthy (free of thrombus, calcification) proximal landing zone (PLZ). This is the location of the aorta that the proximal part of the endograft will land in in relation to the Ishimaru classification (Figure 1.5).[2] Zones 0-2 involve endograft deployment across the arch. Strategies to maintain perfusion of the SAT must be employed for the LCCA and IA, whereas the LSA is typically revascularized in elective settings, but may be covered in emergency settings.

Revascularisation procedures involve arch debranching and extra-anatomical bypasses including LCCA to LSA bypass for zone 2, IA-to-LCCA with/without bypass to the LSA in zone 1, and ascending aorta-to-IA-to-LCCA with/without bypass to the LSA in zone 0 deployment (Figure 1.6). Minimally invasive strategies to maintain perfusion to the SAT include the use of parallel endografts whereby an endograft is deployed into a SAT alongside the TEVAR endograft (chimney, snorkel), scallop endografts that have a 'u-shaped defect aligned to the origin of the SAT, and custom or off the shelf fenestrated/branched TEVAR endografts that have a hole or branch incorporated into the TEVAR endograft (Figure 1.7).[30]

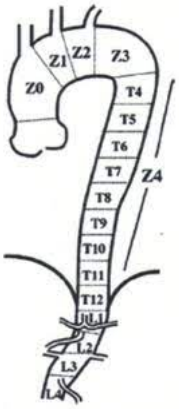


Figure 1.5 Ishimaru proximal landing zone classification. Zone 4 is >20mm distal to the left subclavian artery; Zone 3 within 20mm of the left subclavian artery; Zone 2 is proximal to the left subclavian artery; Zone 1 is proximal to the left common carotid artery; Zone 0 is proximal to the innominate artery.

TEVAR does not require any of the techniques needed in OSR, and has therefore dramatically improved the mortality and morbidity rates associated with ORS as observed in the pivotal trials of all commercially available endografts.[31-33] A recent systematic review with meta-analysis comparing outcomes of OSR to TEVAR on 14,580 patients with DTAA found that TEVAR was significantly associated with a lower rate

of paraplegia, renal failure, and cardiac complications.[34] Another systematic review and meta-analysis of 18,193 patients found that TEVAR for acute type B dissection was associated with lower all-cause operative and 1-year death compared to OSR.[35] Furthermore, a third systematic review and meta-analysis of 1968 patients with traumatic ruptured thoracic aorta found a lower 30-day and 1-year mortality with TEVAR compared to OSR.[36] The early survival advantage of TEVAR over OSR has led to a significant change in practice whereby TEVAR is now a first-line treatment for the management of thoracic aortic diseases throughout the world.[37-39]

Worryingly, these meta-analyses have not found a difference in the stroke rates between OSR and TEVAR.[34-36] Contemporary studies estimate the rate of periprocedural stroke to be anywhere between 2% to 8%,[40-43] increasing to 16% with endograft deployment across the aortic arch.[44] As TEVAR continues to be the primary mode of repair for thoracic aortic disease in current clinical practice and is now considered a treatment option for 'lower-risk' and younger patient populations, it is imperative that the mechanisms of stroke are well understood, and measures are taken to mitigate the risk of stroke.

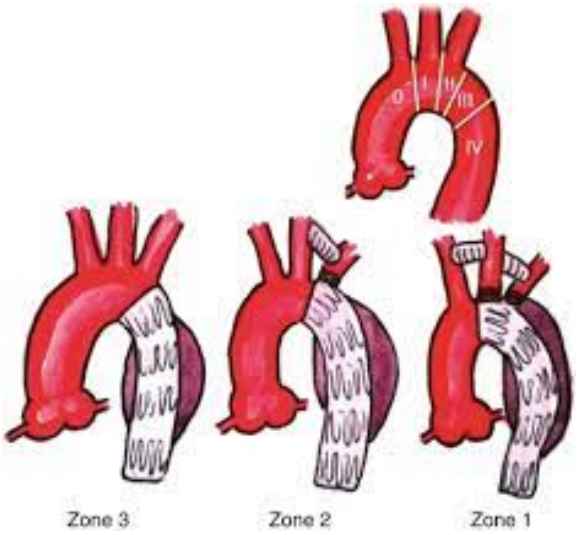


Figure 1.6 Arch debranching and extra-anatomical bypass procedures used in TEVAR.

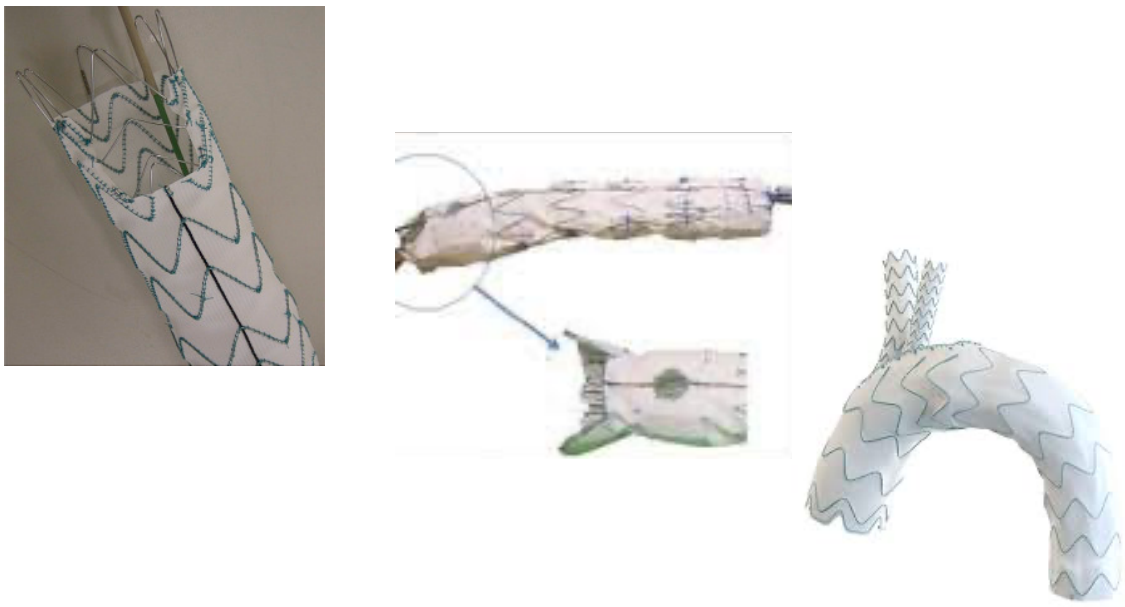


Figure 1.7 Scallop, fenestrated and arch branch TEVAR devices procedures

1.5 Neurological brain injury following TEVAR

In recent years, there is increasing recognition that clinical stroke is simply the ‘tip of the iceberg’ and that TEVAR is associated with a significant risk of neurological brain injury (NBI) that spans a spectrum from overt stroke in its most severe form, to covert injury including neuroradiological evidence of acute cerebral infarcts that are termed ‘silent’ brain infarcts (SBI) to denote the lack of focal neurological symptoms. This form of brain damage is not innocuous and may be related to cognitive dysfunction beyond the perioperative period but remains poorly understood.

1.5.1 Characterising stroke following TEVAR

Clinical stroke is the immediately noticed manifestation of NBI following TEVAR with symptoms often apparent within 24 hours of TEVAR in most patients. Symptoms often prompt neuroimaging to confirm the diagnosis and delineate the mechanism of injury (ischaemia vs. haemorrhage).[42,45] Ischaemic stroke by far outweighs haemorrhagic stroke following TEVAR.[41] Ischaemic infarcts develop in defined cerebrovascular distributions, and stroke following TEVAR has a preponderance for the posterior circulation. Just over 60% of patients will suffer a stroke in the posterior circulation,[41,45] 22-25% will suffer a stroke in the anterior circulation[41,45] and 10%will suffer a stroke affecting both the anterior and posterior circulations.[41] These findings suggest that peri-procedural cerebral embolisation may be the underlying mechanism of stroke following TEVAR.

Stroke following TEVAR has devastating consequences. Aproximately 30% to 50% of affected patients will die in-hospital.[42,46] Prolonged rehabilitation is often necessary for survivors and this can cost up to £23,315 per stroke patient in the UK[47] with up to 30% of patients still left with a permanent disability.[48] Stroke following TEVAR also a significant independent risk factor for 30-day (OR 8.11, P=.004) and 1-year (P=0.006) mortality.[47]

Risk factors stroke following TEVAR may be divided into procedural and patient related factors. Patient related factors include age, prior stroke,[42] chronic kidney disease, and higher grades of atheroma in the aortic arch.[42,45,49] Procedural factors include difficult aortic anatomy, proximal extent of repair,[42,43] intra-operative hypotension,[25] long operative time[40] and coverage of the LSA.[47,50] The LSA provides an important source of blood supply to the left posterior circulation via the vertebral artery, explaining why its coverage may lead to increased risk of stroke as well as spinal cord infarction.

1.5.2 Characterising 'silent' brain infarcts following TEVAR

The widespread availability of diffusion-weighted magnetic resonance imaging (DW-MRI) has led to an increasing recognition that transcatheter based procedures such as TEVAR, transcatheter aortic valve replacement (TAVR), carotid artery stenting (CAS), and even diagnostic procedures in the arch during cardiac catheterisation result in a high frequency (>50%) of DW-MRI infarcts. The absence of overt focal neurological deficits typical of classical stroke syndromes attributable to a DW-MRI infarct has led to the term 'silent' acute ischaemic brain infarcts (SBI).

Following TEVAR, up to 63-81% of patients will develop SBI that are radiologically visible and quantifiable on neuroimaging as early as 24 hours post-procedure. There are only two published reports to document the burden of acute SBI in TEVAR. In their descriptive study, Kahlert et al[51] found multiple DW-MRI infarcts (1 to 6 infarcts per patient) in both the left (16 infarcts) and right hemisphere (13 infarcts) and anterior (20 infarcts) and posterior (9 infarcts) circulations that ranged in size between $15mm^3$ and $300mm^3$. The 63% acute infarction rate contrasts with the 0% apparent periprocedural stroke rate. Perera et al[52] demonstrate a much higher overall infarction rate at 81%, with an 8% clinical stroke rate. A total of 120 new DW-MRI infarcts were detected (1 to 9 DW-MRI infarcts per patient), mainly in the left cerebral hemisphere and in the posterior circulation, with a surface area between 9-$81.5mm^2$). Differences in the strength of the MRI scanner (3T Perera et al[52] versus 1.5T Kahlert et al[51]) may account for the discrepancy in number of DW-MRI infarcts between the two studies. The focal and multi-focal appearance of DW-MRI infarcts further supports periprocedural cerebral embolisation as the mechanism of injury for SBI.

Diffusion weighed imaging (DWI) is the preferred magnetic resonance imaging (MRI) sequence to investigate acute infarction. Acute infarcts are seen as hyperintense bright lesions against the background of dark normal tissue. This occurs as the result of restricted diffusion of water when cytotoxic oedema

develops immediately in ischaemic tissue. DWI has a high sensitivity (sensitivity 0.99) for the rapid detection (within minutes) of ischaemic injury when performed within 12h of symptom onset and can detect new insults for several days after the initial event.[53,54] With time (1-3 weeks), DWI infarcts may increase or decrease in size, cavitate or collapse entirely leaving no trace on the DWI.[55] After the acute phase, T_2-weighted fluid attenuated inversion recovery (FLAIR) provides the most accurate method for detection of infarcts that remain apparent throughout the chronic phase, not DW-MRI.[55]

While the clinical significance of new procedure-related DW-MRI infarcts following TEVAR are not known, such infarcts may not be innocuous with the term 'silent' a misnomer for several reasons.

Firstly, the temporal relationship of the imaged infarct to the procedure suggests this ischaemic damage is a direct complication of TEVAR. Bright infarcts identified by DW-MRI infarcts have been termed 'finger-prints of invasive medical procedures'.[56] The greater prevalence and incidence of SBI, in comparison to overt stroke provides a further measure of their importance. Furthermore, DW-MRI infarcts represent areas of irreversible infarcted neuronal tissue and are pathologically distinct from white matter hyperintensities (gliosis, axonal loss, and ischemic demyelination) and cerebral microbleeds (haemosiderin from a microbleed).[57,58]

While DW-MRI infarcts may reverse or even become invisible on T1 and T2 weighted MRI at 3-30months post-procedure[59,60] histological analysis of the tissue indicates that ischaemic damage has still occurred.[61]This is a particular feature of very small lesions in embolic stroke.[57] Furthermore, while the final T_2 lesion volume is often one-half of the initial DWI lesion, this does not imply tissue salvage.[62] DW-MRI signal reversal is also not associated with functional improvement.[57]

Secondly, we know that patents who develop neurological signs following TAVR have higher number (26 versus 2.7±3, *P*=0.004) and volume (11.9±6 mL versus 1.1±1.1 mL, *P*=0.007) of new cerebral infarcts.[63] It therefore seems plausible that patients who have such a high procedure-related embolic burden following TEVAR should develop focal neurological signs, however subtle. However, patients are not routinely systematically interrogated for neurological deficits in the post-operative period, meaning that many neurological events are likely to be missed or misdiagnosed. Cardiovascular studies that incorporate the routine neurological examination of patients by a neurologist have demonstrated a higher rate of neurological deficits.[64] Furthermore, the neurological examination represents an assessment of only motor and sensory functions of the brain. A full neurological evaluation of brain function requires neuropsychological examination which can only assessed through explicit neuropsychological testing which is even less frequently carried out than expert neurological examination. The clinical impact of apparently 'silent' procedure-related DW-MRI infarcts therefore remains unknown and cannot be classified as 'silent' at this time.

Further support for this assumption comes from a variety of longitudinal studies. In the 2019 prospective NeuroVISION study, 1114 non-cardiac surgery patients underwent a DW-MRI at a median of 5 days postoperatively and neurocognitive assessment at 30 days and 1-year follow-up. The covert stroke rate (DWI- MRI infarcts in a patient with no clinical stroke symptoms) was 7%. Cognitive impairment was found in 42% of participants who had new DWI-MRI infarcts, in comparison to 29% of participants without DWI-MRI infarcts (OR 1·98, 95% CI 1·22–3·20, AR increase 13%; p=0·0055) 1 year after surgery. DWI-MRI infarct positive patients were also at an increased risk of perioperative delirium, overt stroke, or transient ischaemic attack at 1 year.[65] A further study of patients undergoing cardiac surgery found that of the 43% of patients who developed new DWI infarcts, 75% of these patients had objective evidence of cognitive decline in 2 or more tests in the presence of multiple DWI infarcts or single lesions greater than $1cm^3$, in comparison to 28% of patients with a solitary DWI infarct, and 18% of patients with no ischaemic

change (P<0.001) at 6 weeks follow-up. This suggests that cognitive impairment is more severe with greater ischaemic load.[66] Increasing volumes of 'subclinical' procedure-related DW-MRI infarcts have also been associated with cognitive impairment in patients undergoing CAS.[67] Other studies have also associated DW-MRI infarcts to an increased risk of future stroke,[68] depression[69] and dementia.[70]

1.5.3 Cognitive impairment following TEVAR

There is only one TEVAR study that has explored the relationship between DWI-MRI infarcts and cognition. In the study by Perera et al,[52] the rate of neurocognitive decline following TEVAR has been reported to be as high as 88% in those patients with DWI-MRI infarcts, with impairment in six out of seven cognitive domains assessed.

The mechanism by which procedure-related DW-MRI infarcts may lead to cognitive impairment is not fully understood. However, it is plausible that focal or multi-focal infarcts may disrupt the complex and interlinked neuronal circuit, akin to the pathophysiology of infarcts in Alzheimer's disease.[71] Furthermore, whether a DW-MRI infarct results in focal motor and/or sensory deficit or impaired cognition is clearly dependent upon the cerebral location of the infarcts, as well as the number volume.

1.6 Mechanism of neurological brain injury in TEVAR

1.6.1 Periprocedural cerebral embolization and its significance to neurological brain injury

The temporal relationship of stroke and DW-MRI infarcts to TEVAR, and the focal/multi-focal appearance of DW-MRI infarcts supports the theory that peri-procedural cerebral embolisation is the mechanism of NBI following TEVAR. Further support for this theory comes from transcranial doppler (TDC) ultrasound studies of the cerebral arteries.

TCD is a portable tool that provides non-invasive real-time haemodynamic measures of the cerebrovascular vasculature. TCD can also detect circulating cerebral microemboli, based on the backscatter of ultrasound wave from the microemboli, resulting in high intensity transient signals (HITS) in the Doppler waveform, also known as microembolic signals (MES).[72] 'Emboli' appear as uni-directional, short duration (<0.001-0.03s) HITS with a characteristic 'whistling' sound.[73] Five studies to date have investigated periprocedural cerebral embolisation as a risk factor for TEVAR induced NBI, and have defined high-risk procedural manoeuvres that result in emboli entering the brain.[52,74 75 76,77]

Kim et al[77] recruited 23 patients to undergo TCD monitoring during TEVAR. A total of 2383 MES were recorded, more on the right side than the left. Interestingly, strokes were observed in those patients with > 75 MES and who had at least 22 manipulations in the arch, whereas patients with < 75MES did not suffer stroke and had < 18 manipulations in the arch. Most MES occurred with device deployment and post-deployment angiography, especially when the pigtail catheter for angiogram was entered via the right side of the arch. The authors found that all three patients with a bovine arch had more MES in the right MCA, whilst those with normal arch anatomy had more MES in the left MCA. While the PLZ are not described

in this study, the straighter course of the right common carotid artery in a bovine arch may explain the above finding.

In a study of 20 patients undergoing TEVAR for aneurysmal disease, Bismuth et al[74] have shown a significant association between the total number of microembolic signals (MES) and post-operative stroke, TIA (p=0.0055) and death (p=0.0053). Further analysis of MES by phase of TEVAR revealed 1081 and 1141 microembolic signals (MES) during the diagnostic and treatment phase of TEVAR respectively, with the highest MES counts generated during pigtail catheter placement during the diagnostic phase, and by device deployment during the treatment phase. Significantly more MES were counted during deployment in zones 0-2 than 3-4 (p=0.027). Embolic counts to the right/left sides were the same overall (average 53 right, 52 left). Interestingly, when the LSA was covered, no more MES were noted than when the LSA was not covered. Debranching the left subclavian artery did not lead to any more MES outside of the differences already observed to be associated with the landing zone and there was no difference in MES with respect to arch type.

Unfortunately, patients in both studies did not undergo routine DW-MRI or neurocognitive testing. Therefore, it is not possible to quantify the cerebral ischaemic damage following TEVAR or understand the effects of periprocedural embolisation on cognitive dysfunction. The atheroma burden in the arch was also not assessed, preventing a conclusion as to why higher MES are observed with more proximal landing zones.

Perera et al[52] have demonstrated the impact of TCD detected cerebral emboli detected during TEVAR in a much larger study of 52 patients. This study found total of 262 MES in the TEVAR group, in comparison to only 18 MES in the EVAR/FEVAR group where most manipulations are lower down the aorta within

the abdomen. Device manipulation and deployment, followed by contrast injection resulted in the highest rates of embolisation (p=0.001). Embolisation was also significantly detected more frequently with higher aortic atheroma grade 4 and 5 (P=0.042), at more proximal landing zones 0 and 1 in comparison to 3 and 4 (P=0.001) and during arch hybrid procedures (P=0.001). Interestingly, no difference in MES was found between the treated pathologies. This study also found that predictors of TCD detected cerebral emboli include LSCA revascularisation, LSCA bypass, proximal landing zone and arch hybrid procedure on univariate analysis. Univariable analysis also revealed TCD MES to be a significant predictor of memory and recall cognitive decline memory and recall (P =0·009). The development of new DW-MRI infarcts (for both overt and covert stroke) and DW-MRI infarct surface area were not shown to be associated with TCD MES.

Similarly, Benson et al[76] have also shown that TEVAR results in significantly greater numbers of procedural emboli compared with EVAR, with the highest risk phase being guidewire and pigtail catheter insertion. This group have also found that perioperative embolic load (MES>30) in endovascular aortic procedures, not just TEVAR, is associated with cognitive decline in list recall at 30 days compared with a lower embolic load (1-10 MES), but this was not associated with incidence of POD or stroke. The most recent study by Grover et al[75] has found a median number of 453 total MES (IQR, 227-521) with maximum MES at stent manipulation and deployment (median 82, IQR 73-142). The study contrasts to that by Perera et al[52] and Benson et al[76] in demonstrating a positive association between an increase in MES to increased number of DWI infarcts (r_s =0.912; P =0.01). Overall, these studies indicate that MES do not appear randomly during TEVAR and may be a surrogate marker of emboli reaching the brain, resulting in neurological injury in the form of DW-MRI infarcts.

These findings are also in keeping with studies that have detected a positive correlation between the presence of MES and DW-MRI infarcts in other clinical settings such as in carotid endarterectomy and stenting.[78,79] The clinical significance of MES is also evident from studies that have detected a high frequency of DW-MRI infarcts in patients with MES who have suffered acute ischaemic stroke.[80-82] Procedure-related MES have also been associated with cognitive decline following cardiac surgery[83,84] and carotid endarterectomy.[85,86] While there is no study that has explored the relationship between the occurrence of TCD embolic signals and new DW-MRI infarcts in the same TAVR population, Drews et al[87] have demonstrated an 8% incidence of new cerebral infarcts on computed tomography (CT) that was associated with an average procedural total of 730 HITS and 140 MES following TAVR.

1.6.2 The aetiology of peri-procedural emboli

TCD detected emboli travelling to the cerebral circulation during TEVAR are presumed to be 'solid'. TEVAR involves the manipulation of wires, catheters and large diameter devices across a diseased aortic arch as well as the deployment of the endograft against an atherosclerotic wall, all in close proximity to the origins of the supra-aortic vessels that supply the brain.[42,43] Thus there is an assumption that solid particles are dislodged during these manoeuvres that may then embolise to the cerebral circulation under pulsatile flow to cause arterial occlusion and incite ischaemic damage. This theory is unsurprising given that atherosclerotic disease and higher-grade atheroma burden of the thoracic aorta are recognised risk factors for stroke after heart surgery and TEVAR.[42,88]

Furthermore, the prothombotic tendency of wires and catheters used, as well as activation of platelets and the clotting cascade following damage to the endothelium during instrument manipulation,[89] together with suboptimal periprocedural anticoagulation may also lead to thrombus formation. Thrombus may also fragment from the tip of instruments during the procedure.

However, the athero-thrombo-embolic theory may not be the only mechanism of NBI in TEVAR. Grover et al[75] utilised TCD differentiation software to discriminate (differentiate) MES in TEVAR. Differentiation between solid and gaseous emboli is possible because the backscatter of ultrasound from gaseous emboli are higher than that of solid, which in turn are higher than that of blood (embolus to blood ratio, EBR). The amount of reflected ultrasound depends on the size and acoustic impedance, which in turn is dependent on the density of the material. The greater the difference between acoustic impedance of the embolus and blood, the greater the reflection is. Gaseous emboli produce a greater acoustic impendence than solid emboli (because of the lower density of gas than solid) and so cause large ultrasound reflections. Solid emboli however have acoustic impedance similar blood and therefore give a smaller reflection.[73] Furthermore, solid microemboli reflect ultrasound at higher frequency. These characteristics allow the discrimination of solid and gaseous emboli.[90,91]

Out of a median number of 453 MES (IQR, 227-521), Grover et al[75] have found that the majority of MES were gaseous (391, IQR 213-461 vs 32, IQR 17-54 gaseous vs solid MES). Stent manipulation and deployment was again identified as the highest risk phase for MES, with 89% of signals differentiated as gas and only 11% as solid. Furthermore, this study identified a positive correlation between new DW-MRI infarcts and gaseous MES ($r_2 = 0.928$; $p=0.01$).

These findings prompt two questions: (1) 'where does the gas come from?' and (2) 'is it harmful?'

Four recent experimental bench-top studies have demonstrated the release of 'gas' bubbles from all commercially available TEVAR stent-grafts following deployment in water-filled containers, despite flushing with saline (according to instructions for use (IFU)) to de-air the device prior to deployment.[92-94]

The first study to report on this phenomenon was by Inci et al[92] who reported 0.1-0.3ml air release for Medtronic Valiant Thoracic and <0.025 to 0.04 ml for Gore TAG following IFU preparation with saline. The largest bubbles had a diameter of 3mm and could be seen to be released from the proximal end of the MDT device. Rohlffs et al[93] found that the Cook Zenith device released 0.34-1.02ml of gas and again large bubbles appeared at the tip of the device with smaller bubbles released along the length of the graft following 60mls saline flushing. Gagnon et al[94] have deployed Cook, Gore and Medtronic devices and commented on the pooled mean collected volume of 0.18ml (range, 0.125-0.225ml) with a mean bubble size of 2.59mm (range, 1.07-5.21ml). In comparison to the other two studies, they observed large bubbles at the distal end of the Cook and Medtronic devices, and at the proximal end of Gore devices (no comment on the volume of saline used to flush devices). Rylski et al[95] used the Relay Pro NBS system and found a median of 0.138 ml (IQR, 0.106 – 0.150 ml) of gas released with 40mls saline flushing and a median of 0.088ml (0.063- 0.150ml) with 120 mls saline flushing.

The source of the gas released from these devices during deployment may be related to the manufacturing process. Stent-grafts and their delivery systems are manufactured and packaged in room air conditions rather than a vacuum. It is therefore likely that the 'gas' is air trapped within the delivery system as well as within the folds of the compressed stent-graft from the manufacturing processes. It is possible that saline flushing prior to device insertion and deployment into the patient is inadequate at pushing out air trapped pockets because of the pressure needed to force saline through a tightly compressed system.

As the deployment process begins, bubbles may be forcibly directed upwards towards the supra-aortic trunks for several reasons. The natural buoyancy and lower specific gravity of air bubbles released from within the device allows air bubbles to travel retrograde against the direction of blood flow. This is a unique property differs from a solid embolus. Furthermore, during device insertion manipulation for correct

orientation and positioning in the aortic arch and the device is opposed against the aortic wall and causes an occlusive effect within the aorta.[92] At this moment, reduced antegrade flow prevents any bubbles from being 'washed' downwards.

The distribution of air embolisation to the supra-aortic trunks has also been recently demonstrated in an experimental study using a pulsatile thoracic flow model that has shown that deployment in zone 2 (and coverage of the LSA) leads to higher amounts of air to the right side of the 'brain', while zone 3 deployment lead to higher amounts of air in the descending aorta which the authors hypothesise may contribute to visceral ischaemia.[96]

While these experimental studies have slight methodological differences, including the methods for gas collection, the differences in volume and size ranges of bubbles released may also be the result of different device designs (for example, sheathed devices (Cook, Medtronic and Relay Pro) appear to release much larger volumes of gas than non-sheathed devices (Gore)). The varying amounts of air released form the same device design also suggests variability in the manufacturing process for a given manufacturer.

Nevertheless, findings from these bench-top studies demonstrate that TEVAR devices (delivery systems and the endograft itself) release significant volumes of gas that distribute to the supra-aortic trunks according to the Ishimaru zone[2] of endograft deployment and can subsequently be detected as MES on TCD during TEVAR.

1.6.3 The harmful effects of solid versus gaseous emboli

While there is little debate regarding the occlusive effects of solid emboli and 'massive' gaseous embolisation (eg decompression sickness)[97] on ischaemic brain injury and stroke, the clinical significance of microemboli (defined as < 900–1000μ),[98] and in particular cerebral air microemboli (gaseous microemboli, GME) from invasive procedures is the subject of much debate.

In general, GME are presumed to be less dangerous than solid microemboli (SEM) for the brain because of their transient nature (1 second for a 1um radius bubble) under the force of pulsatile blood and rapid resorption within the cerebral circulation. GME are therefore presumed less likely to cause occlusion of the cerebral microvasculature.[99,100]

However, GME have been implicated as a cause of adverse neurological and neurocognitive outcomes following cardiac surgery since the mid-1960's.[101,102] Sources for GME included the bubble oxygenator and venous reservoir[103], air in the cardiopulmonary bypass circuit lines (CPB),[104] insufficient de-airing of the open cardiac chambers [105] and introduction from perfusionist interventions.[106] There are also isolated reports of the introduction of air into the cerebral circulation (cortical arteries) during cerebral angiography[107] and through peripheral intravenous catheter[107,108] that manifest as cerebral infarcts on computed tomography of the brain immediately after the procedure with gas visible in the arteries supplying the infarcted region, but not in other vessels.

Patients with mechanical heart valve (MHV) who are known to chronically produce gaseous microemboli from cavitation suffer with memory deficits compared to matched patients with tissue valves that do not generate emboli, and matched controls.[109]

Animal models of cerebral arterial embolism have provided useful insights into the behavior and harmful consequences of bubbles once introduced into the circulation. Once a bubble has entered the arterial system, it may either lead to (1) mechanical obstruction to blood flow (trapping) and/or (2) cause endothelial irritation and inflammation as the bubble (s) pass and redistribute through the vascular bed (redistribution).[110,111] The final common insult of these two mechanisms is ischemia in downstream tissues.[112]

Once a bubble has entered the arterial system whether trapping or redistribution occurs is dependent on the composition, size, volume and number of the bubbles, the haemodynamic environment, and the cerebral location of where they finally lodge. Bubbles composed of nitrogen (N_2) are less likely to dissolve than those composed of metabolic gases such as oxygen (O_2) and carbon-dioxide (CO_2). Larger sized bubbles are also less likely to dissolve that smaller ones whereby a 200um air bubble takes 32 minutes to dissolve compared to a 50um air bubble that takes 2 minutes to dissolve.[113]

Conversely, bubbles less than 15microns have been observed to pass freely through the cerebral circulation, whereas bubbles larger than this have been found to obstruct blood flow.[114] As bubbles become trapped in a vessel, they typically assume a cylindrical shape with hemispherical ends. At this point, the length of the bubble is greater than its radius and the dissolution time is increased by at least 50% for a spherical bubble with the same initial volume.[115] Larger GME are also more likely to lodge higher up in the arterial tree, with a predilection for trapping in small arterioles of 20-50um in diameter.[116] The boundary between gray and white matter is particularly dense in vessels of this size, [117] and this may account for the high incidence of infarcts seen in this region following GME.[118]

Once in the vasculature, several small bubbles may become larger bubbles through fusion with other bubbles.[119,120] Alternatively, at branch points in a vessel, larger bubbles can split with each bubble taking different paths to each other.[121] A given sized bubble will continue to travel at the velocity of blood and follow the normal circulation, that becomes progressively smaller at more distal locations (7-10um in cerebral microvasculature) until it encounters a smaller vessel to lodge.[122] In reality, it is therefore plausible that a bubble of any size/volume may occlude arterioles/capillaries of any size and lead to subtle localized injury if the diameter of the bubble is greater to the vessel.

Indeed, animal models have shown that air emboli as low as 5ul (0.005ml) in volume and as small as 45um (0.045mm) in diameter can lead to reduction or complete arrest of cerebral blood flow for several minutes (transit time of the bubble) with resultant neurological impairment as well as histological and radiological evidence of small (<1mm) multifocal and widely distributed brain infarcts.[123-126], in contrast to those produced by thromboembolic events.[121]

While small bubbles may not occlude a vessel to significantly interrupt blood flow, they do not remain harmless.[127] Animal models have shown a reduction in cerebral blood flow (CBF) and neuroelectrical function with bubbles as small as 25ul and 10-20um(0.01-0.02mm) in the absence of occlusive effects.[128] During their passage through the circulation, small bubbles strip the endothelium from the basement membrane causing breakdown to the blood brain barrier (BBB).[129] This damage incites an inflammatory response leading to leucocyte infiltration, activation of complement and coagulation systems and release of cytototoxic proteases that cause cellular damage to surrounding structures.[130,131]

Bubbles can also to interact with membrane fragments of these inflammatory cells (for example proteins and lipids on blood cells) that may also lead to their growth and stabilization and increasing the likelihood of occlusive effects.[132,133]

Cerebral haemodynamics of the local environment may exacerbate many of these effects. Hypotension and decreased perfusion pressure have both been found impair the washout and clearance of GME thereby increasing their 'survival' time in the vascular bed of hypoperfused regions, and the severity of ischaemia in both animal models and computational algorithms.[134] Monte Carlo simulation experiments have found that a high blood pressure can reduce the total number of blocked arterioles and duration of embolic blockages by forcing bubbles through the vascular tree rapidly.[126,135] Finally, while all GME do eventually become absorbed following trapping, there is often incomplete normalization of blood flow leading to cerebral ischaemia and impaired neuronal function.[126]

1.7 Neuroprotective adjuncts against neurological brain injury

1.7.1 Solid protection: Cerebral embolic filter devices

Cerebral embolic filter devices (CEPDs) are filters that are designed to deflect or capture emboli 'en-route' to the brain. They are used as an adjunct during vascular transcatheter based procedures where there is a significant periprocedural embolic risk, such as in carotid artery stenting (CAS) and transcatheter aortic valve repair (TAVR).[136-142]

CEPDs are inserted before the transcatheter based procedure and are removed after the procedure. CEPDs vary according to the structure (frame vs cone), access required for insertion (radial/brachial vs femoral), filter pore and sheath size, mechanism of protection (deflection vs filter and capture), location (across the

arch or into supra-aortic vessels) and which supra-aortic vessels are afforded protection (Figure 1.8, Table 1.1).

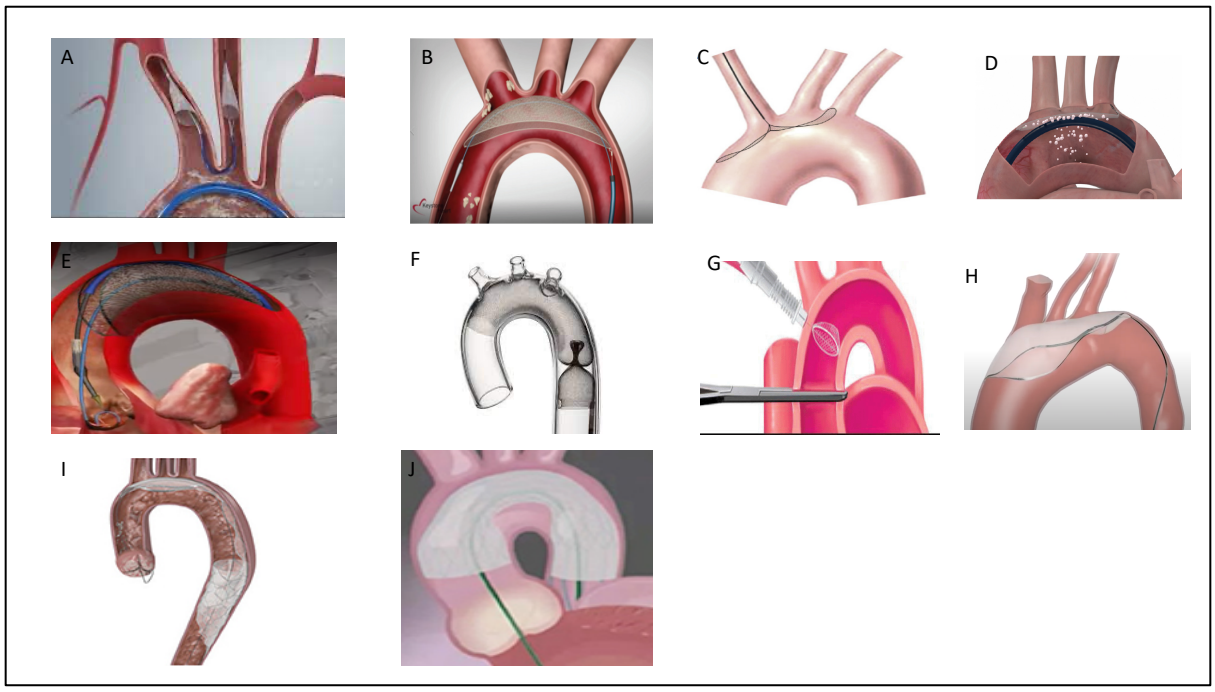


Figure 1.8 Cerebral embolic protection devices currently available for use with transcatheter based procedures; (A) Sentinel^{TM}, (B)TriGuard, (C) Embrella, (D)Protemb, (E) Emblok, (F), Emboline, (G) Embol-X, (H) Point-guard, (I) Filterlex, (J), Embolisher.

Table 1.1 Commercially available cerebral embolic protection devices

	Embrella (Edwards Lifesciences; Irvine, California, United States)	**TriGuard (Keystone Heart Ltd., Herzliya, Israel**	**SENTINEL (Boston Scientific, United States)**
Structure	Two polyurethane membrane/mesh (pore size 100um) mounted on a nitinol frame	Nitinol frame and polymeric membrane/mesh (pore size 115x145um)	Two cone shaped mesh filters (pore size 140um, proximal filter 15mm in size, distal filter 10mm in size) connected by an articulating catheter.
Placement	Aortic Arch	Aortic Arch	Directly into brachiocephalic (proximal filter) and left common carotid artery (distal filter)
Access and Sheath Size	Radial/ulnar/brachial 6F	Femoral 9F	Radial/brachial 6F
Embolic protection method	Deflection	Deflection	Filter and capture
Supra-aortic vessels protected	Brachiocephalic and left common carotid arteries	Brachiocephalic, left common carotid and left subclavian arteries	Brachiocephalic and left common carotid arteries
Vascular territory protection	Anterior circulation	Anterior and posterior circulation	Anterior circulation

The most applicable CEPD for TEVAR is the Sentinel dual-filter system. This involves the percutaneous insertion of a proximal and distal filter directly into the brachiocephalic and left common carotid artery. Other CEPDs (Embrella and TriGuard) protect the supra-aortic trunks by sitting across the arch and are not suitable for TEVAR as they would interfere with the fixation and sealing of the TEVAR endograft.

Three very small feasibility and safety studies of the Sentinel CEPD in TEVAR are reported in the literature (total of 17 patients).[75,143,144] In the largest study to date (n = 10), Grover et al[75] demonstrate a 95% debris capture rate of acute thrombus, arterial wall and foreign material with a median total number and surface area of 937 captures particles (IQR, 146-1687) and 2.66 mm^2 (IQR, 0.08-9.18 mm^2) respectively. No patient experienced a clinical stroke and there were only 23 new infarcts with a median surface area of 6mm^2 on DW-MRI in the CEPD group.

The use of CEPD is more widely documented in in TAVR. A number of randomised and large prospective studies using clinical and radiological end-points in patients undergoing TAVR demonstrate a reduction in post-operative stroke, as well as a reduction in the number and volume of new DW-MRI infarcts when compared to patients who did not receive CEPD (Table 1.2)..[137-142] The SENTINEL trial also observed a

significant correlation between new lesion number and volume, and neurocognitive decline.[142] Histological confirmation of the high embolic load (majority of debris 150-500 mm in diameter) captured by CEPDs further supports the hypothesis that CEPDs have the potential to mitigate periprocedural embolic risk from TAVR.[137,138,142]

The evidence from these studies suggests that CEPDs could also potentially confer neuroprotection in patients undergoing TEVAR. Further evaluation in large studies is necessary in order to support routine clinical use.

Table 1.2 Evidence base for cerebral embolic protection devices

	Embrella	**Triguard**	**Sentinel**
Pivotal study/s	PROTAVI-C	DEFLECT III	CLEAN-TAVI MISTRAL-C SENTINEL CSI-Ulm-TAVR
Methods	Prospective, non-randomised	RCT	1.RCT 2.Prospective non-randomised
Patients (CEPD vs controls)	41 vs 11	46 vs 39	CLEAN-TAVI: 50 vs 50 MISTRAL-C: 32 vs 33 SENTINEL: 244 vs 119 CSI-Ulm-TAVR: 802
Results	**Stroke/TIA** -7.3% CEPD vs control 0% (P>0.05) **DW-MRI:** - Non-significant increase in DW-MRI infarcts in CEPD group (8vs.4, P=0.41) - Significantly lower DW-MRI infarct volumes (40% smaller, P = 0.003) in CEPD group **Neurocognitive** -Mild significant improvement at 30 days compared with baseline in CEPD group (P<0.001) vs no difference in control group over time (P=0.678)	**Stroke/TIA** -2.2% CEPD vs 5.1 control (P=0.46) 3.1% worsening NIHSS score from baseline in CEPD vs 15.4% control (P=0.16) **DW-MRI:** - Greater freedom from DW-MRI infarct in CEPD (21.2 vs. 11.5%), - 44% reduction of median DW-MRI infarct volume (P=0.07) **Neurocognitive:** -At discharge and at 30 days, fewer TriGuard patients in both the ITT and PT populations had a worsening in MoCA scores -Mean MoCA score improved from baseline to discharge and 30 days in the TriGuard group; in the control group, the mean score declined from baseline to discharge and rebounded to approximately baseline levels at 30 days	**Stroke/TIA** -CLEAN-TAVI: 5% CEPD vs control 5% -MISTRAL-C 0% CEPD vs control 7% % -SENTINEL: 5.6% vs. 9.1%; P=0.25) -CSI-Ulm-TAVR: 1.4% vs 4.2% (p=0.03) **DW-MRI** -CLEAN-TAVI: significantly lower number and volume of DW-MRI in CEPD group (P<0.001) -MISTRAL-C: Greater freedom from DW-MRI infarct in CEPD (27% vs 13%), lower number and volume of DW-MRI infarcts -SENTINEL: significant reductions in DW-MRI volume in both protected and all territories in the CEPD group vs controls (p=0.025 and p=0.050 for protected and all territories, respectively. CSI-Ulm-TAVR: **Neurocognitive:** -CLEAN-TAVI: 50 % vs 72.2% overall worsening early MOCA scores -MISTRAL-C: 4% vs 27% cognitive deterioration (p=0.017) -SENTINEL: Significant correlation between change in neurocognitive scores from baseline to 30-day follow-up with median DW-MRI lesion volume in protected territories (P=0.0109 and unprotected territories (P=0.003)

The major drawback of the Sentinel device for use in TEVAR (and TAVR) is incomplete brain protection. The left vertebral artery provides 20% of total brain perfusion and currently remains unprotected by the two-filter Sentinel CEPD. Periprocedural debris can therefore still embolise to the brain through this vessel. Unsurprisingly, Grover et al[75] report that 65% of new infarcts were in the hindbrain territory supplied by the left vertebral artery. Similarly, the randomised TAVR CEPD trials (CLEAN-TAVI, MISTRAL-C and SENTINEL) also demonstrated a lower reduction in lesion volume to the entire brain compared to protected areas of the brain, and the unprotected left vertebral artery in all these studies may account for this finding.[137,138,142]

Recently, the use of a third single filter in the left subclavian artery or vertebral artery has been proposed. Van Gils et al used the Wirion (Allium Medical, Inc., Caesarea, Israel)) into the left vertebral artery, in addition to Sentinel CEPD placement into the brachiocephalic and left common carotid arteries in 11 patients undergoing TAVR. Comparable amounts of embolic debris were obtained between the left vertebral filter to the Sentinel filters.[145]

The Sentinel CEPD cannot be deployed in zone 0 and 1 due to interference with deployment and retrieval of both filters relative to the endograft. Shimamura et al the deployment of three different single filters (Parachute (Tri-Med), Filtrap (Nipro) and FilterWire EZ (Boston Scientific Corporation)) in the supra-aortic vessels and the placement of an occlusion balloon catheter for the left subclavian artery following arch debranching procedures but prior to TEVAR stent-graft deployment in zone 0 and 1 in a complex group of 17 patients. They authors conclude that the use of single filters may prevent stroke during endovascular arch repair.[146] However, a limitation of this technique is that the debranching procedures needed to revascularize the brachiocephalic and left common carotid arteries at landing zones 0 and 1 mean

these vessels are unprotected and manipulation during these extra-anatomical bypasses could also be a further source for embolic stroke.

1.7.2 Solid protection: Carotid clamping and flow reversal

Clamping of the supra-aortic vessels is an alternative method of embolic protection. This has been used in CAS to prevent cerebral embolisation into the internal carotid artery (ICA).[147] Masada et al used a similar technique in TEVAR; clips and occlusion balloons were applied to these vessels to arrest forward blood flow from the left common carotid artery and the left subclavian artery for zone 1 cases and from the LSCA for zone 2 cases prior to delivery and deployment of endografts. This technique was associated with a 21% rate of infarction (24 new infarcts) in this TEVAR cohort to this technique.[148]

Flow reversal to divert blood (and emboli) away from the cerebral vessels during CAS may also be a useful strategy during interventions in the aortic arch. Ribo *et al* used this technique in 65 patients undergoing CAS and reported no air/solid microemboli on TCD monitoring during stent deployment.[149] A recent meta-analysis of single-arm and comparative studies has also demonstrated a pooled stroke rate of 0-4% during CAS with flow reversal.[150]

While promising, these techniques require surgical exposure of the supra-aortic vessels and this may not be necessary for all TEVAR cases. Clamping of the supra-aortic vessels and flow reversal also risk cerebral hypoperfusion, while clamp release may itself lead to cerebral embolisation, all of which risk neurological deficit.

1.7.3 Solid protection: Robotic navigation

The use of robotic catheters has been proposed to be a further mechanism that may reduce cerebral solid embolisation. Wire and pigtail manipulation is the TEVAR step most associated with solid MES.[75] By increasing precise manoeuvrability and stability of endovascular instruments in the arch, this technology may therefore reduce unnecessary catheter movements and contact with the atherosclerotic vessel wall. Rippel et al demonstrate a significant reduction in vessel wall contact (wall-hits) with robotic catheter technology compared to manual techniques in a simulated study of TAVR (median wall-hits: 1 (0-5) vs 6 (2-22), $P < 0.01$).[151] Similarly, Perera *et al* demonstrated a significant reduction in TCD-detected cerebral embolisation of particulate matter during catheter placement in the arch in comparison to manual techniques (median TCD-HITS: 0(0-1) vs 2(1-5), $P<0.01$).[152]

1.7.4 Gaseous protection: TEVAR delivery system flushing techniques

The issue of gas release from TEVAR endografts and their propensity to cause cerebral infarcts that may manifest as stroke and/or cognitive impairment, despite flushing with heparinised saline according to IFU has led many to develop new methods with which to effectively de-air endografts and their delivery systems.

In recent years, flushing endografts with carbon-dioxide (CO_2) prior to saline flushing to purge out retained air has received much attention. This 'inerting' technique is practiced widely in chemical industry whereby inert gases are used to displace (purge) other gases safely to prevent dangerous chemical reactions.[152] CO_2 is the ideal inerting gas as it is readily available and is 1.5 times denser than air and 25 times more soluble to air.[152] The practice of CO_2 field flooding of the cardiac chambers, arterial lines and cardiopulmonary bypass circuit has been invariably practiced since the 1960's. This de-airing technique aims to prevent cerebral air embolisation and its neurological consequences by displacing air and creating a CO_2

atmosphere.[153-162] A recent meta-analysis of CO_2 field flooding in cardiac surgery found a lower rate of neurocognitive impairment with CO_2 field flooding compared to standard cardiac de-airing manoeuvres, although this was not statistically significant (12% vs 21%; p=0.35). The stroke rate was also similar between the two groups (1% vs 1.2%; p=0.62).[163]

With respect to TEVAR, the practice of 'CO_2 flushing' of TEVAR devices is also thought to replace air within the spaces of the delivery system and endograft with a less harmful gas.[164] Kolbel et al report a 3% stroke rate in 36 patients who underwent TEVAR with CO_2 flushing.[164] A recent two centre retrospective analysis from the STEP collaborators (Stroke from Thoracic Endovascular Procedures) demonstrated a 50% rate of DW-MRI infarcts in patients undergoing TEVAR in zones 0-3 with CO_2 flushing. This study however excluded patients who had had a clinical stroke and used a 1.5T MRI scanner, both of which may lead to an underestimation of the infarct rate.[165] Moreover, this study did not evaluate the impact of DW-MRI infarcts on cognitive impairment.

Other device specific de-airing techniques have also been described including the use of 'blood flushing', addition of flushing side ports,[166] and liquid perfluorocarbons, [167] however, there is insufficient clinical data to support their use at this time.

1.7.5 Gaseous protection: Gaseous filter devices

Filters against GEM have also been created. The use of a dynamic bubble trap (HPmedica, Augsburg, Germany) that is incorporated into the cardiopulmonary bypass circuit has been designed to reduce gaseous embolisation has been found to reduce TCD MES. Studies have demonstrated an improved cognitive function 3 months following coronary artery bypass.[168,169,170] This could potentially be used to prevent cerebral air embolisation during TEVAR arch angiography.

The TriGuard 3 CEPD has its design based on the TrigGuard CEPD that sits across the aortic arch and covers the origns of the supra-aortic trunks. The new design has smaller pores and has been shown to reduce cerebral embolisation of particulate and air bubbles under simulated conditions.[171] While further clinical testing is warranted to demonstrate its efficacy in preventing cerebral infarcts, as explained earlier, it is not suitable for TEVAR because of its location within the arch.

In the future, technological developments could focus on the design of supra-aortic vessel filters that prevent the passage of both solid and gaseous microemboli during TEVAR.

1.8 Summary

The importance of TEVAR as a therapeutic option for older, comorbid patients with thoracic aortic disease and the inherent risk of stroke and cognitive decline in this population, as well the expansion of TEVAR to a younger and 'lower-risk' cohort of patients demands the application of strategies that can mitigate all forms of procedure-related brain injury including ischaemic cerebral infarcts.

At this current time, there are no TEVAR-specific neuroprotective systems/adjuncts against neurological brain injury. CEPDs and meticulous preparation of TEVAR delivery systems, that may include the use of carbon-dioxide flushing to prevent periprocedural cerebral embolisation of particulate matter and air offer promising neuroprotective solutions, but further clinical studies are required to show direct correlation between these practices and improved clinical and radiological outcomes.

1.9 Hypothesis

TEVAR is an embologenic procedure that results in gaseous and solid cerebral embolisation; neuroprotective adjuncts may be developed to reduce the embolic burden of TEVAR and in doing so, may mitigate the risk of cerebral injury, stroke, and cognitive impairment.

1.10 Aims

The overall aims of this thesis are to:

1. Test the efficacy of CO_2 flushing of thoracic endografts to prevent gaseous embolization during TEVAR with respect to TCD-detected cerebral embolization, the frequency of new DW-MRI infarcts, stroke, and cognitive impairment, and in doing so determine the clinical safety and feasibility of CO_2 flushed endografts.

2. Validate the efficacy of CO_2 flushing of thoracic endografts to prevent gaseous embolization in an experimental setting.

3. Test the efficacy of cerebral embolic protection filters to prevent solid embolization during TEVAR with respect to TCD-detected cerebral embolization, the frequency of new DW-MRI infarcts, stroke, and cognitive impairment

4. Use the findings of this body of work to inform a future randomised control trial to determine the clinical efficacy of the appropriate and most relevant neuroprotective adjuncts.

1.11 Study outcomes

The primary outcome measures are:

1. Imaging- TCD detected cerebral embolization, DW-MRI infarcts, number, and volume of gas bubbles released during endograft deployment on the experimental model with the ultrasound-based bubble detector

2. Clinical- stroke, cognitive impairment, and major adverse cardiovascular events

3. Histological- analysis of debris captured by CEPD

Chapter 2: Pathology specific incidence and trends in stroke following thoracic endovascular aortic repair (TEVAR) for descending thoracic aortic pathology: a systematic review and meta-analysis.

2.1 Aim

This study aims to (1) perform a systematic review and meta-analysis to determine the incidence and risk factors for stroke following zones 2-4 TEVAR according to aortic pathology, and (2) determine if the stroke rate has changed over the last two decades using meta-regression.

2.2 Methods

This systematic review was conducted in accordance with the Preferred Reporting Items for Systematic Reviews and Meta-Analyses (PRISMA) guidelines and the protocol was registered on the international prospective register of systematic reviews (PROSPERO ID 42020183843).

2.2.1 Search strategy

The population of interest was patients undergoing TEVAR for descending thoracic aortic pathology, defined as TEVAR in zones 2-4 only. The intervention was TEVAR. There was no comparator group. The outcome was clinical and/or radiological neurological brain injury according to the authors' published definition.

The Ovid MEDLINE® and Embase (EMBASE Classic+Embase) were searched until 20th November 2020 using a combination of search terms relating thoracic endovascular aortic repair, TEVAR, descending thoracic aorta aneurysm, type B dissection, blunt adj2 traumatic injury, and stroke, transient isch*emic

attack, TIA, cerebral isch*emia and infarct*. The search was limited to human studies and studies in English only. A second-level hand search of the reference lists of retrieved articles was also undertaken to increase sensitivity. Full text articles were obtained through institutional access and through the British Library.

2.2.2 Selection criteria

All articles (>10 patients) reporting on neurological brain injury following TEVAR for descending aortic pathology were included. Aortic pathology was defined as atherosclerotic/degenerative aneurysms, acute type B dissection (<14 days), chronic type B dissection (>14 days), and blunt aortic injury. Studies that included TEVAR in PLZs 0-1 or mixed pathology were included only if neurological outcomes for zones 2-4, and for each pathology could be extracted. When a distinction between acute and chronic dissection according the 14-day criteria could not be made, studies were excluded.

Studies that reported on outcomes exclusively for 2nd stage TEVAR following ascending and/or arch repair were excluded as these were considered separate pathologies and this group of patients may be at less at risk of stroke given the arch was reinforced with dacron and no longer consisted of an arterial wall. Mixed studies that included this population were only included if this group of patients accounted for <25% of the total population. Emergency TEVAR for DTAA was only included if elective and emergency cases could not be separated and most cases were elective.

Studies utilising neuroprotective adjuncts were excluded. To avoid inclusion of the same patient cohort, the most recent study by a group or the paper with the most relevant data was included. Population-based studies and studies using administrative database were only included if it was clear TEVAR was in zones 2-4. Abstracts and conference papers were included if sufficient information on neurological brain

outcomes could be extracted. Authors were also contacted if further clarification or additional data were required.

2.2.3 Data extraction and analysis

Two independent researchers (Ms Lydia Hanna and Mr Ammar Abdullah, PhD students) performed a title and abstract screen through the COVIDENCE platform against the protocol and inclusion and exclusion criteria. Any disagreements were resolved by a third independent reviewer (Mr Richard Gibbs). Data was extracted (Ms L Hanna, Ms A Perera) separately for atherosclerotic aneurysms, acute type B dissections, chronic type B dissections and blunt traumatic injury on a prespecified excel sheet of outcomes. For each pathology data extraction included study design details, patient demographic data, pathology, stroke definition and diagnosis, total number of patients in the study and number who developed stroked. The number of patients treated in zone 2, 3 and 4, and revascularisation of the left subclavian artery and method of revascularisation was collected when reported.

A meta-analysis of proportions was conducted using the metaprop command[172] within the metafor package[173] in R Studio version 3.6.3 (R Studio, Boston, MA, USA). Observed proportions were transformed using the logit tranformation and subsequently back transformed to provide the pooled summary estimates with confidence limits calculated through the Clopper-Pearson interval.[174] Effect size was calculated using a random effects model and estimated using the DerSimonian and Laird method.[175] Heterogeneity was assessed using Higgin's I^2.[176] An I^2 >50% indicated significant heterogeneity. To determine the impact of time on stroke rate for each pathology, meta-regression was performed by publication year. Scatter/bubble plots that depicted year of publication (independent variable, x) and the weighted proportion of people with stroke (dependant variable, y) were constructed together with the confidence interval. Uni- and multi-variable meta-regression were used to explore the effects of age, sex, and patient co-morbidities on the

primary outcome (stroke). Regression analysis was also performed to determine the relationship between stroke (independent variable, y) and in-hospital mortality (dependant variable, x). Variable significance at univariable meta-regression were included in the multi-variable model. Subgroup/sensitivity analysis was conducted to determine the stroke rate for a given geographical location. For all analyses, a p value < 0.05 was significant.

2.2.4 Risk of bias

Funnel plots and Egger's test were used to examine publication bias. Where statistically significant asymmetry was found via Egger's test, trim-and-fill plots were performed to determine an estimate of the true proportion.[177] Quality assessment of each study was performed using a modification of the National Institute of Health (NIH) quality assessment tool for case series[178] and the Newcastle-Ottawa Scale (NOS)[179] because the majority of studies included in this review were case series and both tools had appropriate domains for assessment. Studies scoring between 7-9 were judged to be high quality, 4-6 high risk of bias, and 0-3 very high risk of bias. The quality of the evidence was graded using the Grades of Recommendation, Assessment, Development and Evaluation (GRADE) approach based on risk of bias (individual study limitations), inconsistency (heterogeneity in the meta-analysis), indirectness (external validity), imprecision (small sample size, wide confidence interval), and publication bias.[180]

2.3 Results

The electronic database search yielded 5583 studies. The PRISMA flow chart is detailed in Figure 2.1

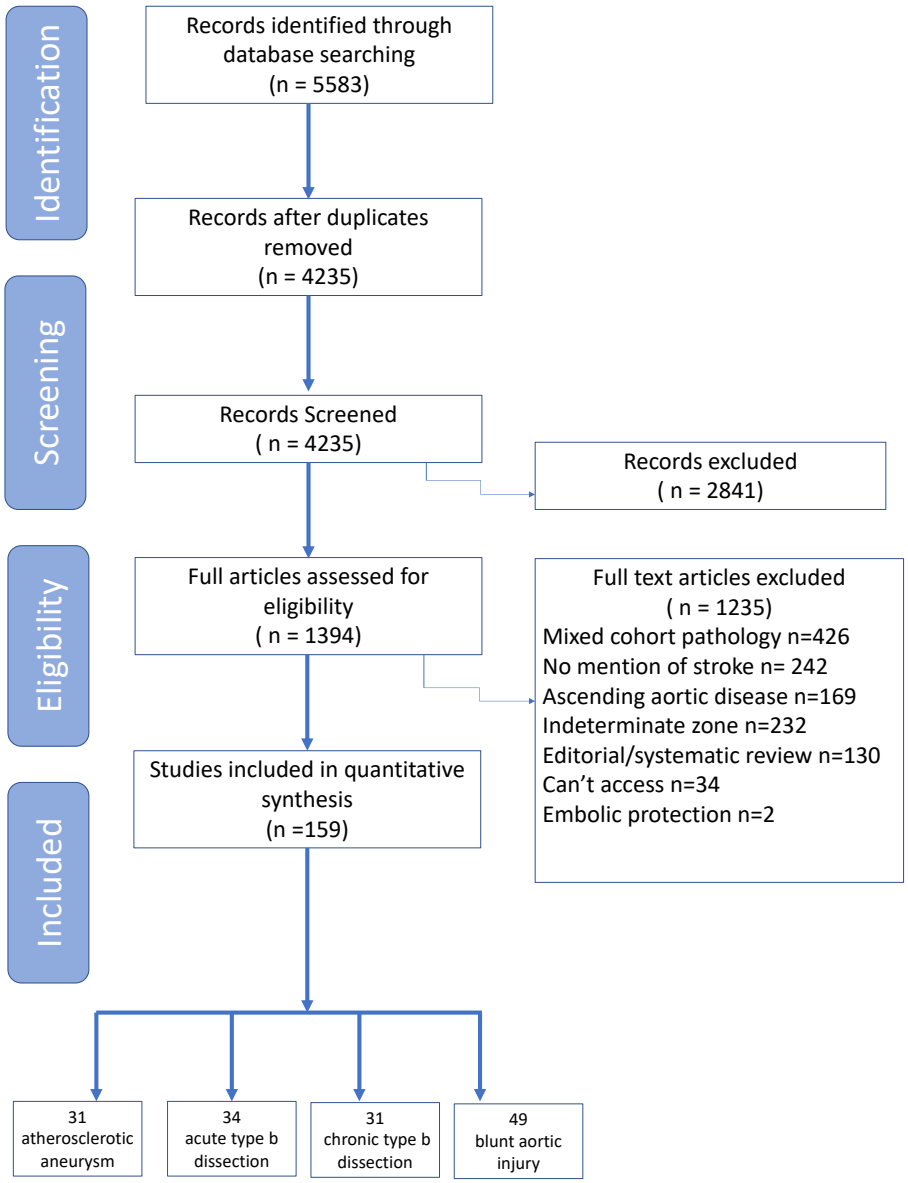


Figure 2.1 PRISMA flow chart

2.3.1 Atherosclerotic aneurysms

31 studies including 9067 patients undergoing TEVAR for atherosclerotic aneurysms were included in the meta-analysis. Eleven studies were from multi-centre industry sponsored trials, [33,181-190]

three multi-centre studies,[191-193] 2 population-based studies[194,195] and 15 single-centre studies[196-210] The study characteristics, TEVAR characteristics, and stroke outcomes are summarised in Table 2.1(a-c). Only eight studies defined stroke and there was no consistent definition used among the studies.[45,185,189,191,193,194,204,206] The aetiology of stroke was also reported in only 8 studies; 8 studies reported embolic infarcts[45,181,182,184,186,192,198,202] and 1 study reported haemorrhagic stroke.[186] The pooled stroke rate was 3.9% (95% CI 3.1% to 4.6%, I^2=46%), p<0.01)(Figure 2.2). Meta-regression using year of publication as a covariate showed no change in the weighted proportion of stroke over time (β_i =-0.016, SE 0.021, p=0.45). No publication bias was detected on Funnel plot analysis (t = -1.36, df = 29, p = 0.18). Risk of bias and justifications for assessments are provided in Table 2.2 and 2.3, respectively.

Table 2.1 Study/patient characteristics (a), TEVAR characteristics (b), stroke and mortality outcomes(c) for atherosclerotic aneurysms.

a. Study/patient characteristics

1st author, Year of publication, Publication type, Country	Study design	Total No. patients	Male % (No.)	Age Mean (SD)	Co-morbidities % (No.)						
					Hypertension	CVA/TIA	IHD	Hypercholestrolaemia	COPD	Smoking	DM
Neuhauser, 2004, full text, Austria	Retrospective, single centre	31	81 (25/31)	Median 73 (IQR 65-81)	77 (24/31)	NR	90 (28/31)	NR	45 (14/31)	36 (11/31)	10 (3/31)
Glade, 2005, full text, Netherlands	Retrospective, multicentre	42	Not reported individually for endo group	Not reported individually for endo group	86 (36/42)	19 (8/42)	62 (26/42)	NR	60 (25/42)	NR	12 (5/42)
Marcheix, 2006, full text, France	Prospective, single centre	45	NR	68 (11)	76 (34/45)	9 (4/45)	53 (24/45)	NR	58 (26/45)	60 (27/45)	27 (12/45
Saratzis, 2007, full text, Greece	Retrospective, single centre	23	100 (23/23)	Median 66 (IQR 45-84)	30 (7/23)	NR	13 (3/23)	17 (4/23)	9 (2/23)	17 (4/23)	4 (1/23)
Makaroun, 2005, full text, USA	Prospective, multicentre TAG registry	142	58 (82/142)	Median 71(IQR 30-86)	NR	10 (14/142)	49 (70/142)	NR	39 (56/142)	83 (118/142)	NR
Azizzadeh, 2019, full text, USA	Prospective, multicentre Valiant EVO clinical trial	87	62 (54/87)	71 (9)	90 (78/87)	17 (15/8)	62 (54/87)	73 (63/86)	33 (28/86)	51 (44/86)	21 (18/87)
Yunoki, 2015, full text, Japan	Retrospective, single centre	36	67 (24/36)	75 (10)	94 (34/36)	14 (5/36)	44 (16/36)	56 (20/36)	14 (5/36)	NR	NR
Ranney, 2018, full text, USA	Retrospective, single centre	192	56 (107/192)	71 (10)	91 (174/192)	11 (21/192)	20 (39/192)	75 (143/192)	33 (63/192)	67 (129/192)	22 (42/192)
Heijmen, 2012, Europe, full text	Prospective, multicentre Valiant Captivia registry	49	78 (38/49)	70 (8)	82 (40/49)	12 (6/49)	80 (39/49)	47 (23/490	31 (15/49)	57 (28/49)	16 (8/49)
Ullery, 2012, USA, full text	Retrospective, single centre	433	Not reported individually for aneurysm group	Not reported individually for aneurysm group	NR	NR	NR	NR	NR	NR	NR
Fairman, 2008, USA, full text	Prospective, multicentre VALOR trial	195	59 (115/195)	70 (11)	87 (170/195)	17 (34/195)	79 (154/195)	44 (85/195)	37 (72/195)	77 (150/195)	16 (31/195)
Matsuyama, 2014, Japan, full text	Retrospective, multicentre	27	Not reported individually for descending thoracic aneurysm group	Not reported individually for descending thoracic aneurysm group	NR	NR	NR	NR	NR	NR	NR
Varkevisser, 2020, USA, full text	Retrospective, population-based study	1762	Not reported individually for thoracic aneurysm group	Not reported individually for thoracic aneurysm group	NR	NR	NR	NR	NR	NR	NR
Shimizu, 2019, Japan, full text	Retrospective, population-based study	3411	NR	NR	NR	NR	NR	NR	NR	NR	NR
Schlosser, 2009, USA, full text	Retrospective, multicentre	72	86 (62/72)	73 (6.8)	NR	NR	NR	NR	NR	NR	NR
Hughes, 2010, USA, full text	Retrospective, single centre	79	56 (44/79)	73 (14)	87 (69/79)	NR	48 (38/79)	NR	54 (43/79)	NR	27 (21/79)
Andrassy, 2011, USA, full text	Retrospective, single centre	53	60 (32/53)	70 (10)	85 (45/53)	NR	40 (21/53)	NR	28 (15/53)	NR	11 (6/53)

Matsumura, 2008, USA, full text	Prospective, multicentre Zenith TX2 trial	160	72 (115/160)	72 (9.6)	89 (143/160)	21 (33/160)	65 (104/160)	NR	44 (71/160)	86 (138/160)	19 (30/160)
Patel, 2016, USA, full text	Prospective, multicentre GORE TBE trial	22	55 (12/22)	74.1 (10.5)	91 (20/22)	0	46 (10/22)	NR	36 (8/22)	50 (11/22)	14 (3/22)
Zamor, 2015, USA, full text	Retrospective, single centre	29	Not reported individually for aneurysm group	Not reported individually for aneurysm group	NR	NR	NR	NR	NR	NR	NR
Kratimenos, 2019, Greece, full text	Retrospective, single centre	30	80 (24/30)	73.7 (6.3)	57 (17/30)	27 (8/30)	7 (2/30)	50 (15/30)	23 (7/30)	70 (21/30)	17 (5/30)
Ziza, 2016, France, full text	Retrospective, single centre	81	Not reported individually for aneurysm group	Not reported individually for aneurysm group	NR	NR	NR	NR	NR	NR	NR
Tanious, 2021, USA, full text	Retrospective, single centre	219	55 (120/219)	74 (10.5)	91 (201/219)	NR	NR	72 (158/219)	31 (67/219)	NR	NR
Malas, 2021, USA, full text	Retrospective, multicentre	45	69 (31/45)	74 (54-85)	96 (43/45)	56 (25/56)	16 (7/45)	62 (28/45)	31 (14/45)	84 (38/45)	18 (8/45)
Farber, 2017, USA, full text	Retrospective, multicentre Bolton Relay trial	133	53 (70/133)	72.8 (10.7)	90 (119/133)	30 (40/133)	50 (66/133)	77 (102/133)	32 (43/133)	77 (103/133)	20 (27/133)
Maldonado, 2013, USA, full text	Retrospective, multicentre	823	Not reported individually for aneurysm group	Not reported individually for aneurysm group	NR	NR	NR	NR	NR	NR	NR
Mezzetto, 2021, Italy, full text	Retrospective, multicentre	129	89 (115/129)	74.9 (7.4)	67 (86/129)	NR	32 (41/129)	42 (54/129)	NR	NR	16 (20/129
Kasirajan, 2011, USA, full text	Retrospective, multicentre	421	63 (265/421)	Male 71.0 (10.8), Female 72.8 (9.5)	NR	10 (42/421)	39 (162/421)	NR	32 (134/421)	67 (282/421)	NR
Fairman, 2012, USA, full text	Prospective, multicentre VALOR II trial	160	59 (95/160)	72.2 (9.1)	94 (150/160)	22 (35/160)	44 (71/160)	74 (118/160)	35 (56/160)	44 (71/160)	21 (34/160)
Jordan, 2015, USA, full text	Prospective, multicentre cTAG trial	66	59 (39/66)	72.2 (9.4)	99 (65/66)	38 (25/66)	61 (40/66)	70 (46/66)	42 (28/66)	70 (46/66)	20 (13/66)
Torsello, 2017, Germany, full text	Prospective, single centre	70	51 (36/70)	70.6 (9.4)	51 (63/70)	20 (14/70)	50 (35/70)	NR	30 (21/70)	30 (21/70)	11 (8/70)

b. TEVAR characteristics

1st author, Year of publication	**Indication for TEVAR**	**TEVAR device**	**PLZ No. in zone 2/zone 3-4**	**Left Subclavian Artery Management**		
				Coverage	Bypass/Transposition	Endovascular
Neuhauser, 2004	Atherosclerotic degenerative descending thoracic aorta aneurysms	Gore Excluder, Medtronic Talent, Boston Scientific Vanguard	8/23	7	1	0
Glade, 2005	Atherosclerotic degenerative descending thoracic aorta aneurysms	1 Medtronic AneuRx, Medtronic Talent, Gore TAG	0/42	NA	NA	NA
Marcheix, 2006	Atherosclerotic degenerative descending thoracic aorta aneurysms	Gore Excluder, Medtronic Talent, 1 Baxter device	6/39	6	0	0
Saratzis, 2007	Atherosclerotic thoracic aneurysms	LeMaitre EndoFit	0/23	NA	NA	NA
Makaroun, 2005	Atherosclerotic degenerative descending thoracic aorta aneurysms	Gore TAG	28/114	0	28	0
Azizzadeh, 2019	Atherosclerotic thoracic aneurysms	Medtronic Navion	NR	1	24	0
Yunoki, 2015	Atherosclerotic descending thoracic aneurysms	Gore TAG	0/36	NA	NA	NA

Ranney, 2018	Degenerative atherosclerotic aneurysms	Gore TAG/cTAG, Medtronic Talent/Valiant, Cook Zenith TX2/Alpha, Bolton Relay, Medtronic AneuRx	NR	76 (partial and complete)	12	0
Heijmen, 2012	Degenerative aneurysms	Medtronic Valiant Captivia	19/30	0	19	0
Ullery, 2012	Degenerative aneurysms	NR	NR	NR	NR	NR
Fairman, 2008	Degenerative aneurysms	Medtronic Talent	13/182	3	10	0
Matsuyama, 2014	Atherosclerotic thoracic aneurysms	Custom-made	9/18	0	0	9
Varkevisser, 2020	Thoracic aortic aneurysm	NR	622/1140	NR	NR	NR
Shimizu, 2019	Descending thoracic aortic aneurysms	NR	NR	NR	NR	NR
Schlosser, 2009	Degenerative aneurysms	NR	10/62	10	0	0
Hughes, 2010	Descending thoracic aneurysms	Gore TAG, Cook Zenith TX2, Medtronic Talent	NR	NR	4	NR
Andrassy, 2011	Degenerative aneurysms	Homemade, Medtronic Talent, Gore Excluder, Cook Zenith TX2	12/41	9	3	0
Matsumura, 2008	Descending thoracic aortic aneurysms and ulcers	Cook Zenith TX2	NR	NR	NR	NR
Patel, 2016	Distal aortic arch aneurysms	GORE thoracic branch endoprosthesis	22/0	0	0	22
Zamor, 2015	Aneurysm	NR	3/26	3	26	0
Kratimenos, 2019	Degenerative atherosclerotic aneurysms	Lifetech Scientific Ankura	3/26	3	0	0
Ziza, 2016	Aneurysm	Mixed- Gore Excluder, Medtronic Talent and Valiant, Cook Zenith	24/57	NR	NR	NR
Tanious, 2021	Descending thoracic aortic aneurysms	Multiple- Cook Zenith TX2 and Alpha, Gore TAG and cTAG, Medtronic Valiant and Talent	NR	78	40	NR
Malas, 2021	Descending thoracic aneurysms	Bolton Relay	10/35	7	3	0
Farber, 2017	Aneurysms and PAUs	Bolton Relay	NR	NR	NR	NR
Maldonado, 2013	Thoracic aneurysm	GORE TAG, Medtronic Talent, Cook TX2, Bolton Relay	254/557	111	143	0
Mezzetto, 2021	Descending thoracic aneurysms	GORE TAG, Bolton Relay	48/81	0	48	0
Kasirajan, 2011	Atherosclerotic fusiform aneurysms	GORE TAG and cTAG	NR	NR	NR	NR
Fairman, 2012	Degenerative descending thoracic aortic aneurysms	Medtronic Valiant	51/106	29	22	0
Jordan, 2015	Thoracic aortic aneurysms	GORE cTAG	22/44	4	18	0
Torsello, 2017	Thoracic aortic aneurysms or PAUs	Cook Zenith Alpha	NR	NR	6	9

c. Stroke characteristics and Mortality

1st author, Year of publication	Stroke diagnosis/definition	Stroke % (No.)	Stroke character (embolic/haemorrhagic)	Risk factors for stroke identified by study
Neuhauser, 2004	NR	3.2 (1/31)	NR	NR
Glade, 2005	NR	0	NA	NA
Marcheix, 2006	NR	13 (6/45)	Embolic	LSA coverage in 1 patient, diffuse injuries consistent with emboli during device manipulation in atherosclerotic arch
Saratzis, 2007	NR	0	NA	NA
Makaroun, 2005	NR	3.5 (5/142)	Embolic	Strokes occurred in 4/5 patients with carotid-subclavian bypass
Azizzadeh, 2019	NR	4.6 (4/87)	Embolic	Proximal landing zone 2 in 3 stroke patients and zone 4 in 1 stroke patient

Yunoki, 2015	NR	0	NA	NA
Ranney, 2018	NR	2 (4/192)	Embolic	NR
Heijmen, 2012	NR	6 (3/49)	NR	NR
Ullery, 2012	Any new focal or global neurologic deficit lasting >24 hours with associated computed tomography or magnetic resonance imaging evidence of acute intracranial abnormality	3.5 (15/433)	Embolic	Analysis of mixed pathology group; Independent risk factors for any perioperative stroke were chronic renal insufficiency and history of prior stroke. Age and zone 2 coverage were additional risk factors for posterior circulation stroke.
Fairman, 2008	NR	3.6 (7/195)	Embolic	History of AAA and PLZ 2 and 3
Matsuyama, 2014	NR	0	NA	NA
Varkevisser, 2020	Stroke was defined by the NSQIP as motor, sensory, or cognitive dysfunction persisting for ≥24 hours and clinical suspicion of stroke	3.4 (60/1762)	NR	NR
Shimizu, 2019	NR	3.3 (113/3411)	NR	NR
Schlosser, 2009	New clinically-evident brain injury present after operation, including focal or global and transient or permanent deficits lasting >24 hours	1.4 (1/72)	NR	NR
Hughes, 2010	New neurologic deficit by clinical exam lasting greater than 24 hours, with or without computed tomographic/magnetic resonance imaging confirmation, or a finding on computed tomographic/magnetic resonance	2.5 (2/79)	NR	NR
Andrassy, 2011	NR	1.9 (1/53)	NR	NR
Matsumura, 2008	Temporary deficit with recovery within 24 hours grade 1 and delayed recovery, infarct on CT or magnetic resonance, permanent deficit with mild impairment grade 2, severe impairment or fatal outcome grade 3	3.1 (5/160)	NR	NR
Patel, 2016	NR	0	NA	NA
Zamor, 2015	Confirmed on CT/MRI + neurology review	3.5 (1/29)	NR	NR
Kratimenos, 2019	NR	0	NA	NA
Ziza, 2016	NR	3.7 (3/81)	NR	NR
Tanious, 2021	NR	4.1 (9/219)	NR	NR
Malas, 2021	NR	2.2 (1/45)	NR	NR
Farber, 2017	A sudden, nonconvulsive loss of neurologic function because of an ischemic or haemorrhagic intracranial vascular event	7.5 (10/133)	NR	NR
Maldonado, 2013	Any clinically relevant stroke or transient ischemic event, regardless of extent of recovery	7.3 (59/810)	NR	Female gender, cerebrovascular disease, smoking
Mezzetto, 2021	NR	1.6 (2/129)	Acute cerebral ischaemia	NR
Kasirajan, 2011	NR	2.9 (12/421)	NR	NR
Fairman, 2012	NR	2.5 (4/160)	2 haemorrhagic and 2 ischaemic	Complete and partial LSCA coverage in the 2 patients with ischaemic stroke
Jordan, 2015	NR	3 (2/66)	NR	NR
Torsello, 2017	NR	0	NA	NA

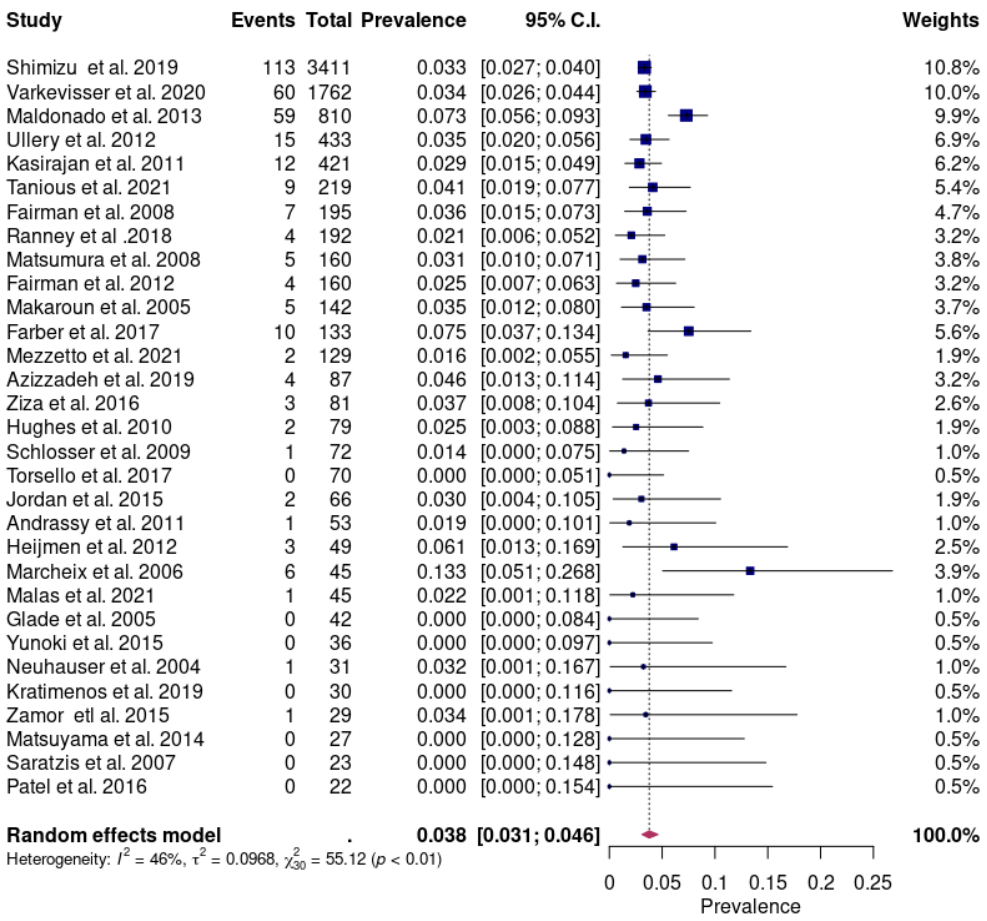


Figure 2.2 Forrest plot for pooled incidence of stroke following TEVAR for atherosclerotic aneurysms.

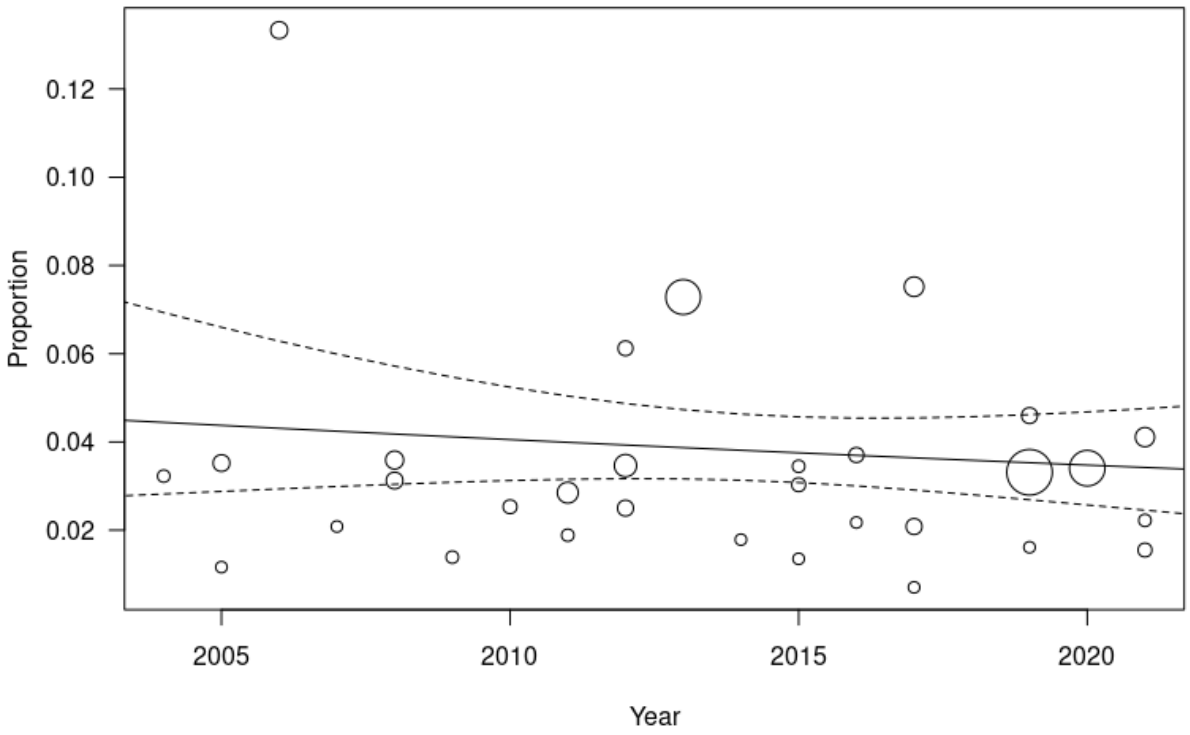


Figure 2.3 Meta-regression (scatter plot) of the relationship between year of publication and stroke as a weighted proportion for atherosclerotic aneurysms (β_i =-0.016, SE 0.021, p=0.45). Each circle represents a study telescoped by its weight in the analysis.

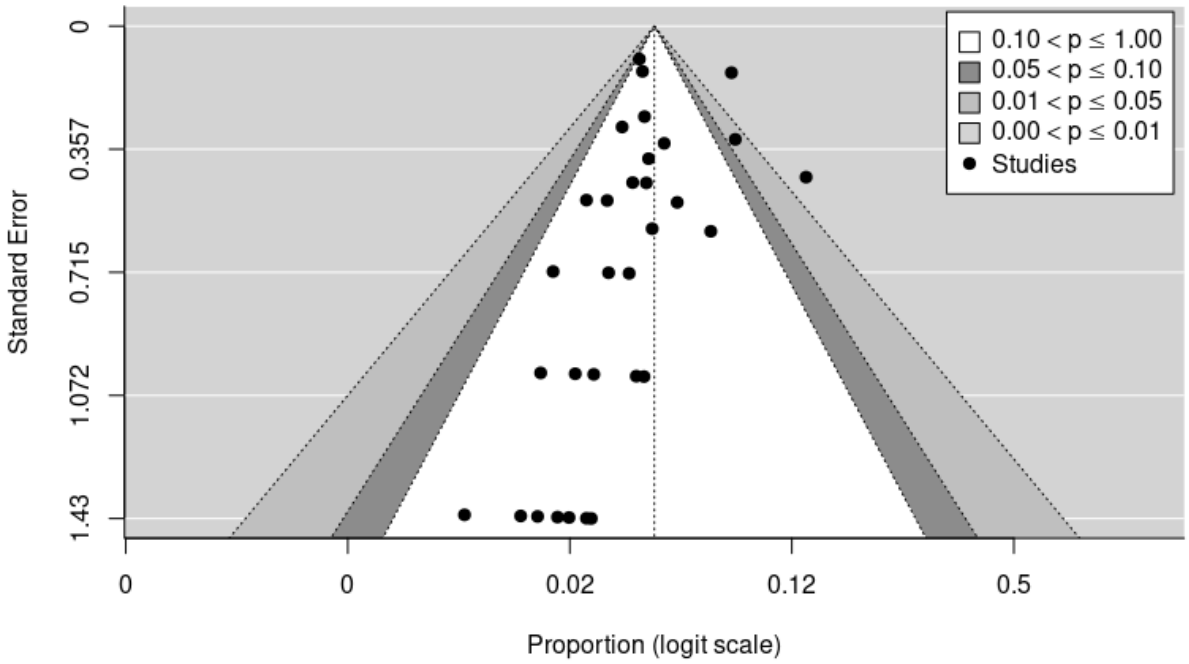


Figure 2.4. Funnel Plot for atherosclerotic aneurysm: (t = -1.36, df = 29, p = 0.18).

Table 2.2 Risk of bias assessment of studies reporting stroke following TEVAR for atherosclerotic aneurysms

Modified Newcastle-Ottawa quality assessment score Key: *=1, -=0, NR=not reported, NA=not applicable

1st author, Year of publication	Selection				Comparability	Outcome			Total score
	Representativeness	Selection of non-exposed cohort (Non-TEVAR control group)	Ascertainment	Stated no stroke at start of study		Method of assessment of stroke	Follow up to minimum 90 days	Adequacy of follow up	
Neuhauser, 2004	*	-	NR	NR	-	NR	*	*	3
Glade, 2005	*	*	*	NR	*	NR	-	NR	5
Marcheix, 2006	*	-	NR	NR	-	*	*	*	4
Saratzis, 2007	-	-	NR	NR	-	NR	*	*	2
Makaroun, 2005	-	-	*	NR	-	*	*	*	4
Azizzadeh, 2019	-	-	*	NR	-	*	-	NR	2
Yunoki, 2015	*	-	NR	NR	-	NR	*	*	3
Ranney, 2018	*	-	*	NR	-	*	*	*	5
Heijmen, 2012	-	-	*	NR	*	NR	-	NR	2
Ullery, 2012	*	-	*	NR	*	*	*	*	6
Fairman, 2008	-	*	*	NR	*	NR	*	*	4
Matsuyama, 2014	*	-	NR	NR	-	NR	*	*	3
Varkevisser, 2020	-	-	*	NR	*	*	-	NR	3
Shimizu, 2019	-	*	*	NR	*	NR	NR	NR	3
Schlosser, 2009	-	-	*	NR	-	*	-	NR	2
Hughes, 2010	NR	-	NR	NR	-	*	*	*	3
Andrassy, 2011	NR	*	NR	NR	*	NR	NR	NR	2
Matsumura, 2008	NR	*	NR	NR	*	*	*	*	5
Patel, 2016	-	-	*	*	-	NR	*	*	4
Zamor, 2015	*	-	*	NR	-	*	*	*	5
Kratimenos, 2019	-	-	NR	NR	-	NR	*	*	2
Ziza, 2016	*	-	*	NR	-	NR	*	*	4
Tanious, 2021	*	-	*	NR	-	NR	*	*	4
Malas, 2021	-	-	*	NR	-	NR	*	*	3
Farber, 2017	-	*	*	NR	*	*	*	*	6
Maldonado, 2013	*	-	NR	NR	*	*	-	NR	3
Mezzetto, 2021	-	-	*	NR	*	NR	*	*	4
Kasirajan, 2011	*	-	*	NR	*	NR	*	*	5
Fairman, 2012	-	-	*	NR	*	*	*	*	5
Jordan, 2015	-	-	NR	NR	-	NR	*	*	2
Torsello, 2017	*	-	NR	NR	-	NR	*	*	3

Table 2.3 Justifications for risk of bias assessment for studies reporting stroke following TEVAR for atherosclerotic aneurysms

Modified Newcastle-Ottawa quality assessment, criteria for grading + 1 where applicable

1st author, Year of publication, Reference	Selection				Comparability	Outcome			Total score
	Representativeness	Selection of non-exposed cohort (Non TEVAR control group)	Ascertainment	Stated no stroke at start of study		Method of assessment of stroke	Follow up to minimum 90 days	Adequacy of follow up	
Neuhauser, 2004	Consecutive series of cases						Range 4-69 months	Clinical examination	3
Glade, 2005	Consecutive patients	Open group	Medical records		Open group				4
Marcheix, 2006	Consecutive patients					Imaging, modality not reported	Range 6 months-6.7 years	Aortic imaging	4
Saratzis, 2007							Range 8-40 months	Full clinical + neurologic examination + aortic imaging	2
Makaroun, 2005			Monitored research forms			Imaging, modality not reported	Mean 24 months, range 7-1626 days	Aortic imaging + physical examination	4
Azizzadeh, 2019			ClinicalTrials.gov results database			Imaging, modality not reported			2
Yunoki, 2015	Consecutive cases						Mean 33 months	Aortic imaging + clinical status assessment at outpatient clinic	3
Ranney, 2018	Consecutive cases inferred		Retrospective review of prospectively maintained database			Imaging, modality not reported	Range 3-141 months	Clinical	5
Heijmen, 2012			ClinicalTrials.gov results database		Comparison of aneurysm vs acute vs chronic dissection				2
Ullery, 2012	Consecutive cases inferred		Retrospective review of prospectively collected database		Assessed risk factors for anterior vs posterior stroke	Imaging (CT/MRI) and clinical evaluation by stroke neurologist	Mean 49 months (SD 26.6)	Clinical	6
Fairman, 2008		Retrospective open surgical cohort	ClinicalTrials.gov results database		Retrospective open surgical cohort		Up to 12 months reported	CT aorta + Clinical examination	5
Matsuyama, 2014	Consecutive patients						Range 36-164 months	Aortic imaging	3
Varkevisser, 2020			American College of Surgeons National Surgical Quality Improvement Program (NSQIP) registry		With vs without left subclavian artery revascularisation	Clinical			3
Shimizu, 2019		Open and hybrid repair comparative group	Japan Cardiovascular Surgery Database		Open and hybrid repair group and different pathologies				3
Schlosser, 2009			Retrospective review of prospectively maintained database			Clinical			2

Hughes, 2010						Clinical or imaging	Range 6-55 months	Clinical examination + CT aorta	3
Andrassy, 2011		Historic open surgery group			Historic open surgery group				2
Matsumura, 2008		Comparison between TEVAR and open repair			Open group	Clinical +/- imaging	Up to 12 months	Aortic imaging	5
Patel, 2016			Protocol-specific case report forms	Pre-operative modified Rankin scores			Mean 232 days (Range 3 to 435 days)	Physical assessment + aortic imaging	4
Zamor, 2015	All cases of TEVAR during study period		Electronic medical records			Imaging + clinical specialist review	Mean 24.9 months	Clinical + aortic imaging	5
Kratimenos, 2019							Median 32 months	Aortic imaging	2
Ziza, 2016	Consecutive cases inferred		Prospectively maintained database				Median 29.9 months (range, 1.25-171.8)	Clinical examination + aortic CT	4
Tanious, 2021	Consecutive cases inferred		Thoracic Aortic Centre database				Range 0.5-5 years	Aortic imaging	4
Malas, 2021			Clinical trial database				Mean follow up 2.3 years	Aortic imaging	3
Farber, 2017		Retrospective open surgical cohort	ClinicalTrials.gov results database		Open group	Clinical + imaging	Mean 3.2 years	Clinical + aortic imaging	6
Maldonado, 2013	Consecutive patients				Left subclavian artery coverage vs revascularisation	Clinical			3
Mezzetto, 2021			Departmental database		ePTFE vs Dacron graft		Median follow up 32 months, range 1-156 months	Aortic imaging +/- clinical	4
Kasirajan, 2011	All patients in GORE clinical trials		Database		Male vs Female		1 year	Aortic imaging	5
Fairman, 2012			ClinicalTrails.gov results database		Medtronic Valiant vs Talent stent-graft	Cerebral imaging	12 months	CT aorta + Clinical examination	5
Jordan, 2015							12 months	Aortic imaging	
Torsello, 2017	Consecutive patients						Mean follow up 22 months	Aortic imaging	3

2.3.2 Acute type B dissection

45 studies including 4246 patients undergoing TEVAR for acute type B dissection were included in the meta-analysis. Six studies were from multi-centre industry sponsored studie,[183,211-215] 2 population-based studies,[195,216] 5 multi-centre studies[217-221] and 31 single-centre studies,[45,222-251] 1 randomised controlled trial (ADSORB).[252] The study/patient characteristics, TEVAR characteristics, and stroke and mortality outcomes are summarised in Table 2.4(a-c). Only 4 studies defined stroke, [45,212,234,239] and only 6 studies characterised the stroke aetiology with embolic infarcts reported in 5 studies[226,243,247,250,251] and watershed infarcts in the remaining study.[239] The pooled stroke rate was 4.2% (95% CI 3.2% to 5.5%, I^2= 48%, p<0.01) (Figure 2.5). Meta-regression using year of publication as the covariate demonstrated no change in the weighted proportion of stroke over time (β_i=-0.003, SE, 0.029, p=0.93)(Figure 2.6). Significant publication bias was detected (t = -4.09, df = 43, p = 0.0002) (Figure 2.7). This was explored further with Trim and Fill plots (Figure 2.8) to determine the true estimate. The stroke rate was found to be 5.7% ((95% CI 4.4 to 7.4], z= -19.49, p<0.001, I^2 =53.08%, p<.0001). Risk of bias and justifications for risk of bias are summarised in Tables 2.5 and 2.6, respectively.

Table 2.4 Study/patient characteristics (a), TEVAR characteristic(b), stroke and mortality (c) for acute type b dissection

a. Study/patient characteristics

1st author, Year of publication, Publication type, Country	Study design	Total No. patients	Male % (No.)	Age Mean (SD)	Co-morbidities % (No.)						
					Hypertension	CVA/TIA	IHD	Hypercholestrolaemia	COPD	Smoking	DM
Zhang, 2017, full text, China	Retrospective, single centre	60	72 (43/60)	63.2 (11.3)	82 (49/60)	8 (5/60)	3 (2/60)	8 (5/60)	5 (3/60)	60 (36/60)	12 (7/60)
Gao, 2019, China, full text	Retrospective, single centre	343	NR individually for acute group	NR individually for acute group	NR	NR	NR	NR	NR	NR	NR
Zha, 2019, full text, China	Retrospective, single centre	63	83 (52/63)	59.13 (9.91)	92 (58/63)	8 (5/63)	3 (2/63)	NR	3 (2/63)	65 (41/63)	18 (11/63)
Zhang, 2018, China, full text	Retrospective, multicentre	38	NR individually for acute group	NR individually for acute group	NR	NR	NR	NR	NR	NR	NR
Shu, 2011, China, full text	Retrospective, single centre	45	73 (33/45)	42.6 (31-47)	22 (10/45)	13 (6/34)	NR	NR	13 (6/34)	NR	18 (8/45)
Du, 2019, China, full text	Retrospective, single centre	163	83 (136/163)	51.06 (10.79)	75 (122/163)	15 (24/163)	16 (26/163)	20 (33/163)	NR	32 (52/163)	4 (7/163)
Zhan-kui, 2016, China, full text	Retrospective, single centre	264	76 (201/264)	58.38 (10.63)	81 (213/264)	4 (11/264)	3 (7/264)	NR	1 (3/264)	61 (160/264)	5 (12/264)
He, 2015, China, full text	Retrospective, single centre	148	82 (122/148)	TEVAR group 43 (5), TEVAR + bare stent group 42 (12)	97 (144/148)	13 (19/148)	NR	NR	10 (14/148)	NR	8 (12/148)
Ruan, 2014, China, full text	Retrospective, single centre	62	71 (44/62)	56 (10.29)	76 (47/62)	29 (18/62)	NR	NR	11 (7/62)	58 (36/62)	13 (8/62)
Zhu, 2017, China, full text	Retrospective, single centre	130	88 (114/130)	53.7 (13.1)	89 (115/130)	NR	NR	NR	NR	55 (72/130)	6 (8/130)
Huang, 2015, China, full text	Retrospective, single centre	81	86 (70/81)	With 51 (9) and without 55(10) type 1a endoleak	74 (60/81)	11 (9/81)	NR	NR	NR	52 (42/81)	5 (4/81)
Shimizu, 2019, Japan, full text	Retrospective, population-based study	636	NR	NR	NR	NR	NR	NR	NR	NR	NR
Lombardi, 2020, USA, full text	Prospective, multicentre	73	66 (48/73)	60.7 (10.9)	86 (63/73)	22 (16/73)	11 (8/73)	NR	21 (15/73)	75 (55/73)	4 (3/73)
Stelzmueller, 2019, Austria, full text	Retrospective, single centre	55	73 (40/55)	Median 52 (IQR 17-86)	78 (43/55)	11 (6/55)	6 (3/55)	NR	6 (3/55)	NR	6 (3/55)
Cambria, 2015, USA, full text	Prospective, multicentre	50	74 (37/50)	57.1 (31-83)	94 (47/50)	30 (15/50)	16 (8/50)	32 (16/50)	20 (10/50)	54 (27/50)	18 (9/50)
Parsa, 2010, USA, full text	Retrospective, single centre	22	NR	NR	NR	NR	NR	NR	NR	NR	NR
Szeto, 2008, USA, full text	Retrospective, single centre	35	63 (22/35)	58.6 (13.4)	89 (31/35)	NR	14 (5/35)	NR	40 (14/35)	NR	NR
Zeeshan, 2010, USA full text	Retrospective, single centre	45	71 (32/45)	59.1 (13.2)	87 (39/45)	20 (9/45)	4 (2/45)	NR	16 (7/45)	47 (21/45)	18 (8/45)
Bavaria, 2015, USA, full text	Prospective, multicentre, Medtronic DISSECTION trial	50	80 (40/50)	57.2 (12.9)	90 (45/50)	6 (3/50)	4 (2/50)	NR	NR	NR	8 (4/50)
Desai, 2015, USA, full text	Retrospective, single centre	114	60 (68/114)	Intervention groups; Early 63.9 (12.8) and delayed 64.3 (14.3)	94 (107/114)	NR	11 (12/114)	NR	NR	47 (53/114)	16 (18/114)
Ullery, 2012, USA, full text	Retrospective, single centre	81	Not reported individually for acute	Not reported individually for acute dissection group	NR	NR	NR	NR	NR	NR	NR

			dissection group								
Lou, 2020, USA, full text	Retrospective, single centre	91	73 (66/91)	52.6 (13.9)	89 (81/91)	NR	8 (7/91)	26 (24/91)	6 (5/91)	34 (31/91)	4 (4/91)
Afifi, 2015, USA, full text	Retrospective, single centre	37	68 (25/37)	61.3 (15.3)	NR	19 (7/37)	11 (4/37)	NR	16 (6/37)	38 (14/37)	38 (14/37)
Pearce, 2008, USA, full text	Retrospective, single centre	15	80 (12/15)	61 (11.5)	NR	NR	NR	NR	NR	NR	NR
Torrent, 2021, USA, full text	Retrospective, population-based study	446	62 (278/446)	60.7 (13.4)	89 (397/446)	2 (9/446)	7 (31/446)	NR	17 (76/446)	36 (159/446)	12 (54/446)
Pruitt, 2020, USA, full text	Retrospective, single centre	154	75 (116/154)	60.5 (13.8)	89 (137/154)	16 (24/154)	5 (7/154)	35 (54/154)	10 (16/154)	40 (62/154)	12 (18/154)
Mastroroberto, 2010, Italy, full text	Retrospective, single centre	13	54 (7/13)	74.3 (8.4)	77 (10/13)	8 (1/13)	8 (1/13)	NR	8 (1/13)	NR	8 (1/13)
Steuer, 2013, Switzerland, full text	Retrospective, dual-centre	102	66 (67/102)	Median 69 (IQR 36-86)	69 (70/102)	27 (27/102)	NR	NR	NR	38 (39/102)	4 (4/102)
Faure, 2018, France, full text	Retrospective, single centre	41	83 (34/41)	Median 61 (IQR 23-87)	66 (27/41)	NR	NR	NR	NR	NR	NR
Sobocinski, 2020, Sweden, full text	Retrospective, dual-centre	41	78 (32/41)	58.8 (12.7)	59 (24/41)	10 (4/41)	5 (2/41)	NR	10 (4/41)	61 (25/41)	5 (2/41)
Ehrlich, 2013, Europe, full text	Prospective, multicentre	29	76 (22/29)	Median 61 (IQR 22-78)	86 (25/29)	28 (8/29)	NR	NR	14 (4/29)	NR	NR
Heijmen, 2012, Europe, full text	Prospective, multicentre Valiant Captivia registry	19	74 (14/19)	58.4 (13.5)	79 (15/19)	21 (4/19)	5 (1/19)	58 (11/19)	5 (1/19)	47 (9/19)	5 (1/19)
Guangqi, 2009, China, full text	Retrospective, single centre	72	90 (65/72)	56.4 (11.3)	99 (71/72)	NR	NR	NR	NR	NR	NR
Jing, 2008, China, full text	Retrospective, single centre	32	88 (28/32)	67.8 (11.2)	75 (24/32)	NR	6 (2/32)	NR	6 (2/32)	59 (19/32)	16 (5/32)
Khoynezhad, 2009, USA, full text	Retrospective, multicentre	28	68 (19/28)	62 (15)	NR	25 (7/28)	11 (3/28)	NR	25 (7/28)	NR	NR
Eggebrecht, 2005, Germany, full text	Retrospective, single centre	15	NR	NR	NR	NR	NR	NR	NR	NR	NR
Kato, 2002, Japan, full text	Retrospective, single centre	14	10	66 (6)	79 (11/14)	7 (1/14)	0	NR	NR	NR	NR
Palma, 2002, Germany, full text	Retrospective, single centre	70	51	57.6 (13.3)	NR	NR	NR	NR	NR	NR	NR
Rodriguez, 2008, USA, full text	Retrospective, single centre	59	NR	NR	NR	NR	NR	NR	NR	NR	NR
Chen, 2006, China, full text	Retrospective, single centre	43	NR	NR	93 (40/43)	NR	NR	NR	NR	NR	12 (5/43)
Chemelli-Steingruber, 2010, Austria, full text	Retrospective, single centre	38	76 (29/38)	Median 64 (IQR 35-89)	87 (33/38)	29 (11/38)	NR	NR	24 (9/38)	5 (2/38)	8 (3/38)
Qin, 2016, China, full text	Retrospective, multicentre	179	NR	NR	NR	NR	NR	NR	NR	NR	NR
Brunkwall, 2014, Europe, full text	Prospective, multicentre, randomised study	30	70 (21/30)	Median 63.6 (IQR 41.8-75.6)	NR	NR	NR	NR	NR	NR	NR
Sze, 2009, USA, full text	Retrospective, single centre	23	NR	NR	NR	NR	NR	NR	NR	NR	NR
Torsello, 2010, Germany, full text	Retrospective, multicentre	32	78 (25/32)	63.3 (11.3)	NR	NR	NR	NR	NR	NR	NR

b. TEVAR characteristics

1st author, Year of publication	Indication for TEVAR	TEVAR device	PLZ No. in zone 2/zone 3-4	Left Subclavian Artery Management		
				Coverage	Bypass/Transposition	Endovascular

Zhang, 2017	Acute complicated type B dissection	NR	NR	NR	NR	NR
Gao, 2019	Acute phase, <14 days	China GRIMED, Medtronic Talent and Valiant, MicroPort Hercules, Cook, Bolton Relay, Jotec E-vita	NR	NR	NR	NR
Zha, 2019	Acute aortic dissection, <14 days	MedtronicCaptivia, Cook Zenith, Lifetech Scientific Ankura	26/37	23	0	3
Zhang, 2018	Type B aortic dissection, acute phase	Lifetech Scientific Ankula, Microport Medical Hercules and Castor branched aortic stent grafts, Medtronic Valiant +/- distal Medtronic Endurant extender aortic cuff	NR	NR	NR	NR
Shu, 2011	Complicated acute type B aortic dissection	Medtronic Talent, Cook Zenith, Bolton Relay, MicroPort Aegis	2/43	2	0	0
Du, 2019	Acute type B aortic dissection	Lifetech Scientific Ankura, Medtronic Talent and Endurant	28/135	28	0	0
Zhan-kui, 2016	Acute type B aortic dissection, <2 weeks	Medtronic Talent and Valiant, Cook Zenith	NR	NR	NR	NR
He, 2015	Complicated acute type B aortic dissection	Cook Zenith TX2, Bolton relay, MicroportHercules, MedtronicTalent +/- distal bare stent (OptiMed Sinus-XL)	78/70	26	19	23
Ruan, 2014	Complicated type B acute aortic dissection	Medtronic Talent, Cook Zenith	NR	NR	NR	NR
Zhu, 2017	Acute type B aortic dissection, <14 days	Medtronic Talent	15/115	1	12	2
Huang, 2015	Acute type B aortic dissection, <14 days	MedtronicTalent, Cook Zeith TX2, MicroportHercules	52/29	33	19	0
Shimizu, 2019	Acute aortic dissection	NR	NR	NR	NR	NR
Lombardi, 2020	Acute complicated type B aortic dissection, <14 days	Zenith Dissection Endovascular System (Zenith TX2 dissection graft with Pro-Form and bare metal stent)	28/45	NR	15	NR
Stelzmueller, 2019	Acute complicated type B aortic dissection, <14 days	Gore TAG, Medtronic Talent and Valiant, Bolton Relay, Cook Zenith TX2	21/34	21	0	0
Cambria, 2015	Acute complicated type B aortic dissection, <14 days	Gore cTAG	27/23	19	9	0
Parsa, 2010	Complicated acute dissection, <14 days	Gore TAG, Cook Zenith TX2	NR	NR	NR	NR
Szeto, 2008	Acute complicated type B dissection, <14 days	Gore TAG, Cook Zenith, Medtronic Talent	25/10	25	0	0
Zeeshan, 2010	Acute dissection, <14 days	Gore TAG, Medtronic Talent, Cook Zenith	NR	NR	1	NR
Bavaria, 2015	Acute complicated type B dissection	Medtronic Valiant Captivia	22/28	18	4	0
Desai, 2015	Acute type B dissection, <14 days	NR	48/66	38	10	0
Ullery, 2012	Acute type B dissection	NR	NR	NR	NR	NR

Lou, 2020	Complicated acute type B aortic dissection	Cook Zenith TX2, Gore TAG	7/84	0	7	0
Afifi, 2015	Acute type B dissection, <14 days	NR	NR	NR	NR	NR
Pearce, 2008	Complicated acute type B aortic dissection, <14 days	Gore TAG	7/8	7	0	0
Torrent, 2021	Uncomplicated acute type b aortic dissection, <14 days	NR	NR	NR	NR	NR
Pruitt, 2020	Acute complicated type B aortic dissection	Gore TAG and cTAG, Cook Zenith TX2 and Alpha, Medtronic Valiant and Navion, Bolton Relay	102/54	NR	38	NR
Mastroroberto, 2010	Acute type b aortic dissection, <14 days	Medtronic Talent	5/8	5	0	0
Steuer, 2013	Acute complicated type B aortic dissection, <14 days	NR	NR	NR	NR	NR
Faure, 2018	Complicated acute type B aortic dissection	TEVAR + STABILISE technique- Gore cTAG, Cook Zenith TX2, Bolton Relay	NR	NR	NR	NR
Sobocinski, 2020	Complicated acute type B aortic dissection, <14 days	NR	NR	NR	6	NR
Ehrlich, 2013	Acute complicated aortic type B dissection	Medtronic Talent	1/28	1	0	0
Heijmen, 2012	Acute type B aortic dissection, <14 days	MedtronicValiant Captivia	14/5	8	6	0
Guangqi, 2009	Acute type B aortic dissection, <14 days	MedtronicTalent, Cook Zenith, Lifetech Scientific Ankura, MicroPort Aegis	25/47	25	0	0
Jing, 2008	Acute aortic dissection, <14 days	MedtronicTalent, Cook Zenith, MicroPort Aegis	2/30	2	0	0
Khoynezhad, 2009	Complicated acute type B aortic dissection, <14 days	Medtronic Talent and Gore TAG	NR	NR	NR	NR
Eggebrecht, 2005	Acute type B aortic dissection, <14 days	MedtronicTalent	NR	NR	NR	NR
Kato, 2002	Acute type B aortic dissection	Custom-made	NR	NR	NR	NR
Palma, 2002	Acute type B aortic dissection, <15 days	Gore Excluder, Medtronic Talent	14/56	14	0	0
Rodriguez, 2008	Acute type B aortic dissection, <14 days	Gore Tag, Medtronic Talent, Endomed Endofit	4/55	NR	NR	NR
Chen, 2006	Acute type B aortic dissection, <14 days	Microport Angiolet, Xianjian Angcover	2/41	2	0	0
Chemelli-Steingruber, 2010	Acute type B aortic dissection	Medtronic Talent, Gore Excluder and TAG	13/25	13	0	0
Qin, 2016	Uncomplicated type B acute aortic dissection	Medtronic Talent, Zenith Cook, Gore TAG, Aegis MicroPort, Ankura Lifetech Scientific	12/167	3	0	9
Brunkwall, 2014	Acute uncomplicated type b dissection, <14 days	Gore TAG	NR	NR	NR	NR
Sze, 2009	Acute complicated type	Gore TAG	13/10	NR	NR	NR

	b dissection, <14 days					
Torsello, 2010	Acute type b aortic dissection	Valiant Medtronic	14/18	NR	NR	NR

c. Stroke characteristics and mortality

1st author, Year of publication	Stroke diagnosis/definition	Stroke % (No.)	Stroke character (embolic/haemorrhagic)	Risk factors for stroke identified by study
Zhang, 2017	NR	1.7 (1/60)	NR	NR
Gao, 2019	NR	0	NA	NA
Zha, 2019	NR	4.8 (3/63)	NR	NR
Zhang, 2018	NR	0	NA	NA
Shu, 2011	NR	0	NA	NA
Du, 2019	NR	0.6 (1/163)	Acute cerebral infarction	Partial left subclavian artery coverage in patient with ischaemic stroke
Zhan-kui, 2016	NR	0.38 (1/264)	NR	NR
He, 2015	NR	0	NA	NA
Ruan, 2014	NR	3.2 (2/62)	NR	NR
Zhu, 2017	NR	3.1 (4/130)	NR	NR
Huang, 2015	NR	0	NA	NA
Shimizu, 2019	NR	4.1 (26/636)	NR	NR
Lombardi, 2020	NR	6.9 (5/73)	NR	NR
Stelzmueller, 2019	NR	3.6 (2/55)	NR	NR
Cambria, 2015	NR	18 (9/50)	NR	NR
Parsa, 2010	NR	0	NA	NA
Szeto, 2008	Clinical examination and CT head	2/9 (1/35)	Basal ganglia infarct	NR
Zeeshan, 2010	NR	6.7 (3/45)	NR	NR
Bavaria, 2015	NR	8 (4/50)	NR	NR
Desai, 2015	NR	5.3 (6/114)	NR	NR
Ullery, 2012	Any new focal or global neurologic deficit lasting >24 hours with associated computed tomography or magnetic resonance imaging evidence of acute intracranial abnormality	4.9 (4/81)	Embolic	Analysis of mixed pathology group; Independent risk factors for any perioperative stroke were chronic renal insufficiency and history of prior stroke. Age and zone 2 coverage were additional risk factors for posterior circulation stroke.
Lou, 2020	NR	5.5 (5/91)	NR	NR
Afifi, 2015	NR	8.1 (3/37)	NR	NR
Pearce, 2008	Clinical assessment and MRI	5.3 (1/15)	Watershed cerebral infarct	NR
Torrent, 2021	NR	3.6 (16/446)	NR	NR
Pruitt, 2020	NR	13.6 (21/154)	NR	NR
Mastroroberto, 2010	NR	0	NA	NA
Steuer, 2013	NR	5.9 (6/102)	NR	NR
Faure, 2018	NR	0	NA	NA
Sobocinski, 2020	NR	2.4 (1/41)	NR	NR
Ehrlich, 2013	NR	10.3 (3/29)	NR	NR
Heijmen, 2012	NR	0	NA	NA
Guangqi, 2009	NR	4.2 (3/72)	Embolic	NR
Jing, 2008	NR	0	NA	NA
Khoynezhad, 2009	NR	3.6 (1/28)	NR	NR
Eggebrecht, 2005	NR	0	NA	NA
Kato, 2002	NR	0	NA	NA
Palma, 2002	NR	2.9 (2/70)	Embolic	NR
Rodriguez, 2008	NR	5.1 (3/59)	NR	NR
Chen, 2006	NR	4.7 (2/43)	NR	NR
Chemelli-Steingruber, 2010	NR	2.6 (1/38)	Embolic	NR
Qin, 2016	NR	0	NA	NA
Brunkwall, 2014	NR	0	NA	NA
Sze, 2009	NR	8.7 (2/23)	Embolic	Coverage of left subclavian artery
Torsello, 2010	NR	0	NA	NA

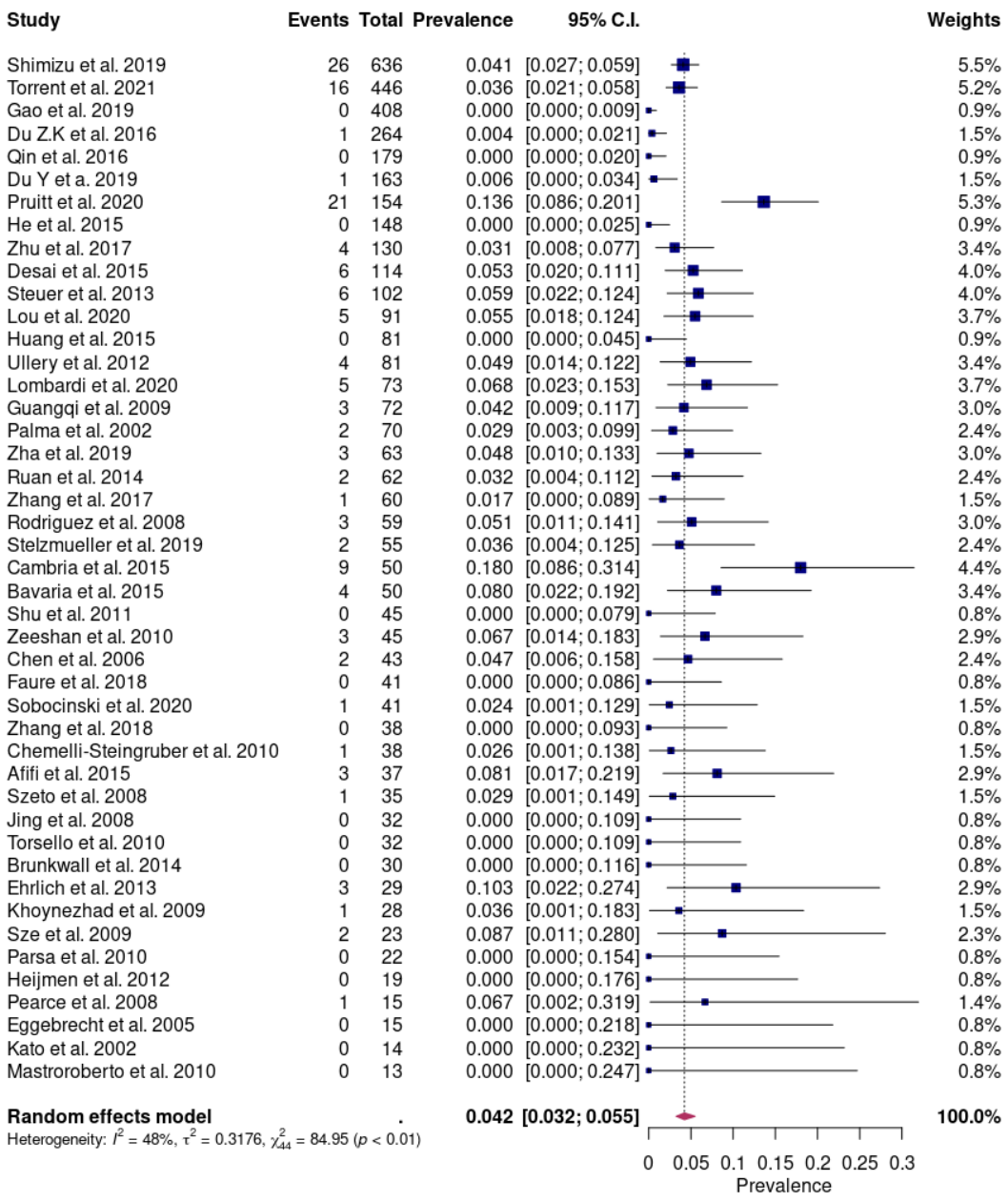


Figure 2.5 Forrest plot for pooled incidence of stroke following TEVAR for acute type B dissection

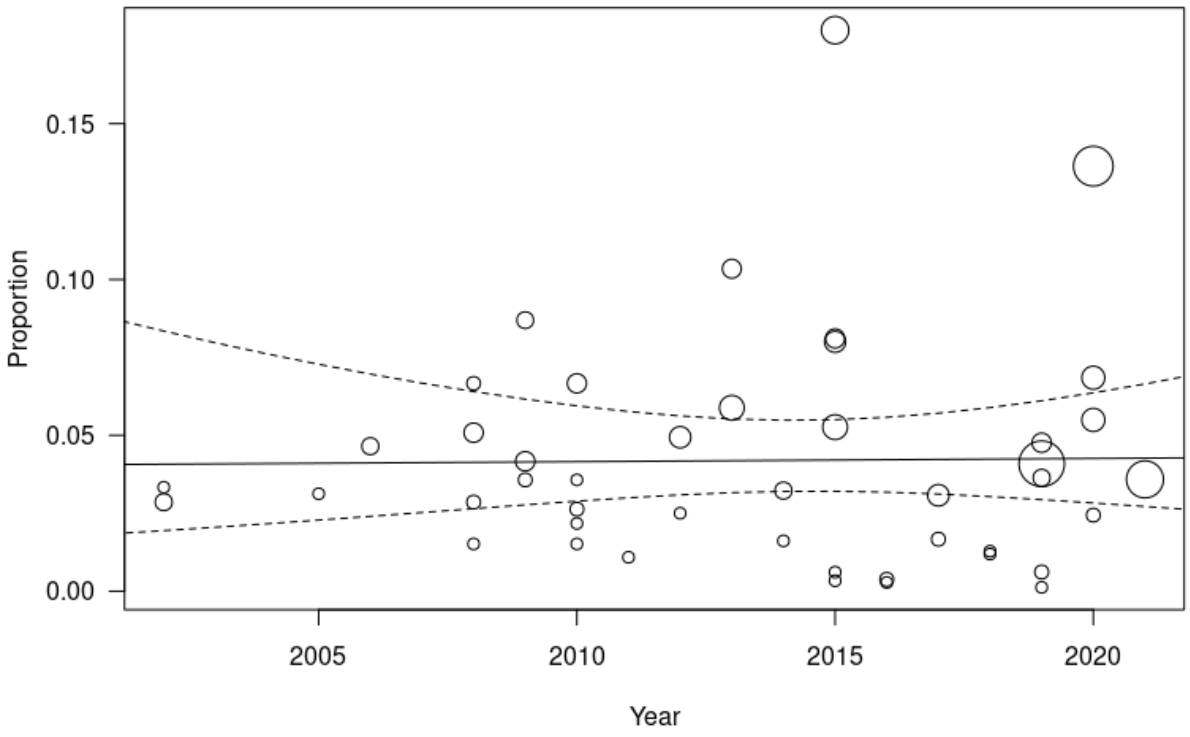


Figure 2.6 Meta-regression (scatter plot) of the relationship between year of publication and stroke as weighted proportion following TEVAR for acute type b dissection (β_i=-0.003, SE, 0.029, p=0.93). Each circle represents a study telescoped by its weight in the analysis.

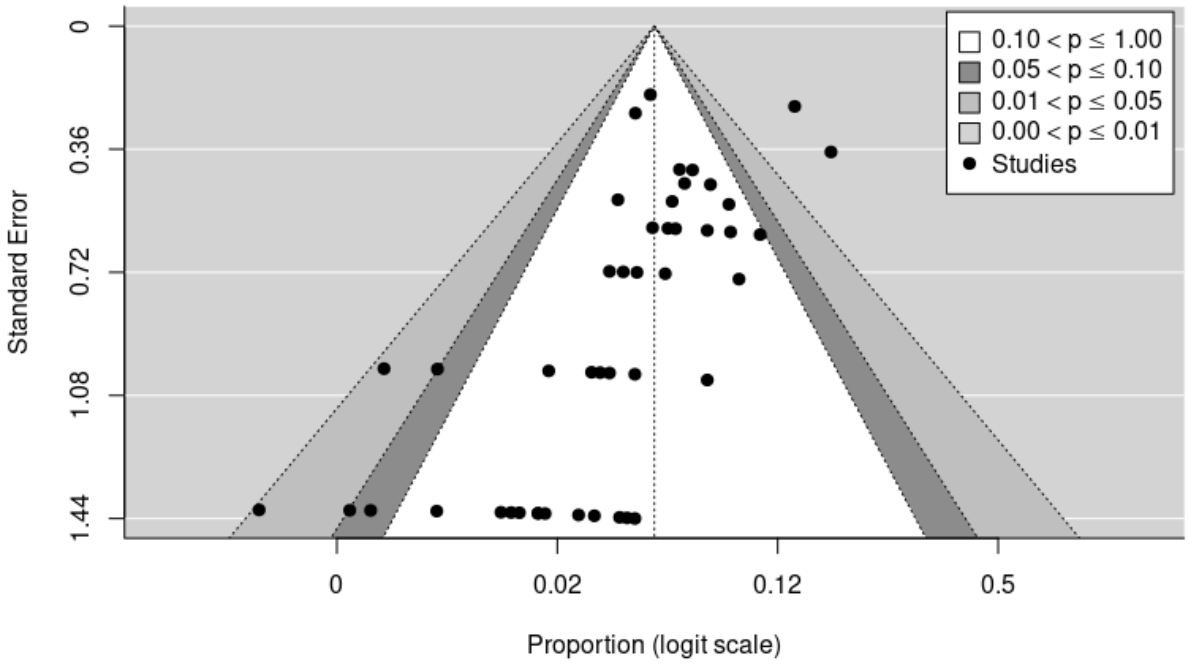


Figure 2.7 Funnel Plot for acute type B dissection (t= -4.09, df=43, p=0.0002)

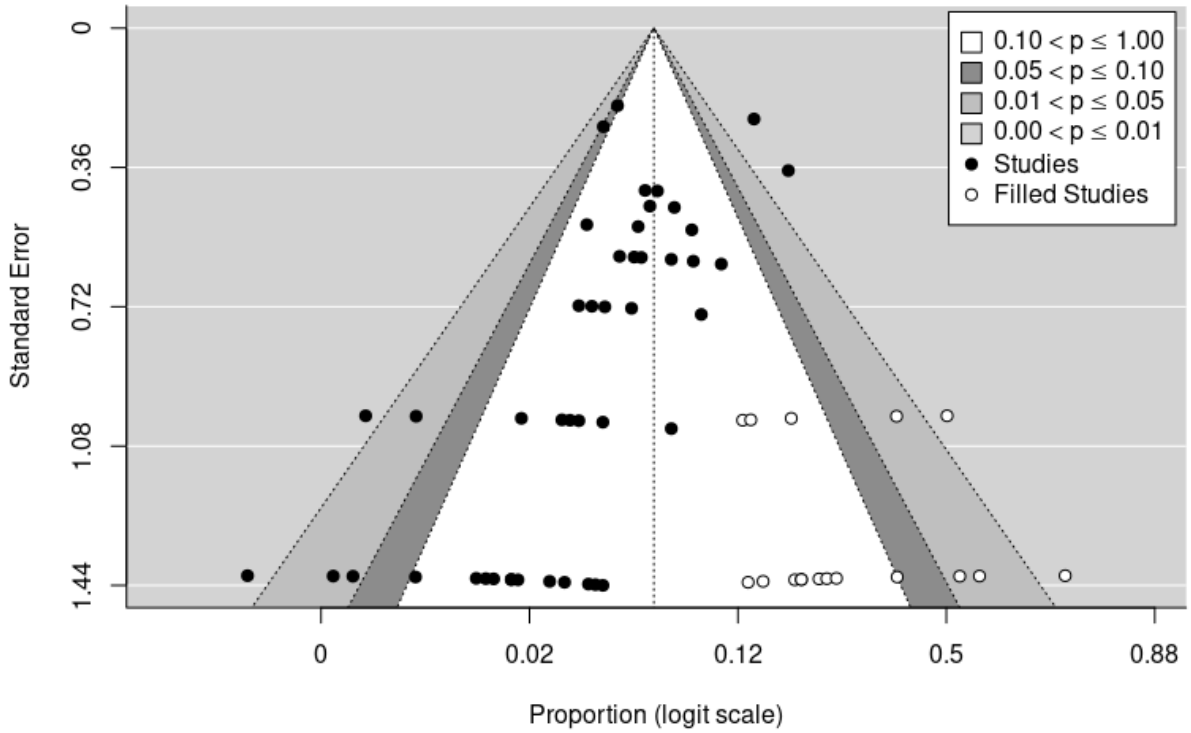


Figure 2.8 Trim and fill plots for acute type B dissection

Study	**Prevalence [95% CI]**	**W**
Shimizu et al. 2019	0.041 [0.028,0.059]	3.90%
Torrent et al. 2021	0.036 [0.022,0.058]	3.73%
Gao et al. 2019	0.001 [0.000,0.019]	0.83%
Du Z.K et al. 2016	0.004 [0.001,0.026]	1.39%
Qin et al. 2016	0.003 [0.000,0.043]	0.83%

Du Y et a. 2019	0.006 [0.001,0.042]	1.39%
Pruitt et al. 2020	0.136 [0.091,0.200]	3.80%
He et al. 2015	0.003 [0.000,0.051]	0.83%
Zhu et al. 2017	0.031 [0.012,0.079]	2.77%
Desai et al. 2015	0.053 [0.024,0.112]	3.11%
Steuer et al. 2013	0.059 [0.027,0.125]	3.10%
Lou et al. 2020	0.055 [0.023,0.125]	2.95%
Huang et al. 2015	0.006 [0.000,0.090]	0.83%
Ullery et al. 2012	0.049 [0.019,0.124]	2.75%
Lombardi et al. 2020	0.068 [0.029,0.154]	2.94%
Guangqi et al. 2009	0.042 [0.014,0.121]	2.47%
Palma et al. 2002	0.029 [0.007,0.107]	2.06%
Zha et al. 2019	0.048 [0.015,0.138]	2.47%
Ruan et al. 2014	0.032 [0.008,0.120]	2.06%
Zhang et al. 2017	0.017 [0.002,0.109]	1.38%
Rodriguez et al. 2008	0.051 [0.016,0.146]	2.46%
Stelzmueller et al. 2019	0.036 [0.009,0.134]	2.05%
Cambria et al. 2015	0.18 [0.096,0.311]	3.31%
Bavaria et al. 2015	0.08 [0.030,0.195]	2.72%

Shu et al. 2011	0.011 [0.001,0.151]	0.83%
Zeeshan et al. 2010	0.067 [0.022,0.187]	2.45%
Chen et al. 2006	0.047 [0.012,0.168]	2.04%
Faure et al. 2018	0.012 [0.001,0.164]	0.83%
Sobocinski et al. 2020	0.024 [0.003,0.154]	1.37%
Zhang et al. 2018	0.013 [0.001,0.175]	0.82%
Chemelli-Steingruber et al. 2010	0.026 [0.004,0.165]	1.37%
Afifi et al. 2015	0.081 [0.026,0.223]	2.43%
Szeto et al. 2008	0.029 [0.004,0.177]	1.36%
Jing et al. 2008	0.015 [0.001,0.201]	0.82%
Torsello et al. 2010	0.015 [0.001,0.201]	0.82%
Brunkwall et al. 2014	0.016 [0.001,0.211]	0.82%
Ehrlich et al. 2013	0.103 [0.034,0.276]	2.40%
Khoynezhad et al. 2009	0.036 [0.005,0.214]	1.36%
Sze et al. 2009	0.087 [0.022,0.289]	2.00%
Parsa et al. 2010	0.022 [0.001,0.268]	0.82%
Heijmen et al. 2012	0.025 [0.002,0.298]	0.82%
Pearce et al. 2008	0.067 [0.009,0.352]	1.33%
Eggebrecht et al. 2005	0.031 [0.002,0.350]	0.81%

Kato et al. 2002	0.033 [0.002,0.366]	0.81%
Mastroroberto et al. 2010	0.036 [0.002,0.384]	0.81%
Filled: Chemelli-Steingruber et al. 2010	0.124 [0.019,0.508]	1.37%
Filled: Heijmen et al. 2012	0.13 [0.009,0.712]	0.82%
Filled: Sobocinski et al. 2020	0.133 [0.021,0.527]	1.37%
Filled: Parsa et al. 2010	0.147 [0.010,0.740]	0.82%
Filled: Zhang et al. 2017	0.184 [0.030,0.620]	1.38%
Filled: Brunkwall et al. 2014	0.189 [0.014,0.792]	0.82%
Filled: Jing et al. 2008	0.199 [0.015,0.802]	0.82%
Filled: Torsello et al. 2010	0.199 [0.015,0.802]	0.82%
Filled: Zhang et al. 2018	0.228 [0.018,0.828]	0.82%
Filled: Faure et al. 2018	0.241 [0.019,0.838]	0.83%
Filled: Shu et al. 2011	0.258 [0.021,0.850]	0.83%
Filled: Du Y et a. 2019	0.383 [0.080,0.816]	1.39%
Filled: Huang et al. 2015	0.384 [0.037,0.910]	0.83%
Filled: Du Z.K et al. 2016	0.502 [0.124,0.878]	1.39%
Filled: He et al. 2015	0.532 [0.066,0.948]	0.83%
Filled: Qin et al. 2016	0.579 [0.079,0.957]	0.83%
Filled: Gao et al. 2019	0.758 [0.163,0.980]	0.83%

Number of studies combined: k = 62 with 17 added studies)

Random-Effects model: 0.057 [0.044, 0.074], z= -19.49, p<0.001

Quantifying heterogeneity:

tau^2 (estimated amount of total heterogeneity): 0.4912 (SE = 0.2238)

tau (square root of estimated tau^2 value): 0.7009

I^2 (total heterogeneity / total variability): 53.08%

H^2 (total variability / sampling variability): 2.13

Test for Heterogeneity:

Q(df = 61) = 130.0218, p-val < .0001

Table 2.5 Risk of bias assessment of studies reporting stroke following TEVAR for acute dissection

Modified Newcastle-Ottawa quality assessment score. Key: *=1, -=0, NR=not reported, NA=not applicable

1st author, Year of publication, publication type, Country	Selection				Comparability	Outcome			Total score
	Representativeness	Selection of non-exposed cohort (Non-TEVAR control group)	Ascertainment	Stated no stroke at start of study		Method of assessment of stroke	Follow up to minimum 90 days	Adequacy of follow up	
Zhang, 2017	*	-	NR	NR	*	NR	*	*	4
Gao, 2019	-	-	NR	NR	*	NA	*	*	3
Zha, 2019	*	-	*	NR	*	NA	*	*	5
Zhang, 2018	-	-	NR	NR	*	NA	*	*	3
Shu, 2011	*	-	NR	NR	-	NA	*	*	3
Du, 2019	*	-	*	NR	-	NR	*	*	4
Zhan-kui, 2016	*	-	NR	NR	-	NR	*	*	3
He, 2015	*	-	NR	NR	*	NA	*	*	4
Ruan, 2014	-	-	*	NR	-	NR	*	*	3
Zhu, 2017	-	-	-	NR	-	NR	*	*	2
Huang, 2015	-	-	NR	NR	*	NR	*	*	3
Shimizu, 2019	-	*	*	NR	*	NR	NR	NR	3
Lombardi, 2020	-	-	*	NR	-	NR	*	*	3
Stelzmueller, 2019	-	-	NR	NR	*	NR	*	*	3
Cambria, 2015	-	-	NR	NR	-	*	*	*	3
Parsa, 2010	-	-	NR	NR	*	NR	*	*	3
Szeto, 2008	-	-	NR	NR	-	*	*	*	3
Zeeshan, 2010	-	*	*	NR	*	NR	*	*	5
Bavaria, 2015	-	-	*	NR	-	NR	*	*	3
Desai, 2015	-	-	*	NR	*	NR	NR	NR	2
Ullery, 2012	*	-	*	NR	*	*	*	*	6
Lou, 2020	*	-	*	NR	*	NR	*	*	5
Afifi, 2015	-	*	NR	*	*	NR	*	*	5
Pearce, 2008	*	-	*	NR	-	*	*	*	5
Torrent, 2021	-	-	*	NR	*	NR	NR	NR	2
Pruitt, 2020	*	-	*	NR	-	NR	*	*	4
Mastroroberto, 2010	*	*	NR	NR	*	NR	NR	NR	3
Steuer, 2013	*	-	NR	NR	*	NR	NR	*	3
Faure, 2018	-	-	*	NR	-	NR	*	*	3
Sobocinski, 2020	*	-	NR	NR	*	NR	NR	NR	2
Ehrlich, 2013	*	-	*	NR	-	NR	*	*	4
Heijmen, 2012	-	-	*	NR	*	NR	-	NR	2
Guangqi, 2009	*	-	NR	NR	*	NR	*	*	4
Jing, 2008	-	-	NR	NR	*	NR	*	*	3
Khoynezhad, 2009	*	-	*	NR	-	NR	*	*	4
Eggebrecht, 2005	-	-	NR	NR	*	NR	*	*	3
Kato, 2002	*	-	NR	NR	*	NR	*	NR	3
Palma, 2002	*	-	NR	NR	-	NR	*	*	3
Rodriguez, 2008	NR	-	NR	NR	*	NR	*	*	3
Chen, 2006	*	-	NR	NR	*	NR	*	*	4
Chemelli-Steingruber, 2010	-	*	-	NR	*	NR	*	*	4
Qin, 2016	-	*	-	NR	*	NR	*	*	4
Brunkwall, 2014	-	*	*	NR	*	NR	*	*	5
Sze, 2009	NR	-	NR	NR	*	NR	*	*	3
Torsello, 2010	-	-	*	NR	-	NR	*	*	3

Table 2.6 Justifications for risk of bias assessment for studies reporting stroke following TEVAR for acute dissection

Modified Newcastle-Ottawa quality assessment, criteria for grading + 1 where applicable

1st author, Year of publication, publication type, Country	Selection				Comparability	Outcome			Total score
	Representativeness	Selection of non-exposed cohort (Non-TEVAR control group)	Ascertainment	Stated no stroke at start of study		Method of assessment of stroke	Follow up to minimum 90 days	Adequacy of follow up	
Zhang, 2017	Consecutive				Acute vs chronic dissection groups		Mean 24 months	Aortic CT	4
Gao, 2019					Acute vs chronic dissection groups		Median 70 months	Aortic CT	3
Zha, 2019	Consecutive		Registry data		Acute vs chronic dissection groups		Median 34 months	Aortic CT	5
Zhang, 2018					TEVAR vs TEVAR + distal aortic extender cuff, acute vs subacute vs chronic phase		Median 15 months	Aortic CT	3
Shu, 2011	Consecutive						Mean 13 months	Clinical review and aortic CT	3
Du, 2019	Consecutive		Hospital records				Median 48 months	Clinical examination and aortic CT	4
Zhan-kui, 2016	Consecutive						Mean 34 months	Clinical visit	3
He, 2015	Consecutive				TEVAR +/- distal bare stent		Mean 10 months	Clinical examination and aortic CT	4
Ruan, 2014			Hospital records				Median 52 months	Physical examination and contrast CT	3
Zhu, 2017							Median 29 months	Aortic CT	2
Huang, 2015					Comparison of patients with and without immediate type 1a endoleaks		Average 12 months	Aortic CT	3
Shimizu, 2019		Open and hybrid repair comparative group	Japan Cardiovas-cular Surgery Database		Open and hybrid repair group and different pathologies				3
Lombardi, 2020			ClinicalTrials.gov results database				>1 year	Clinical + Aortic CT	3
Stelzmueller, 2019					Comparison of acute complications; malperfusion/rupture vs persistent pain		Median 6 months	Aortic imaging	3
Cambria, 2015						Clinical assessment by Clinical Events Committee which included 2 neurologists	Mean 647 days	Physical examination and CT angiography	3
Parsa, 2010					Acute vs chronic type B dissection		Median 7.1 months	Clinical examination and aortic CT	3

Szeto, 2008						Clinical examination and CT head	Range 3-47 months	Clinical review and aortic imaging	3
Zeeshan, 2010		Open surgery cohort	University of Pennsylvania aortic database		TEVAR vs open surgery vs medical therapy		Mean 37 months	Aortic CT	5
Bavaria, 2015			ClinicalTrials.gov results database				12 months	Physical examination and aortic CT	3
Desai, 2015			Prospectively collected clinical perioperative registry		Acute early vs delayed vs subacute TEVAR timing				2
Ullery, 2012	Consecutive cases inferred		Retrospective review of prospectively collected database		Assessed risk factors for anterior vs posterior stroke	Imaging (CT/MRI) and clinical evaluation by stroke neurologist	Mean 49 months (SD 26.6)	Clinical	6
Lou, 2020	Consecutive		Emory aortic database		Standard vs extended aortic endograft coverage		Median 3.1 years	Aortic imaging +/- clinical	5
Afifi, 2015		Open surgical group		Postoperative outcomes were defined as deficits not present before the intervention	Uncomplicated vs complicated acute type B dissection, and medical, open surgery and TEVAR management		Median 4.6 years	Clinical	5
Pearce, 2008	All patients		Prospectively maintained vascular registry			Clinical assessment and MRI	Mean 5.8 months	Clinical and radiographic	5
Torrent, 2021			Vascular Quality Initiative (VQI) TEVAR registry		Acute vs subacute groups				2
Pruitt, 2020	Consecutive		Medical records				Mean 16 months	Aortic CT	4
Mastroroberto, 2010	Consecutive	Open surgery group			Medical therapy vs open surgery vs TEVAR				3
Steuer, 2013	Consecutive				Acute vs subacute groups			Aortic CT	3
Faure, 2018			Prospectively maintained database of acute dissections				Median 12 months	Aortic CT	3
Sobocinski, 2020	Consecutive				TEVAR vs STABLE cohort (composite device design)				2
Ehrlich, 2013	Consecutive		Sub-set of Talent Thoracic Registry				Mean 53 months	Aortic CT	4
Heijmen, 2012			ClinicalTrials.gov results database		Comparison of aneurysm vs acute vs chronic dissection				2
Guangqi, 2009	Consecutive				Acute vs chronic groups		2 years	Aortic CT	4
Jing, 2008					Acute vs chronic groups		Mean 17 months	Blood pressure monitoring and aortic imaging	3
Khoynezhad, 2009	Consecutive		Electronic database				Mean 36 months	Physical examination + aortic CT	4
Eggebrecht, 2005					Acute vs chronic groups		>1 year	Clinical examination and aortic CT	3
Kato, 2002	Consecutive cases inferred				Acute type A vs acute type B acute vs chronic type B groups		Range 6-53 months		3
Palma, 2002	Consecutive cases inferred						Mean 14 months	Aortic imaging	3
Rodriguez, 2008					Acute vs chronic groups		Mean 15 months	Aortic CT	3
Chen, 2006	Consecutive				Acute (early vs late) vs chronic groups		Mean 27 months	Clinical and aortic CT	4
Chemelli-Steingruber, 2010		TEVAR vs Medical therapy			TEVAR vs Medical therapy		Mean 33 months	Clinical examination and aortic CT	4

Qin, 2016	TEVAR vs best medical therapy		TEVAR vs best medical therapy	Mean 30 months	Aortic CT	4
Brunkwall, 2014	Best medical therapy vs TEVAR + best medical therapy	ClinicalTrials.gov results database	Best medical therapy vs TEVAR + best medical therapy	1 year	Aortic CT	5
Sze, 2009			Acute vs subacute vs chronic groups	Mean 22 months	Clinical evaluation and aortic CT	3
Torsello, 2010		TRAVIATA (Thoracic Repair Analysis using Valiant in Indications of the Thoracic Aorta) registry		Mean 22 months	Clinical evaluation and aortic CT	3

2.3.3 Chronic type B dissection

34 studies including 3626 patients undergoing TEVAR for chronic type B dissection were included in the meta-analysis. There was only 1 randomised control (INSTEAD),[253] 1 multi-centre industry sponsored trial,[183] 4 multi-centre study,[217,218,254,255] and 2 population-based study.[195,216] There were a total of 26 single-centre studies.[222,224,233,236,243-246,248,249,251,256-270] No study reported a stroke definition. Only one study reported the stroke aetiology, which was embolic.[243] The study/patient characteristics, TEVAR characteristics, and stroke and mortality outcomes are summarised in Table 2.8(a-c). The pooled stroke rate was 1.8% (95% CI, 1.4% to 2.4%, I^2 =0%, p=0.98) (Figure 2.9). Meta-regression showed no change in the stroke rate over time using year of publication as the co-variate (β_i =-0.029, SE 0.028, p=0.31) (Figure 2.10). There was no publication bias (t = 1.25, df = 32, p = 0.22) (Figure 2.11). Risk of bias and justifications for risk of bias assessments are sumamrised in Tables 2.8, and 2.9, respectively.

Table 2.7 Study/patient characteristics, TEVAR characteristics, and stroke and mortality outcomes for chronic type B dissection

a. Study/patient characteristics

1st author, Year of publication, Publication type, Country	Study design	Total No. patients	Male % (No.)	Age Mean (SD)	Co-morbidities % (No.)						
					Hypertension	CVA/TIA	IHD	Hypercholestrolaemia	COPD	Smoking	DM
Kazimierczak, 2019, full text, Poland	Retrospective, single centre	20	70 (14/20)	59.7 (11.57)	NR	NR	NR	NR	NR	NR	NR
Nozdrzykowski, 2013, full text, Germany	Retrospective, single centre	32	72 (23/32)	Median 62, IQR 54-67.5	100 (32/32)	NR	6 (2/32)	NR	22 (7/32)	NR	28 (9/32)
Lee, 2013, full text, Korea	Retrospective, single centre	71	70 (50/71)	54.7 (12)	82 (58/71)	3 (2/71)	3 (2/71)	NR	NR	39 (28/71)	6 (4/71)
Lee, 2020, full text, Korea	Retrospective, multicentre	52	65 (34/52)	Early chronic 56.6 (11.2), late chronic 61.9 (9.2)	79 (41/52)	19 (10/52)	6 (3/52)	NR	NR	29 (15/52)	23 (12/52)
Zhang, 2017, full text, China	Retrospective, single centre	25	64 (16/25)	65.5 (10)	88 (22/25)	4 (1/25)	4 (1/25)	8 (2/25)	0	40 (10/25)	16 (4/25)
Zha, 2019, full text, China	Retrospective, single centre	23	78 (18/23)	55.92 (12.06)	87 (20/23)	4 (1/23)	0	NR	9 (2/23)	70 (16/23)	17 (4/23)
Zhang, 2018, full text, China	Retrospective, multicentre	119	NR individually for chronic group	NR individually for chronic group	NR	NR	NR	NR	NR	NR	NR
Gao, 2019, China, full text	Retrospective, single centre	343	NR individually for chronic group	NR individually for chronic group	NR	NR	NR	NR	NR	NR	NR
Xu, 2010, China, full text	Retrospective, single centre	84	82 (69/84)	53.3 (11.6)	80 (67/84)	NR	NR	NR	NR	31 (26/84)	11 (9/84)
Shimizu, 2019, Japan, full text	Retrospective, population-based study	1180	NR	NR	NR	NR	NR	NR	NR	NR	NR
Kitamura, 2014, Japan, full text	Retrospective, single centre	45	94 (50/53)	55.5 (13.1)	NR	NR	NR	NR	NR	NR	NR
Mizoguchi, 2017, Japan, full text	Retrospective, single centre	16	88 (14/16)	65 (12)	100 (16/16)	13 (2/16)	19 (3/16)	69 (11/16)	13 (2/16)	100 (16/16)	NR
Parsa, 2010, USA, full text	Retrospective, single centre	33	NR	NR	NR	NR	NR	NR	NR	NR	NR
Andersen, 2014, USA, full text	Retrospective, single centre	44	64 (28/44)	Median 56 (IQR 47-65)	98 (43/44)	11 (5/44)	0	48 (21/44)	16 (7/44)	59 (26/44)	11 (5/44)
Desai, 2015, USA, full text	Retrospective, single centre	18	67 (12/18)	64.1 (14.8)	100 (18/18)	NR	17 (3/18)	NR	NR	67 (12/18)	11 (2/18)
Dohle, 2020, USA, full text	Retrospective, single centre	17	65 (11/17)	61.9 (11.8)	100 (17/17)	41 (7/17)	NR	59 (10/17)	41 (7/17)	35 (6/17)	24 (4/17)
Andacheh, 2012, USA, full text	Retrospective, single centre	73	71 (52/73)	58	NR	NR	NR	NR	NR	NR	NR
Lou, 2018, USA, full text	Retrospective, single centre	87	68 (59/87)	59.5 (11.8)	92 (80/87)	NR	9 (8/87)	NR	13 (11/87)	22 (19/87)	15 (13/87)
Kang, 2011, USA, full text	Retrospective, single centre	76	65 (49/76)	61.5 (12.5)	99 (75/76)	38 (29/76)	12 (9/76)	34 (26/76)	22 (17/76)	42 (32/76)	11 (8/76)
Torrent, 2021, USA, full text	Retrospective, population-based study	242	66 (160/242)	59.9 (12.1)	96 (232/242)	12 (30/242)	8 (19/242)	NR	15 (36/242)	29 (70/242)	13 (32/242)
Heijmen, 2012, Europe, full text	Prospective, multicentre Valiant Captivia registry	23	61 (14/23)	61.6 (9.6)	100 (23/23)	26 (6/23)	0	44 (10/23)	4 (1/23)	52 (12/23)	4 (1/23)
Nienaber, 2009, Europe, full text	Prospective, multicentre RCT	72	86 (62/72)	60 (10.7)	10 (7/72)	NR	NR	NR	13 (9/72)	24 (17/72)	7 (5/72)
Massara, 2020, Italy, full text	Retrospective, single centre	13	NR	NR	NR	NR	NR	NR	NR	NR	NR
Steuer, 2013, Switzerland, full text	Retrospective, dual-centre	22	64 (14/22)	Median 58 (IQR 34-81)	82 (18/22)	18 (4/22)	NR	NR	NR	59 (13/22)	5 (1/22)

Guangqi, 2009, China, full text	Retrospective, single centre	49	94 (46/49)	57.1 (10)	96 (47/49)	NR	NR	NR	NR	NR	NR
Jing, 2008, China, full text	Retrospective, single centre	35	86 (30/35)	69 (12.7)	80 (28/35)	NR	3 (1/35)	NR	11 (4/35)	66 (23/35)	26 (9/35)
Eggebrecht, 2005, Germany, full text	Retrospective, single centre	28	NR	NR	NR	NR	NR	NR	NR	NR	NR
Kato, 2002, Japan, full text	Retrospective, single centre	14	86 (12/14)	61 (14)	64 (9/14)	7 (1/14)	0	NR	NR	NR	NR
Palma, 2002, Germany, full text	Retrospective, single centre	13	85 (11/13)	Median 60.6 (IQR 39-79)	NR	NR	NR	NR	NR	NR	NR
Rodriguez, 2008, USA, full text	Retrospective, single centre	47	NR	NR	NR	NR	NR	NR	NR	NR	NR
Chen, 2006, China, full text	Retrospective, single centre	19	95 (18/19)	60.1 (7.2)	84 (16/19)	NR	NR	NR	NR	NR	11 (2/19)
Sze, 2009, USA, full text	Retrospective, single centre	14	NR	NR	NR	NR	NR	NR	NR	NR	NR
Manning, 2009, Sweden, full text	Retrospective, single centre	10	80 (8/10)	Median 63 (IQR 45-79)	NR	NR	NR	NR	NR	NR	NR
Nienaber, 1999, Germany, full text	Retrospective, multicentre	12	75 (9/12)	62 (11)	92 (11/12)	NR	NR	NR	33 (4/12)	NR	NR

b. TEVAR characteristics

1st author, Year of publication	Indication for TEVAR + time since initial event	TEVAR device	PLZ No. in zone 2/zone 3-4	Left Subclavian Artery Management		
				Coverage	Bypass/Transposition	Endovascular
Kazimierczak, 2019	Chronic type B aortic dissection with aneurysmal degeneration, >90 days	Petticoat strategy (Medtronic Talent stent graft in the thoracic, plus additional distal bare stent into the abdominal and infrarenal aorta, followed by parallel stent grafts into common iliac arteries	0/20	0	0	0
Nozdrzykowski, 2013	Chronic type B aortic dissection, >14 days	NR	NR	NR	NR	NR
Lee, 2013	Complicated chronic type B aortic dissection, >14 days	S&G Biotech SEAL, Taewoong Medical Taewoong, Medtronic Valiant, Cook Zenith TX2	2/69	0	2	0
Lee, 2020	Type B aortic dissection, >14 days (acute <6 weeks excluded, early chronic 6 weeks to 1 years), late chronic (>1 year)	S&G Biotech SEAL, Medtronic Valiant, Cook Zenith TX2	29/23	NR	NR	NR
Zhang, 2017	Complicated type B aortic dissection, >14 days	NR	NR	NR	NR	NR
Zha, 2019	Type B aortic dissection, >14 days	MedtronicCaptivia, Cook Zenith, Lifetech Scientific Ankura	13/10	13	0	0
Zhang, 2018	Type B aortic dissection, >14 days	Lifetech Scientific Ankula, Microport Medical Hercules and Castor branched aortic stent grafts, Medtronic Valiant +/- distal Medtronic Endurant extender aortic cuff	NR	NR	NR	NR
Gao, 2019	Type B aortic dissection, >14 days	China GRIMED, Medtronic Talent and Valiant, MicroPort Hercules, Cook, Bolton Relay, Jotec E-vita	NR	NR	NR	NR
Xu, 2010	Chronic type B aortic dissection, >14 days	Medtronic Talent, LeMaitre EndoFit, MicroPort	4/80	4	0	0

		Hercules, Vascore Vasoflow, Grikin Advanced Materials Co. China Grikin				
Shimizu, 2019	Chronic aortic dissection	NR	NR	NR	NR	NR
Kitamura, 2014	Non-acute type B aortic dissection, >14 days	Handmade or Matsui-Kitamura (M-K, Japan) stent grafts	NR	NR	NR	NR
Mizoguchi, 2017	Early chronic type B aortic dissection, >14 days to 4 months	Gore TAG and cTAG, Cook Zenith TX2 and TXD	4/12	NR	NR	NR
Parsa, 2010	Chronic type B aortic dissection, >14 days	Gore TAG, Cook Zenith TX2	NR	NR	NR	NR
Andersen, 2014	Chronic type B aortic dissection, >14 days	NR	33/11	NR	NR	NR
Desai, 2015	Subacute type B dissection, 14 days-6 weeks	NR	9/9	4	5	0
Dohle, 2020	Chronic aortic dissection, >90 days	NR	2/15	0	2	0
Andacheh, 2012	Complicated chronic aortic dissection	Medtronic Talent and Valiant Captivia	NR	NR	NR	NR
Lou, 2018	Type B aortic dissection chronic phase	NR	NR	NR	NR	NR
Kang, 2011	Complicated chronic distal aortic dissection, >14 days	Cook TX1 and TX2, Gore TAG, Medtronic Talent, homemade devices	29/47	21	8	0
Torrent, 2021	Uncomplicated acute type b aortic dissection, 15-90 days	NR	NR	NR	NR	NR
Heijmen, 2012	Chronic type B aortic dissection, >14 days	MedtronicValiant Captivia	12/11	3	9	0
Nienaber, 2009	Uncomplicated type B dissection, 2-52 weeks	Medtronic Talent	17/55	15	2	0
Massara, 2020	Chronic type B aortic dissection	MedtronicValiant, Gore Thoracic Excluder, Bolton Relay	10/3	7	3	0
Steuer, 2013	Sub-acute, >14 days	NR	NR	NR	NR	NR
Guangqi, 2009	Chronic type B aortic dissection, >14 days	MedtronicTalent, Cook Zenith, Lifetech Scientific Ankura, MicroPort Aegis	12/37	11	1	0
Jing, 2008	Chronic type B aortic dissection, >14 days	MedtronicTalent, Cook Zenith, MicroPort Aegis	2/33	2	0	0
Eggebrecht, 2005	Chronic type B aortic dissection, >14 days	MedtronicTalent	NR	NR	NR	NR
Kato, 2002	Chronic type B aortic dissection, >1 month	Custom-made	NR	NR	NR	NR
Palma, 2002	Chronic type B dissection	Gore Excluder, Medtronic Talent	10/3	10	0	0
Rodriguez, 2008	Chronic dissection, >14 days	Gore Tag, Medtronic Talent, Endomed Endofit	8/39	NR	NR	NR
Chen, 2006	Type B aortic dissection chronic phase, >2 weeks	Microport Angiolet, Xianjian Angcover	1/18	1	0	0
Sze, 2009	Type B aortic dissection subacute and chronic, >14 days	Gore Excluder and TAG	7/7	NR	NR	NR
Manning, 2009	Chronic type B aortic dissection, >14 days	Cook Zenith, Gore excluder	3/7	3	0	0
Nienaber, 1999	Subacute and chronic type B dissection, >14 days	Medtronic Talent	0/12	0	0	0

c. Stroke characteristics and mortality

1st author, Year of publication, publication	Stroke diagnosis/definition	Stroke % (No.)	Stroke character (embolic/haemorrhagic)	Risk factors for stroke identified by study
Kazimierczak, 2019	NR	0	NA	NA
Nozdrzykowski, 2013	New-onset neurological deficit and/or evident brain injury visualized by CT-scan	5 (1/20)	NR	NR
Lee, 2013	NR	0	NA	NA
Lee, 2020	NR	3.9 (2/52)	NR	NR

Zhang, 2017	NR	4 (1/25)	NR	NR
Zha, 2019	NA	0	NA	NA
Zhang, 2018	NR	0	NA	NA
Gao, 2019	NR	0	NA	NA
Xu, 2010	NR	0	NA	NA
Shimizu, 2019	NR	1.4 (27/1880)	NR	NR
Kitamura, 2014	NR	3.8 (2/53)	NR	NR
Mizoguchi, 2017	NR	0	NA	NA
Parsa, 2010	NR	0	NA	NA
Andersen, 2014	Neurological deficit lasting >72 hours	0	NA	NA
Desai, 2015	NR	0	NA	NA
Dohle, 2020	NR	0	NA	NA
Andacheh, 2012	NR	1.4 (1/73)	NR	NR
Lou, 2018	NR	0	NA	NA
Kang, 2011	NR	1.3 (1/76)	NR	NR
Torrent, 2021	NR	2.2 (5/232)	NR	NR
Heijmen, 2012	NR	0	NA	NA
Nienaber, 2009	NR	1.4 (1/72)	NR	One stroke with PLZ 2 after left subclavian artery revascularisation
Massara, 2020	NR	7.7 (1/13)	NR	NR
Steuer, 2013	NR	0	NA	NA
Guangqi, 2009	NR	2 (1/49)	NR	NR
Jing, 2008	NR	0	NA	NA
Eggebrecht, 2005	NR	0	NA	NA
Kato, 2002	NR	0	NA	NA
Palma, 2002	NR	0	NA	NA
Rodriguez, 2008	NR	4.3 (2/47)	NR	NR
Chen, 2006	NR	0	NA	NA
Sze, 2009	NR	0	NA	NA
Manning, 2009	NR	0	NA	NA
Nienaber, 1999	NR	0	NA	NA

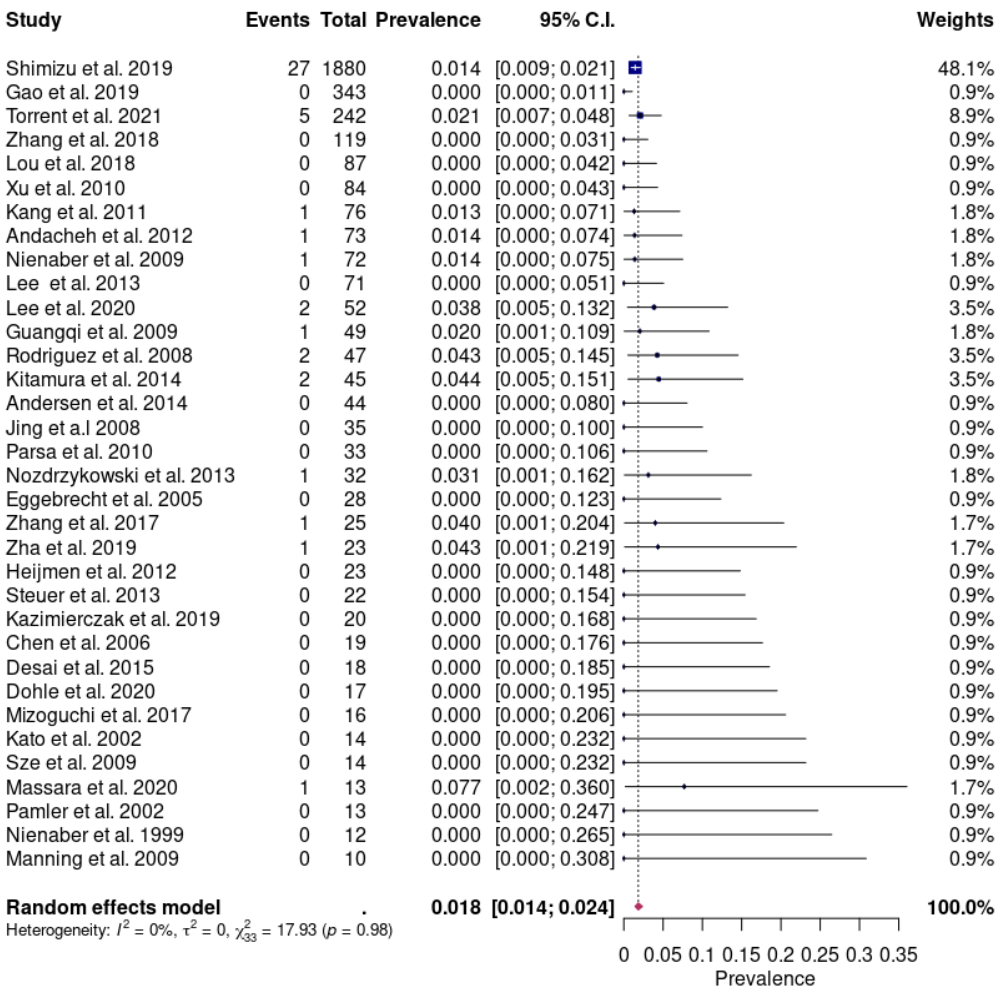


Figure 2.9 Forrest plot for pooled incidence of stroke following TEVAR for chronic type B dissection

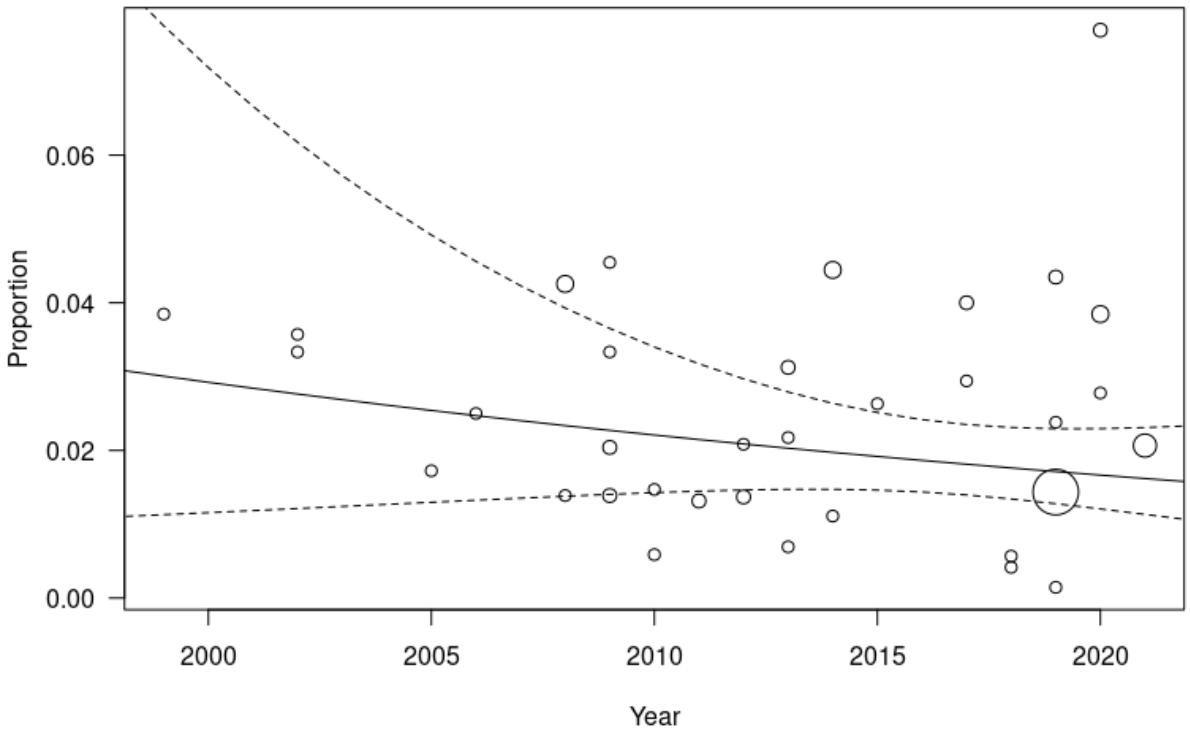


Figure 2.10 Meta-regression (scatter plot) of the relationship between year of publication and stroke as a weighted proportion following TEVAR for chronic type B dissection (β_i =-0.029, SE 0.028, p=0.31). Each circle represents a study telescoped by its weight in the analysis.

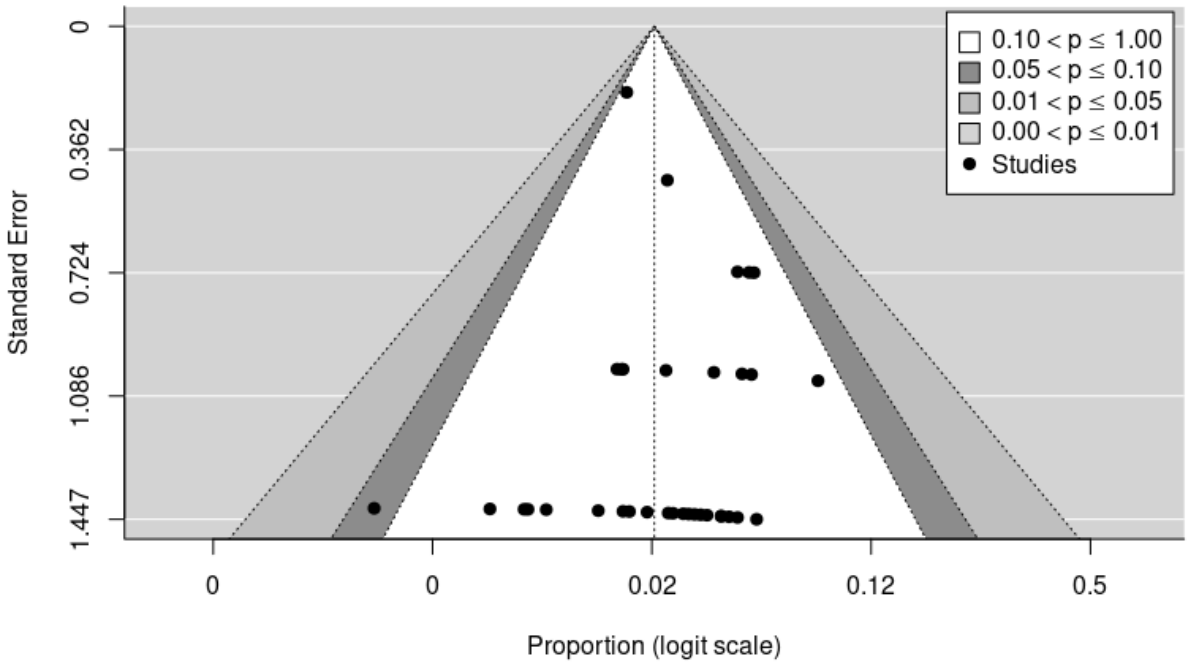


Figure 2.11 Funnel Plot for chronic type B dissection (t = 1.25, df = 32, p = 0.22).

2.8 Risk of bias assessment of studies reporting stroke following TEVAR for chronic type B dissection

Modified Newcastle-Ottawa quality assessment score Key: *=1, -=0, NR=not reported, NA=not applicable

1st author, Year of publication	Selection				Comparability	Outcome			Total score
	Representativeness	Selection of non-exposed cohort (Non-TEVAR control group)	Ascertainment	Stated no stroke at start of study		Method of assessment of stroke	Follow up to minimum 90 days	Adequacy of follow up	
Kazimierczak, 2019	-	-	NR	NR	-	NR	*	*	2
Nozdrzykowski, 2013	-	*	NR	NR	*	*	NR	NR	3
Lee, 2013	*	-	NR	NR	-	NA	*	*	3
Lee, 2020	-	-	NR	NR	*	NR	*	*	3
Zhang, 2017	*	-	NR	NR	*	NR	*	*	4
Zha, 2019	*	-	*	NR	*	NA	*	*	5
Zhang, 2018	-	-	NR	NR	*	NA	*	*	3
Gao, 2019	-	-	NR	NR	*	NA	*	*	3
Xu, 2010	-	-	*	NR	-	NA	*	*	3
Shimizu, 2019	-	*	*	NR	*	NR	NR	NR	3
Kitamura, 2014	*	-	*	NR	-	NR	*	*	4
Mizoguchi, 2017	-	-	NR	NR	*	NR	NR	*	2
Parsa, 2010	NR	-	NR	NR	*	NR	*	*	3
Andersen, 2014	*	-	*	NR	-	*	*	*	5
Desai, 2015	-	-	*	NR	*	NR	NR	NR	2
Dohle, 2020	-	-	*	NR	*	NA	*	*	4
Andacheh, 2012	NR	-	NR	NR	-	NR	*	*	2
Lou, 2018	-	*	*	NR	*	NA	*	*	5
Kang, 2011	*	-	*	NR	-	NR	*	*	4
Torrent, 2021	-	-	*	NR	*	NR	NR	NR	2
Heijmen, 2012	-	-	*	NR	*	NR	-	NR	2
Nienaber, 2009	*	*	*	NR	*	NR	*	*	6
Massara, 2020	-	-	*	NR	*	NR	NR	NR	2
Steuer, 2013	*	-	NR	NR	*	NR	NR	*	3
Guangqi, 2009	*	-	NR	NR	*	NR	*	*	4
Jing, 2008	-	-	NR	NR	*	NR	*	*	3
Eggebrecht, 2005	-	-	NR	NR	*	NR	*	*	3
Kato, 2002	*	-	NR	NR	*	NR	*	NR	3
Palma, 2002	*	-	NR	NR	-	NR	*	*	3
Rodriguez, 2008	NR	-	NR	NR	*	NR	*	*	3
Chen, 2006	*	-	NR	NR	*	NR	*	*	4
Sze, 2009	NR	-	NR	NR	*	NR	*	*	3
Manning, 2009	*	-	*	NR	-	NR	*	*	4
Nienaber, 1999	*	*	NR	NR	*	NR	*	*	5

2.9 Justifications for risk of bias assessment for studies reporting stroke following TEVAR for chronic type B dissection

Modified Newcastle-Ottawa quality assessment, criteria for grading + 1 where applicable

1st author, Year of publication	Selection				Comparability	Outcome			Total score
	Representativeness	Selection of non-exposed cohort (Non-TEVAR control group)	Ascertainment	Stated no stroke at start of study		Method of assessment of stroke	Follow up to minimum 90 days	Adequacy of follow up	
Kazimierczak, 2019							Range 12-27 months	Aortic imaging	2
Nozdrzykowski, 2013		Medical vs TEVAR vs conventional open surgery			Medical vs TEVAR vs conventional open surgery	Clincial +/- CT			3
Lee, 2013	All patients						Median 49 months	Aortic CT	3
Lee, 2020					Comparison of groups based on time from index event		Minimum 1 year	Aortic CT	3
Zhang, 2017	Consecutive				Acute vs chronic dissection groups		Mean 28 months	Aortic CT	4
Zha, 2019	Consecutive		Registry data		Acute vs chronic dissection groups		Median 36 months	Aortic CT	5
Zhang, 2018					TEVAR vs TEVAR + distal aortic extender cuff, acute vs subacute vs chronic phase		Median 15 months	Aortic CT	3
Gao, 2019					Acute vs chronic dissection groups		Median 70 months	Aortic CT	3
Xu, 2010			Database				Mean 33 months	Aortic CT	3
Shimizu, 2019		Open and hybrid repair comparative group	Japan Cardiovas-cular Surgery Database		Open and hybrid repair group and different pathologies				3
Kitamura, 2014	Consecutive inferred		Medical records				Mean 5 years	Aortic CT	4
Mizoguchi, 2017					Early vs late chronic type B dissection			Aortic CT	2
Parsa, 2010					Acute vs chronic type B dissection		Median 7.1 months	Clinical examination and aortic CT	3
Andersen, 2014	All patients		Prospectively maintained Duke Thoracic Aortic Surgery Database			Clinical	87% 1-year survival	Aortic CT	5
Desai, 2015			Prospectively collected clinical perioperative registry		Acute early vs delayed vs subacute TEVAR timing				2
Dohle, 2020			Prospective database		Acute (<90 days) vs chronic (>90 days)		Mean 3.8 years	Aortic CT	4
Andacheh, 2012							Mean >18 months	Aortic CT	2
Lou, 2018		Optimal medical therapy control group	Institutional aortic database		Complicated vs uncomplicated, and uncomplicated TEVAR vs open vs medical therapy		>12 months	Aortic imaging	5
Kang, 2011	Consecutive		Medical records and radiographic information				>12 months	Aortic CT	4

Torrent, 2021			Vascular Quality Initiative (VQI) TEVAR registry		Acute vs subacute groups			2
Heijmen, 2012			ClinicalTrials.gov results database		Comparison of aneurysm vs acute vs chronic dissection			2
Nienaber, 2009	Consecutive	Optimal medical therapy control group	ClinicalTrials.gov results database		TEVAR vs optimal medical therapy	2 years	Aortic imaging	6
Massara, 2020			TEVAR database		Dissection vs aneurysm vs traumatic rupture			2
Steuer, 2013	Consecutive				Acute vs subacute groups		Aortic CT	3
Guangqi, 2009	Consecutive				Acute vs chronic groups	2 years	Aortic CT	4
Jing, 2008					Acute vs chronic groups	Mean 17 months	Blood pressure monitoring and aortic imaging	3
Eggebrecht, 2005					Acute vs chronic groups	>1 year	Clinical examination and aortic CT	3
Kato, 2002	Consecutive cases inferred				Acute type A vs acute type B acute vs chronic type B groups	Range 6-53 months		3
Palma, 2002	Consecutive cases inferred					Mean 14 months	Aortic imaging	3
Rodriguez, 2008					Acute vs chronic groups	Mean 15 months	Aortic CT	3
Chen, 2006	Consecutive				Acute (early vs late) vs chronic groups	Mean 27 months	Clinical and aortic CT	4
Sze, 2009					Acute vs subacute vs chronic groups	Mean 22 months	Clinical evaluation and aortic CT	3
Manning, 2009	Consecutive inferred		Prospectively maintained institutional vascular database			>1 year	Aortic CT	4
Nienaber, 1999	Consecutive	Matched open surgical controls		Matched open surgical controls		3 months	Aortic MRI	5

2.3.4 Blunt traumatic injury

49 studies including 1770 patients were included in the meta-analysis. Three studies were prospective multi-centre industry sponsored registry studies,[271-273] 8 retrospective multi-centre studies,[274-281] 38 single centre.[45,208,282-317] The study/patient characteristics, TEVAR characteristics, and stroke and mortality outcomes are summarised in Table 2.10(a-c). Only 4 studies defined stroke.[45,280,316,317] Seven studies reported the aetiology.[272,273,276,285,295,302,316] The pooled stroke rate was 3.3% (95% CI 2.5% to 4.3%, I^2 =0%, p=0.99) (Figure 2.12). Meta-regression demonstrated no change to the stroke rate over time using the year of publication as the co-variate (β_i=-0.035, SE 0.031), p= 0.25) (Figure 2.13). There was evidence of publication bias (t = -2.94, df = 47, p = 0.005) (Figure 2.14). On further exploration with Trim and Fill plots (Figure 2.15), the true estimate was 4.8% (95% CI 3.8% to 6.1%), z.24.23, p<0.001), I^2 =0%, p=0.77). Risk of bias assessment and justifications are summarised in Tables 2.11 and 2.12, respectively.

Table 2.10 Study/patient characteristics(a), TEVAR characteristics(b), and stroke and mortality outcomes(c) for blunt aortic injury

a. Study/patient characteristics

1st author, Year of publication, Publication type, Country	Study design	Total No. patients	Male % (No.)	Age Mean (SD)	Co-morbidities % (No.)						
					Hypertension	CVA/TIA	IHD	Hypercholestrolaemia	COPD	Smoking	DM
Pacini, 2005, full text, Italy	Retrospective, single centre	15	NR	NR	NR	NR	NR	NR	NR	NR	NR
Antonello, 2013, full text Italy	Prospective, single centre	31	90 (28)	35 (range 16-77)	NR	NR	NR	NR	NR	NR	NR
Martinelli, 2013, full text, Italy	Retrospective, single centre	27	82 (22)	Range 20-69	NR	NR	NR	NR	NR	NR	NR
Di Eusanio, 2013, full text, Italy	Retrospective, single centre	44	NR	33.4 (36.7)	NR	NR	NR	NR	NR	NR	NR
Rousseau, 2005, full text, France	Retrospective, single centre	29	NR	37 (19)	NR	NR	NR	NR	NR	NR	NR
Ziza, 2016, full text, France	Retrospective, single centre	58	80 (47)	43.2 (17.2)	90 (46)	0	5 (3)	17 (10)	2 (1)	19 (11)	7 (4)
Andrassy, 2006, full text, Germany	Retrospective, single centre	15	80 (12)	39 (18)	NR	NR	NR	NR	NR	NR	NR
Buz, 2008, full text, Germany	Retrospective, single centre	39	87 (34)	36 (range 15-82)	NR	NR	NR	NR	NR	NR	NR
Scheinert, 2004, full text, Germany	Retrospective, single centre	10	60 (6)	38.6 (15)	20 (2)	0	10 (1)	10 (1)	0	NR	0
Geisbüsch, 2009, full text, Germany	Retrospective, single centre	14	NR	30 (range 19-77)	NR	NR	NR	NR	NR	NR	NR
Reyes, 2018, full text, Spain	Prospective, single centre	34	79 (27)	36 (range 15-84)	NR	NR	NR	NR	NR	NR	NR
Mosquera, 2018, full text, Spain	Retrospective, single centre	15	93 (14)	50 (15.9)	NR	NR	NR	NR	NR	NR	NR
Fernandez, 2010, full text, Spain	Retrospective, single centre	20	70 (14)	31.8 (range 15-65)	NR	NR	NR	NR	NR	NR	NR
Skripochnik, 2018, full text, USA	Retrospective, single centre	30	70 (21)	38.7 (19.8)	NR	NR	NR	NR	NR	NR	NR
Shackford, 2017, full text, USA	Retrospective, multicentre	176	71 (125)	Median 46 (IQR 28-60)	21 (36)	NR	NR	NR	5 (8)	NR	NR
Starnes, 2015, full text, USA	Prospective, multicentre clinical trial	50	88 (44)	43 (19)	26 (13)	0	4 (2)	NR	2 (1)	46 (23)	8 (4)
Patel, 2011, full text, USA	Retrospective, single centre	19	84 (16)	49.3 (18.3)	37 (7)	11 (2)	37 (7)	NR	11 (2)	26 (5)	5 (1)
Ullery, 2012, full text, USA	Retrospective, single centre	16	Not reported individually for trauma group	Not reported individually for trauma group	NR	NR	NR	NR	NR	NR	NR
Go, 2007, full text, USA	Retrospective, single centre	10	50 (5)	44 (20-84)	NR	NR	NR	NR	NR	NR	NR
Farber, 2013, full text, USA	Prospective, multicentre	51	67 (34)	44.1 (19.9)	26 (13)	4 (2)	12 (6)	14 (7)	6 (3)	29 (15)	8 (4)
Garcia-Toca, 2010, full text, USA	Retrospective, single centre	24	71 (17)	41 (range 20-71)	NR	NR	NR	NR	NR	NR	NR
Estrera, 2013, full text, USA	Retrospective, single centre	69	70 (48)	31.3 (19.6)	NR	NR	NR	NR	NR	NR	NR
Mansour, 2012, full text, USA	Retrospective, single centre	19	68 (13)	42 (range 18-80)	NR	NR	NR	NR	NR	NR	NR
Azizzadeh, 2014, full text, USA	Retrospective, single centre	82	70 (57)	39.5 (20)	NR	NR	NR	NR	NR	NR	NR
DuBose, 2015, full text, USA	Retrospective, multicentre	198	NR	41.7 (17.1)	NR	NR	NR	NR	NR	NR	NR

Riesenman, 2012, full text, USA	Retrospective, single centre	26	73 (19)	40 (20)	NR	NR	NR	NR	NR	NR	NR
Kenel-Pierre, 2019, full text, USA	Retrospective, single centre	77	74 (57)	41 (range 15-83)	NR	NR	NR	NR	NR	NR	NR
Khoynezhad, 2013, full text, USA	Prospective, multicentre clinical trial	50	76 (38)	41 (17)	24 (12)	0	0	NR	4 (2)	NR	2 (1)
Kim, 2019, full text, Korea	Retrospective, multicentre	99	55 (54)	47 (17)	29 (29)	3 (3)	5 (5)	NR	1 (1)	NR	10 (10)
Li, 2017, full text, China	Retrospective, single centre	36	69 (25)	48.7 (15.8)	33 (12)	NR	NR	NR	NR	NR	NR
Shan, 2016, full text, China	Retrospective, single centre	13	92 (12)	35.7 (range 19-62)	NR	NR	NR	NR	NR	NR	NR
Tigkiropoulos, 2018, full text, Greece	Retrospective, single centre	23	83 (19)	44 (range 18-73)	NR	NR	NR	NR	NR	NR	NR
Spiliotopoulos, 2014, full text, Greece	Retrospective, single centre	76	90 (68)	46.2 (18.5)	NR	NR	NR	NR	NR	NR	NR
Kaneyuki, 2019, full text, Japan	Retrospective, single centre	33	70 (23)	45 (19)	NR	NR	NR	NR	NR	NR	NR
Cindy, 2011, full text, Belgium	Retrospective, single centre	24	Not reported individually for TEVAR group	Not reported individually for TEVAR group	NR	NR	NR	NR	NR	NR	NR
Steuer, 2012, full text, Sweden	Retrospective, single centre	17	88 (15)	42 (range 18-77)	NR	NR	NR	NR	NR	NR	NR
Agostinelli, 2006, full text, Italy	Prospective, single centre	15	73 (11)	42 (range 22-69)	NR	NR	NR	NR	NR	NR	NR
Broux, 2006, full text, France	Retrospective, single centre	13	NR	46 (18)	NR	NR	NR	NR	NR	NR	NR
Dunham, 2004, full text, Canada and USA	Retrospective, dual centre	16	69 (11)	33.7 (17)	NR	NR	NR	NR	NR	NR	NR
Fattori, 2002, full text, Italy	Retrospective, single centre	19	NR	39.4 (13.5)	NR	NR	NR	NR	NR	NR	NR
Hoornweg, 2006, full text, Netherlands	Retrospective, multicentre	28	NR	NR	NR	NR	NR	NR	NR	NR	NR
Pratesi, 2006, full text, Italy	Retrospective, single centre	11	100 (11)	48 (7.3)	9 (1)	0	0	0	9 (1)	0	0
Orend, 2002, full text, Germany	Retrospective, single centre	11	82 (9)	NR	NR	NR	NR	NR	NR	NR	NR
Latchat, 2002, full text, Switzerland	Prospective, single centre	12	100 (12)	48 (14)	NR	NR	NR	NR	NR	NR	NR
Melnitchoux, 2004, full text, Switzerland	Retrospective, single centre	15	100 (15)	45	20 (3)	0	0	0	7 (1)	0	7 (1)
Demetriades, 2008, full text, USA	Prospective, multicentre	125	73 (95)	42.2 (18)	NR	NR	NR	NR	NR	NR	NR
Dake, 2001, full text, USA	Retrospective, multicentre	60	68 (41)	46.5 (18)	25 (15)	2 (1)	2 (1)	0	10 (6)	28 (17)	5 (3)
Steingruber, 2007, full text, Austria	Retrospective, single centre	22	77 (17)	38.7 (range 16-82)	NR	NR	NR	NR	NR	NR	NR
Tehrani, 2008, full text, USA	Retrospective, dual centre	30	80 (24)	43 (17)	NR	NR	NR	NR	NR	NR	NR

b. TEVAR characteristics

1st author, Year of publication	Indication for TEVAR	TEVAR device	PLZ No. in zone 2/zone 3-4	Left Subclavian Artery Management		
				Coverage	Bypass/Transposition	Endovascular
Pacini, 2005	Traumatic aortic rupture	Medtronic Talent, Gore Excluder	0/15	1	0	0
Antonello, 2013	Traumatic DTA transection	Medtronic Valiant	27/4	27	0	0
Martinelli, 2013	Blunt aortic injury-Partial rupture, segmental dissection or false aneurysm	Cook Zenith TX1/TX2, Gore TAG/ cTAG, Medtronic Valiant/ Talent	4/23	4	0	0
Di Eusanio, 2013	Blunt traumatic thoracic aortic injury	Medtronic Valiant/ Talent	2/42	2	0	0
Rousseau, 2005	Thoracic aortic rupture from blunt trauma	Medtronic Talent Gore Excluder, Boston Scientific Vanguard device	6/23	6	0	0
Ziza, 2016	Traumatic aortic transection	Gore TAG/cTAG, Medtronic Valiant/Talent, Cook Zenith TX1/TX2	15/43	NR	NR	NR
Andrassy, 2006	Acute traumatic injury to the thoracic aorta	Homemade, Medtronic Talent, Cook Zenith	NR	NR	NR	NR
Buz, 2008	Acute traumatic rupture	Medtronic Talent, JOTEC E-vita, Bolton Relay	20/19	15	5	0
Scheinert, 2004	Traumatic transection	Medtronic Talent Gore Excluder	NR	NR	NR	NR
Geisbüsch, 2009	Traumatic aortic transection	Gore TAG, Medtronic Talent/Valiant, Cook Zenith	8/6	NR	NR	NR
Reyes, 2018	Blunt traumatic thoracic aortic injury	Bolton Relay, Medtronic Talent/Valiant, Gore Excluder/TAG , Cook Zenith	24/10	24	0	0
Mosquera, 2018	Acute traumatic aortic injury	Medtronic Talent/Valiant	1/14	0	1	0
Fernandez, 2010	Acute or subacute traumatic thoracic aortic injuries	Medtronic Talent/Valiant, Gore Excluder/TAG , Bolton Relay, Cook Zenith TX2	10/10	10	0	0
Skripochnik, 2018	Blunt thoracic aortic injury	Medtronic Valiant/Talent/ AneuRx, Gore cTag, Cook Alpha	7/23	7	0	0
Shackford, 2017	Blunt thoracic aortic injury	NR	16/161	NR	NR	NR
Starnes, 2015	Blunt thoracic aortic injury	Cook Zenith Alpha	21/29	21	0	0
Patel, 2011	Blunt thoracic aortic injury	Gore TAG, Medtronic	10/9	2	8	0

		Talent, Cook Zenith TX2				
Ullery, 2012	Traumatic transection	NR	NR	NR	NR	NR
Go, 2007	Acute/subacute traumatic aortic transection with contained pseudoaneurysm	Gore TAG, Cook Zenith TX2	2/8	2	0	0
Farber, 2013	Traumatic aortic transection	Gore cTAG	17/34	14	3	0
Garcia-Toca, 2010	Acute blunt thoracic aortic injury	Gore Excluder/TAG, Medtronic AneuRx	7/17	1	6	0
Estrera, 2013	Blunt thoracic aortic injury	NR	NR	NR	NR	NR
Mansour, 2012	Thoracic aortic injury	Gore TAG, Cook TX2, aortic cuff-Gore Excluder and Medtronic AneuRx	3/16	3	1	0
Azizzadeh, 2014	Traumatic aortic injury	Gore TAG/cTAG, Medtronic Talent/Valiant, Cook Zenith TX2	32/50	32	0	0
DuBose, 2015	Blunt thoracic aortic injury	NR	82/116	82	0	0
Riesenman, 2012	Acute blunt injury to the descending thoracic aorta	Gore TAG/cTAG, Medtronic Talent, Cook Zenith TX2	NR	NR	NR	NR
Kenel-Pierre, 2019	Blunt thoracic aortic injury	NR	NR	NR	NR	NR
Khoynezhad, 2013	Blunt thoracic aortic injury	Medtronic Valiant Captivia	20/30	20	4	0
Kim, 2019	Blunt traumatic aortic injury	Biotech Korea Seal thoracic stent graft	82/17	74	8	0
Li, 2017	Traumatic aortic transection	Medtronic and Cook	10/26	10	0	0
Shan, 2016	Blunt thoracic aortic injury	Medtronic Talent, Microport (China) Hercules, Grikin (China) Grikin	3/10	3	0	0
Tigkiropoulos, 2018	Blunt thoracic aortic injury	LeMaitre Endofit, Gore TAG, Bolton Relay, Medtronic Valiant, Lifetech Scientific Ankura	7/16	5	1	1
Spiliotopoulos, 2014	Blunt thoracic aortic injury	MedtronicTalent/ Valiant Bolton Relay, Jotec E-Vita	11/65	11	0	0
Kaneyuki, 2019	Blunt traumatic thoracic aortic injury	Homemade, Medtronic Valiant, Cook Zenith TX2/ Alpha	20/13	19	1	0
Cindy, 2011	Traumatic aortic rupture	Medtronic Talent/Valiant, Gore Excluder	10/14	9	1	0
Steuer, 2012	Traumatic thoracic aortic transection	Gore TAG, Medtronic Talent, Cook Zenith	8/9	8	0	0
Agostinelli, 2006	Blunt aortic injury	Medtronic Talent	2/13	2	0	0
Broux, 2006	Blunt thoracic aortic injury	Gore Excluder, Medtronic Talent	NR	NR	NR	NR

Dunham, 2004	Acute blunt aortic injury	World Medical Talent Thoracic Coiltrac device, Medtronic AneuRx cuff extender, Guidant Corp Ancure stent device	7/9	7	0	0
Fattori, 2002	Traumatic aortic injury	Medtronic Talent, Gore Excluder	0/19	0	0	0
Hoornweg, 2006	Acute traumatic rupture of the thoracic aorta	Medtronic Talent, Gore TAG	9/19	9	0	0
Pratesi, 2006	Acute traumatic rupture of the thoracic aorta	Medtronic Talent/Valiant	0/11	0	0	0
Orend, 2002	Acute traumatic descending aortic transection	Gore Excluder	11/0	10	1	0
Lachat, 2002	Acute traumatic aortic rupture of the descending aorta	Gore Excluder, Medtronic Talent, Boston Scientific Shneider covered Wallstent	0/12	0	0	0
Melnitchoux, 2004	Acute traumatic aortic rupture	Gore Excluder, Medtronic Talent, Corvita Corvita	NR	NR	NR	NR
Demetriades, 2008	Blunt traumatic thoracic aortic injury	Gore TAG, Cook Zenith, Medtronic Talent, Boston Scientific Vanguard	NR	NR	NR	NR
Dake, 2001	Traumatic thoracic aortic transections	NR	5/55	5	1	0
Steingruber, 2007	Acute traumatic thoracic aortic rupture	Medtronic Talent, Boston Scientific Vanguard	6/16	6	0	0
Tehrani, 2008	Traumatic thoracic aortic transection	Gore Excluder/TAG , Braile Biomedica Braile, Medtronic AneurRx	4/26	0	4	0

c. Stroke characteristics and mortality

1st author, Year of publication, Reference	Stroke diagnosis/definition	Stroke % (No.)	Stroke character (embolic/haemorrhagic)	Risk factors for stroke identified by study
Pacini, 2005	NR	0	NA	NA
Antonello, 2013	NR	0	NA	NA
Martinelli, 2013	NR	0	NA	NA
Di Eusanio, 2013	NR	2.3 (1/44)	NR	Left subclavian artery coverage
Rousseau, 2005	NR	0	NA	NA
Ziza, 2016	NR	0	NA	NA
Andrassy, 2006	NR	0	NA	NA
Buz, 2008	NR	2.6 (1/39)	Ischemia	NA
Scheinert, 2004	NR	0	NA	NA
Geisbüsch, 2009	Transient ischemic attack post-operative day 1	7.1 (1/14)	NR	NR
Reyes, 2018	NR	0	NA	NA
Mosquera, 2018	NR	0	NA	NA
Fernandez, 2010	NR	0	NA	NA
Skripochnik, 2018	NR	0	NA	NA
Shackford, 2017	NR	2.8 (5/176)	NR	NR
Starnes, 2015	NR	2 (1)	Embolic	NR
Patel, 2011	NR	10.5 (2)	NR	1=post-operative hypotension, 1=post-operative atrial flutter

Ullery, 2012	Any new focal or global neurologic deficit lasting >24 hours with associated computed tomography or magnetic resonance imaging evidence of acute intracranial abnormality	6.3 (1/16)	Embolic	Analysis of mixed pathology group; Independent risk factors for any perioperative stroke were chronic renal insufficiency and history of prior stroke. Age and zone 2 coverage were additional risk factors for posterior circulation stroke.
Go, 2007	NR	0	NA	NA
Farber, 2013	NR	3.9 (2)	1 hypoxic encephalopathy, 1 ischemic stroke	NR
Garcia-Toca, 2010	NR	0	NA	NA
Estrera, 2013	NR	2.9 (2/69)	NR	NR
Mansour, 2012	NR	0	NA	NA
Azizzadeh, 2014	NR	2.4 (2/82)	NR	NR
DuBose, 2015	NR	1.0 (2/198)	NR	NR
Riesenman, 2012	NR	7.7 (2/26)	NR	NR
Kenel-Pierre, 2019	NR	1.3 (1/77)	Embolic	Secondary atrial fibrillation
Khoynezhad, 2013	NR	0	NA	NA
Kim, 2019	NR	2 (2/99)	NR	NR
Li, 2017	NR	0	NA	NA
Shan, 2016	NR	0	NA	NA
Tigkiropoulos, 2018	NR	4.4 (1/23)	NR	NR
Spiliotopoulos, 2014	NR	0	NA	NA
Kaneyuki, 2019	NR	6.1 (2/33)	Ischemic	Causes of CVA not identified. Early and late neurological events in 20% patients with LSCA coverage and in 0% of patients with preserved LSCA.
Cindy, 2011	NR	4.2 (1/24)	NR	NR
Steuer, 2012	NR	0	NA	NA
Agostinelli, 2006	NR	0	NA	NA
Broux, 2006	NR	0	NA	NA
Dunham, 2004	NR	6.3 (1/16)	NR	NR
Fattori, 2002	NR	0	NA	NA
Hoornweg, 2006	NR	0	NA	NA
Pratesi, 2006	NR	0	NA	NA
Orend, 2002	NR	0	NA	NA
Lachat, 2002	NR	0	NA	NA
Melnitchoux, 2004	NR	0	NA	NA
Demetriades, 2008	NR	1.6 (2/125)	NR	NR
Dake, 2001	CVA is defined as thrombotic or hemorrhagic stroke; excludes transient ischemic attack	10 (6/60)	NR	40% (2/5) LSCA coverage with no revascularisation developed CVA
Steingruber, 2007	NR	0	NA	NA
Tehrani, 2008	NR	3.3 (1/30)	NR	NR

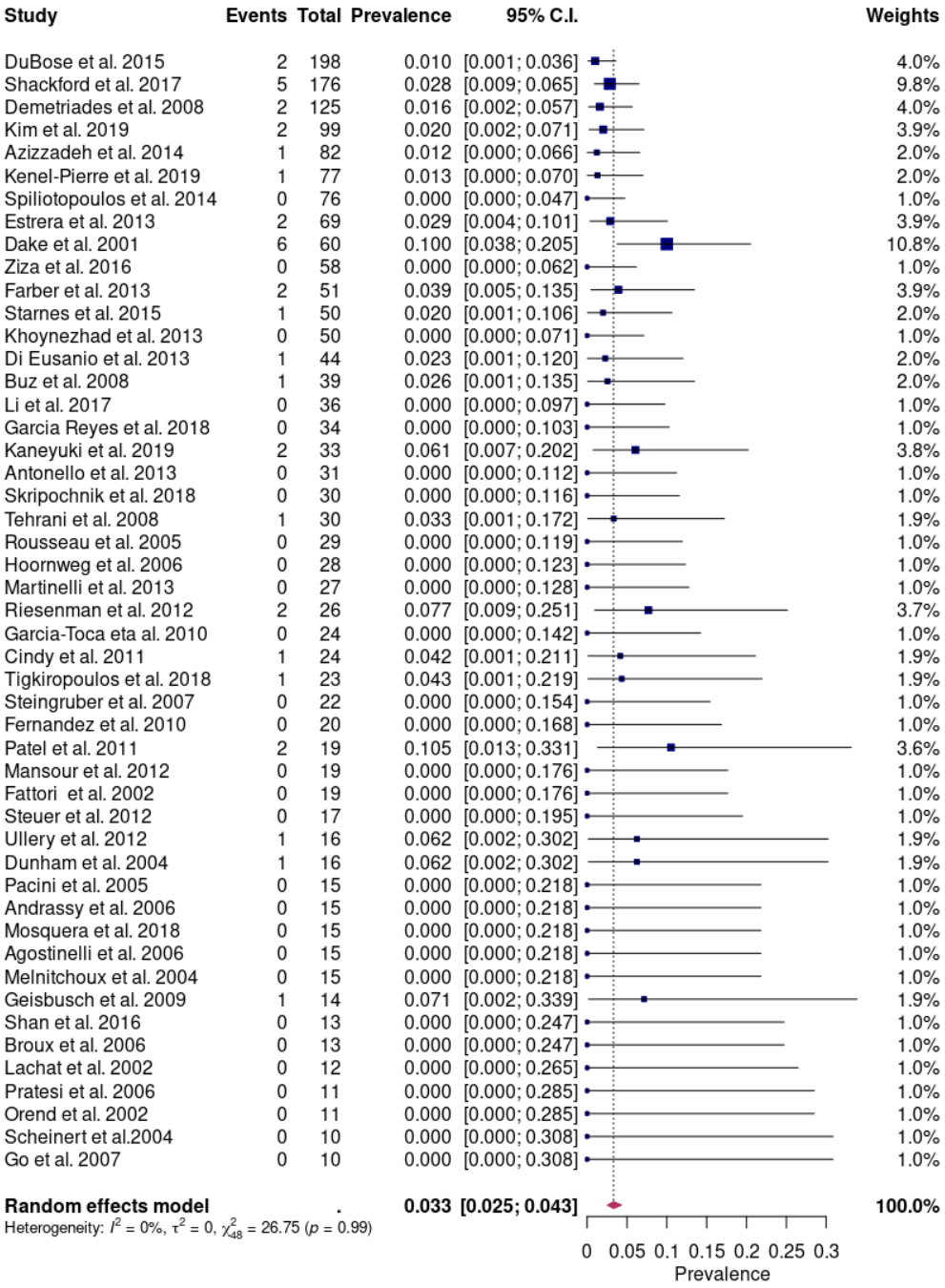


Figure 2.12 Forrest plot for pooled incidence of stroke following TEVAR for blunt aortic injury

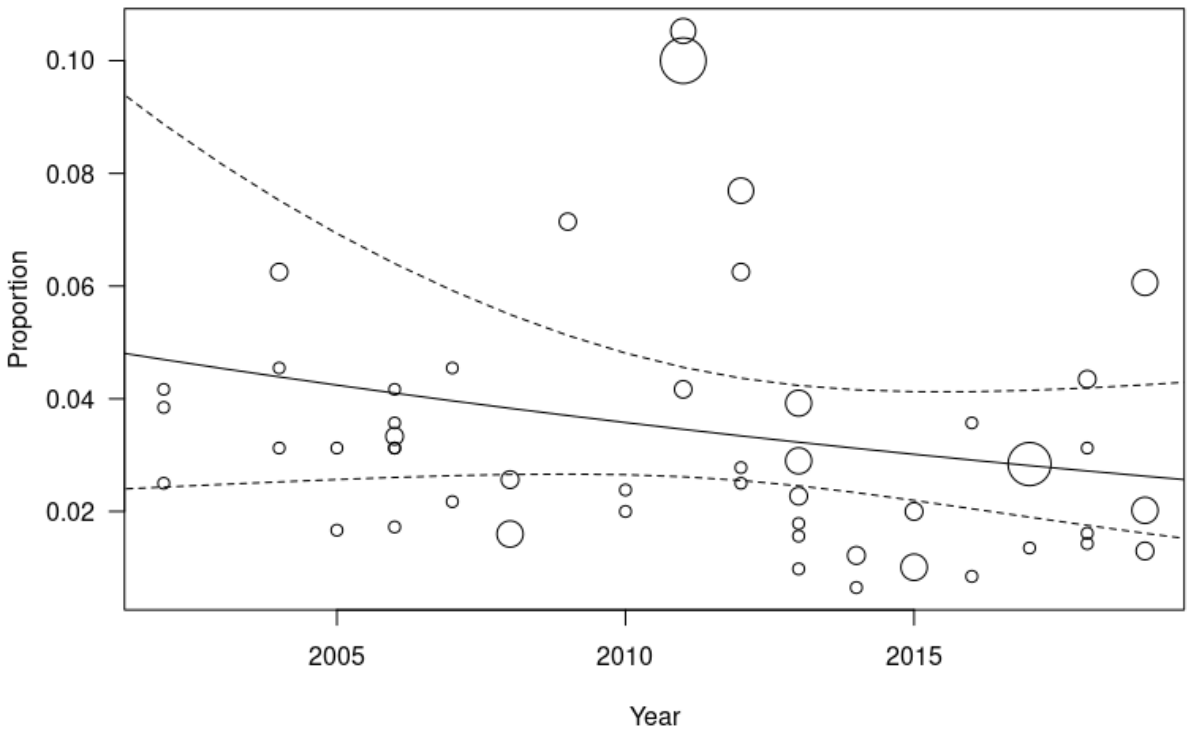


Figure 2.13 Meta-regression (scatter plot of the relationship between year of publication and stroke as a weighted proportion following TEVAR for blunt aortic injury (β_i=-0.035, SE 0.031, p=0.25). Each circle represents a study telescoped by its weight in the analysis.

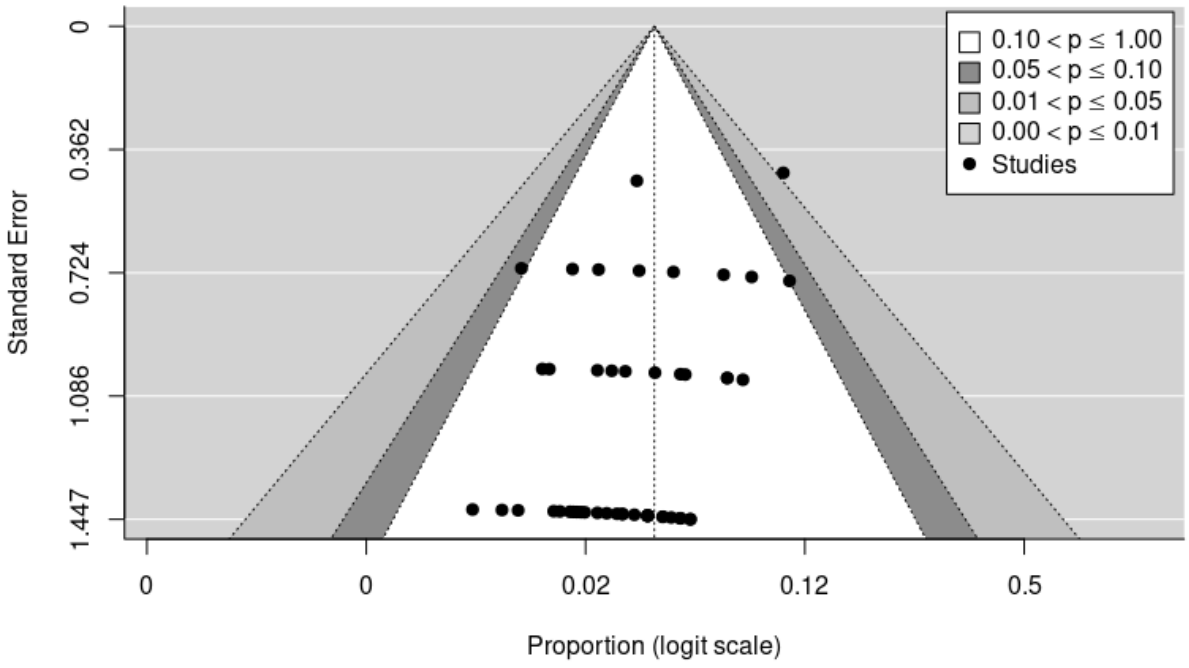


Figure 2.14 Funnel Plot for blunt aortic injury (t = -2.94, df = 47, p = 0.005)

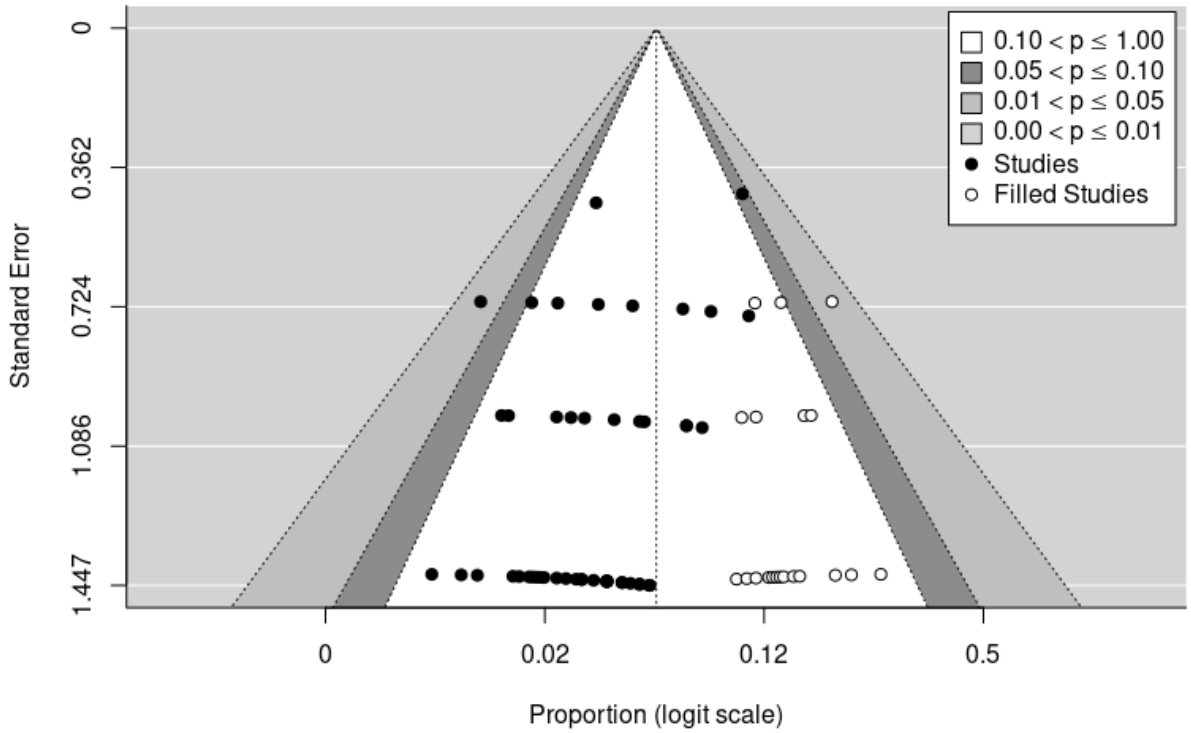


Figure 2.15 Trim and fill plots for blunt aortic injury

Author	**Prevalence [95% CI]**	**W**
DuBose et al. 2015	0.010 [0.003, 0.039]	3.00%
Shackford et al. 2017	0.028 [0.012, 0.066]	7.36%
Demetriades et al. 2008	0.016 [0.004, 0.062]	2.98%
Kim et al. 2019	0.020 [0.005, 0.077]	2.97%
Azizzadeh et al. 2014	0.012 [0.002, 0.081]	1.50%
Kenel-Pierre et al. 2019	0.013 [0.002, 0.086]	1.50%

Spiliotopoulos et al. 2014	0.006 [0.000, 0.095]	0.75%
Estrera et al. 2013	0.029 [0.007, 0.109]	2.94%
Dake et al. 2001	0.100 [0.046, 0.205]	8.18%
Ziza et al. 2016	0.008 [0.001, 0.121]	0.75%
Farber et al. 2013	0.039 [0.010, 0.144]	2.91%
Starnes et al. 2015	0.020 [0.003, 0.129]	1.49%
Khoynezhad et al. 2013	0.010 [0.001, 0.138]	0.75%
Di Eusanio et al. 2013	0.023 [0.003, 0.144]	1.48%
Buz et al. 2008	0.026 [0.004, 0.161]	1.48%
Li et al. 2017	0.014 [0.001, 0.182]	0.75%
Garcia Reyes et al. 2018	0.014 [0.001, 0.191]	0.75%
Kaneyuki et al. 2019	0.061 [0.015, 0.212]	2.85%
Antonello et al. 2013	0.016 [0.001, 0.206]	0.75%
Skripochnik et al. 2018	0.016 [0.001, 0.211]	0.75%
Tehrani et al. 2008	0.033 [0.005, 0.202]	1.46%
Rousseau et al. 2005	0.017 [0.001, 0.217]	0.75%
Hoornweg et al. 2006	0.017 [0.001, 0.223]	0.74%
Martinelli et al. 2013	0.018 [0.001, 0.230]	0.74%
Riesenman et al. 2012	0.077 [0.019, 0.261]	2.80%

Garcia-Toca eta al. 2010	0.020 [0.001, 0.251]	0.74%
Cindy et al. 2011	0.042 [0.006, 0.244]	1.45%
Tigkiropoulos et al. 2018	0.043 [0.006, 0.252]	1.45%
Steingruber et al. 2007	0.022 [0.001, 0.268]	0.74%
Fernandez et al. 2010	0.024 [0.001, 0.287]	0.74%
Patel et al. 2011	0.105 [0.026, 0.337]	2.71%
Mansour et al. 2012	0.025 [0.002, 0.298]	0.74%
Fattori et al. 2002	0.025 [0.002, 0.298]	0.74%
Steuer et al. 2012	0.028 [0.002, 0.322]	0.74%
Ullery et al. 2012	0.062 [0.009, 0.335]	1.42%
Dunham et al. 2004	0.062 [0.009, 0.335]	1.42%
Pacini et al. 2005	0.031 [0.002, 0.350]	0.73%
Andrassy et al. 2006	0.031 [0.002, 0.350]	0.73%
Mosquera et al. 2018	0.031 [0.002, 0.350]	0.73%
Agostinelli et al. 2006	0.031 [0.002, 0.350]	0.73%
Melnitchoux et al. 2004	0.031 [0.002, 0.350]	0.73%
Geisbusch et al. 2009	0.071 [0.010, 0.370]	1.41%
Shan et al. 2016	0.036 [0.002, 0.384]	0.73%
Broux et al. 2006	0.036 [0.002, 0.384]	0.73%

Lachat et al. 2002	0.038 [0.002, 0.403]	0.73%
Pratesi et al. 2006	0.042 [0.003, 0.425]	0.73%
Orend et al. 2002	0.042 [0.003, 0.425]	0.73%
Scheinert et al.2004	0.045 [0.003, 0.448]	0.72%
Go et al. 2007	0.045 [0.003, 0.448]	0.72%
Filled: Fernandez et al. 2010	0.095 [0.006, 0.635]	0.74%
Filled: Di Eusanio et al. 2013	0.099 [0.015, 0.445]	1.48%
Filled: Steingruber et al. 2007	0.104 [0.007, 0.656]	0.74%
Filled: Kim et al. 2019	0.111 [0.030, 0.335]	2.97%
Filled: Starnes et al. 2015	0.112 [0.017, 0.477]	1.49%
Filled: Garcia-Toca eta al. 2010	0.112 [0.008, 0.674]	0.74%
Filled: Martinelli et al. 2013	0.124 [0.009, 0.698]	0.74%
Filled: Hoornweg et al. 2006	0.128 [0.009, 0.705]	0.74%
Filled: Rousseau et al. 2005	0.131 [0.009, 0.712]	0.75%
Filled: Skripochnik et al. 2018	0.135 [0.009, 0.719]	0.75%
Filled: Demetriades et al. 2008	0.136 [0.038, 0.390]	2.98%
Filled: Antonello et al. 2013	0.139 [0.010, 0.725]	0.75%
Filled: Garcia Reyes et al. 2018	0.150 [0.011, 0.743]	0.75%
Filled: Li et al. 2017	0.158 [0.011, 0.753]	0.75%

Filled: Kenel-Pierre et al. 2019	0.163 [0.026, 0.584]	1.50%
Filled: Azizzadeh et al. 2014	0.172 [0.028, 0.599]	1.50%
Filled: DuBose et al. 2015	0.201 [0.059, 0.503]	3.00%
Filled: Khoynezhad et al. 2013	0.206 [0.016, 0.808]	0.75%
Filled: Ziza et al. 2016	0.231 [0.018, 0.829]	0.75%
Filled: Spiliotopoulos et al. 2014	0.282 [0.024, 0.864]	0.75%

Number of studies combined: k = 69 with 20 added studies)

Random-Effects model: 0.048 [0.038, 0.061], z= -24.2345, p<0.001

Quantifying heterogeneity:

tau^2 (estimated amount of total heterogeneity): 0 (SE = 0.1816)

tau (square root of estimated tau^2 value): 0

I^2 (total heterogeneity / total variability): 0.00%

H^2 (total variability / sampling variability): 1.00

Test for Heterogeneity:

Q(df = 68) = 59.2216, p-val = 0.7673

Table 2.11 Risk of bias assessment of studies reporting stroke following TEVAR for blunt aortic injury

1st author, Year of publication,	Selection				Comparability	Outcome			Total score
	Representativeness	Selection of non-exposed cohort (Non-TEVAR control group)	Ascertainment	Stated no stroke at start of study		Method of assessment of stroke	Follow up to minimum 90 days	Adequacy of follow up	
Pacini, 2005	-	*	*	NR	*	NR	*	*	5
Antonello, 2013	*	-	*	NR	-	*	*	*	5
Martinelli, 2013	-	-	-	NR	-	NR	*	*	2
Di Eusanio, 2013	-	*	-	NR	*	NR	*	*	4
Rousseau, 2005	*	*	*	NR	*	NA	*	*	6
Ziza, 2016	*	-	*	NR	-	NR	*	*	4
Andrassy, 2006	-	*	-	NR	*	NR	*	*	4
Buz, 2008	-	*	-	NR	*	*	*	-	4
Scheinert, 2004	-	-	-	NR	-	*	*	*	3
Geisbüsch, 2009	*	*	-	NR	*	*	*	*	6
Reyes, 2018	-	-	-	NR	-	NA	*	*	2
Mosquera, 2018	-	*	-	NR	*	NA	*	-	3
Fernandez, 2010	-	-	-	NR	-	NA	*	*	2
Skripochnik, 2018	-	-	*	NR	-	NA	-	-	1
Shackford, 2017	*	*	*	NR	*	NR	*	*	6
Starnes, 2015	-	-	*	NR	-	*	-	*	3
Patel, 2011	-	*	-	NR	*	*	*	-	4
Ullery, 2012	*	-	*	NR	*	*	*	*	6
Go, 2007	-	-	-	NR	-	NA	*	*	2
Farber, 2013	-	-	-	NR	-	NR	*	*	2
Garcia-Toca, 2010	*	-	-	NR	-	NR	*	*	3
Estrera, 2013	-	*	*	NR	*	NR	*	*	5
Mansour, 2012	-	-	-	NR	-	NA	*	*	2
Azizzadeh, 2014	-	-	*	NR	-	NR	*	*	3
DuBose, 2015	-	*	*	NR	*	NR	-	-	3
Riesenman, 2012	-	*	*	NR	*	NR	-	*	4
Kenel-Pierre, 2019	-	-	-	NR	*	NR	*	-	2
Khoynezhad, 2013	-	-	*	NR	-	NA	-	*	2
Kim, 2019	-	-	-	NR	-	NR	*	*	2
Li, 2017	*	-	-	NR	-	NA	*	*	3
Shan, 2016	*	-	-	NR	-	NA	*	*	3
Tigkiropoulos, 2018	*	-	-	NR	*	NR	*	*	4
Spiliotopoulos, 2014	*	-	-	NR	-	NR	*	*	3
Kaneyuki, 2019	*	-	-	NR	-	*	*	*	4
Cindy, 2011	*	*	-	NR	*	NR	*	-	4
Steuer, 2012	*	-	*	NR	-	NR	*	*	4
Agostinelli, 2006	*	-	-	NR	-	NA	*	*	3
Broux, 2006	-	*	-	NR	*	NA	-	-	2
Dunham, 2004	*	-	-	NR	-	NR	*	*	3
Fattori, 2002	*	-	-	NR	-	NR	*	*	3
Hoornweg, 2006	-	-	-	NR	-	NA	*	*	2
Pratesi, 2006	*	-	-	NR	-	NA	*	*	3
Orend, 2002	*	-	-	NR	-	NA	*	*	3
Lachat, 2002	-	-	-	NR	-	NA	*	NR	1
Melnitchoux, 2004	-	-	-	NR	-	NA	*	*	2
Demetriades, 2008	-	*	-	NR	*	NR	-	-	2
Dake, 2001	-	-	*	NR	-	*	*	*	4
Steingruber, 2007	*	-	-	NR	-	*	*	*	4
Tehrani, 2008	*	-	-	NR	-	-	*	*	3

Table 2.12 Justifications for risk of bias assessment for studies reporting stroke following TEVAR for blunt aortic injury

1st author, Year of publication, publication type, Country	Selection				Comparability	Outcome			Total score
	Representativeness	Selection of non-exposed cohort (Non-TEVAR control group)	Ascertainment	Stated no stroke at start of study		Method of assessment of stroke	Follow up to minimum 90 days	Adequacy of follow up	
Pacini, 2005		Open surgery group	Medical records		TEVAR vs open surgery		Up to 7 years	Clinical and imaging with aortic CT	5
Antonello, 2013	Consecutive cases inferred		Prospective study			Clinical evaluation by neurologist	Mean 36 months	Neurological examination and aortic CTA	5
Martinelli, 2013							Median 67 months	Aortic CTA	2
Di Eusanio, 2013		Open surgery group			TEVAR vs open surgery		Mean 95 months	Aortic imaging	4
Rousseau, 2005	Consecutive	Open surgery and medical therapy alone	Medical records		Open surgery vs stent-graft vs medical therapy alone		Mean 46 months	Transesophageal echocardiography and aortic CT	6
Ziza, 2016	Consecutive cases inferred		Prospectively maintained database				Median 29.9 months	Clinical examination + aortic CT	4
Andrassy, 2006		Open surgery group			TEVAR vs open surgery		Mean 36 months	CT	4
Buz, 2008		Open surgery group			Open surgery vs endovascular repair	Imaging	Mean 2.2 years		4
Scheinert, 2004						Clinical/imaging	Median 15 months	Aortic CT	3
Geisbüsch, 2009	All patients	Open surgery group			Open repair vs TEVAR	Clinical and imaging	Mean 52 months	Clinical examination and aortic imaging	6
Reyes, 2018							Mean 98 months	Aortic CT	2
Mosquera, 2018		Open surgery group			Conservative vs open surgery vs endovascular		Median 9.5 years		3
Fernandez, 2010							Mean 43.5 months (range, 5.5-108)	Clinical examination and angio-CT	2
Skripochnik, 2018			Institutional database						1
Shackford, 2017	All patients	Open surgery group	Research Electronic Data Capture		TEVAR vs open surgery vs non-operative management		Median 13 months	Chest radiograph and CT	6
Starnes, 2015			ClinicalTrails.gov results database			Imaging		Clinical examination and aortic CT	3
Patel, 2011		Open surgery group			Open surgery vs TEVAR	Imaging	Mean 36 months		4
Ullery, 2012	Consecutive cases inferred		Retrospective review of prospectively collected database		Assessed risk factors for anterior vs posterior stroke	Imaging (CT/MRI) and clinical evaluation by stroke neurologist	Mean 49 months	Clinical	6
Go, 2007							Mean 20 months	Clinical review and chest CTA	2
Farber, 2013							76% at 6 months	Aortic CT	2

Garcia-Toca, 2010	Consecutive					Mean 21 months	CT	3
Estrera, 2013		Open surgery group	Houston trauma centre registry	Open surgery vs TEVAR		Mean 2.5 years	Clinic visit and CTA	5
Mansour, 2012						Median 32 months	Clinical and CTA	2
Azizzadeh, 2014			Institutional trauma registry			Median 2.3 years	Telephone/Clinic visit and CTA	3
DuBose, 2015		Open surgery group	Trauma registries	Open surgery vs TEVAR				3
Riesenman, 2012		Open surgery group	Institutional trauma registry database	TEVAR vs open surgery vs nonintervention			CT	4
Kenel-Pierre, 2019				Intraoperative heparinisation-full vs partial vs none		Mean 31 months		2
Khoynezhad, 2013			ClinicalTrails.gov results database				Physical examination and aortic imaging	2
Kim, 2019						Mean 49 months	Medical record review and CTA	2
Li, 2017	All patients					Mean 13 months	CTA	3
Shan, 2016	Consecutive cases inferred					Median 24 months	CTA	3
Tigkiropoulos, 2018	Consecutive cases inferred			Prescence and absence of post-implantation hypertension investigated		Median 48 months	Clinical examination and CT	4
Spiliotopoulos, 2014	Consecutive					Median 3 years	Clinical examination and imaging	3
Kaneyuki, 2019	Consecutive				Cerebral imaging (CT/MRI)	Median 6 years	Clinical examination and CT	4
Cindy, 2011	Consecutive	Open surgery group		Open surgery vs TEVAR		Mean 39 months		4
Steuer, 2012	Consecutive cases inferred		National Vascular Registry (Swedvasc), local registry of interventional radiology, and In-Patient registry			Median 36 months	CT and clinical status	4
Agostinelli, 2006	Consecutive cases inferred					Mean 29 months	CT	3
Broux, 2006		Open surgery group		Open repair vs TEVAR				2
Dunham, 2004	All patients					Mean 10.7 months	CT and chest radiograph	3
Fattori, 2002	Consecutive series					Mean 20 months	CT	3
Hoornweg, 2006						Median 26.5 months	CTA	2
Pratesi, 2006	Consecutive cases inferred					Mean 18 months	Clinical examination, chest x-ray, CT	3
Orend, 2002	Consecutive cases inferred					Mean 14 months	CT and chest x-ray	3
Lachat, 2002						Mean 17 months		1
Melnitchoux, 2004						Mean 34 months	Clinical examination and CT	2
Demetriades, 2008		Open surgery group		TEVAR vs open surgery, critical vs no extra-thoracic injuries, high vs low volume centres				2
Dake, 2001			Catastrophic thoracic aortic indications database		Imaging	Total follow up to 1 year	Clinical	4

Steingruber, 2007	Consecutive	Neurological examination	Mean 23 months	Clinical examination and CT	4
Tehrani, 2008	All patients		Mean 11.6 months	Clinical and CT	3

2.4 Meta-regression analysis

On univariate analysis, diabetes significantly increased the risk of stroke (regression coefficient (Exp (B)), 7.57, [standard error 3.79], p=0.04)) following TEVAR for atherosclerotic aneurysms. Multi-variable regression analysis was not possible. On univariate analysis, hypertension (3.18[1.5], p=0.03) and coronary artery disease (4.47[2.19], p=0.04) increased the risk of stroke following TEVAR for acute type B dissection with only hypertension significantly associated on multi-variate analysis. No variables were associated with stroke following TEVAR for chronic dissection. COPD was significantly associated with stroke following TEVAR for blunt aortic injury (19.1 [6.75], p=0.0005). Stroke was not a significant predictor of in-hospital mortality for any of the pathologies.

2.5 Sensitivity analysis

Studies were grouped according to geographical locations (America, Asia, and Europe). There was no significant difference in the stroke rate for atherosclerotic aneurysms (Figure 2.16), chronic type B dissection (Figure 2.18) or blunt aortic injury (Figure 2.19). A significant difference in the stroke rate was observed following TEVAR for acute type B dissection with the highest rate observed in studies published from America (Figure 2.17).

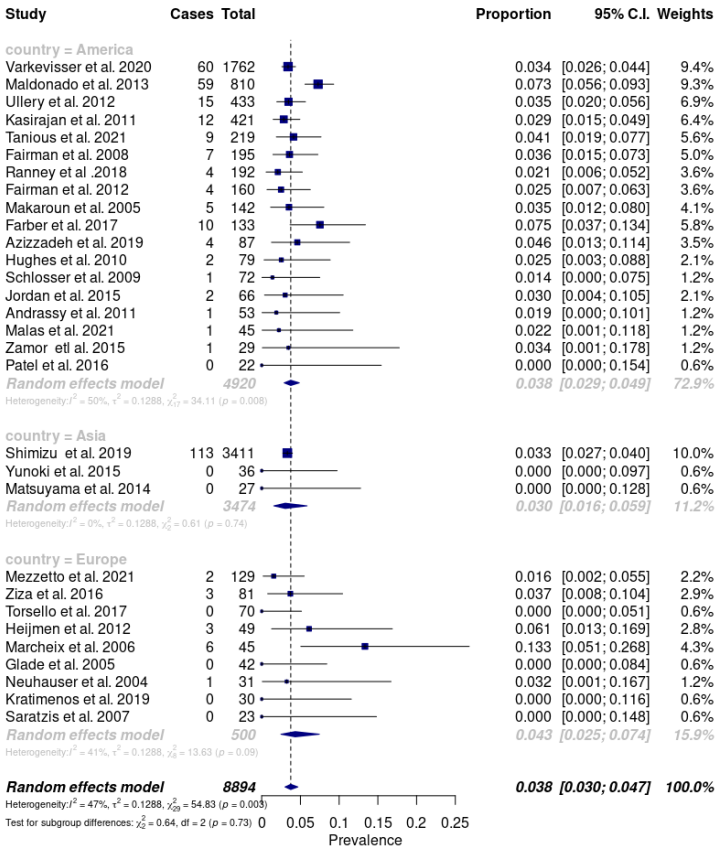


Figure 2.16 Forrest plot of pooled incidence or stroke rate following TEVAR for atherosclerotic aneurysms by geographical region (study by Matsumura et al.[185] excluded due to inclusion data from several countries.

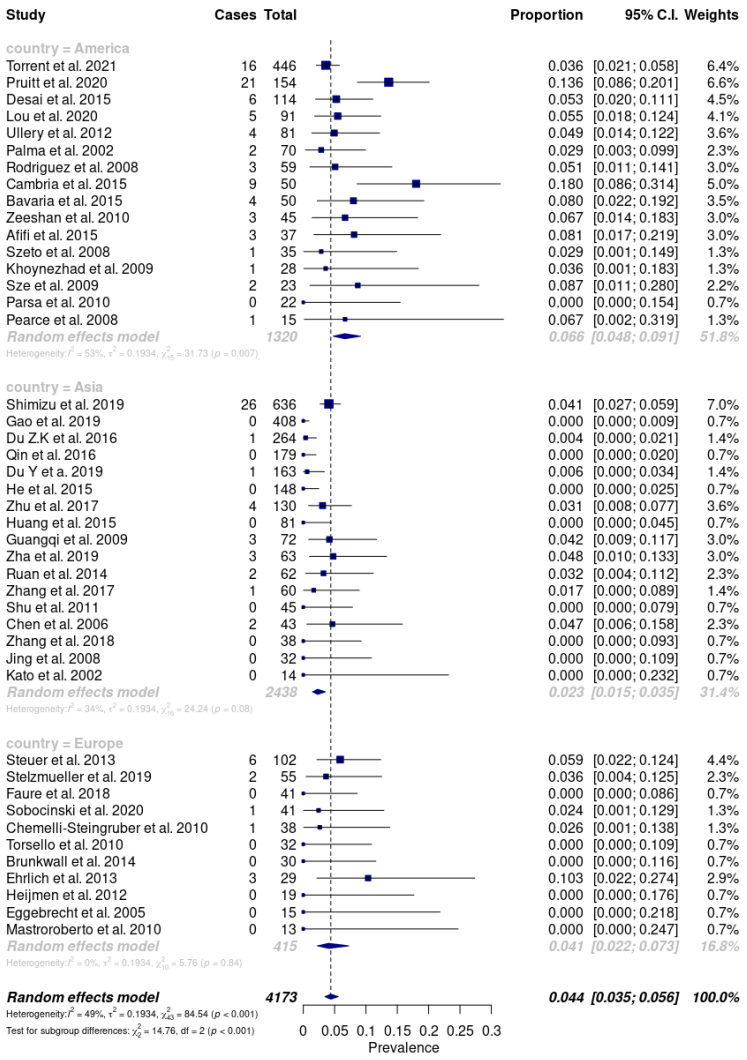


Figure 2.17 Forrest plot of pooled incidence or stroke rate following TEVAR for acute type b dissection by geographical region (study by Lombardi et al.[211] excluded as data from Japan and USA)

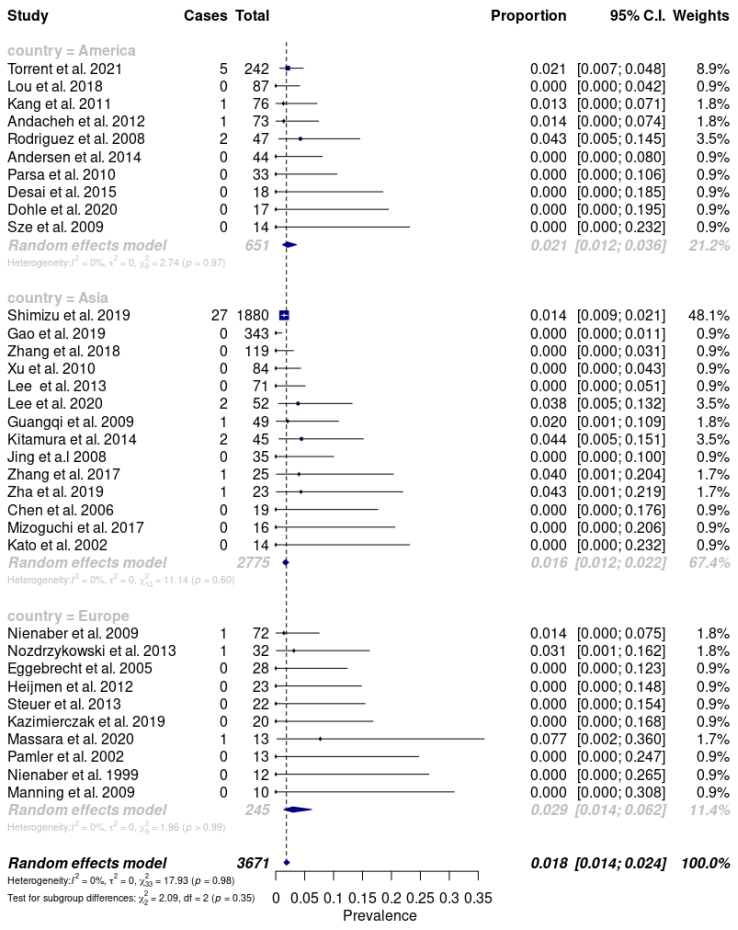


Figure 2.18 Forrest plot of pooled incidence or stroke rate following TEVAR for chronic type B dissection by geographical region

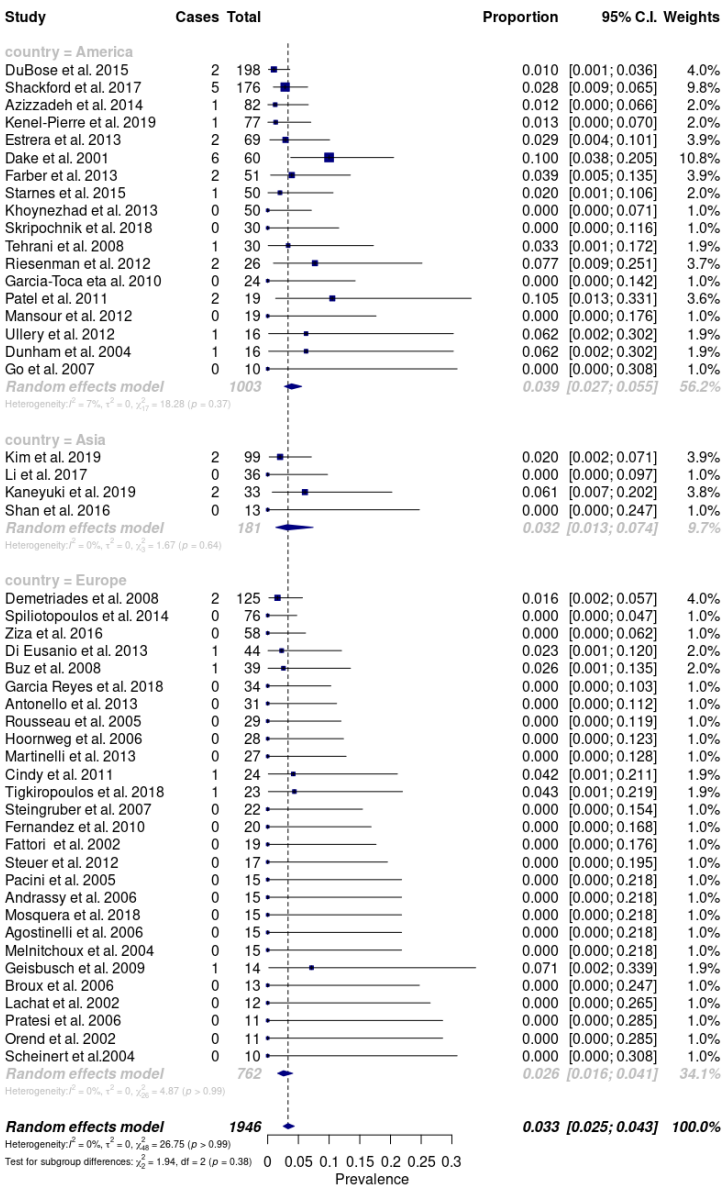


Figure 2.19 Forrest plot of pooled incidence or stroke rate following TEVAR for blunt aortic injury by geographical region

2.6 Risk of bias and quality of the evidence

The risk of bias was found to be low to very low for studies reporting stroke following TEVAR for atherosclerotic aneurysms (Tables 2.2 and 2.3), acute type B dissection (Tables 2.5 and 2.6), chronic type B dissection (Tables 2.8 and 2.9) and blunt aortic injury (Tables 2.11 and 2.12). The GRADE assessment is shown in Table 2.13. The overall certainty of the evidence was found to be very low for acute type b dissection and low for all other pathologies.

Table 2.13 GRADE assessment of studies reporting stroke following TEVAR for aneurysm, acute type B dissection, chronic type B dissection and blunt aortic injury.

Pathology and outcome	**Certainty assessment**						**Summary of findings**
	Risk of bias (Individual study limitations)	**Inconsistency (Heterogeneity in meta-analysis)**	**Indirectness (external validity)**	**Imprecision (Small sample size, wide CIs)**	**Publication bias**	**Overall certainty of evidence**	**Effect (95% CI)**
Aneurysm							
Stroke	Serious	Serious	Low	Low	None	LOW	3.8 (3.1- 4.6)
Acute type b dissection							
Stroke	Serious	Serious	Low	Low	Serious	VERY LOW	4.2 (3.2-5.5)
Chronic dissection							
Stroke	Serious	None	Low	Low	Low	LOW	1.8(1.4-2.4)
Blunt aortic injury							
Stroke	Serious	Low	Low	Low	Serious	VERY LOW	3.3 (2.5-4.3)

2.7 Discussion

2.7.1 Summary of findings

This systematic review and meta-analysis with meta-regression demonstrated that the risk of stroke following TEVAR in zones 2-4 varies across different aortic pathologies, and geographical locations. The highest stroke rate was observed in acute type B aortic dissection, with the highest rate observed in studies published from America. The stroke rate has not significantly changed over time for any aortic pathology.

2.7.2 Overall completeness, applicability, and quality of the evidence

This systematic review with meta-regression represents a comprehensive and rigorous analysis of the best available literature to derive the post-procedural stroke risk following TEVAR limited to zones 2-4 by pathology. Despite efforts to systematically address the risk of studies with overlapping populations by careful review of authors, institutions, and dates of study recruitment, the meta-analysis may have included overlapping studies that were overlooked. The low level of evidence was an expected finding given the observational nature of the included studies and systemic bias associated with such study designs. Despite efforts to limit heterogeneity and deduce the stroke rate limited to TEVAR in zone 2-4 for each pathology and by geographical location, and the use of a random effects model approach to the meta-analysis, the low to moderate heterogeneity between studies could have affected the estimate of stroke following TEVAR.

Heterogeneity in patient selection, operative details, surgeon, and institutional experience, as well as a lack of reporting standards for stroke with inconsistent and incomplete reporting of the definition of stroke, its assessment, and aetiology may present bias and limit the applicability of the findings. These factors also limited further meta-regression analysis to determine risk factors of stroke and account for potential patient and procedure related confounding factors such as atrial fibrillation, and the management of the left subclavian artery and its impact on stroke. It was my intention to conduct a comparative analysis of stroke

rates between zone 2 and 3-4, and the impact of LSA coverage versus revascularisation in zone 2 TEVAR, but there was a paucity of studies providing such data prohibiting such analyses. Funnel plot asymmetry was observed for aneurysms, acute type B dissections and trauma. Most studies were located towards the left of the plots suggesting that higher stroke rates are not being reported. However, statistically significant publication bias was only detected for acute type B dissection and trauma. Trim-and-fill plot analysis resulted in similar (albeit increased) effect estimates for these two pathologies. Thus, the true effect estimate of stroke is likely to be higher than our original analysis. While the lack of a control group makes the results difficult to place into context, the rates of open surgery are declining in favour of the less invasive approach of TEVAR, making this comparative analysis in contemporary practice less applicable.[318] Furthermore, most papers describing outcomes of stroke between TEVAR and open surgery rely on historical controls of open surgery, increasing the risk of bias.

2.7.3 Clinical interpretation of the data

Peri-procedural stroke remains one of the most feared complications by patients and clinicians following TEVAR. When reported, the common mechanism of stroke was cerebral embolisation as evidenced by the presence of cerebral infarcts on neuroimaging. In support of this is the identification of high intensity signals (HITS) on transcranial doppler studies of the middle cerebral artery, indicative of emboli within the cerebral circulation, that appear at several high-risk phases of TEVAR when endovascular instruments are manoeuvred across the aortic arch,[52] dislodging thrombotic, atherosclerotic debris as well as the release of air from catheters and delivery systems. Other mechanisms of stroke include cerebral haemorrhage, hypovolaemia, and cerebral encephalopathy. There is increasing recognition that stroke following TEVAR varies according to pathology and zone. However, stroke rates according to pathology *and* zone are not well known because most series and device registries do not report rates of stroke stratified according to pathology *and* zone. Data from the MOTHER registry[319] noted a 5% stroke rate for thoracic aneurysms compared to 2% stroke rate for chronic type b dissection, however this data was not stratified according to

zone of TEVAR. Similarly, data from the GREAT registry[320] quoted a 30-day stroke rate of 1.6%, however, on analysis according to PLZ, the stroke rate was 13.3%, 2.9%, 2.5%, 0.6% and 0.4% for zone 0,1,2,3,4(1% for zones 2-4). These data, however, were not stratified according to pathology. At this present time, there have been two systematic reviews with meta-analysis that aimed to determine the stroke rate following TEVAR for descending aortic aneurysms. In 2016, Biancari et al.[321] reviewed the stroke rate in patients undergoing TEVAR in the descending thoracic aorta (defined as zone 2-4) and reported a pooled rate of 2.7% (95% CI 1.5% to 3.9%), slightly lower to the findings of the results of this meta-analysis. In 2017, Von Allmen et al.[322] quote a 4.1% (95% CI 2.9% to 5.5%) pooled prevalence of stroke, which is slightly higher than the result of this meta-analysis. However, this latter study ended up including studies that were heterogenous with respect to pathology (primary atherosclerotic aneurysms and aneurysms results from chronic dissections, and TEVAR deployment in more proximal landing zones (0-1) beyond the descending thoracic aorta.

2.7.4 Implications for research and wider clinical practice

An important finding of this meta-analysis is that the stroke rate has not change significantly over time, despite the reported improvements in patient selection, newer generation devices, overall perioperative care, and the reconfiguration of vascular surgery services whereby TEVAR is limited to high-volume and experienced centres. As such research efforts are urgently needed to further our understanding of the pathophysiology as well as the patient and operative factors that increase the risk of peri-operative stroke. Furthermore, there is an urgent need to develop neuroprotective adjuncts for TEVAR that can mitigate the risk of stroke and all forms of brain injury following TEVAR. While there is a plethora of data regarding stroke rates stemming from device registries, population-based studies, and institutional series, it is imperative that the 'Reporting standards for thoracic endovascular aortic repair (TEVAR)'[323] and the 'Standardised neurological endpoints for cardiovascular clinical trials'[324] are adhered to overcome many of the shortcomings of the current literature.

2.8 Conclusion

Stroke following TEVAR in zones 2-4 varies according to pathology with the highest stroke rate observed in acute type B aortic dissection. The stroke rate for aortic pathologies has not changed over time. The quality of the evidence was low, and the true stroke rate is likely underestimated because of inconsistent and incomplete reporting standards.

Chapter 3: Methods

The following studies were conducted and/or analysed for this research thesis:

Clinical

1. Pilot study of carbon-dioxide flushing of TEVAR endografts

2. Comparative study between carbon-dioxide flushing and standard saline flushing of TEVAR endografts

3. Cerebral embolic protection filter (CEPD) study

Experimental

1. Benchtop experimental study to quantify the volume, composition, and distribution of gas release from a variety of TEVAR endografts and the impact that CO_2 flushing has on these endpoints.

3.1 Ethical approval

Ethical approval was obtained from the United Kingdom (UK) Research Ethics Committee (REC) reference 08/H0711/59 for 'Neurological injury in Aortic Stenting' study (NIAS) that was conducted between 2012-2015. This study was set up by my predecessor Ms. Anisha Perera and aimed to quantify the spectrum of neurological injury patients experienced following TEVAR. The main findings have been published in 2018 in the British Journal of Surgery.[52]

A substantial amendment was obtained in 2015 by Ms Gagandeep Grover who took over NIAS from MS Perera (once Ms Perera had finished her research in 2015) to study the use of the two-filter Sentinel CEPD in patients undergoing TEVAR. Ms Grover obtained a Stroke project grant to fund this project and was responsible for recruitment of patients undergoing TEVAR to receive the Sentinel CEPD between 2015 to 2018. Ms Grover left the research team in April 2018. Data analysis for this project was undertaken by me and is presented in this thesis.

I started my PhD in October 2017 and my research time overlapped with Ms Grover. During October 2017 to April 2018, I was responsible for obtaining a second substantial amendment was to recruit patients undergoing TEVAR to receive CO_2 flushing of TEVAR endografts at St Mary's Hospital, London and St Thomas's Hospital, London, followed by recruitment of patients to receive three-vessel CEPD at St Mary's Hospital, London only upon completion of the CO_2 study. The CO_2 study recruited patients between April 2018 to 2021 with the last patient recruited in May 2021. The first patient for three-vessel CEPD was recruited on the 9th of July 2021. Patients that did not consent to receive CEPD or CO_2 flushing or that could not receive these interventions due to logistic reasons (for example no available trained personnel for CEPD insertion or difficulty obtaining the CO_2 tank) were offered the opportunity to participate in the study as a control participant and were offered standard care and underwent the research procedures.

3.2 CO_2 Study

3.2.1 Study design and setting

This was a multi-centre prospective non-randomised observational study recruited patients who were eligible for TEVAR to undergo CO_2 flushing followed by heparinised saline flushing (standard treatment) of TEVAR endografts prior to insertion into the body. Recruitment took place between May 2018 to May 2021. All patients were planned to be followed up to 6-months post-procedure. The two sites are St Mary's Hospital (SMH), Imperial College Healthcare NHS Trust and St Thomas's Hospital (STH), NHS Foundation Trust. Both sites are high volume (>20 cases/year) centres for TEVAR.

Most patients were recruited from SMH as this was the main base location for Ms Lydia Hanna who was responsible for recruitment into this study. Towards the latter part of the study, the research team were contacted by Baylor Scott and White Heart Hospital (BSWH), Baylor Plano, Texas, United States, who expressed an interest to recruit into this study according to the research protocol design at Imperial College London. Recruitment was conducted by research nurses at this hospital with all data analysis conducted by the Imperial College London research team.

3.2.2 Study objectives

Document the rate of cerebral embolisation by transcranial doppler, new DW-MRI infarcts seen on post-operative cerebral DW-MRI, clinical neurological deficit (stroke) and neurocognitive impairment during TEVAR with CO_2 flushed TEVAR endografts.

3.2.3 Participants

Inclusion criteria: All adult (>18 years) patients who are deemed (1) anatomically suitable to undergo TEVAR for any aortic pathology (aneurysm, dissection, trauma) according to the local multi-disciplinary team, (2) able to consent, (3) participate in follow-up neurological and neurocognitive assessments.

Exclusion criteria: (1) unwilling/unable to consent, (2) contraindication to MRI (for example pacemaker), (3) haemodynamically unstable, (4) pregnant.

A control group comprised of participants that had been prospectively recruited by Ms Anisha Perera, Ms Gagandeep Grover and Ms Lydia Hanna between 2012 to 2020 will comprise those patients who do not wish to receive CO_2 flushing but wish to participate in the study and its research procedures.

Participants were identified from the weekly vascular multi-disciplinary meetings, vascular operating lists and suitable patients admitted onto a ward at each site. The researchers maintained close collaborative links and contact with Vascular consultant surgeons, ward teams and administrative staff to aid participant identification.

A researcher (Ms Lydia Hanna) approached all eligible patients for participation. Patients were provided with a participant information leaflet (PIS, Appendix 1)) and were only enrolled once written and fully informed consent was given (Appendix 2).

3.2.4 Study procedures: TEVAR

Patients underwent TEVAR using any of the commercially available thoracic endografts. Endografts were flushed with 100% medical grade CO_2 followed by 60mls of heparinised saline prior to insertion and deployment. All the procedures were performed under general or local anaesthesia according to standardised practice with ultrasound guided percutaneous puncture or surgical cut-down for exposure of the common femoral artery (CFA) according to surgeon preference. Cerebrospinal fluid drainage to prevent spinal cord ischaemia was selectively utilised based on established criteria.[325] Heparin was given throughout the procedure to maintain an activated clotting time of 250 seconds. Systolic blood pressure was pharmacologically reduced to 80mmHg for endograft deployment only and rapid pacing was used in zone 0 cases to counteract the windsock effect and aid precise proximal endograft placement.

Arch debranching and extra-anatomical bypasses were performed to achieve the PLZ. Due to technological advancement during the study, perfusion to the supra-aortic trunks was also maintained with the use of scallop,[326] fenestrated[327] or branched arch endografts.[328] Staging of arch debranching and/or visceral hybrid repairs was at the discretion of the treating surgeon. All patients were nursed in an intensive care unit/high dependency unit post-operatively.

3.2.5 Study procedures: CO_2 flushing technique

All devices were flushed with 100% medical grade CO_2 followed by 60mls heparinised saline. For sheathed devices (Cook, Medtronic, Terumo Aortic), there devices are designed with a side-port attached onto the delivery system through which CO_2 and saline can be used to flush the delivery system as well as the endograft enclosed within the sheath (Figure 3.1). For unsheathed devices (CTAG, Gore), only the catheter guidewire may be flushed, however this endograft itself cannot be flushed. An alternative therefore had to be determined. Following discussion with Gore, the research team decided on the following steps: the

endograft is removed from its packaging and inserted into a W.L Gore Dryseal Sheath (CE marked) that is used in clinical practice for CTAG insertion into the CFA. This sheath has two flush ports, one flush port (white) for inflation of a balloon which acts as a valve to prevent leakage of blood once in the CFA, and the other (blue) for flushing of the main body of the Dryseal. The blue flush port is used to flush through CO_2 followed by saline. One stent needs to be left exposed to allow CO_2 (and saline) to exit. The open end of the Dryseal is capped off with a thumb to prevent leakage of CO_2 and saline (Figure 3.2). The purpose of the Dryseal is to create a chamber full of CO_2 that can then push out all the air and allow saline to dissolve the CO_2 as for sheathed devices.

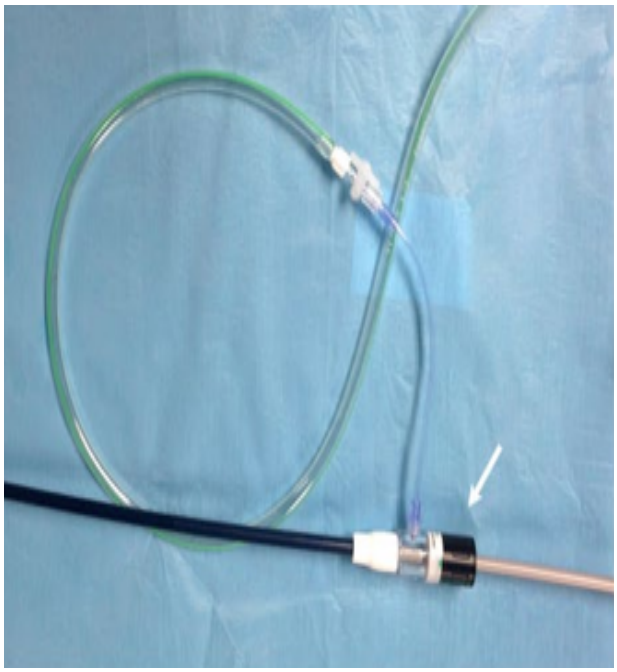


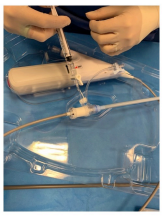
Figure 3.1 Flushing of Cook device



1. Insert Ctag into Dryseal



2. 1cm of Ctag exposed



3. Inflate dryseal VALVE port with 5ml saline



3. Connect dryseal FLUSH port to CO2 tubing



4. Saline flush into dryseal port and guidewire lumen port



5. Remove CTAG from dryseal and leave submerged under saline in tray

Figure 3.2 Flushing of CTAG device

The flush ports of the sheathed devices or the Dryseal are connected to the pressure regulator with PurpleMedical flush tubing. This is typically used in laparoscopic surgery and has an in-line filter to prevent any contamination. The shorter length of this tubing must be cut in half to fit onto the nipple of the pressure regulator that screws onto the CO_2 tank. The longer length is what attached to the flush ports (Figure 3.3).



Figure 3.3 Pressure regulator and Purple Medical laparoscopic tubing with in-line filter, 0.02um pores.

I decided to flush for two minutes at 2-bar pressure (1500mmHg). The flush time was taken from a recent paper that described this technique (Rohlffs et al)[93] and noted a significant reduction in the volume of 'gas' released. Unfortunately, to date there is no description of the specifics of the CO_2 flush technique in sufficient detail for all commercially available endografts.

At the time of this clinical study, we were unable to secure endografts from Industry to be able to determine the optimal flow and pressure that would be most effective at reducing the gas released. From presentations given by Rohlffs et al[93] our research team deduced that what was most likely being used was a 1.2bar pressure regulator typically used in CO_2 angiography.

In a small safety test, I connected a 1.2 bar (900mmHg), 2 bar (1500mmHg) and 4 bar (3000 mmHg) pressure regulator (BOC medical) to the CO_2 tank and then to the Purple medical tubing with in-line filter. CO_2 regulators 1.2 bar, very little CO_2 reached the end of the tubing, leading me to conclude that perhaps this was not a high enough pressure to overcome the in-line filter, and once connected to the endograft,

which introduces a further point of resistance, even less CO_2 may be able to get through the endograft and reach the end. The in-line filter is crucial, and I did not want to try tubing without this filter as even though medical grade CO_2 is sterile and inert, this has not been officially tested in this study. While the Purple tubing is also sterile, one end of it needs to be connected to the pressure regulator and this is not a sterile connection. I therefore did not want t chance even a small risk of contamination of the endograft as endograft infection is a devastating complication with abysmal outcomes.

I subsequently tried a 4-bar pressure (without regulated flow), however this pressure was too high and resulted in significant leaks from the tubing either side of the in-line filter, and this would likely result in variable pressures being delivered to the endograft thereby limiting the efficacy of CO_2.

I settled on 2-bar pressure regulator and the tubing seemed to tolerate this pressure with no leakage. I then was able to secure one expired Medtronic Valiant device and connected the system. I was able to observe (feel and hear) CO_2 reach the endograft and there were no leaks at any points in the system (pressure regulator-to-CO_2 tank, pressure regulator-to-purple tubing- purple tubing to endograft device). As a pragmatic approach, I settled on this 2-bar pressure regulator.

The flushing technique has further been refined upon completion of this pilot clinical study as described further in section 3.4 once I was able to acquire endografts for benchtop testing.

3.2.6 Study procedures: Clinical pre-operative evaluation

All patients needing TEVAR as decided upon at the weekly multi-disciplinary team meeting underwent a thorough pre-operative work-up to ensure 'fitness' to proceed with TEVAR at the respective vascular unit.

As a routine, this included:

- Computed tomography of the aorta (CTA) to determine anatomical suitability for TEVAR and establish the PLZ and distal landing zone (DLZ). This CTA was also used to determine if patients were more suitable to receive a scallop endograft and/or needed arch debranching and extra-anatomical bypass.

- Dobutamine stress echocardiography and pulmonary function tests

- Bilateral carotid dopplers only for those patients needing extra-anatomical bypass, fenestrated or arch branch repairs

-Radioisotope renogram in patients planned to undergo visceral hybrid repair

3.2.7 Study procedures Research pre-operative CTA evaluation

All CT images required for clinical use were acquired using the Brilliance iCT 256 slice scanner (Phillips Healthcare, Netherlands) using the following clinical parameters; 200mA, 12kEV, 1mm slice thickness, matrix 1024 x 1024. All images were acquired with intravenous iodinated contrast for opacification of the aorta. Multi-planar 3-dimensional image reconstruction on dedicated CT workstations (Extended Brilliance Workspace, V3 5.0.2254, Philips Medical Systems) allowed for centre line creation and accurate aortic diameter measurements.

The CTA of all participants was subsequently evaluated for the arch grade and atheroma burden by an interventional radiologist blinded to operative and clinical details of a participant. The arch grade was according to that descried by Kotelis et al based on the relationship of the origins of the supra-aortic vessels

to perpendicular planes (Figure 3.4).[329] Atheroma was graded based on the thickest point captured by the contrast-enhanced CTA (Figure 3.5).[88]

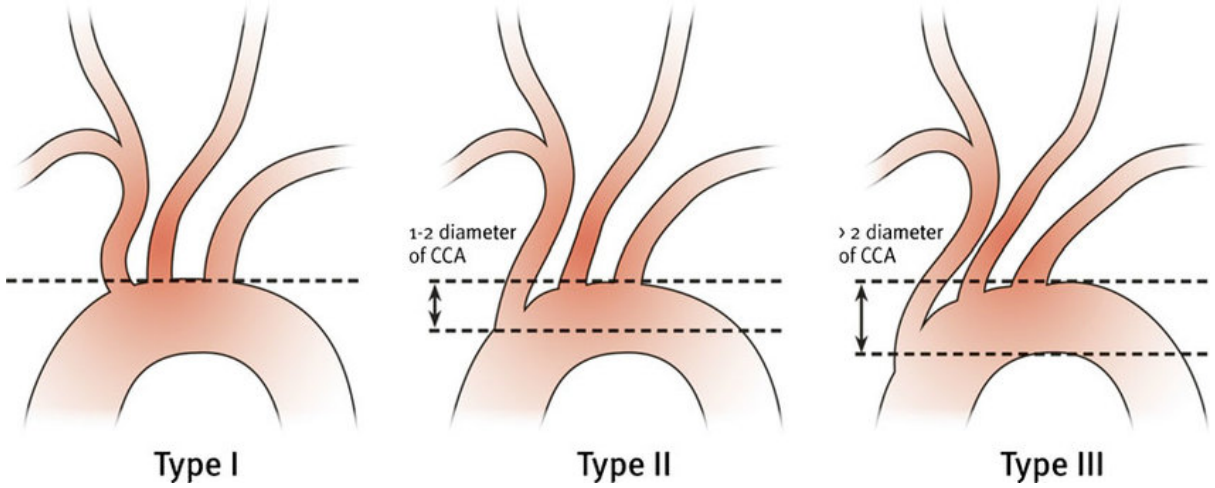


Figure 3.4 Classification of aortic arch type I to III. Image taken from Kotelis D et al.[329]

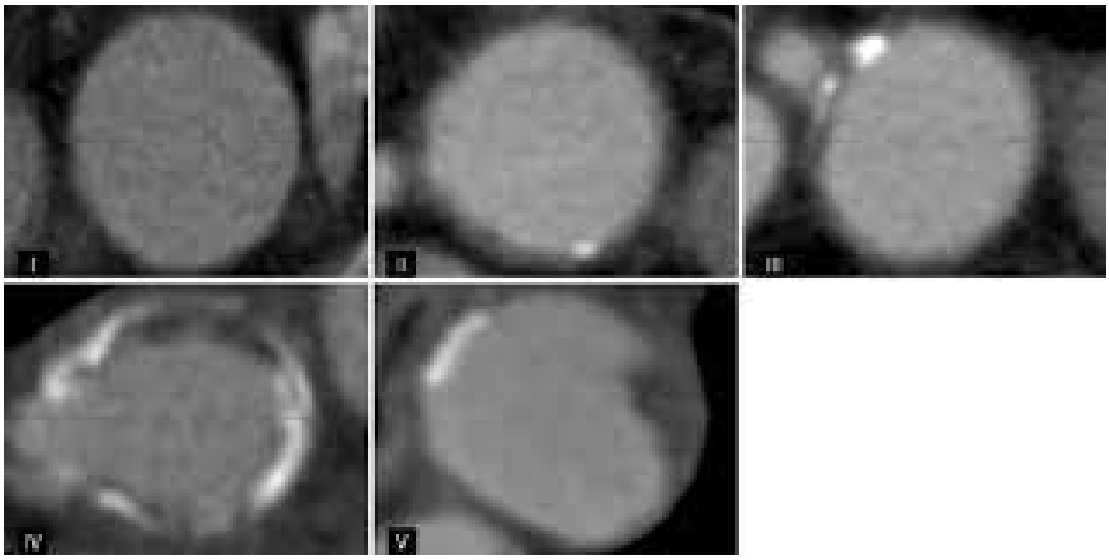


Figure 3.5 Quantitative grading of atheroma I-V; I, normal; II, intimal thickening; III, atheroma < 5mm; IV, atheroma > 5mm; V, mobile lesion.[88]

3.2.8 Study procedures: Intra-operative Transcranial doppler monitoring

Transcranial doppler (TCD) ultrasound monitoring (EmboDop DWL, Compumedics Ltd, Germany) of the cerebral arteries was used to detect HITS characteristic of emboli within the cerebral circulation at certain steps of the procedure (time-stamping procedural steps to embolic activity). TCD transducer probes connected by a headset was placed over the temporal bone as the 'acoustic window' to allow bilateral insonation of the cerebral arteries. Where possible, the middle cerebral arteries (MCA) were insonated as this artery provides blood supply to the largest cerebral territory and is the most easily insonated (Figure 3.6). However, where it is not possible to insonate the MCA, the anterior cerebral arteries (ACA) or the posterior cerebral arteries (PCA) was also insonated. TCD monitoring was undertaken with the DWL® Doppler device with 2-channel emboli detection software. This system uses 2 MHz transducer probes with a sampling volume of 8mm, median soft gain of 25 (range 13-38), filter setting 150Hz, and an intensity threshold of >9dB. The TCD waveform signal is recorded continuously throughout the procedure. A trained assessor (Ms. Lydia Hanna) recorded the time of key procedural steps of TEVAR.

The TEVAR procedure was divided into the following steps:

-Knife to skin and femoral cut-down or percutaneous access

-Extra-anatomical bypass and arch debranching manoeuvres

-Wire and catheter manipulation – wire and catheter placement and/or manipulations into the thoracic aorta

-Stiffwire manipulation - stiffwire placement and/or manipulation into the thoracic aorta

-Endograft manipulation – placement and/or manipulation of the endograft into the thoracic aorta (including withdrawal) for every endograft used

-Endograft deployment – opening of the endograft in the thoracic aorta for every endograft used.

-Arch angiography – IV contrast angiography in the arch with the automatic pump or hand injections.

The trained researcher was responsible for all TCD data acquisition and analysis. Blinding to the procedural steps or analysis was therefore not possible at either stage. While the TCD machine provides automated reporting of an embolus as a HIT from artefact, with further automated differentiation into a gas or solid HIT, offline manual analysis was conducted as a stepwise approach by Ms. Lydia Hanna. First, a HIT was classified as an embolus if it met the following criteria according to consensus committee on microembolus detection.[73]

1. High intensity signal (detected by the system)

2. unidirectional signal within the Doppler velocity spectrum

3. short duration signal (<300 ms)

4. the presence of an audible noise (heard as a crackle, thud, chirp, moan)

Secondly, the differentiation between a solid and gas embolus was dependent upon the following conditions (Figure 3.7)[90]:

1.solid emboli tend to appear lower in the spectral waveform

2. solid emboli have reduced ultrasound reflectivity

3. solid emboli have a shorter duration of travel with reduced acoustic impendence

Where there were showers of emboli at a given procedural step (for example during arch angiography) it was not always possible to differentiate solid and gaseous signals and so the automated machine count was used for this for pragmatic reasons (Figure 3.8).

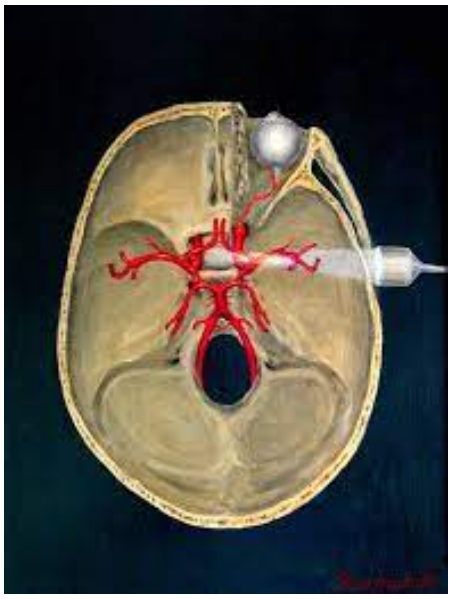


Figure 3.6 Transcranial doppler monitoring of the middle cerebral artery through the temporal bone.

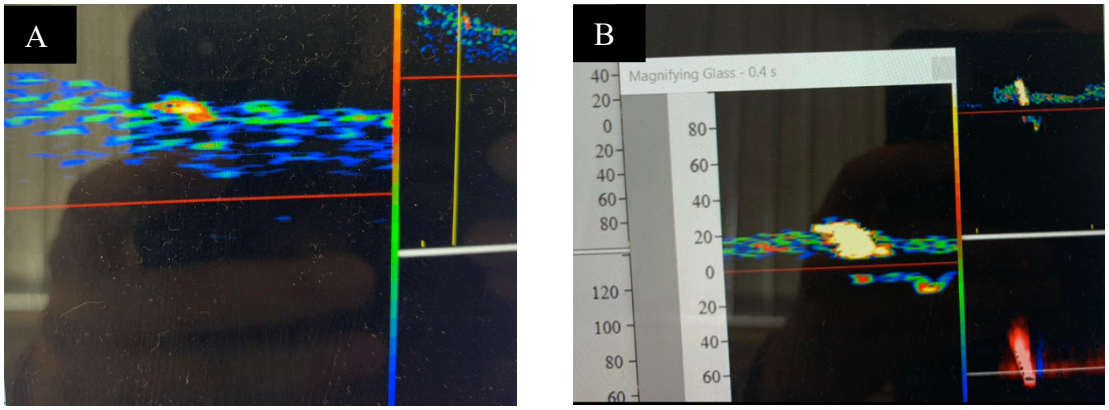


Figure 3.7 Solid (A) and Gas (B) embolus

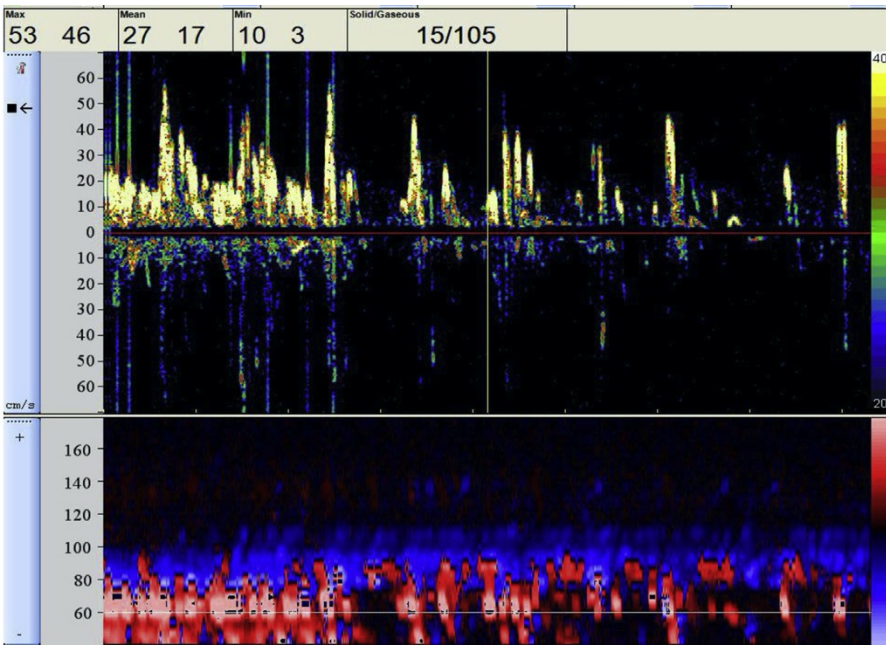


Figure 3.8 Shower of emboli released during procedural step

3.2.9 Study procedures: Diffusion-weighted Magnetic Resonance Imaging

DW-MRI scans were performed post-operatively within 72hrs or when the patient was medically stable to look for new DW-MRI. A 3-Tesla Discovery MR750w system (GE healthcare, UK) was used. The MRI sequences consist of : axial DWI ASSET slice thickness 5mm, gap 1mm; axial T2-weighted fluid-attenuated inversion recovery (FLAIR) slice thickness 5mm, gap 1mm; coronal T1-weighted FSPGR 3D, slice thickness 1mm, no gap and MRA Time of Flight (ToF) to look for completeness of Circle of Willis. These sequences were modified for STH patients to ensure consistency with the 3T sequences at SMH as only a 1.5T scanner was available following discussions with the local MR department. Chronic small vessel ischemia was classified using the Fazekas Scale.[330]

A consultant neurointerventional radiologist, blinded to all clinical and operative details of the patients reported the number, laterality, and vascular territory (anterior or posterior circulation, or border zone

territory) of new DW-MRI infarcts according to a specified protocol (Appendix 3). Maximum diameter and surface area of new DW-MRI infarcts was also recorded. DW-MRI infarct surface area was measured on the slice of largest lesion diameter. DW-MRI infarcts were considered as separate if there is no continuity between them on the same slice and adjacent slices.

3.2.10 Study procedures: Stroke assessment

All participants underwent a full clinical neurological exam by Ms. Lydia Hanna during their in-patient stay. According to the American Heart Association/American Stroke Association, stroke is defined as an 'episode of neurological dysfunction caused by focal cerebral infarction (ischaemic stroke) or focal collection of blood within the brain parenchyma or ventricular system not caused by trauma.[331] Transient ischaemic attack was defined as symptoms of stroke lasting <24 hours.[331] If a clinical stroke was suspected, a neurological assessment by the clinical neurology team was requested. Stroke diagnosis was confirmed by a consultant neurologist and functional neurological outcome was scored on the modified Rankin scale (mRs, Appendix 4).

3.2.11 Study procedures: Neuropsychological assessment

Neuropsychological assessment was undertaken pre-operatively (1-7 days pre-TEVAR) and at 6-weeks and 6-months post-operatively to detect sub-clinical neuropsychological deficits. Neurocognitive assessments consisted of a series of paper-based tests (supplementary Table 1).[6] The timing and nature of all assessments were in-line with a Consensus Statement on Assessment of Neurobehavioral Outcome after Cardiac Surgery.[332]

The tests included:

1.**REY auditory verbal learning test** (Appendix 5). This test is comprised of two components to test both verbal learning and memory. For the verbal learning component, the participant is read a set of 15 words and asked to remember as many of them as possible and is then asked to repeat as many of the words as they can remember, in any order. This is repeated 5 times. The total number of words at trial 5 are counted up and form the final score. Next, a different set of words are read to the participant who again needs to remember these and repeat these back to the assessor (inference trial). The participant is then asked to recall as many words as possible from the first list that was repeated 5 times without any prompts by the assessor. This comprises the memory component of the test. Alternative forms of lists were used at the three time points to reduce practice effect.

2.**Trail making test part A** (Appendix 6). This test assesses visual search and motor skills. The participant is required to join up numbered circles (1-25) dot-to-do as quickly as possible and without taking their hand off the page. The numbered circles are distributed in a random pattern. The total time taken to complete the task in seconds is recorded. If the participant makes a mistake, the assessor points them to the correct order and the time this takes is factored into the final time.

3. **Trail making test part B** (Appendix 6). This test assesses higher cognitive functions such as mental flexibility and switching. The participant is required to join up circles that contain numbers and letters distributed randomly on the page, but must join these up in order for example, 1 to A, 2 to B, etc. The total time taken to complete is the final score.

4. **Grooved pegboard** (Appendix 7). This test assesses mental dexterity, fine motor skills and complex visuo-motor co-ordination of both the dominant and non-dominant hand. A pegboard is placed in front of the participant who is required to place randomly orientated pegs into the grooves with only one hand, in an orderly line. For the left hand, the pegs must be placed from right to left and vice versa for the right hand. The pegs needs to be placed from the top row to the bottom row. The participant is encourage to place the pegs correctly as quickly as possible but without making any drops. The final score is based on the time it takes to complete the task (in seconds). A second is added onto the final score for every peg dropped. The number of correctly placed pegs is also added to the final score.



Figure 3.9 Grooved pegboard

5. **Controlled oral word association test (COWAT)** (Appendix 8). This is a test for executive functioning. The participant is asked to identify as many words as they can in a minute that begin with F, then A, then S. The words cannot be people or places. A different set of letters is used for the 6-week and 6-month testing to avoid practice effect. The total score is based on the total number of words.

3.2.12 Study endpoints

The **primary endpoint** of this study was the incidence of DW-MRI infarcts (the proportion of patients with a new DW-MRI infarct). The **secondary endpoints** included solid and gaseous TCD HITS, number and size (in mm^2) of new DW-MRI infarcts according to specified vascular distributions of the brain, peri-operative clinical stroke and neurocognitive impairment at 6-weeks and 6-months follow-up.

3.2.13 Sample size calculation

The largest study to document the incidence of DW-MRI infarcts was by Perera et al[332] in 52 TEVAR patients. This study observed that 81% of patients had evidence of cerebral infarction post TEVAR. To reduce the incidence of DW-MRI infarcts by 30% (a conservative estimate) following discussions with the Imperial Clinical Trials Unit (ICTU) with CO_2 flushing, at 0.05 alpha level and 90% power would require 48 patients. To account for a 30% MRI drop-out rate (worse case estimate), an extra 14 patients would be required. A total of 62 patients were therefore planned for recruitment to make up the initial cohort.

3.3 Sentinel dual-filter CEPD study

3.3.1 Study design

This single-centre prospective non-randomised study was conducted at St Mary's Hospital, Imperial College Healthcare NHS Trust between June 2015, and April 2018. The study recruited 18 consecutive patients to undergo TEVAR with a CEPD and compared pre-specified outcomes to 17 patients not receiving CEPD (recruited after the CEPD group). In additional to local REC ethics, the Institution's National Health Service Trust New Devices Committee. All participants provided written informed consent for CEPD insertion and histological analysis of tissue captured in the filters. Patients were evaluated with pre- and post-operative diffusion-weighted magnetic resonance imaging (DW-MRI), neurological examination and

neurocognitive tests. Study design, ethical approval and participant recruitment was undertaken by Ms. Gagandeep Grover. Data analysis and interpretation was undertaken by Ms. Lydia Hanna.

3.3.2 Study Objectives

The study objective was to determine the effect of the CEPD to reduce cerebral embolisation to the brain with respect to DW-MRI, clinical stroke and to histologically evaluate the debris captured with the filters.

3.3.3 Participants

All patients undergoing TEVAR for any thoracic pathology between June 2015 and April 2018 were eligible for inclusion if they were (1) able to consent, (2) participate in follow-up neurological and neurocognitive assessments, (3) anatomically suitable for TEVAR with stent-graft deployment in Ishimaru zones 2-4[2] (deployment in zones 0-1 could result in CEPD entrapment) and (4) anatomically suitable for Sentinel™ CEPD insertion. CEPD anatomical suitability included innominate artery diameter between 9 to 15mm and left common carotid artery diameter between 6.5 to 10mm, without excessive tortuosity or > 70% obstructive atherosclerotic disease. Exclusion criteria included stroke within last 6 months, supra-aortic vessel stenosis > 70%, haemodynamic instability including aortic rupture, contraindication to MRI and procedural time > 180mins to reduce risk of thrombus formation on the filters.

3.3.4 Study procedures: TEVAR

TEVAR procedure was according to standard clinical practice as described in section 3.2.4.

3.3.5 Study procedures: Sentinel CEPD insertion

The Sentinel™ CEPD is the most compatible with TEVAR workflow as it does not require filter deployment within the aortic arch which would otherwise interfere with the thoracic stent-graft deployment. The CEPD system is inserted prior to TEVAR delivery system insertion and is withdrawn following removal of the TEVAR delivery system. Following right brachial access, the proximal filter was deployed in the innominate artery, providing protection to cerebral territories supplied by the right carotid and vertebral arteries. The distal filter was deployed into the left carotid artery providing protection to most of the left cerebral hemisphere. The left vertebral artery and its cerebrovascular territory remain unprotected (Figure 3.10). Accordingly, the Sentinel™ CEPD provides complete protection of 74% of the brain, partial protection to 24% of the brain and leaves 2% unprotected (Figure 3.11).

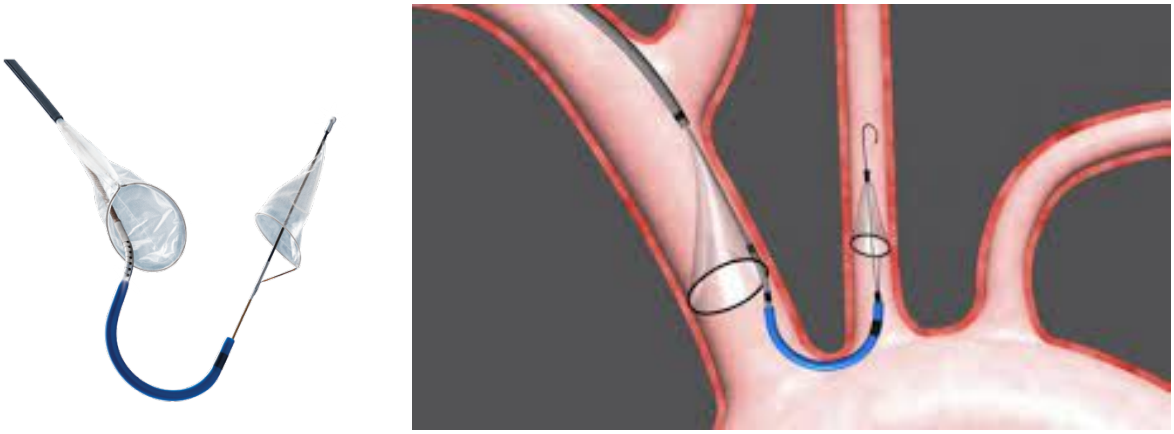
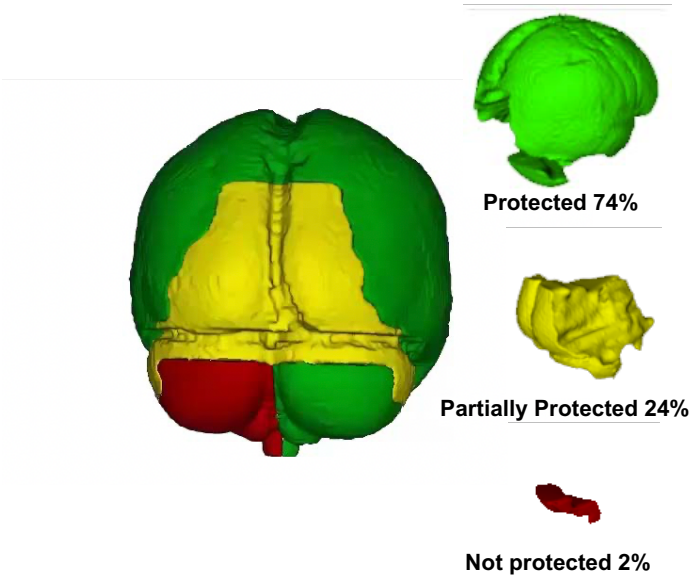


Figure 3.10 Sentinel cerebral embolic protection system with two filters; one in the innominate artery and one in the left common carotid artery. The left subclavian remains unprotected.



Cerebrovascular territory	Left hemisphere	Right hemisphere
Anterior cerebral artery terminal branches	P	P
Anterior cerebral artery central branches	P	P
Middle cerebral artery terminal branches	P	P
Middle cerebral artery central branches	P	P
Posterior cerebral artery terminal branches	PP	PP
Posterior cerebral artery central branches	PP	PP
Anterior choroidal artery	PP	PP
Superior cerebellar artery	PP	PP
Anterior inferior cerebellar artery	PP	PP
Basilar artery anterior	PP	PP
Basilar artery anteromedial	PP	PP
Basilar artery lateral	PP	PP
Basilar artery dorsal	PP	PP
Posterior inferior cerebellar artery	N	P

P: protected; PP, partially protected; N, not protected

Figure 3.11 Cerebral territories protected by the Sentinel dual-filter system.

3.3.6 Study procedures: Clinical pre-operative evaluation

Clinical pre-operative evaluation is described in 3.2.6

3.3.7 Study procedures: Research pre-operative CTA evaluation

Pre-operative CT evaluation is described in 3.2.7.

3.3.8 Study procedures: Intra-operative Transcranial doppler monitoring

Intra-operative TCD monitoring is described in 3.2.8.

3.3.9 Study procedures: Diffusion-weighted magnetic resonance imaging

Pre- and post-operative DW-MRI scans were undertaken in this study given the invasive nature of inserting cerebral embolic protection devices. The sequences are described in section 3.2.9.

3.3.10 Study procedures: Stroke Assessment

This is described in section 3.2.10.

3.3.11 Study procedures: Neuropsychological assessment

This is described in section 3.2.11.

3.3.12 Histological filter assessment

Filters from the CEPD arm were stored in 10% buffered formalin and analysed by a core lab (CV Path, Santa Rosa, Calif). Debris composition and morphometric analysis (particle count, diameter, and surface area) were all recorded.

3.3.13 Study endpoints

The **primary endpoint** was the reduction in the number of new DW-MRI cerebral infarcts on post-operative MRI scans for protected territories of the brain and all territories of the brain. 'Protected territories' of the brain are defined as brain territories perfused by vessels protected by the CEPD; 'all territories' refers to the entire brain. **Secondary endpoints** included the reduction in the surface area (mm^2), stroke rate and neurocognitive impairment, and TCD HITS between the CEPD and control arms.

3.3.14 Sample size calculation

This is the first study to assess the potential effect of CEPD to reduce cerebral solid embolisation in TEVAR. No formal sample size calculation was undertaken. The numbers recruited are in keeping with pilot study recommendations.[333]

3.4 Statistical analysis for clinical studies

Statistical analysis was performed using SPSS software package (version 27 and 28; SPSS, Chicago, IL). Summary statistics for demographic, procedural, radiological data are presented as the mean and standard deviation (SD) or median and interquartile range (IQR) depending on the spread of the data. Categorical variables are presented as frequencies and percentage. For comparative analysis, Mann-Whitney U, Kruskal-wallis and Friedman tests were used as appropriate given the non-parametric spread of the data. Where data was heavily skewed and non-normally distributed, logarithmic transformation was conducted as appropriate.

Neurocognitive impairment is defined as significant deterioration (>20% decline in change scores for each test from baseline to postoperatively, and from baseline to 6-weeks follow-up) on ≥2 of the tests used for each patient as a 'composite' cognitive performance score. Neurocognitive change scores were calculated by subtracting the postoperative or 6-week score (X_2) from the baseline (X_1) and dividing this by the baseline score:

20% method: $\frac{X_2 - X_1}{X_1}$ [334]

Univariate and multi-variate analysis was performed. Entry criteria into multi-variate models was dependent upon a statistical significance level of $p<0.05$. Linear regression was used for continuous variables and logistic regression of binary variables.

3.5 Benchtop Study

A series of benchtop experimental studies were conducted to determine the optimal time and flow rate to achieve the lowest amount of gas released following endograft deployment according to IFU and following CO_2 flushing, and to determine the composition of released gas when the endograft was flushed according to IFU and with CO_2. The aim of these experiments was to standardise the technique for use in the clinic and develop an evidence base.

Experiments were conducted mainly on the sheathed Medtronic Valiant endograft due to difficulty in obtaining endografts of the same size in appropriate quantity to allow repeated measures from other endograft manufacturers. As a sheathed endograft, the delivery system has a pullback system that allows endografts to be re-sheathed in a much easier way than other sheathed devices. Endografts needed to be re-sheathed for re-use due to the limited supply of a standard set of endografts.

A big factor in standardising the CO_2 flush technique is to ensure the equipment for use is authorised for use in medical practice. I was able source a CO_2 flow regulator that operates at fixed 4-bar pressure from Oxylitre Ltd (Figure 3.12). This is the pressure/flow regulator used by cardiothoracic units in the UK who favour CO_2 field flooding to reduce cerebral air embolisation. Under European practice, all CO_2 regulators are calibrated at 4-bar pressure. All benchtop experiments were thereore conducted on this pressure/flow regulator.



Figure 3.12 Flow/pressure regulator specific to CO_2 gases used within the European Union

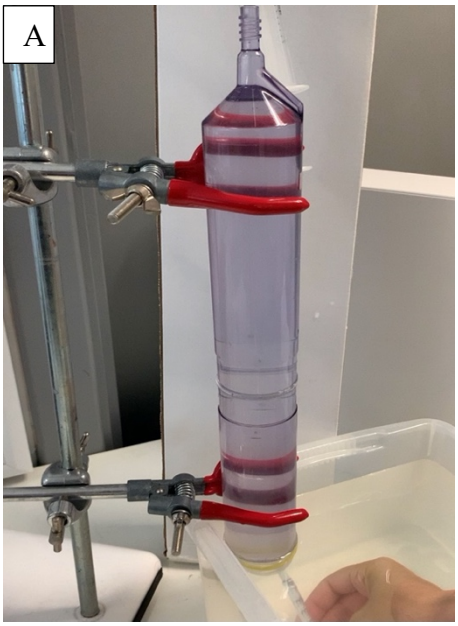
There was concern that given this clinical pressure/flow regulator is set to 4-bar pressure (similar to the BOC 4-bar flow unregulated pressure regulator) it would also be too high for use. Using the water displacement method of gases, whereby heavier gases will push water down in a submerged system, I inserted a Medtronic endografts into a water submerged plastic see through container with graduated litre markings and flushed the endograft with CO_2 underwater for 1 -minute using the BOC 4-bar pressure regulator. I found that in 1 minute, >5L of water was displaced by the CO_2. From this I concluded that the combination of 4-bar pressure and an unregulated flow may therefore be too great for use in the clinic.

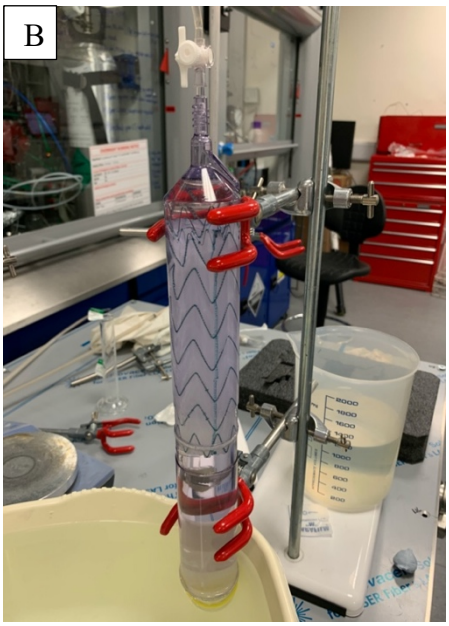
I also applied the same method using the BOC 2-bar pressure regulator used in the clinical study and this displaced 5L of water, providing me with a reference point for this benchtop work. The advantage of switching to the Oxylitre flow/pressure regulator was that flow would be regulated at a given pressure (4-bar) ensuring there would be enough pressure to drive flow through the delivery system and overcome the resistance that is expected at the filter of the tubing, and at the point of contact with the compressed endograft.

The analysis of ‘gas concentration/ was evaluated in a Hiden Analytical HPR-20 mass spectrometer located at Imperial College London.[335] This equipment is suited for continuous gaseous streams at near atmospheric conditions, with quoted detection limits from 5 parts per billion to 100%. It uses one of two detector types: Faraday or Secondary Electro Multiplier (SEM); the last allows a faster and more sensitive analysis, but is limited to a smaller concentration range.[336] Furthermore, given the equipment’s baseline fluctuations and high dependence on the mixture being analysed, the obtained results were only considered from a qualitative point of view. The output data provided by the mass spectrometer can plot the CO_2 signal and nitrogen signal (Nitrogen [N_2,] and Oxygen [O_2] surrogate marker of air) as a function of time.

Experiments regarding time and gas composition were conducted at the same time at the Department of Chemical Engineering, Imperial College London, under the supervision of Dr Chris Tighe, Senior lecturer, and in conjunction with Dr Artur Rolo De Andrade (PhD student chemical engineering) and Mr Tom Hess (5^{th} year medical student).

All endograft deployments to release gas for the time, gas composition and volumetric analysis were conducted on a straight plastic tube (deployment chamber) that I was able to fashion from two syringe pumps used in angiography. The deployment chamber was submerged underwater in a water filled tub. The deployment chamber was 4.5cm in diameter and had a cone tip allowing a three-way tap to be connected to it. The three-way tap had a 5cm tube and then end of this was also connected to a three-way tap allowing syringes to attach onto it for the aspiration of released gas (Figure 3.13). For gas composition experiments, a fixed (2ml) volume of argon was injected into the chamber, and this was the carrier gas for any released bubbles (see section 3.5.2). This was not necessary for the volumetric experiments.





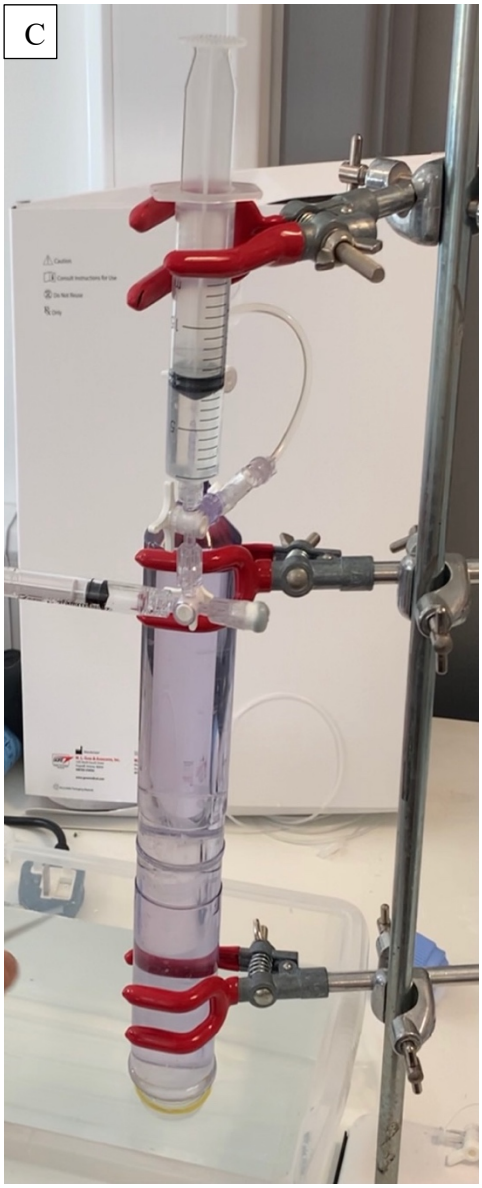


Figure 3.13 Deployment chamber (plastic tube) for all deployments for collection of gas bubbles for composition and volume analysis (A); with endograft deployed (B); three-way tap and line that was

connected onto another three-way tap allowing gas to be aspirated in a 20mls syringe and then transferred to a 2.5, 5 or 10ml syringe for volumetric analysis and compositional analysis(C).

3.5.1 Time quantification

To determine the time CO_2 takes to reach the end of the endograft and reach a steady state and therefore the minimum time necessary to fully purge an endograft with CO_2, the tip of a 46mm (proximal diameter)-46mm (distal diameter)-152mm (length) Medtronic valiant endograft was placed inside a stainless-steel tube which was connected to a mass spectrometer via a 1/8" PFA flexible tube (Figure 3.14). CO_2 at 2L, 4L and 6L at 4 bar-pressure was flushed through the endograft and the time taken to reach a steady state of CO_2 was recorded.

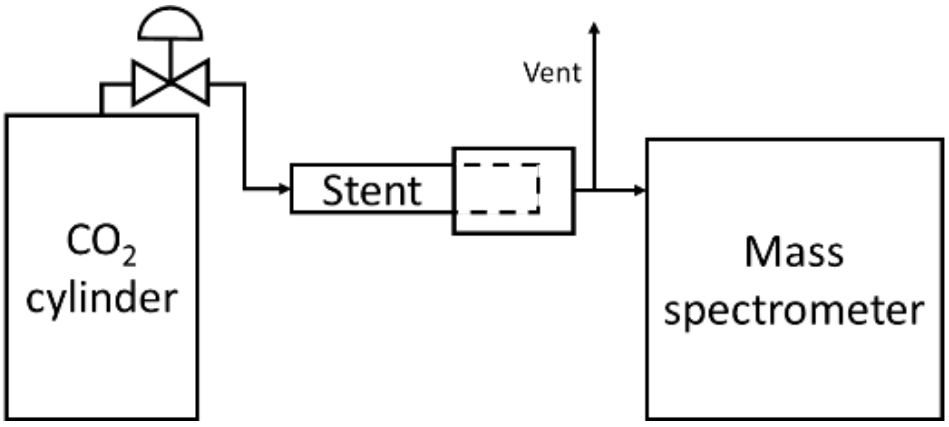


Figure 3.14 Schematic of the setup used to continuously measure a stream's composition.

Changes in pressure (and thus peak intensity, which would interfere with the accuracy of the 100% CO_2 baseline) were mitigated by use of a vent situated downstream of the stent-tube apparatus (such that the analysed gas mixture was at the same conditions each experiment).

Given the system's tubular configuration, it is expected that CO_2 moves across the system as a wave front subject to small deformations.[337] This was traced in the mass spectometer using the detector suited for higher concentrations. For each flowrate, the time between starting the purging feed and achieving a constant CO_2 at the outlet was measured. The same procedure was conducted without the endograft, i.e. connecting the steel tube directly to the regulator in the CO_2 cylinder. The difference between these two times consisted of the residence time in the endograft itself, being an indication of the time required to purge it.

Time taken for CO_2 to move from the end of the stent to the mass spectrometry detector:

Minimum CO_2 purge duration (s) = CO_2 purge via stent (s) – mass spectrometry-CO_2 delay (s)

3.5.2 Composition ascertainment

The objective of this experiment was composition analysis of the bubbles released during a endograft deployment following flushing with no intervention, saline (IFU) and CO_2 at varying flowrates. Given their small volume (less than 0.1 mL), the tested stents were deployed into an argon atmosphere to allow for a >1ml sample which was fully collected in a syringe (carrier gas). Inert gases are gaseous substances that are chemically nonreactive with other substances under standard temperature and pressure conditions. The non-reactive property of inert gases makes them suitable for a host of industrial processes as they prevent explosions, corrosion, and other unfavourable phenomena. Argon is a widely-used inert gas in industry. Argon makes up a small fraction (0.934% by volume) of atmospheric alongside oxygen (20.95% by volume) and nitrogen (78.09% by volume), making it the ideal carrier gas for the purposes of these experiments.

The sample was inserted in a ¼” stainless steel tee and swiped by a continuous flow of argon (199.8 ± 0.2 mL/min, Figures 3.16 and 3.16)

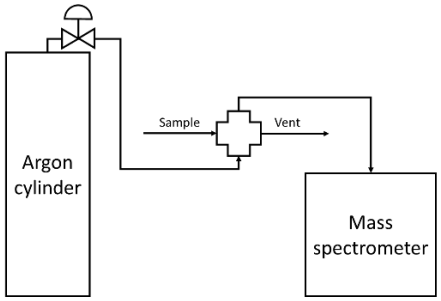


Figure 3.15 Schematic of the setup used to individually analyse a sample composition.



Figure 3.16 Endograft inserted into stainless steel tube that was then connected to the mass spectrometer.

The collected samples considered different endograft conditioning before deployment (Table 3.1):

1. Deployment of the endograft without any purging to establish the composition of gas (baseline)

2.Deployment of the endograft following 60mls saline solution flushing (IFU, to establish the composition of gas following saline flush

3. CO_2 followed by 60mls saline flushing at the flow rates for a time that was determined by the time experiments in section 3.5.1.

Table 3.1 Endograft conditions

Group A endograft were not flushed
Group B endograft were flushed with 60 mL saline only.
Group C endograft were flushed with CO_2 (2 $Lmin^{-1}$, 4 bar) for x minute, then 60 mL saline
Group D endograft were flushed with CO_2 (4 $Lmin^{-1}$, 4 bar) for x minute, then 60 mL saline
Group E endograft were flushed with CO_2 (6 $Lmin^{-1}$, 4 bar) for x minute, then 60 mL saline
Group F endograft were flushed with CO_2 (8 $Lmin^{-1}$, 4 bar) for x minute, then 60 mL saline
Group G endograft were flushed with CO_2 (10 $Lmin^{-1}$, 4 bar) for x minute, then 60 mL saline

The protocol of flushing included:

Protocol:

1. 6 x 20 mL saline prepared and manually de-gassed.

2. Central cannula wire line flushed with same intervention as endogaft, and sealed with air-tight stopcock to prevent air from coming back into the device and being released underwater

3.Delivery system (and endograft) flushed ready for deployment

Flushing was conducted vertically, from low-to-high. Saline syringes were de-gassed using manual (negative pressure) techniques.[338] Syringes were not fully injected and care was taken not to introduce room air into the system when attaching and removing syringes.

Prior to all deployments and analysis, a control sample of the argon atmosphere was injected into the experimental system/apparatus thus establishing a detection limit.

Accurate compositional analysis of the gas sample was accomplished by using an inverted, degassed, saline-filled 1 mL syringe to extract a sample of the gas mixture, while maintaining a saline-seal for transport between collection apparatus and mass spectrometer. Care was taken to avoid introducing room air into the sample when removing the 1 mL syringe from the collection apparatus.

The signal of CO_2 and O_2 (surrogate of air) were measured for all samples and corresponding signal areas were calculated (not proportional to CO_2 and O_2 concentration, until signal-concentration gradient made). For each analysis and molecule, a single peak was obtained, being integrated numerically, accounting for any changes in the baseline. Given the high dilution of these species in argon, it was possible to use the more sensitive SEM detector.

Due to the limited number of endografts of the same size and length, following deployments, all endografts were tried under hot air, and the delivery system was dried by purging with compressed air under a heater. Endografts were then re-loaded onto the delivery system.

3.5.3 Volume quantification

The same set-up used for compositional analysis was also used for volumetric analysis. The 46mm endografts could no longer be used due to wear and tear and I was able to obtain 3x 22 (proximal diameter)-22 (distal diameter)-152 (length) mm that needed to be re-used. The same endograft was used for a given

intervention. All endografts were dried thoroughly as described above before re-sheathing. The three way-tap allowed for a variety of leur-lock syringes to be attached to it, allowing for accurate aspiration and quantification of bubbles. Once deployment was complete, a 10ml syringe was used to aspirate the gas release 'en-block' and for accurate quantification, this was transferred into a 5ml, 2.5ml or 1ml syringe.

The same flushing protocol described above was used but testing was limited to saline only, 2L CO_2 +saline, 4L CO_2 +saline and 6LCO_2 +saline. As explained in results, this was because at 8L and 10L CO_2 the tubing connected the pressure/flow regulator to the endograft started leaking, and therefore it was deemed that these flow rates were not feasible.

3.5.4 Gas distribution quantification

To determine the distribution of gas release following endograft deployment, it was necessary to develop a model that replicated the geometrical and mechanical properties of the aorta and its physiological conditions, in vitro. The following pre-requisites needed to be considered in conducting this experiment.

1. Accuracy of the mechanical and geometric features: Accurate in vitro human anatomy of the thoraco-abdominal and cerebral circulatory system and that would allow introduction and accurate deployment of endografts, with arch anatomy that would allow characterisation of distribution of gas bubbles released.

2. Realistic haemodynamic environment: Deployments to be conducted under pulsatile conditions whereby there are realistic pressure/flow characteristics. This would also be dependent on model specifications and its mechanical properties.

3.5.5 Anatomy of the model

I designed a silicone thoracoabdmominal model that was custom-made by Elastrat®. The original schematic picture is depicted in Figure 3.17). This was modified by Elastrat® to meet their manufacturing capabilities. The final model and its dimensions are shown in Figure 3.18. The model included an aortic valve that connected onto a chamber that simulated the ventricle distally, stubs of coronary arteries (13mm in diameter), ascending aorta (28-29mm diameter), aortic arch (26-25mm in diameter), supra-aortic vessels that were between 6.5mm to 7mm in diameter. A PLZ of 20mm in length was incorporated in-between the LSA and a DTAA (width 57mm and length 66mm). The DTA diameter was 25mm.

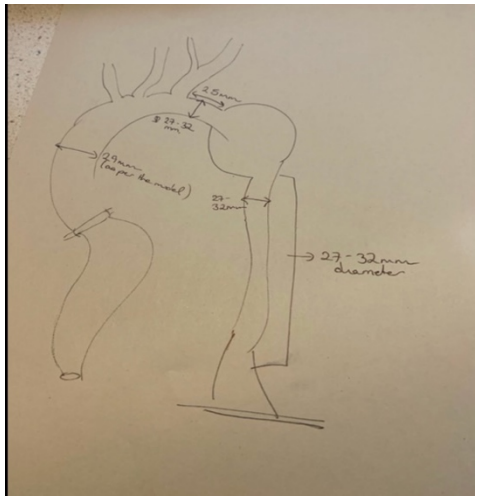


Figure 3.17 Schematic drawing of model

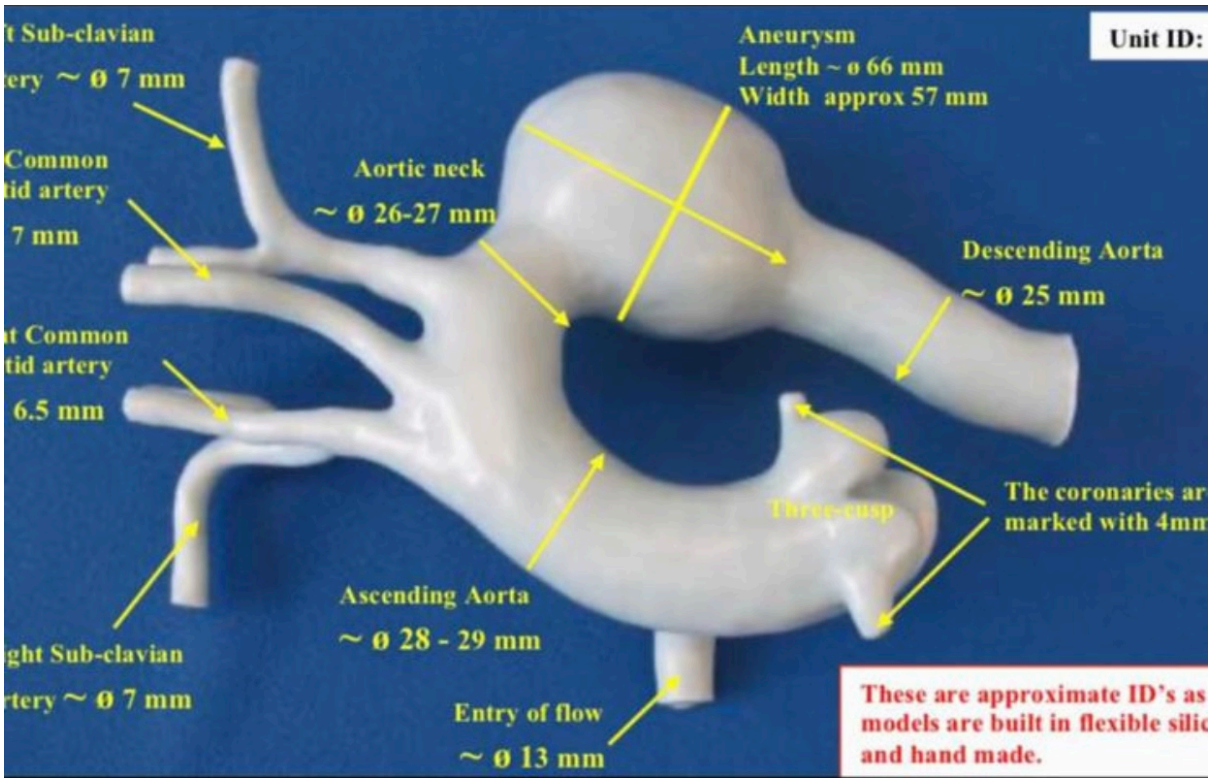


Figure 3.18 Dimensions of the arch of the thoracoabdominal model.

The left vertebral artery left common carotid and right common carotid arteries were connected to 3/8inch diameter PVC tubes. To replicate real-life set-up, the flow model was kept supine and not elevated (Figure 3.19).

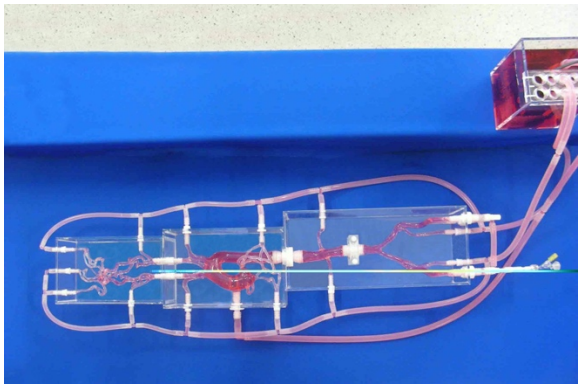


Figure 3.19 Thoracoabdominal model in its entirety.

3.5.6 Physiology of the model

The Harvard pulsatile pump (Figure 3.20) was used to circulate blood (blood mimicking fluid BMF) and provide antegrade perfusion. This is a piston driven pulsatile pump that can deliver human physiologic flow rates and pressures in waveforms similar to those produced by the heart. To ensure the correct physiological flow rate are generated throughout the arterial tree, calipers were applied to the PVC tubes to vary diameter (resistance) and flow rate. Pressure and arterial waveform validation prior to stent-graft deployment were carried out by an experienced senior sonographer (CP) from the Irvine vascular lab, Imperial College London, by placement of an ultrasound probe to display arterial waveforms at the aortic arch, innominate artery, left common carotid artery, left subclavian artery, and proximal and distal descending thoracic aorta, and iliac arteries. The stroke rate was controlled to maintain a flow rate of 6l/minute.



Figure 3.20 Harvard pulsatile pump

The flow model was filled with Model 046 Blood Mimicking Fluid (BMF) made by CIRS at a temperature of 37 degrees. This is intended for use in any flow phantom with any type of pumping mechanism. It is formulated to simulate the acoustic and physical properties of blood, providing a stable and reliable fluid for Doppler studies and system evaluations. The fluid is fully degassed prior to packaging to minimize noise

from any additional air bubbles and to ensure that any air bubbles within the flow model are only from the stent-grafts. It has a viscosity of 4mPa (human blood is 4.4mPa), density of 1037kgm^3 (human blood 1053), velocity of 1548 ms^{-1} (human blood 1583), acoustic attenuation 0.05 dB/cm^{-1}MHz (human blood 0.15 dB/cm MHz).

3.5.7 Quantification of air bubbles and emboli

Air bubbles passing through the supra-aortic vessels were measured in size, volume and distribution through a C.E marked bubble counter BCC300(GAMPT GmbH, Merseburg, Germany)(Figure 3.21). This has three ultrasonic probes that will each be placed at the innominate (IA), left common carotid (CCA) and left vertebral artery(VA) 10cm away from the arch, during deployment of each stent-graft of the respective group to provide a measure of air reaching the right side of the brain (IA), left side of the brain(left CCA), and hindbrain (left VA).

The BCC300 can transform each 'embolism' event into an acoustic signal for the determination of micro bubble number, size, and volume. It is capable of safely detecting and classifying microbubbles as small as 20μm in diameter. Air bubble release was recorded at the following steps; Introduction of endograft in arch, primary deployment to intermediate diameter (leading to trailing unlacing of sleeve), secondary deployment (trailing to leading end unlacing of sleeve withdrawal of delivery system) to full diameter. The patterns of air bubble distribution during these steps, especially with respect to unlacing of the two sleeves was observed and analysed. Deployment was filmed with a high-resolution camera.

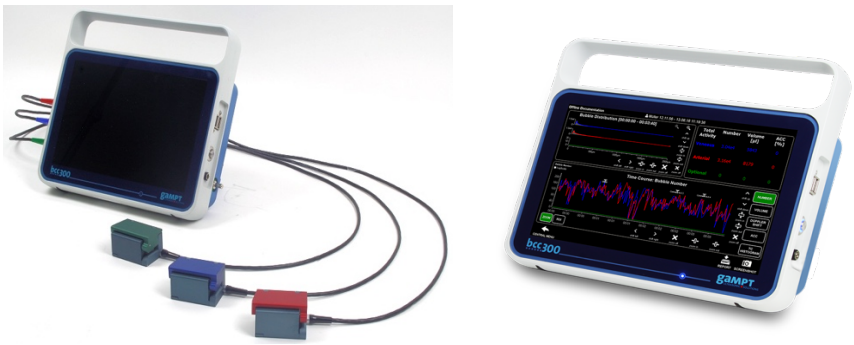


Figure 3.21 GAMPT bubble detector

3.6 Statistical analysis for benchtop work

The Students T test (two-sided) with unequal variance was used for all comparative analyses. A $p<0.05$ was statistically significant.

Chapter 4: CO_2 Study

4.1 Aim

This study was performed to determine the effect of CO_2 flushing of thoracic endografts on TCD-detected cerebral air embolisation, incidence of new procedure-related DW-MRI infarcts, and the incidence of stroke and cognitive impairment in patients undergoing TEVAR.

4.2 Results

4.2.1 Study population

A total of 75 patients undergoing TEVAR were recruited into this study and were available for analysis. Seventy patients were recruited from SMH and STH with a further 5 patients recruited from BSWH. Patient demographics and procedural data of the 75 patients are shown in Table 4.1 and 4.2 respectively.

Table 4.1 Patent demographics

Characteristics	Patients (n=75)
Demographics	
Age (years)	69.8 ± 12
Male	52 (69)
Co-morbidities	
Hypertension	67 (89)
Atrial fibrillation	5 (7)
Ischaemic heart disease	26 (35)
Hypercholestrolaemia	47 (63)
Diabetes mellitus	7 (9)
Chronic obstructive pulmonary disease	29 (39)
Chronic kidney disease (eGFR < 60ml/min)	13 (17)
Previous TIA/CVA	6 (8)
Previous thoracic surgery	9 (12)
Previous abdominal surgery	4 (5)
Smoking history	50 (67)
Medication	
Anticoagulation	14 (19)
Antiplatelets	48 (64)
Statins	51 (68)
Fazekas scale: PVWM	
0	5 (7)
1	27 (36)
2	19 (25)
3	24 (32)
Fazekas scale: DWM	
0	7 (9)
1	31 (41)
2	22 (29)
3	15 (20)
***Arch atheroma grade**	
1	17 (24)
2	31 (44)
3	10 (14)
4	12 (17)
***Arch grade**	
1	26 (37)
2	35 (50)
3	9 (13)

eGFR, estimated glomerular filtration rate; PVWM, periventricular white matter lesions; DWM, deep white matter lesions. Data are presented as n (%) or mean standard ± deviation. *5 patients from BSWH could not be analysed due to suboptimal CT imaging.

Table 4.2 Procedural characteristics for 75 patients

Characteristics	Patients (n=75)
Indication	
Atherosclerotic aneurysm	36 (48)
Chronic type b dissection aneurysm	14 (19)
Trauma	1 (1)
Acute type b dissection	12 (16)
Coarctation	1 (1)
Mycotic aneurysm	3 (4)
Penetrating aortic ulcer	6 (8)
Endoleak relining	2 (3)
Rupture/contained ruptured aortic pathology	5 (7)
Urgency	
Elective	52 (69)
Semi-elective	3 (4)
Emergency	20 (27)
***ASA**	
1	1 (1)
2	7 (10)
3	42 (60)
4	20 (29)
VPOSSUM mortality	6.5 ± 12.5
VPOSSUM morbidity	44.0 ± 24.5
Ishimaru Zone	
0	5 (7)
1	2 (3)
2	15 (20)
3	42 (56)
4	11 (14)
Endografts	
Gore cTAG	37
Medtronic (Valiant and Navion)	15
Custom-made Relay Proximal Scallop/fenestrated	8
Relay Tapered	4
Custom-made Relay Arch Branch	1
Cook (Zenith Alpha and TX2)	12
Cook arch fenestrated +stent	1
Cook Arch fenestrated	0
Cook BEVAR (abdominal)	3
Cook FEVAR (abdominal)	0
Total number of TEVAR endografts used per patient; median (IQR)	118; 1 (1-3)
Upper extremity access	13 (17)
Management of the LSA	
Uncovered	53 (71)
Covered	6 (8)

Revascularized	16 (21)
Spinal drain	12 (16)
Operative time (mins)	160.1 ± 114.5
Total time of intra-operative hypotension (<80mmHg, mins)	9.8 ± 12.2
Intra-operative transfusion	19 (25)

*No data available for 5 patients from BSWH. Data are presented as n (%) or mean standard ± deviation LSA, left subclavian artery; TEVAR, thoracic endovascular aortic repair; ASA, American Society of Anaesthesiology Score.

4.2.2 Clinical outcomes

Clinical outcomes are shown in Table 4.3. All endografts were deployed satisfactorily with no conversion to open repair. There were no cases of on-table retrograde type A aortic dissection (RTAD). Ten patients died in hospital; 1 died from RTAD on day 5 (confirmed on post-mortem examination). This patient had a zone 2 TEVAR with carotid-subclavian bypass and suddenly became hypertensive on ITU, lost cardiac output, and died despite resuscitative efforts. This patient also suffered a large right sided cerebellar stroke having presented with dysarthria on day 1 post-operatively. One patient died of a massive myocardial infarction day 0; he was extubated and woke up briefly and suddenly suffered a cardiac arrest. He underwent a zone 0 TEVAR with rapid pacing. The third patient died from abdominal rupture of a type II TAAA secondary to chronic dissection; whilst on the ward he also became hypertensive and lost cardiac output and died despite resuscitative efforts. His zone 3 TEVAR 3 days prior was uneventful. Only one patient died of a post-TEVAR stroke; this patient underwent a zone 0 TEVAR with chimney stents to the IA. She sadly woke up with the dense left sided hemiplegia and dysphasia, was transferred to a rehabilitation ward and had a protracted stay where she aspirated and sadly died.

Of the remaining two patients who died of cardiac causes, one suffered a cardiac arrest on day 10 post-operatively, and the other patient developed hospital acquired pneumonia, acute kidney injury and heart failure day 23 post-operatively. Both patients underwent TEVAR for ruptured aneurysmal disease.

Four patients died of respiratory failure following TEVAR; one patient underwent a zone 0 TEVAR for ruptured DTAA with chimney implantation into the IA, one patient underwent zone 3 TEVAR for iatrogenic TBAD following CERAB procedure, one underwent emergency zone 2 TEVAR and carotid subclavian bypass for acute aortic dissection. The last patient underwent zone 2 TEVAR with coverage of the LSA for ruptured DTAA.

Five patients developed a clinical stroke during their in-hospital admission. The first patient (zone 2 TEVAR) is described above who developed a right sided cerebellar stroke with a large (1671mm^2) infarction in the right posterior circulation (mRS 4). The second patient is also described above underwent zone 0 TEVAR for ruptured DTAA with chimney to the IA and suffered a respiratory complication (mRS 4). This patient had infarcts to the left and right cerebral hemispheres in both the anterior and posterior circulations (total infarcted cerebral tissue 125mm^2). She suffered a dense right sided hemiplegia. The third patient underwent a zone 2 TEVAR with a scallop endograft for the LSA and complained of diplopia to the left eye day 1 post-operatively (mRS 2). His brain DW-MRI showed infarcts in the left anterior and posterior circulations, with the largest infarct (67mm^2) in the left posterior circulation. The fourth patient (zone 0 TEVAR) is described above who died of a stroke (total infarcted cerebral tissue 437mm^2, mRS 4). The final patient underwent a zone 2 TEVAR with a scallop endograft for the LSA and presented with diplopia in the left eye (mRS 2). Two infarcts located in the left posterior circulation only (total of 10mm^2 infarcted cerebral tissue) were detected on DW-MRI. The stroke mortality was 20% (1/5 patients).

Table 4.3 Clinical outcomes for 75 patients

Characteristics	Patients (n=75)
In-hospital complications	
Death	10 (13)
Cause of death	
Retrograde aortic dissection	1
Abdominal rupture	1
Respiratory failure	4
Cardiac	3
Stroke	1
Cardiac	3 (4)
Respiratory	9 (12)
Stroke	5 (7)
Spinal cord ischaemia	2 (3)
Retrograde aortic dissection	1 (13)
Gastrointestinal	0 (0)
Haemofiltration/dialysis	0 (0)
Lower limb	2 (3)
Wound related/pseudoaneurysm	6 (8)
Return to theatre	7 (9)
Length of ITU stay	4.3 ± 5.6
Length of hospital stay	9.1 ± 9.4

ITU, intensive care unit. Data are presented as n (%) or mean standard ± deviation

4.2.3 Intra-operative TCD-detected cerebral embolisation

Intra-operative TCD data was available for 61 patients; bilateral insonation was available for 50 patients, with data for the left side in 60 patients and data for the right side for 51 patients. Reasons for lack of data included no signal (n = 8), recording lost due to software malfunction (n = 2) and logistic reasons for example probe interfering with central line access or extra-anatomical bypass procedures (n = 10), not possible to conduct TCD at BSWH (n = 5).

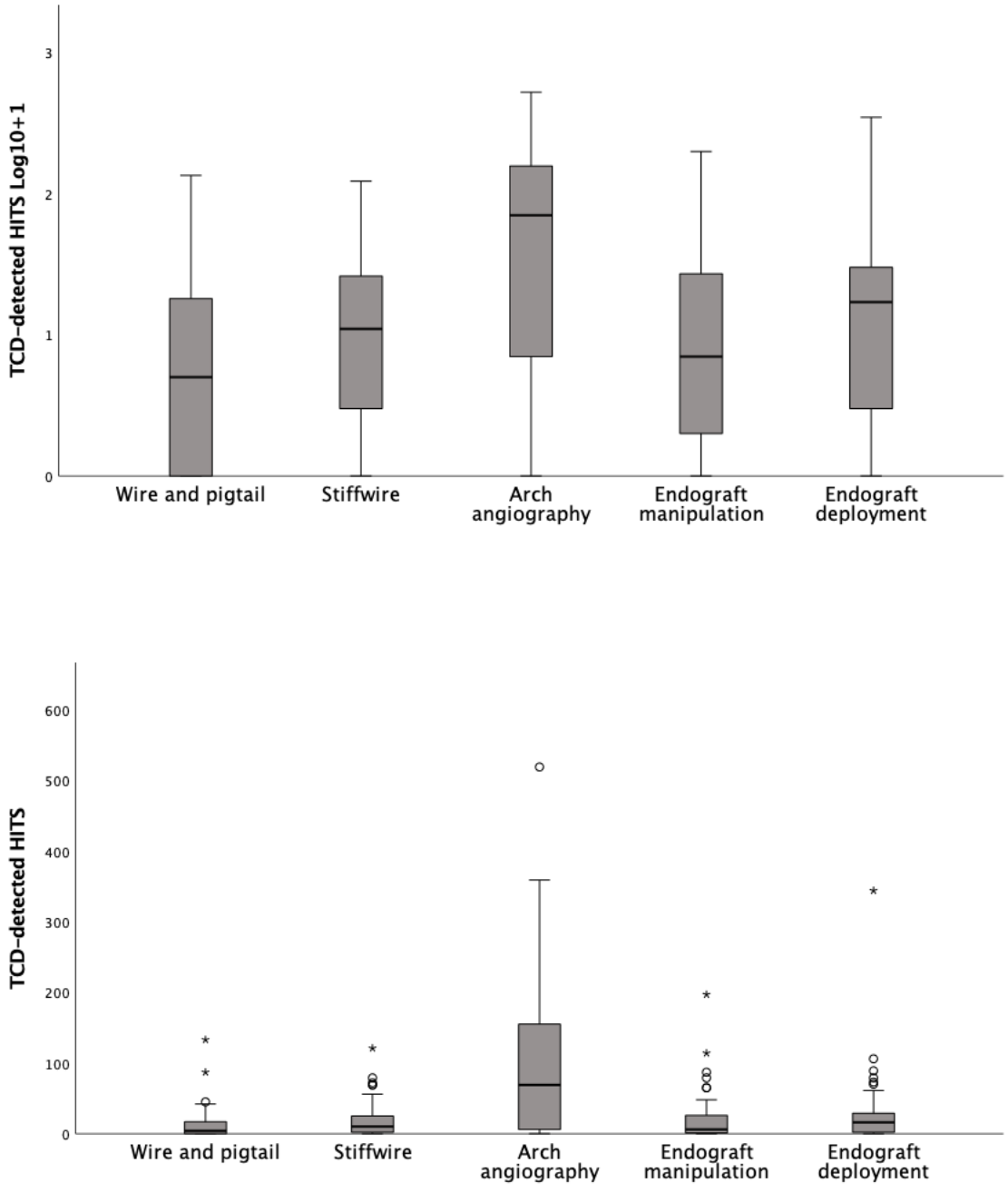
The left MCA was insonated in 58 patients (median depth 50mm, range 45-57) and the left ACA was insonated in the remaining patients. The right MCA was insonated in 47 patients (median depth 49mm,

range 46-58) and the right ACA was insonated in the remaining patients. HITS from the MCA and ACA for a given side were combined to aid data analysis.

The phase of TEVAR associated with the greatest number of TCD-detected HITS was arch angiography (Figures 4.1a), with most HITS found to be gaseous in composition (Figure 4.1b). There were significantly more HITS detected on the left side than the right side (figure 4.1c). Greater TCD-detected HITS were associated with higher arch atheroma grades, arch grades (Figure 4.1d-e respectively) with more gaseous HITS with higher grade (Figure 4.1f-g). Greater TCD-detected HITS were also observed with more severe deep white matter disease but not periventricular white matter disease (figure 4.1h-i, respectively). There were significantly more HITS detected in zone 1>2>3>4 (figure 4.1j-k). However there was no significant difference in the number of HITS according to aortic pathology (figure 4.1l-m).

Figure 4.1

a. TCD-detected HITS by procedural step for **undifferentiated data**



N = 61

The data was found to be extremely positively skewed with many extreme outliers. A Log_{10} +1 transformation of the data was necessary to graphically represent undifferentiated TCD-detected HITS according to procedural steps only. Despite the Log_{10} +1 transformation, the data remained positively skewed. The data below are the non-transformed data, and the non-parametric Friedman statistical test was used.

Wire and pigtail: median 4.0 (IQR 0.0-17.0)

Stiff wire: median 10.0 (IQR 2.0-25.0)

Arch angiography: median 69.0 (IQR 6.0-155.0)

Endograft manipulations: median 6.0 (IQR 1.0-26.0)

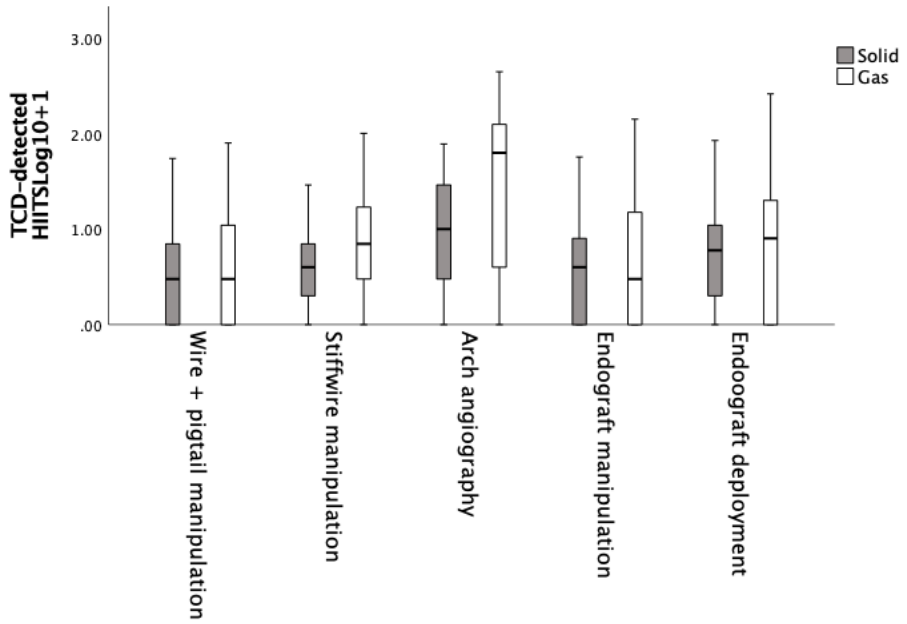
Endograft deployments: 16.0 (IQR 2-29.0)

Friedman test: $p < 0.001$

Pairwise comparisons were performed with a Bonferroni correction for multiple comparisons. Adjusted p values are presented. This post-hoc analysis revealed statistically significant differences in median number of TCD-detected HITS as shown below.

Group comparison for TCD-detected HITS	**P value**
Wire and pigtail and stiffwire	0.046
Wire and pigtail and endograft deployment	0.042
Wire and pigtail and arch angiography	<0.001
Endograft manipulation and arch angiography	<0.001
Stiffwire and arch angiography	<0.001
Endograft deployment and arch angiography	<0.001

b. TCD-detected HITS by procedural step and differentiated into **solid and gas**



N= 61

The data was found to be extremely positively skewed with many extreme outliers. A Log_{10} +1 transformation of the data was necessary to graphically represent differentiated TCD-detected HITS according to procedural steps only. Despite the Log_{10} +1 transformation, the data remained positively skewed. The data below are the non-transformed data, and the non-parametric Friedman statistical test was used.

Wire and pigtail solid: median 2.0 (IQR 0.0-6.0)

Wire and pigtail gas: median 2.0 (IQR 0.0 -10)

Stiffwire solid: median 3.0 (IQR 1.0-6.0)

Stiffwire gas: median 6.0 (IQR 2.0-16.0)

Arch angiography solid: median 9.0 (2.0-28.0)

Arch angiography gas: median 62.0 (3.0-124.0)

Endograft manipulations solid: median 3.0 (0.0-7.0)

Endograft manipulations gas: median 2.0 (0.0-14.0)

Endograft deployments solid: median 5.0 (1.0-10.0)

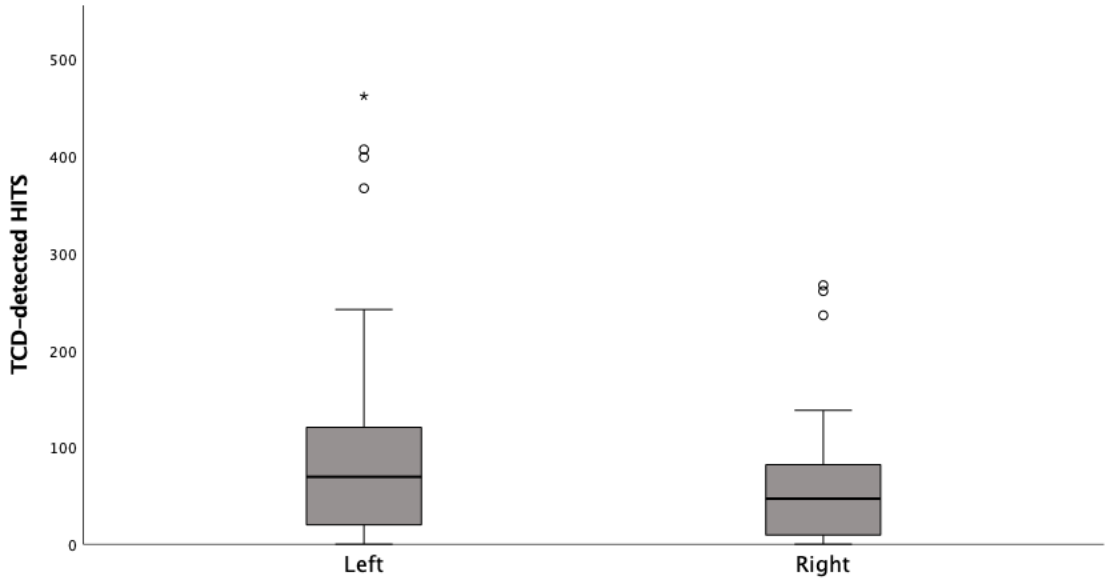
Endograft deployments gas: median 7.0 (0.0-19.0)

Friedman test: $p < 0.0001$

Pairwise comparisons were performed with a Bonferroni correction for multiple comparisons. Adjusted p values are presented. This post-hoc analysis revealed statistically significant difference in median number of TCD-detected HITS as shown below.

Group comparison for TCD-detected HITS	**P value**
Wire and pigtail solid /endograft deployment gas	<0.001
Wire and pigtail solid/arch angiography solid	<0.001
Wire and pigtail solid/stiffwire gas	<0.001
Wire and pigtail solid/arch angiography gas	<0.001
Wire and pigtail gas/arch angiography solid	0.004
Wire and pigtail gas and stiffwire gas	<0.001
Wire and pigtail gas and arch angiography gas	<0.001
Stiffwire solid and arch angiography solid	0.008
Stiffwire solid and stiffwire gas	0.001
Stiffwire solid and arch angiography gas	<0.001
Endograft manipulation solid and stiffwire gas	0.009
Endograft manipulation solid and arch angiography gas	<0.001
Endograft manipulation gas and stiff wire gas	0.041
Endograft manipulation gas and arch angiography gas	<0.001
Endograft deployment solid and arch angiography gas	<0.001
Endograft deployment gas and arch angiography gas	0.001
Arch angiography solid and arch angiography gas	0.012

c. TCD-detected HITS according to **left and right cerebral arteries**



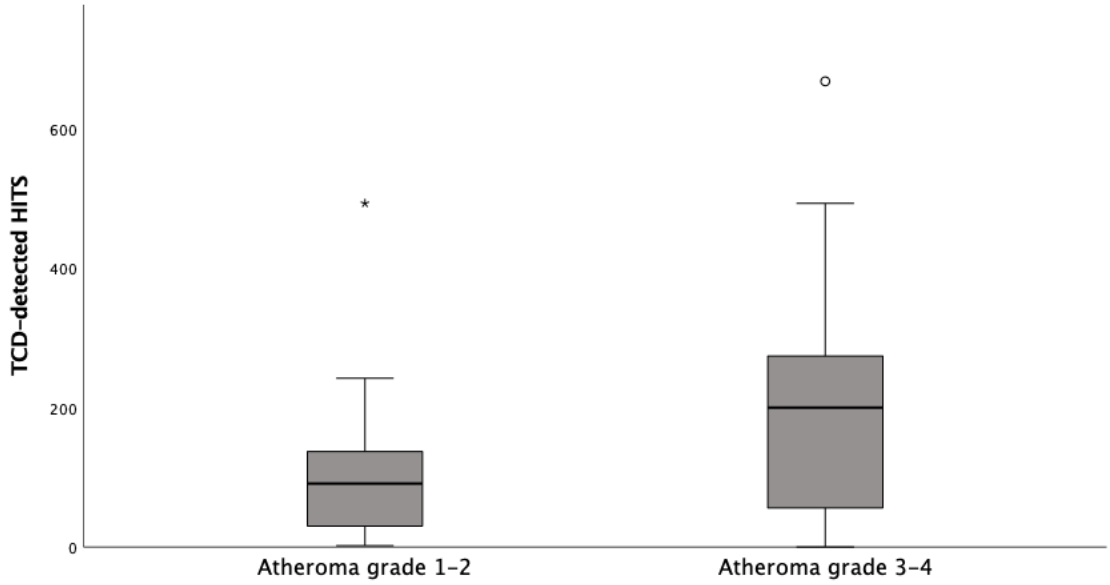
N = 61

Left: median 69.5 (IQR 20.0 – 119.25)

Right: median 47.5 (IQR 12.25-82.5)

Wilcoxon signed rank test: p=0.000033

d. TCD-detected HITS according to **atheroma grade**

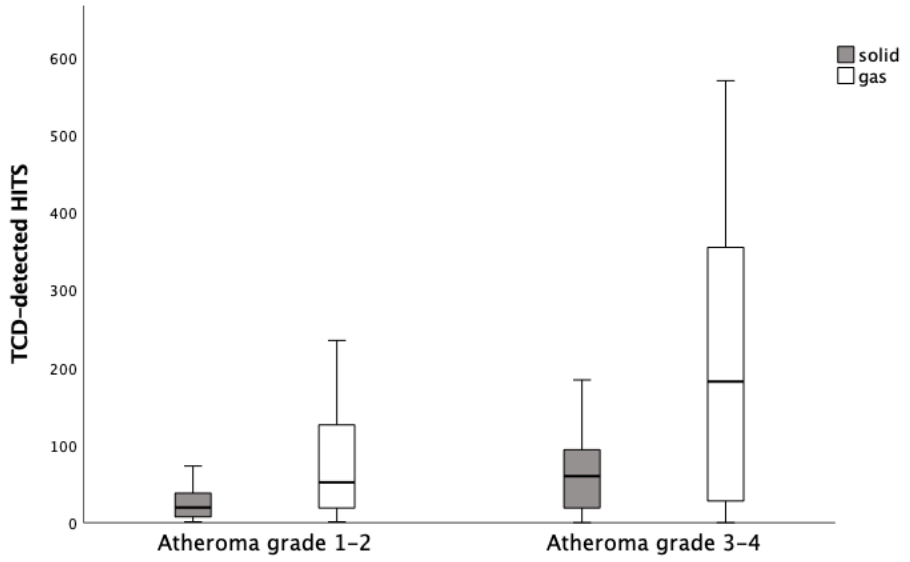


Grade 1-2: median 56.0 (IQR 28.0 – 128.0)

Grade 3-4: median 235.0 (IQR 117.5 – 340.0)

Mann-Whitney U test p = 0.004

e. Differentiated TCD-detected HITS according to **atheroma grade**



Grade 1-2 solid: median 19.5 (IQR 7.75-37.5)

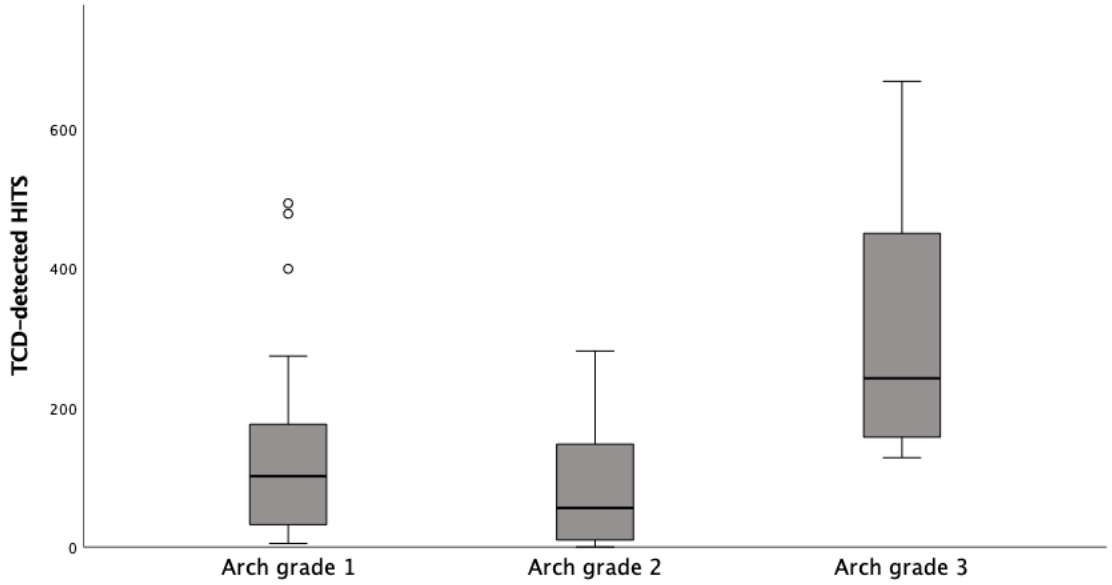
Grade 1-2 gas: median 52 (IQR 20-125)

Grade 3-4 solid: median 60 (IQR 19-94)

Grade 3-4 gas: median 182 (IQR 28-355)

Group comparison for differentiated TCD-detected HITS using Wilcoxon signed rank test	**P value**
Atheroma grade 1-2 solid and gas	<0.001
Atheroma grade 3-4 solid and gas	<0.001
Group comparison for differentiated TCD-detected HITS using Mann Whitney U test	
Atheroma grade 1-2 solid and atheroma grade 3-4 solid	0.004
Atheroma grade 1-2 gas and atheroma grade 3-4 gas	0.048

f. TCD-detected HITS according to **arch grade**



Arch grade 1: median 101.5 (IQR 33.5-174.75)

Arch grade 2: median 56.0 (IQR 10.0- 147.5)

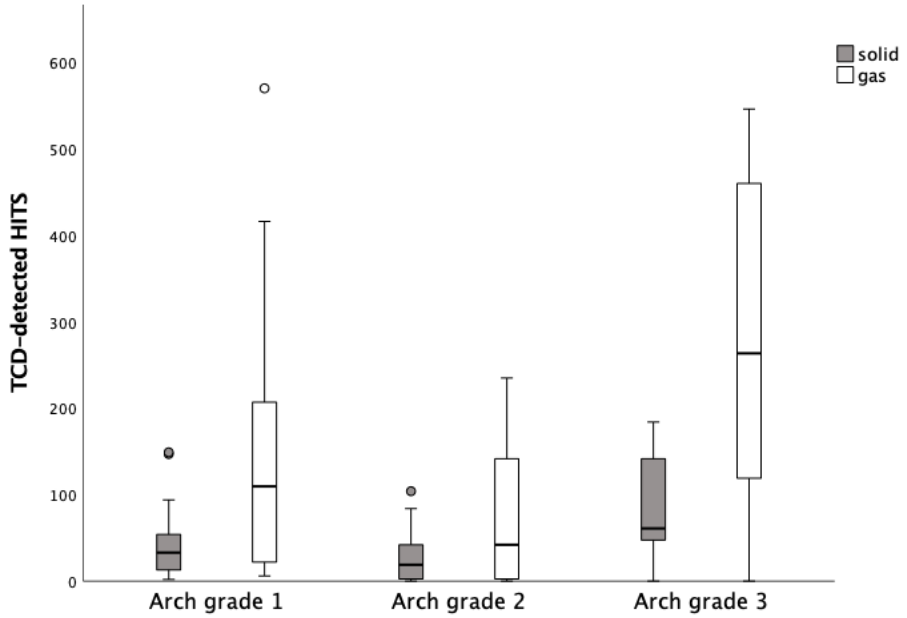
Arch grade 3: median 242 (IQR 157.5-450)

Kruskal Wallis test: p = 0.004

Pair wise comparisons were performed using Dunn's (1964) procedure with a Bonferroni correction for multiple comparisons. Adjusted p values are presented. This post hoc analysis revealed statistically significant differences in median number of TCD HITS between arch grade 3 and arch grade 2 (p=0.006).

Group comparison TCD-detected HITS	**P value**
Arch grade 1 and 2	0.561
Arch grade 2 and 3	0.006
Arch grade 1 and 3	0.176

g. Differentiated TCD-detected HITS according to **arch grade**



Arch grade 1 solid: median 33 (IQR 13-53.5)

Arch grade 1 gas: median 109.5 (23.5 – 205)

Arch grade 2 solid: median 19 (IQR 2.5-42)

Arch grade 2 gas: median 42(2.5-141.5)

Arch grade 3 solid: median 61 (IQR 48.25 -136.75)

Arch grade 3 gas: median 263 (121.5 – 439.5)

Group comparison for differentiated TCD-detected HITS using Wilcoxon signed rank test)	**P value**
Arch grade 1 gas and solid	<0.001
Arch grade 2 gas and solid	<0.001
Arch grade 3 gas and solid	0.063

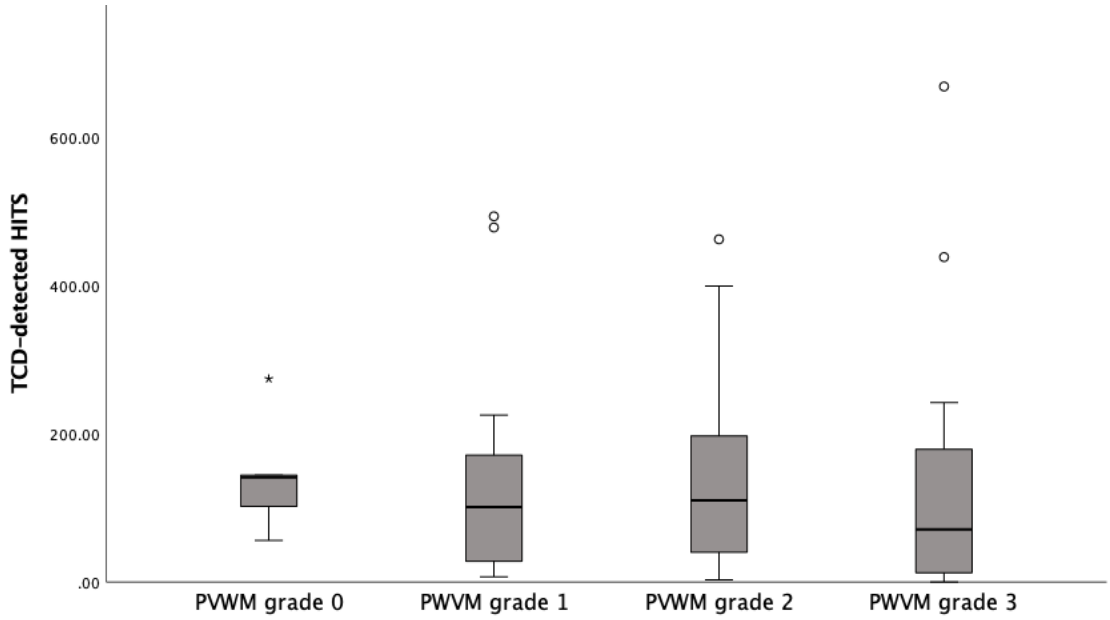
The Kruskal-Wallis test demonstrated significant differences between solid TCD-detected HITS for arch grade 1, 2 and 3 (p=0.024). On post-hoc analysis, pairwise comparisons with a Bonferroni correction for multiple comparisons revealed statistically significant differences in median number of TCD-detected HITS for arch grade 2 and 3 only.

Group comparison for solid TCD-detected HITS	P value
Arch grade 1 and 2	0.412
Arch grade 2 and 3	0.024
Arch grade 1 and 3	0.309

The Kruskal-Wallis test demonstrated significant differences between gaseous TCD-detected HITS for arch grade 1, 2 and 3 (p=0.013). On post-hoc analysis, pairwise comparisons with a Bonferroni correction for multiple comparisons revealed statistically significant differences in median number of TCD-detected HITS for arch 2 and 3.

Group comparison for gas TCD-detected HITS	P value
Arch grade 1 and 2	0.126
Arch grade 2 and 3	0.022
Arch grade 1 and 3	0.590

h. TCD-detected HITS according to Fazekas **periventricular white matter (PVWM) disease**



PVWM grade 0: 141.0 median (IQR 102.0 – 144.0)

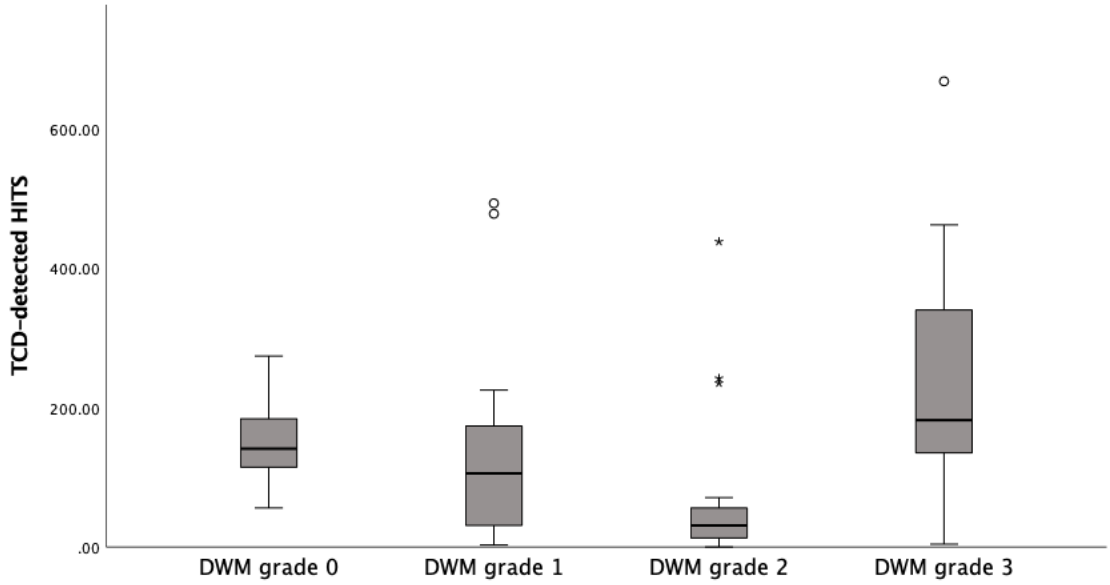
PVWM grade 1: 101 median (IQR 28.0-171.0)

PVWM grade 2: median 110.0 (IQR 40.0-197.0)

PVWM grade 3: median 71.0 (IQR 12.5-179.0)

Kruskal Wallis test: p = 0.723

i. TCD-detected HITS according to Fazekas **deep white matter (DWM) disease**



DWM grade 0: median 141.0 (IQR 114.5 – 184.0)

DWM grade 1: median 105.5 (IQR 31.5- 172.25)

DWM grade 2: median 31.0 (IQR 13.25 – 56.0)

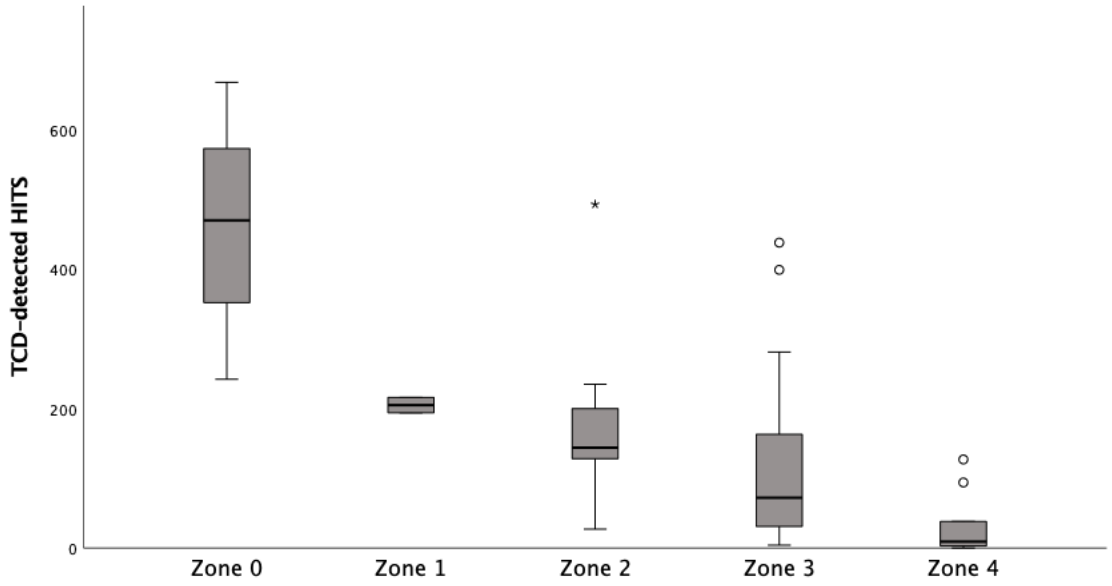
DWM grade 3: median 182.0 (IQR 135.0 -340.0)

Kruskal Wallis test: p=0.006

Pair wise comparisons were performed using Dunn's (1964) procedure with a Bonferroni correction for multiple comparisons. Adjusted p values are presented. This post hoc analysis revealed statistically significant differences in median number of TCD HITS between DWM disease grade 2 and 3 (p=0.006).

Group comparison for TCD-detected HITS	**P value**
DWM disease grade 2 and 1	0.261
DWM disease grade 2 and 0	0.138
DWM disease grade 2 and 3	0.006
DWM disease grade 1 and 0	1.000
DWM disease grade 1 and 3	0.521
DWM disease grade 0 and 3	1.000

j. TCD-detected HITS according to **proximal landing zone**



Zone 0: median 470.0 (IQR 407.0 – 525.5)

Zone 1: median 205.0 (IQR 199.5 – 210.5)

Zone 2: median 144 (IQR 128 – 200)

Zone 3: median 72 (IQR 31-163)

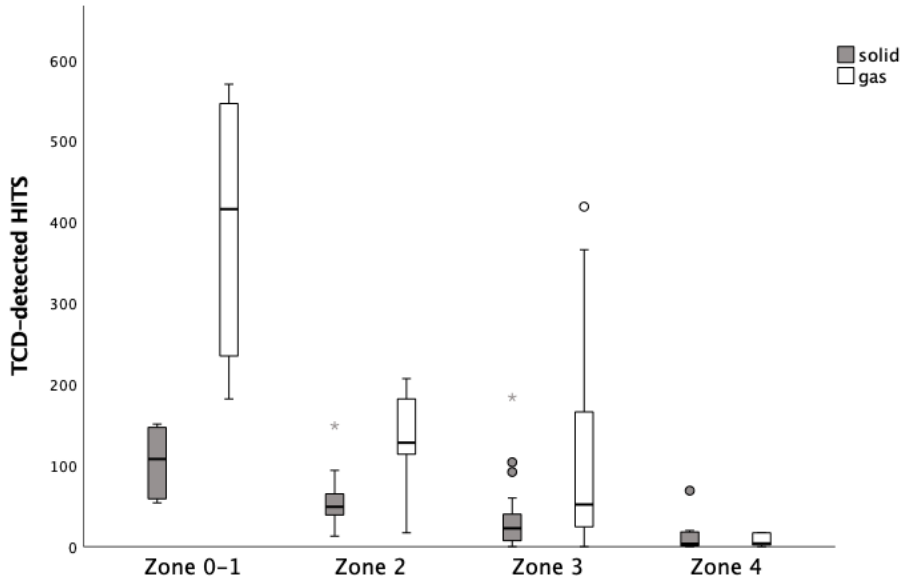
Zone 4: median 9 (IQR 3-32)

Kruskal Wallis test: p = 0.000016 (zone 0 and 1 were considered one zone for statistical analyses).

Pair wise comparisons were performed using Dunn's (1964) procedure with a Bonferroni correction for multiple comparisons. Adjusted p values are presented. The results of this post hoc analysis are presented below.

Group comparison for TCD-detected HITS	**P value**
Zone 4 and zone 3	0.039
Zone 4 and zone 2	0.002
Zone 4 and zone (0-1)	<0.0001
Zone 3 and zone 2	0.636
Zone 3 and zone (0-1)	0.010
Zone 2 and (0-1)	0.459

k. Differentiated TCD-detected HITS according to **proximal landing zone**



Zone 0-1 solid: median 108 (IQR 65.25-143.25)

Zone 0-1 gas: median 416 (259-546)

Zone 2 solid: median 49 (39-65)

Zone 2 gas: median 128(114-182)

Zone 3 solid: median 22.5 (7.75-38)

Zone 3 gas: median 52 (25.75-157)

Zone 4 solid: median 3.5 (1.25-15.5)

Zone 4 gas: median 4(2-14.5)

Group comparison for differentiated TCD-detected HITS using Wilcoxon signed rank test)	P value
Zone (0-1)gas and solid	0.028
Zone 2 gas and solid	0.001
Zone 3 gas and solid	<0.001
Zone 4 gas and solid	0.204

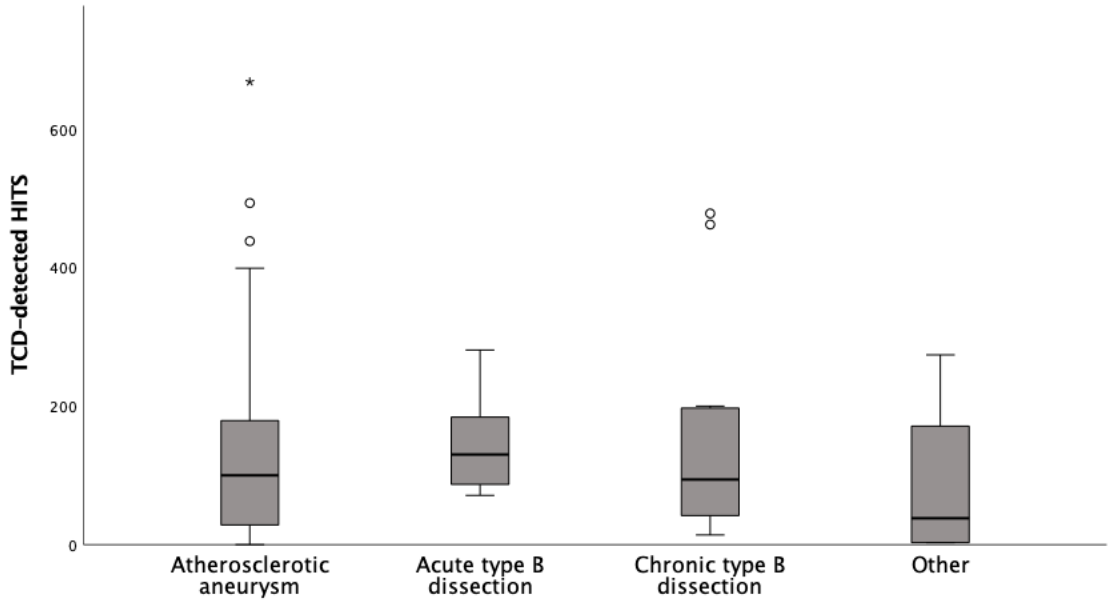
The Kruskal-Wallis test demonstrated significant differences between solid TCD-detected HITS for zone 0-1, zone 2, zone 3 and 4 ($p<0.001$). On post-hoc analysis, pairwise comparisons with a Bonferroni correction for multiple comparisons revealed statistically significant differences in median number of TCD-detected HITS zone 4 and zone 2, zone 4 and zone (0-1), and zone 3 and zone 3 and zone (0-1).

Group comparison for solid TCD-detected HITS	P value
Zone 4 and zone 3	0.336
Zone 4 and zone 2	0.002
Zone 4 and zone (0-1)	<0.001
Zone 3 and zone 2	0.086
Zone 3 and zone (0-1)	0.007
Zone 2 and zone (0-1)	1.000

The Kruskal-Wallis test demonstrated significant differences between gaseous TCD-detected HITS zone 0-1, zone 2, zone 3 and 4 ($p<0.001$). On post-hoc analysis, pairwise comparisons with a Bonferroni correction for multiple comparisons revealed statistically significant differences in median number of TCD-detected HITS for zone 4 and zone 2, zone 4 and zone (0-1), and zone 3 and zone (0-1).

Group comparison gas TCD-detected HITS)	P value
Zone 4 and zone 3	0.115
Zone 4 and zone 2	0.014
Zone 4 and zone (0-1)	<0.001
Zone 3 and zone 2	1.000
Zone 3 and zone (0-1)	0.007
Zone 2 and zone (0-1)	0.237

l. TCD-detected HITS according to **pathology**



Atherosclerotic aneurysm (including chronic PAU and coarctation): median 100.0 (IQR 29.25 – 177.5)

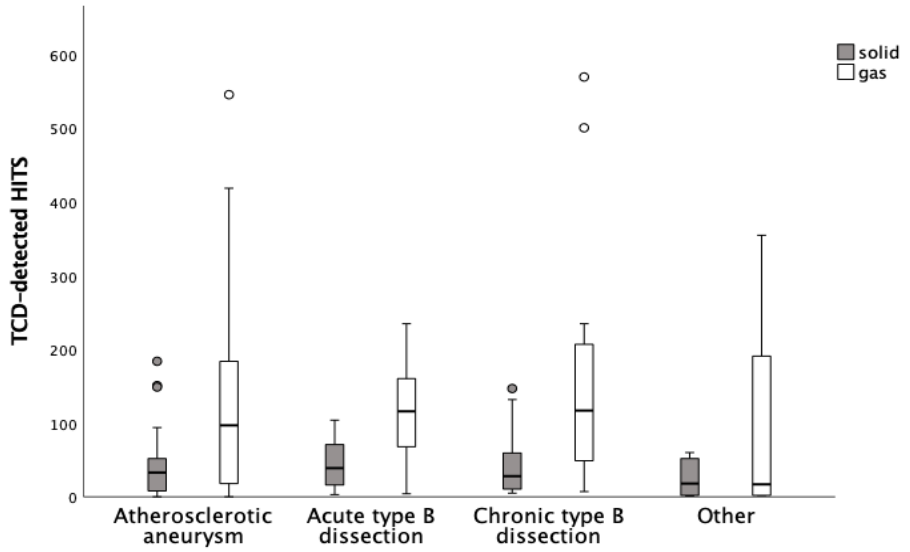
Acute type B dissection (including PAU and IMH): median 130.0 (IQR 94.5 – 164.0)

Chronic Type B dissection: median 94.0 (IQR 42.0-197.0)

Other (including trauma, mycotic aneurysm, endoleak relining): median 38.0 (3.0-171.0)

Kruskal Wallis test: p = 0.630

m. Differentiated TCD-detected HITS by **pathology**



Atherosclerotic aneurysm solid: median 33 (IQR 8-52)

Atherosclerotic aneurysm gas: median 97.5 (IQR 18-184)

Acute type b dissection solid: median 39 (IQR 17.5-70)

Acute type b dissection gas: median 116 (IQR 81-139.75)

Chronic type b dissection solid: median 28 (IQR 10.5-59.5)

Chronic type b dissection gas: median 117 (IQR 49-207)

Other solid: median 18 (IQR 2-52)

Other gas: median 17 (IQR 2-191)

Group comparison for differentiated TCD-detected HITS using Wilcoxon signed rank test)	P value
Atherosclerotic aneurysm solid and gas	<0.001
Acute type b dissection solid and gas	0.012
Chronic type b dissection solid and gas	0.003
Other solid and gas	0.197

Distributions according to gas and solid TCD-detected HITS were not similar for all groups as assessed by visual inspection of the boxplot. A post hoc analysis was undertaken.

The Kruskal-Wallis test demonstrated no differences between solid TCD-detected HITS for the various pathologies (p=0.732), No further analysis was conducted.

The Kruskal-Wallis test demonstrated no differences between gaseous TCD-detected HITS for the various pathologies (p=0.664). No further analysis was conducted.

4.2.4 Clinical stroke, DW-MRI and TCD outcomes

A total of 65 out of 75 patients underwent a DW-MRI brain scan according to the protocol. Ten patients did not undergo an MRI due to post-operative death 0 (n = 2) claustrophobia/refusal (n=3), pacemaker insertion (n =1), medically unstable (n = 2), unable to access scan (n = 1), penile implant (n=1).

Post-operative scans were performed at a median of 4 days (IQR 3-6) following TEVAR. The clinical stroke rate was 6.6% (5/76). Three strokes were in Zone 2 and two strokes were in Zone 0. The DW-MRI infarction rate (inclusive of those who had stroke was 43.1% (28/65). The DW-MRI infarction rate excluding the 5 patients who had a stroke was 38% (23/60).

A total of 116 new DW-MRI infarcts (median 0 (IQR 0-1, range 0-31)), with a total DW-MRI infarct surface area of 3736mm^2 (median 0 (IQR 0-34) were identified. Sixteen patients (25%) had more than one DW-MRI infarct, and bilateral infarcts were observed in 10 patients (15%). There was an even distribution of DW-MRI infarcts with respect to laterality; 58(50%) infarcts were in the left hemisphere, and 58 (50%) infarcts were in the right hemisphere. There was also a relatively even distribution of infarcts between the anterior and posterior vascular territories with 56 (48%) infarcts located in the anterior circulation and 53 (46%) located in the posterior circulation. Seven (6%) infarcts were in borderzone regions. The distribution of the DW-MRI infarcts is described in Table 4.4

Table 4.4 MRI features of the 28 patients with an infarct

Patient number	**MRI outcome**	**Clinical outcome**	**Characteristic of infarct** ***No.*** ***Surface area*** ***Territory***
1	DW-MRI infarct	NAD	2 225mm^2 Left posterior circulation Right posterior circulation
2	DW-MRI infarct	Stroke	5 1679mm^2 Left anterior circulation Right posterior circulation
3	DW-MRI infarct	NAD	1 30mm^2 Right anterior circulation
4	DW-MRI infarct	NAD	1 58mm^2 Right anterior circulation
5	DW-MRI infarct	Stroke	13 125mm^2 Left anterior circulation Right anterior circulation Left posterior circulation Right posterior circulation
6	DW-MRI infarct	NAD	10 48mm^2 Left anterior circulation Right anterior circulation

			Left posterior circulation Right posterior circulation
7	DW-MRI infarct	NAD	4 58mm^2 Right anterior circulation Left borderzone
8	DW-MRI infarct	NAD	1 6mm ^{2} Left borderzone
9	DW-MRI infarct	Stroke	5 71mm^2 Left anterior circulation Left posterior circulation
10	DW-MRI infarct	NAD	3 58mm^2 Left posterior circulation Right posterior circulation
11	DW-MRI infarct	NAD	3 42mm^2 Left posterior circulation
12	DW-MRI infarct	NAD	3 34mm^2 Right anterior circulation Right posterior circulation
13	DW-MRI infarct	NAD	1 6mm^2 Right anterior circulation
14	DW-MRI infarct	NAD	1 12mm^2 Left anterior circulation
15	DW-MRI infarct	NAD	5 27mm^2 Left anterior circulation Left posterior circulation Left borderzone
16	DW-MRI infarct	NAD	6 48mm^2 Left anterior circulation Right anterior circulation Left posterior circulation Right posterior circulation
17	DW-MRI infarct	NAD	1 6mm^2 Right anterior circulation
18	DW-MRI infarct	NAD	1 24mm^2 Right anterior circulation
19	DW-MRI infarct	NAD	2 26mm^2 Left posterior circulation

			Right posterior circulation
20	DW-MRI infarct	Stroke	31 437mm^2 Left anterior circulation Right anterior circulation Left posterior circulation Right posterior circulation Left borderzone Right borderzone
21	DW-MRI infarct	NAD	1 72mm^2 Left anterior circulation
22	DW-MRI infarct	Stroke	2 10mm^2 Left posterior circulation
23	DW-MRI infarct	NAD	1 36mm^2 Right anterior circulation
24	DW-MRI infarct	NAD	1 2mm^2 Right posterior circulation
25	DW-MRI infarct	NAD	1 20mm^2 Left anterior circulation
26	DW-MRI infarct	NAD	5 44mm^2 Left posterior circulation
27	DW-MRI infarct	NAD	5 265mm^2 Right anterior circulation Left posterior circulation Right posterior circulation
28	DW-MRI infarct	NAD	1 12mm^2 Left anterior circulation

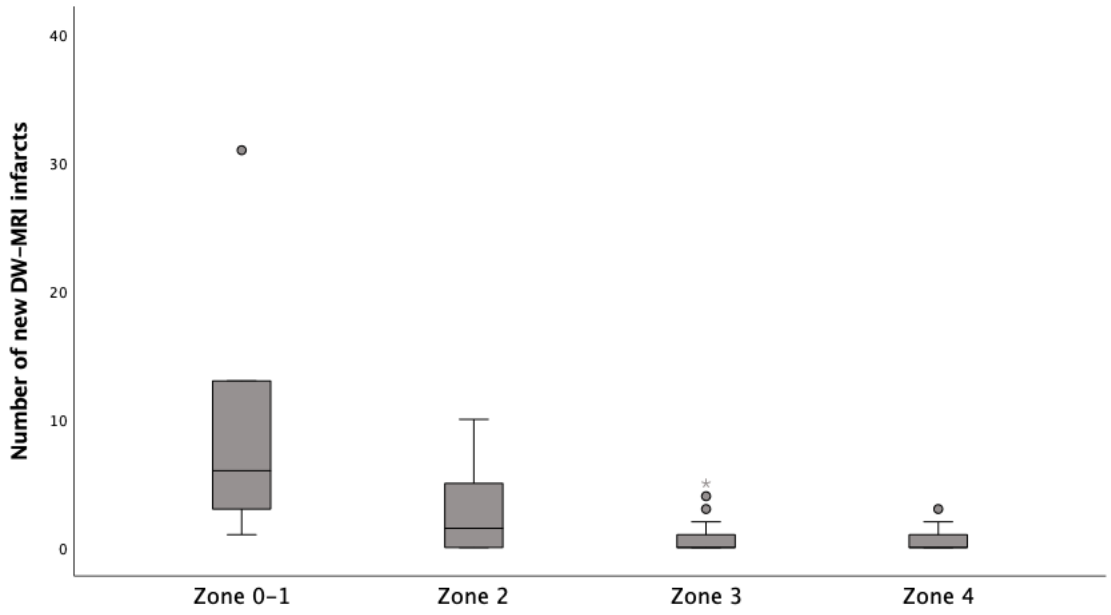
There was a significant difference in the number and surface area of infarcts according to PLZ. Zone 0 and 1 TEVAR were associated with the greatest number and largest surface area of new DW-MRI infarcts (figure 4.2.a and b). The greatest number of infarcts and largest surface area of infarcts were observed in patients with acute type B aortic dissection; however, this was not statistically significant (figure 4.2c and d).

Median number of TCD-detected HITS was highest in patients who developed a stroke, followed by those with new DW-MRI infarcts. Patients with no MRI abnormalities had the lowest number of TCD-detected HITS (figure 4.3a). A similar trend was observed when TCD-detected HITS were analysed according to solid/gas differentiation, however this was not statistically significant (figure 4.3b).

Statistically significant correlations were observed between number and surface area of new DW-MRI infarcts and solid and gaseous TCD-detected HITs, respectively (figures 4.4a and b).

Figure 4.2

a. Distribution of number of DW-MRI infarcts according to **proximal landing zone**



N=65

Zone 0+1: median 6.0 (IQR 3.0-13.0)

Zone 2: median 1.5 (IQR 0.0-5.5)

Zone 3: median 0.0 (IQR 0.0-1.0)

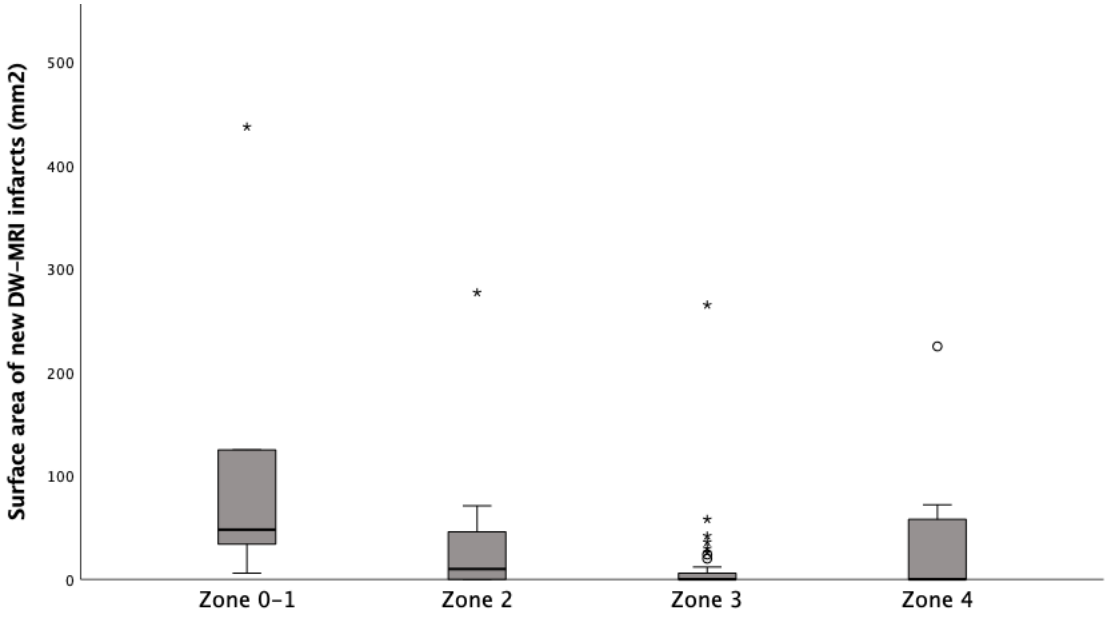
Zone 4: median 0.0 (IQR 0.0-1.0)

Kruskal Wallis test: p=0.001

Pair wise comparisons were performed using Dunn's (1964) procedure with a Bonferroni correction for multiple comparisons. Adjusted p values are presented. The results of this post hoc analysis are presented below.

Group comparison	**P value**
Zone 3 and zone 4	1.000
Zone 3 and zone 2	0.160
Zone 3 and zone (0-1)	0.002
Zone 4 and zone 2	0.695
Zone 4 and (0-1)	0.013
Zone 2 and zone (0-1)	0.363

b. Distribution of DW-MRI infarct surface area according to **proximal landing zone**



N=65 (1 patient excluded from graph as outlier for scaling purposes but not excluded from statistical analysis)

Zone 0+1: median 48.0 (IQR 34.0-125.0)

Zone 2: median 11.0 (IQR 0.0-53.75)

Zone 3: median 0.0 (IQR 0.0-7.5)

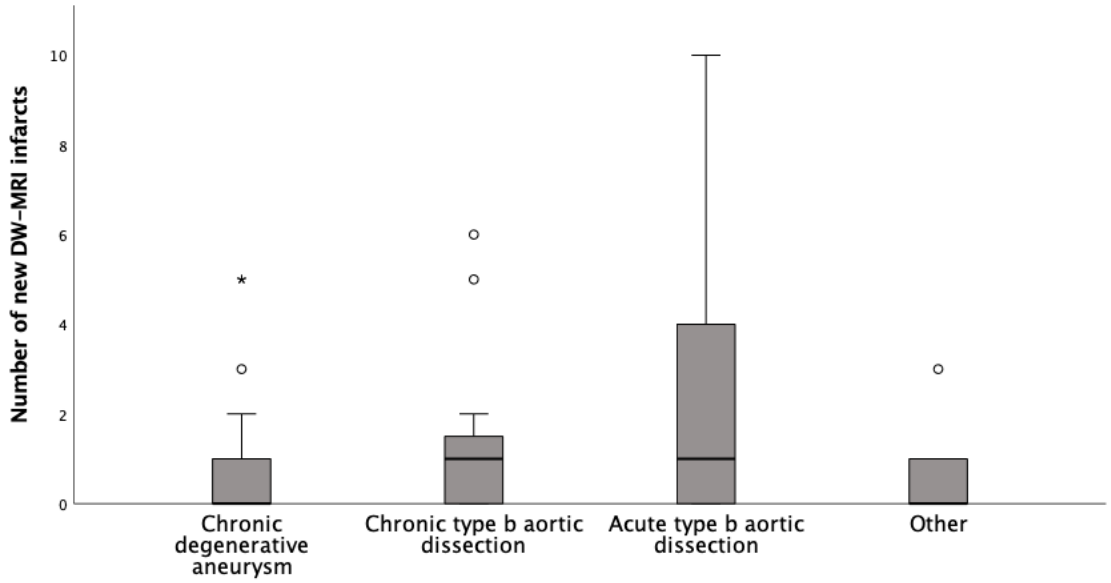
Zone 4: median 0.0 (IQR 0.0-58)

Kruskal Wallis test: p=0.008

Pair wise comparisons were performed using Dunn's (1964) procedure with a Bonferroni correction for multiple comparisons. Adjusted p values are presented. The results of this post hoc analysis are presented below.

Group comparison	**P value**
Zone 3 and zone 4	1.000
Zone 3 and zone 2	0.292
Zone 3 and zone (0-1)	0.012
Zone 4 and zone 2	1.000
Zone 4 and zone (0-1)	0.173
Zone 2 and zone (0-1)	0.746

c. Distribution of number of DW-MRI infarcts according to **pathology**



N=65 (6 patients excluded from graph as outliers for scaling purposes but not excluded from statistical analysis)

Chronic degenerative aneurysm (including chronic PAU and coarctation): median 0.0 (IQR 0.0-1.0)

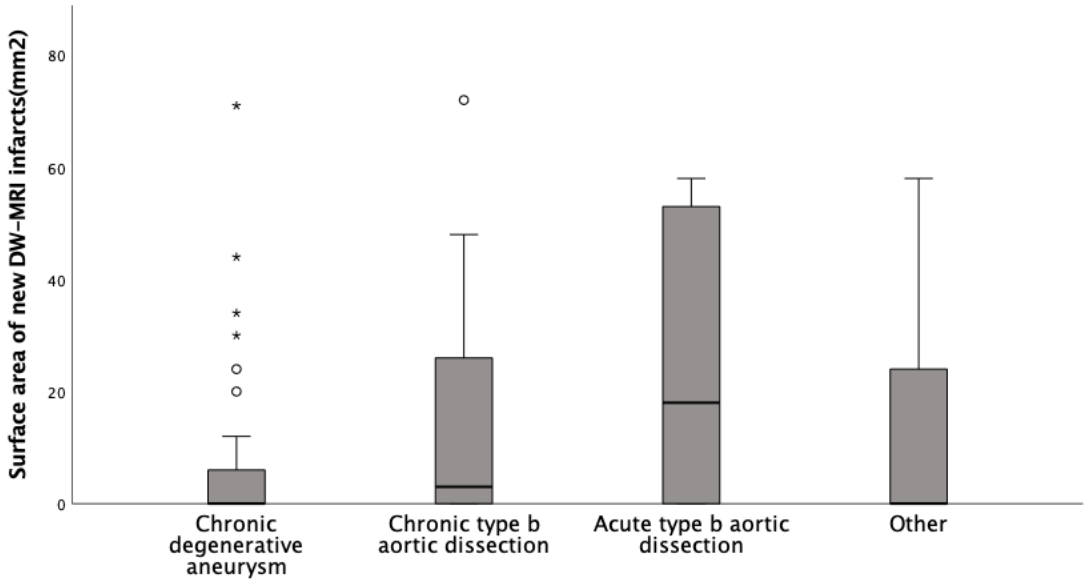
Chronic type B aortic dissection: median 1.0 (IQR 0.0-1.6)

Acute aortic dissection: median 1.0 (IQR 0.0-4.0)

Other (trauma, endoleak relining, mycotic aneurysm): median 0.0 (IQR 0.0-1.0)

Kruskal Wallis test: p = 0.54

d. Distribution of DW-MRI infarct surface area according to **pathology**



N=65 (6 patients excluded from graph as outliers for scaling purposes but not excluded from statistical analysis)

Chronic degenerative aneurysm (including chronic PAU and coarctation): median 0.0 (IQR0.0-18.0)

Chronic type B aortic dissection: median 6.0 (IQR 0.0-37.0)

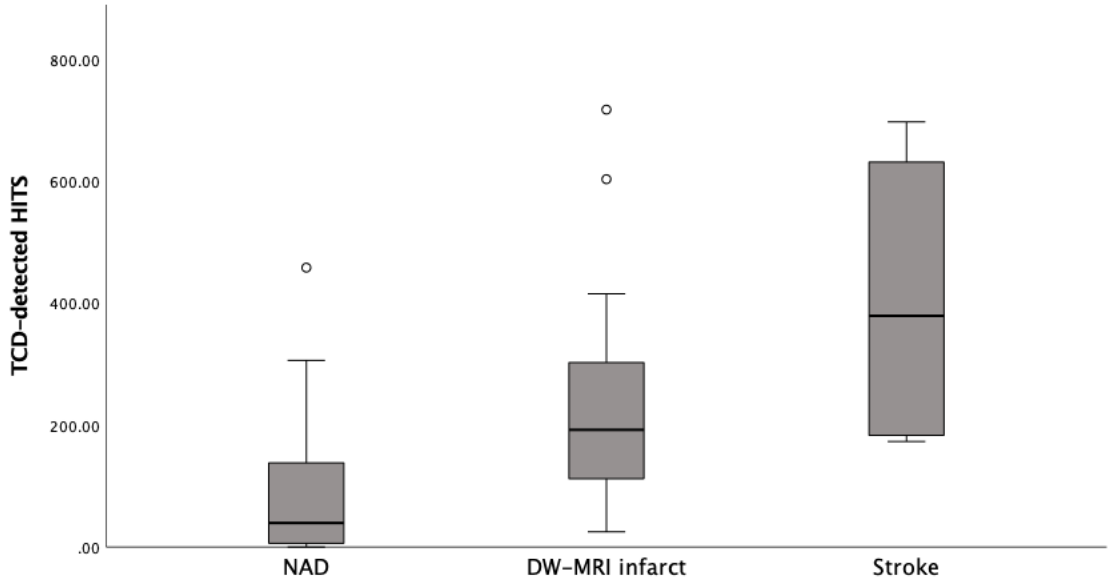
Acute aortic dissection: median 36.0 (IQR 0.0-58.0)

Other(trauma, endoleak relining, mycotic aneurysm: median 0.0 (IQR 0.0-24.0)

Kruskal Wallis test: 0.484

Figure 4.3

a. TCD-detected HITS according to **clinical outcome**



N=56 with complete TCD, DW-MRI and stroke evaluation (*N= 65 DW-MRI, N= 61 TCD, N= 75 Stroke evaluation)*

No abnormality detected (NAD): median 39.5 (IQR 5.5 – 117.0)

Diffusion-weighted magnetic resonance infarcts (DW-MRI infarct): median 188.0 (97.25 – 301.75)

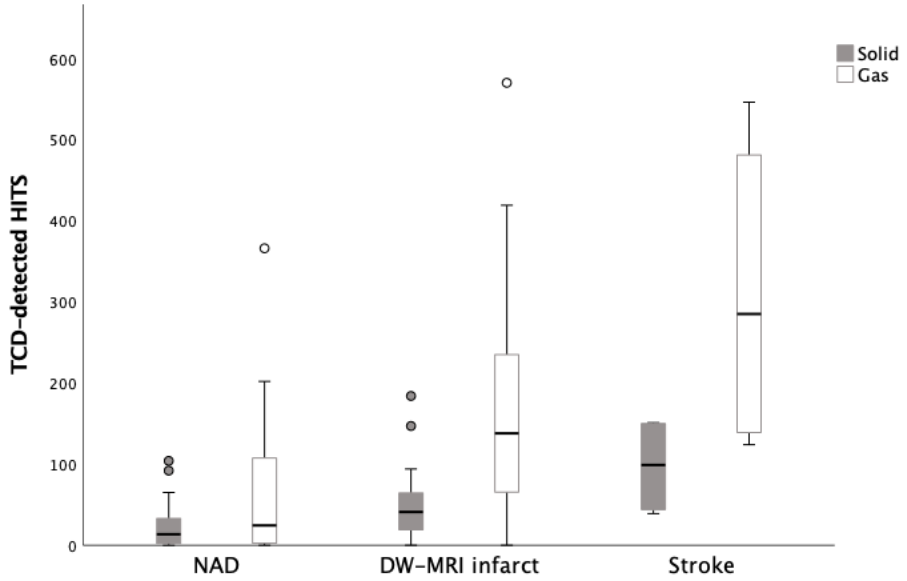
Stroke: median 379.0 (IQR 188.0 – 598.0)

Kruskal Wallis test: p = 0.001

Pair wise comparisons were performed using Dunn's (1964) procedure with a Bonferroni correction for multiple comparisons. Adjusted p values are presented. The results of this post hoc analysis are presented below.

Group comparison of TCD detected HITS	P value
NAD and DW-MRI infarct	0.010
NAD and stroke	0.017
DW-MRI infarct and stroke	0.780

b. Differentiated TCD-detected HITS according to **clinical outcome**



N=56 with complete TCD, DW-MRI and stroke evaluation (*N= 65 DW-MRI, N= 61 TCD, N= 75 Stroke evaluation)*

NAD solid: median 13.5 (IQR 2.0-33.0)

NAD gas: median 24.5 (IQR 2.75-102.75)

DW-MRI infarct solid: median 41.0 (IQR 19.5-62.25)

DW-MRI infarct gas: median 138.0 (IQR 79.25-235)

Stroke solid: median 99.0 (IQR 46.5-149.5)

Stroke gas: median 285.0 (IQR 146.5- 448.5)

Group comparison of differentiated TCD detected HITS using Wilcoxon signed rank test	**P value**
NAD gas and solid	<0.001
DW-MRI infarct gas and solid	<0.001
Stroke gas and solid	0.068

The Kruskal-Wallis test demonstrated significant differences between solid TCD-detected HITS for NAD, DW-MRI infarct, and stroke (p=0.001). On post-hoc analysis, pairwise comparisons with a Bonferroni correction for multiple comparisons revealed statistically significant differences in median number of TCD-detected HITS for NAD and DW-MRI infarct and NAD and stroke.

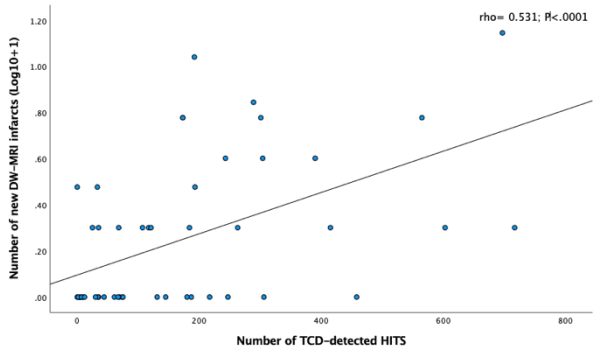
Group comparison solid TCD-detected detected HITS	**P value**
NAD and DW-MRI infarct	0.029
NAD and stroke	0.016
DW-MRI infarct and stroke	0.549

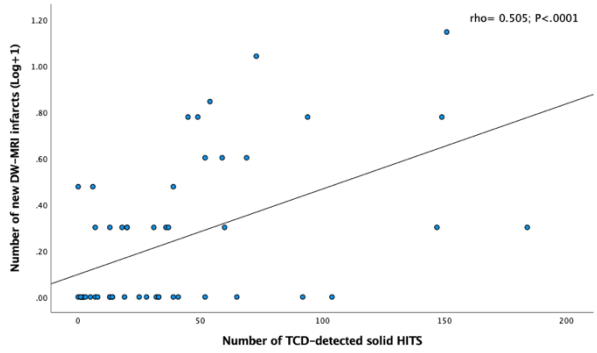
The Kruskal-Wallis test demonstrated significant differences between gaseous TCD-detected HITS for NAD, DW-MRI infarct, and stroke (p=0.003). On post-hoc analysis, pairwise comparisons with a Bonferroni correction for multiple comparisons revealed statistically significant differences in median number of TCD-detected HITS for NAD and DW-MRI infarct and NAD and stroke

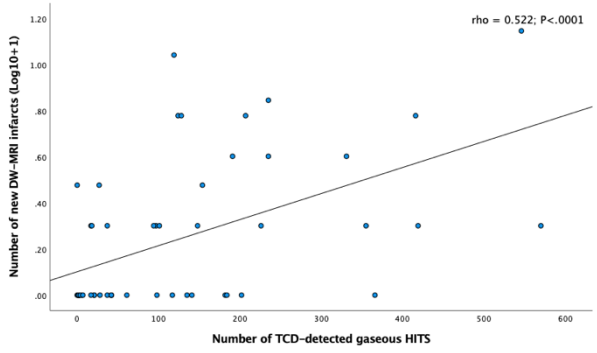
Group comparison (gas detected HITS)	**P value**
NAD and DW-MRI infarct	0.008
NAD and stroke	0.016
DW-MRI infarct and stroke	0.791

Figure 4.4

a. Correlation between number of TCD-detected HITs, solid and gaseous TCD-detected HITS, and number of new DW-MRI infarcts.



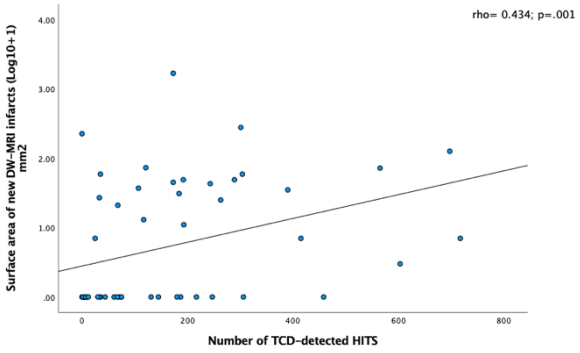


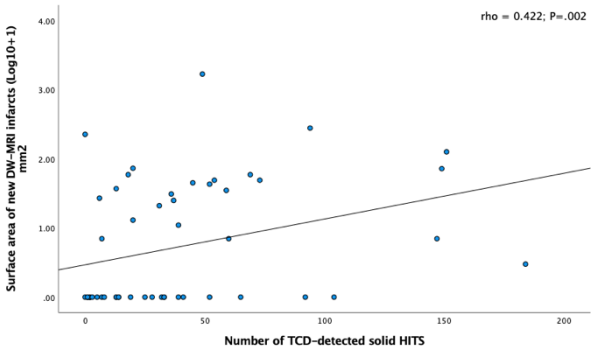


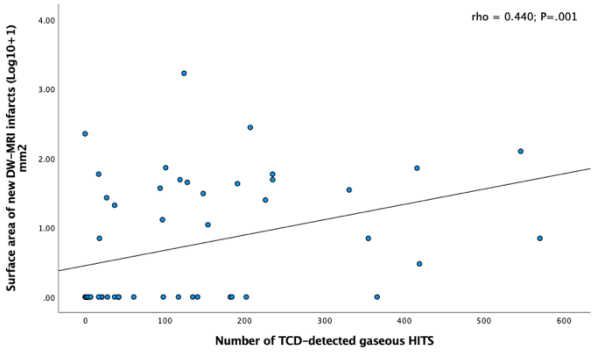
N=56 with complete TCD and DW-MRI (*N= 65 DW-MRI, N= 61 TCD).*

Number of DW-MRI infarct data are transformed to the $\log_{10}$ +1 for graphical representation. Spearman test was used on the non-transformed data.

b. Correlation between number of TCD-detected HITs, solid and gaseous TCD-detected HITS, and surface area of new DW-MRI infarcts.







N=56 with complete TCD and DW-MRI (*N= 65 DW-MRI, N= 61 TCD).*

Surface area of DW-MRI infarct data are transformed to the $\log_{10}+1$ for graphical representation. Spearman test was used on the non-transformed data.

4.2.5 Predictors of TCD-detected HITS

On univariate linear regression, only zone 0-1 and zone 2 were significant predictors of TCD-detected HITS. Age, previous stroke, PVWM, DWM, arch grade, arch atheroma were not found to be significant predictors.

Table 4.5 Predictors of TCD-detected HITS on univariate linear regression analysis

Risk factor	Exp (B)	CI	P value
Zone 0-1	3.96	3.14-5.00	<0.001
Zone 2	3.06	2.50-3.76	0.001

4.2.6 Predictors of Stroke and DW-MRI infarcts

On univariable analysis, arch grade 2-3, PLZ 0-1 and 2, total TCD-detected HITS, solid HITS, and gaseous HITS, infarct number and surface area all significantly predicted the development of stroke (Table 4.6).

Table 4.6 Predictors of stroke on univariate logistic regression analysis

Risk factor	Exp (B)	CI	P value
Arch atheroma 2-3	10.4	1.43-212	0.042
Zone 0-1	8.67	0.977-66.1	0.036
Zone 2	7.25	1.09-59.8	0.040
HITS	1.01	1.01-1.02	0.023
Solid HITS	1.02	1.01-1.03	0.022
Gas HITS	1.01	1.02-1.04	0.026
DW-MRI number	1.59	1.19-2.49	0.010
DW-MRI surface area	1.01	1.02-1.04	0.02

Predictors of new DW-MRI infarcts included total TCD-detected HITS, solid HITS, and gaseous HITS. PLZ 3 was found to reduce the risk of new DW-MRI infarcts (Table 4.7).

Table 4.7 Predictors of new DW-MRI infarct on logistic regression

Risk factor	Exp (B)	CI	P value
HITS	1.01	1.01-1.03	0.004
Solid HITS	1.03	1.01-1.05	0.011
Gas HITS	1.01	1.01-1.02	0.0035
Zone 3	0.208	0.05-0.66	0.10

None of these variables could be confirmed by multivariable analysis for stroke or for new DW-MRI infarcts as the dependant variable. Other demographic and operative variables such as age, sex, previous stroke/TIA, hypertension, diabetes mellitus, hypercholesterolaemia, COPD, chronic kidney disease, smoking, atrial fibrillation, antiplatelet and anticoagulant, statin, grade 2 and 3 DWM and PVW disease, emergency status, operative time, LSA coverage were not shown to be predict the development of TCD-detected HITS, stroke, or DW-MRI infarcts on multivariate analysis.

4.2.7 Neurocognitive outcomes

A total of 44 patients completed pre- and post-operative neuropsychological testing and 42 patients had paired pre- and post-operative neuropsychological testing and a post-operative DW-MRI. New DW-MRI infarcts were present in 17 (40%) patients.

Two patients who completed testing did not undergo MRI due to penile implant and patient refusal. Six-week follow-up tests after TEVAR were conducted at a median of 50 days (IQR 46-55). Reasons for non-completion of testing in the remaining 29 patients included death before 6-week follow-up (n = 4), refusal

(n = 1), emergency presentation (n= 23), stroke deficit precluding unbiased testing (n = 2), loss to follow-up (n = 1). A total of 36 patients had paired pre- and post-operative neurocognitive tests and TCD data.

Only 6 patients completed neuropsychological testing a 6-months follow-up. Due to speedy recruitment during the latter half of the study period, the 6-month follow-up for many patients coincided with the COVID-19 pandemic and a significant proportion were lost due the lockdown in England and all face-to-face hospital visits being cancelled. Thus, there were insufficient numbers of patients who completed 6-month testing to conduct statistical analysis and this data is omitted from this thesis.

Statistical analysis was conducted on the 42 patients with paired DW-MRI and 6-week neuropsychological testing and 36 patients with paired TCD data and 6-week neuropsychological testing.

4.2.8 Neurocognitive outcomes in relation to DW-MRI outcomes

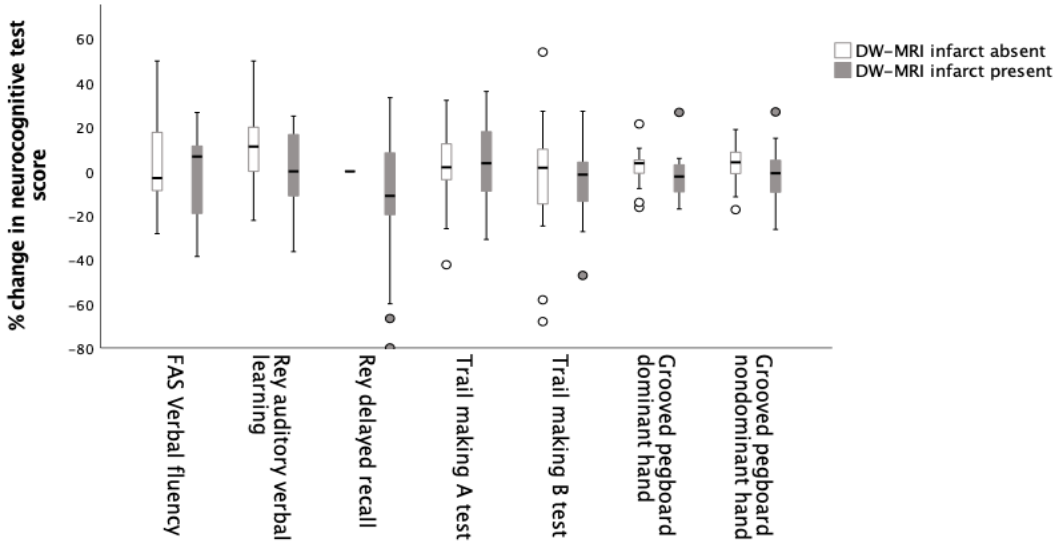
A 20% decline in neuropsychological testing in at least 1 test was observed in 52% (22/42) patients (50% [22/44] patients for whole cohort irrespective of MRI outcome). Nine patients (21% [9/42]) declined in >2 tests [9/44= 20% whole cohort). When neurocognitive impairment was stratified according to the presence and absence of new DW-MRI infarcts, 71% (12/17) of patients with new DW-MRI infarcts exhibited a 20% decline in at least one neurocognitive test compared to 24% (10/25) of patients with no DW-MRI infarcts (p=0.051; Chi square test). Only two patients who developed a clinical stroke were able to undergo neurocognitive testing; one of these patients had a 20% decline on neurocognitive testing (50%).

When the neurocognitive data for *each test* was stratified according to the presence of absence of a new DW-MRI infarct, patients without a DW-MRI infarct displayed significantly less cognitive decline on groove pegboard testing (manual dexterity) for both the dominant and non-dominant hand compared to patients with DW-MRI infarcts (Figure 4.5a).

The present of more than 3 DW-MRI infarcts was also significantly associated with significantly greater cognitive decline in the FAS and REY delayed memory tests (Figures 4.5b and d, respectively).

Figure 4.5

a. Percentage change score for each neurocognitive test according to the presence of a DW-MRI infarct and no DW-MRI infarct.

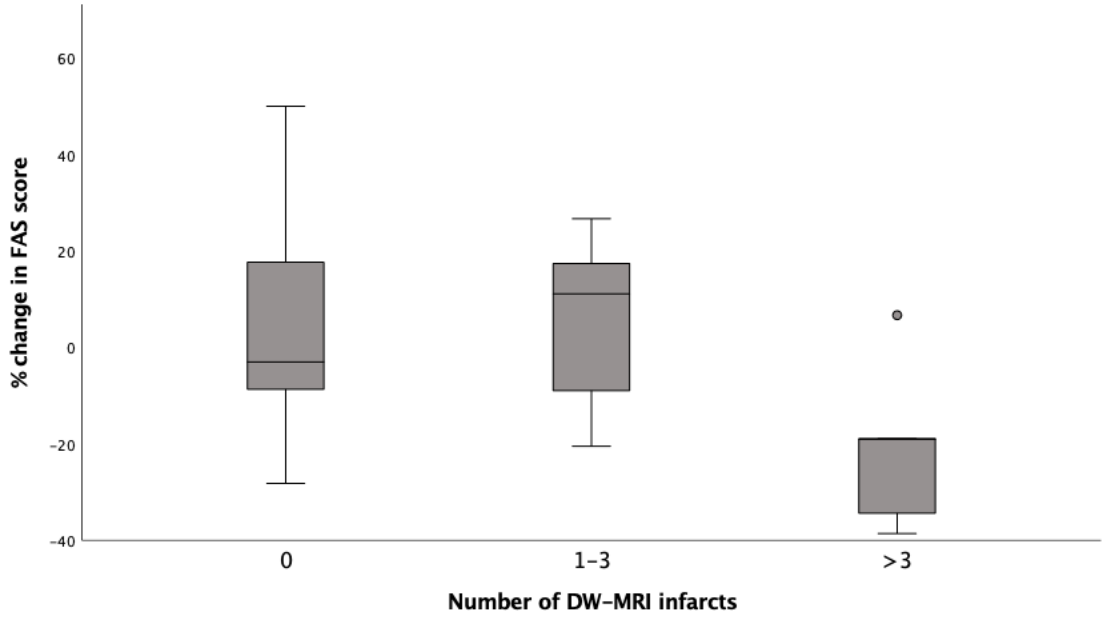


N= 42 *(31 outliers excluded from graph for scaling purposes but not from statistical analysis)*

Cognitive test	**DW-MRI infarct absent (n=25)**	**DW-MRI infarct present (n=17)**	**P value**
FAS	-3.03 (-8.70 - 17.65)	6.67 (-19.05-11.43)	0.434
Rey verbal	10.0 (0.0 - 20.0)	0 (-11.11- 20.0)	0.728
Rey delayed recall	0.0(0.0 -14.29)	-5.56 (-16.96 -18.75)	0.183
Trail making A	1.82 (-3.79 -12.40)	3.66 (-16.87-17.94)	0.868
Trail making B	1.96 (-6.81 - 11.24)	-1.47(-14.20-4.34)	0.377
Grooved pegboard dominant hand	3.66 (-0.86 - 5.16)	-4.10 (-9.70-2.86)	0.032
Grooved pegboard non-dominant hand	4.05 (-1 – 8.70)	-1.03 (-16.66 -2.88)	0.042

Values are reported as median % change score (interquartile range). Mann Whitney U test used.

b. Percentage change in FAS score according to number of infarcts



0 DW-MRI-lesions: median% change in score -3.03 (IQR -8.70 – 17.65)

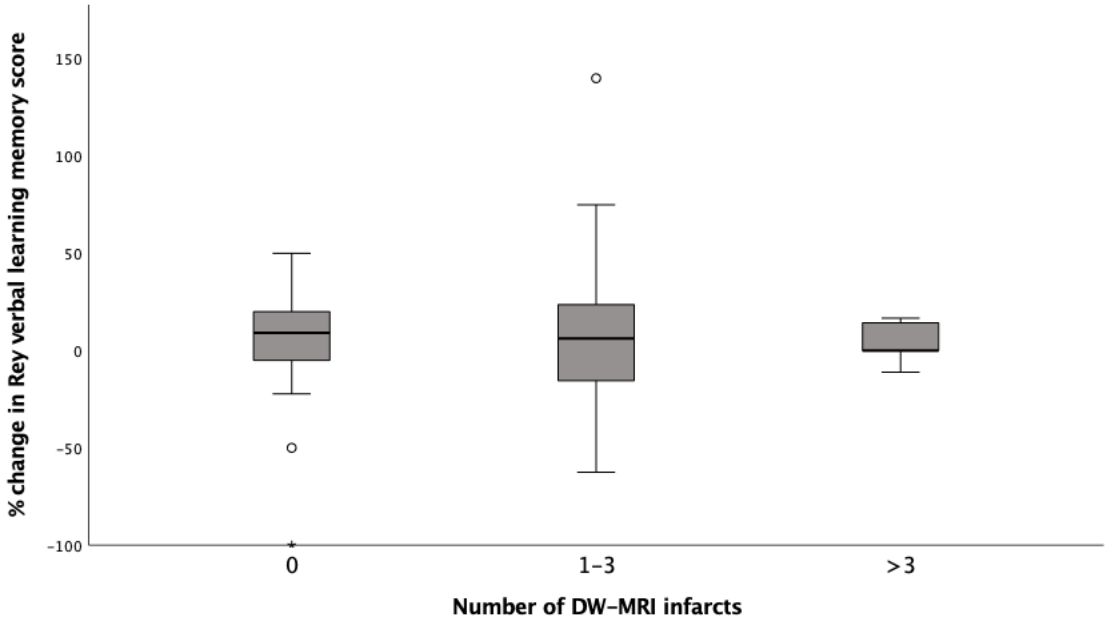
1-3 DW-MRI lesions: median % change in score 11.11 (IQR -6.88 – 17.39)

>3 DW-MRI lesions: median % change in score -19.04 (IQR -34.38—18.92)

Kruskal Wallis p = 0.036

Number of infarcts	**Mann Whitney U test, p value**
0 and >3 infarcts	0.015
0 and 1-3	0.689
1-3 and >3 infarcts	0.019

c. Percentage change in REY auditory verbal learning according to number of infarcts



0 DW-MRI-lesions: median% change in score 10.0 (IQR0.0-20.0)

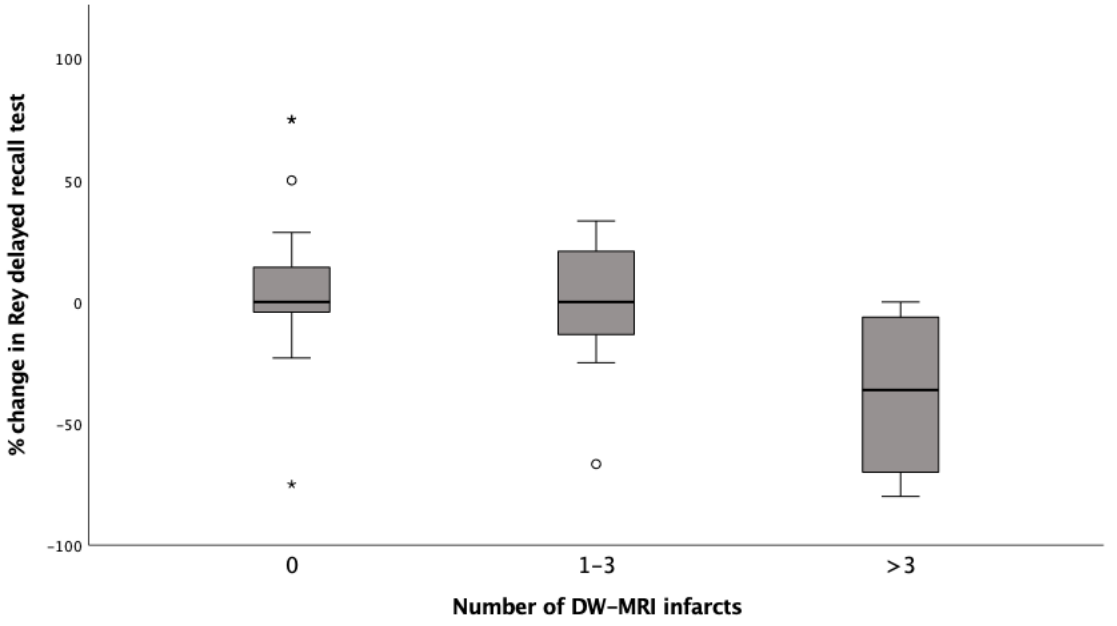
1-3 DW-MRI lesions: median % change in score 6.25 (IQR -14.88-2.92)

>3 DW-MRI lesions: median % change in score 0.0 (IQR 0.0-14.29)

Kruskal Wallis p = 0.864

Number of infarcts	Mann Whitney U test, p value
0 and >3 infarcts	0.516
0 and 1-3	0.987
1-3 and >3 infarcts	0.959

d. Percentage change in REY delayed recall according to number of infarcts



0 DW-MRI-lesions: median% change in score 0 .0 (IQR 0.0-14.29)

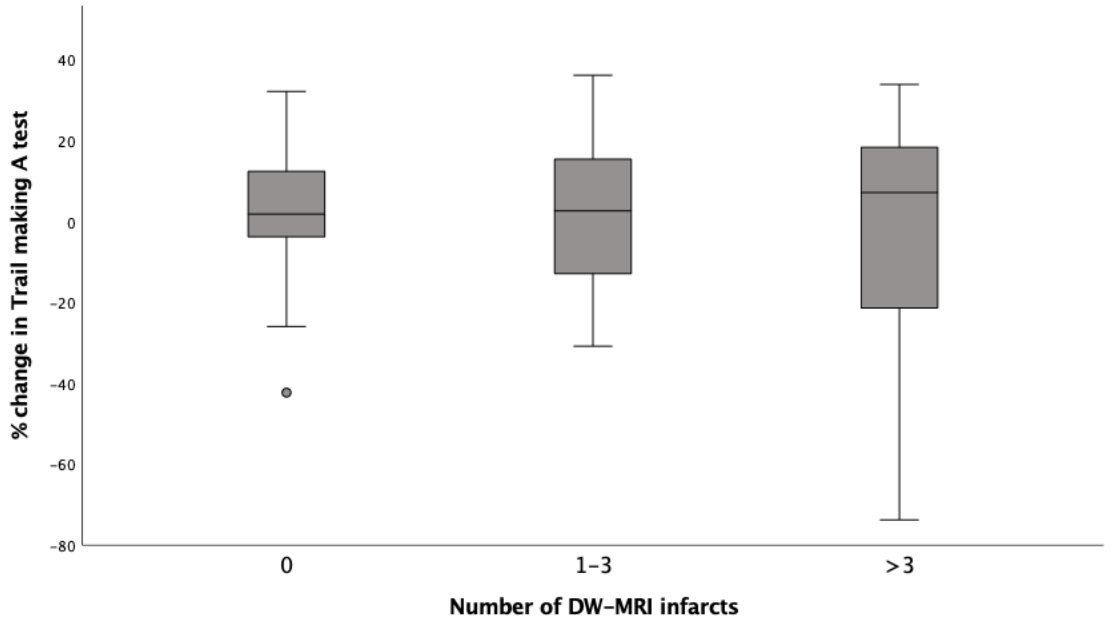
1-3 DW-MRI lesions: median % change in score 0.0 (IQR -12.95 – 25.89)

>3 DW-MRI lesions: median % change in score -36.25 (IQR -65.0 to -9.38)

Kruskal Wallis p = 0.103

Number of infarcts	Mann Whitney U test, p value
0 and >3 infarcts	0.030
0 and 1-3	0.786
1-3 and >3 infarcts	0.103

e. Percentage change in Trail making test A according to number of infarcts



0 DW-MRI-lesions: median% change in score 1.82 (IQR -3.79 - 12.40)

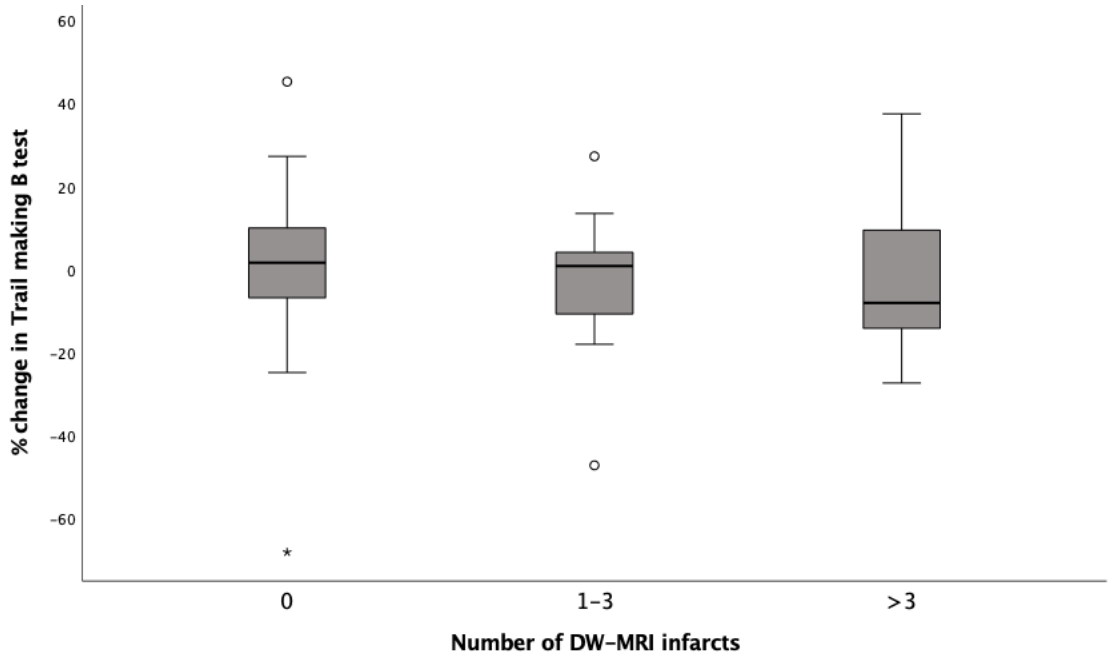
1-3 DW-MRI lesions: median % change in score 2.61 (IQR -10.92-14.16)

>3 DW-MRI lesions: median % change in score 7.14 (IQR -21.39 – 18.36)

Kruskal Wallis p = 0.987

Number of infarcts	Mann Whitney U test, p value
0 and >3 infarcts	0.914
0 and 1-3	0.936
1-3 and >3 infarcts	0.959

f. Percentage change in Trail making test B according to number of infarcts



0 DW-MRI-lesions: median% change in score 1.96 (IQR -6.82 – 11.24)

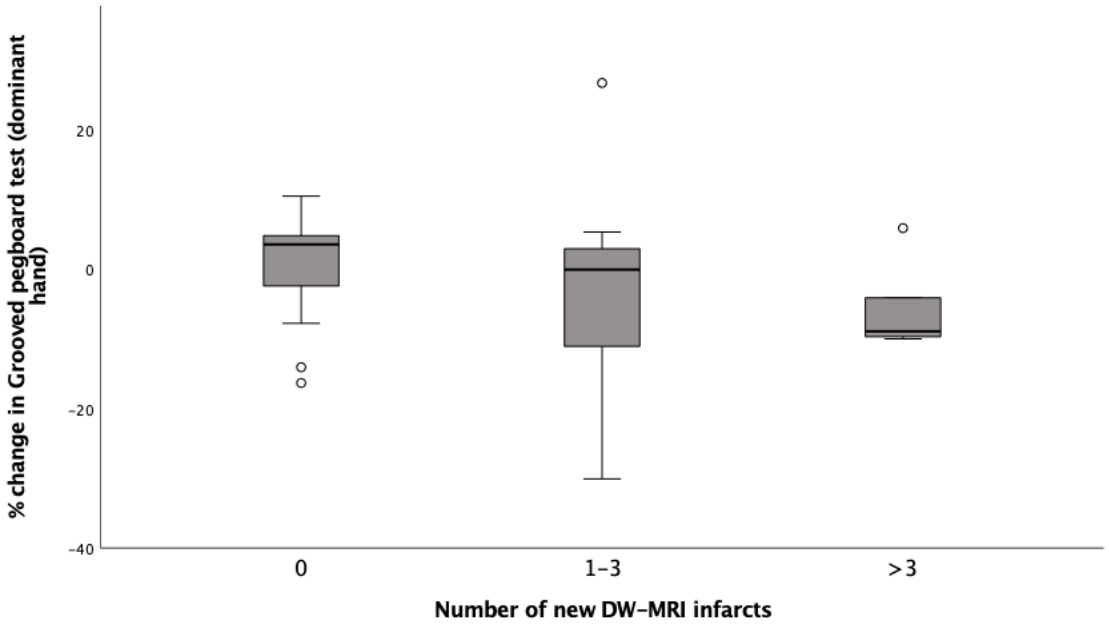
1-3 DW-MRI lesions: median % change in score -0.32 (IQR =14.31 – 4.02)

>3 DW-MRI lesions: median % change in score -8.05 (IQR -14.17 – 9.45

Kruskal Wallis p = 0.367

Number of infarcts	Mann Whitney U test, p value
0 and >3 infarcts	0.627
0 and 1-3	0.432
1-3 and >3 infarcts	0.879

g. Percentage change in Grooved peg board (dominant hand) according to number of infarcts



0 DW-MRI-lesions: median% change in score 3.66 (IQR -0.86- 5.16)

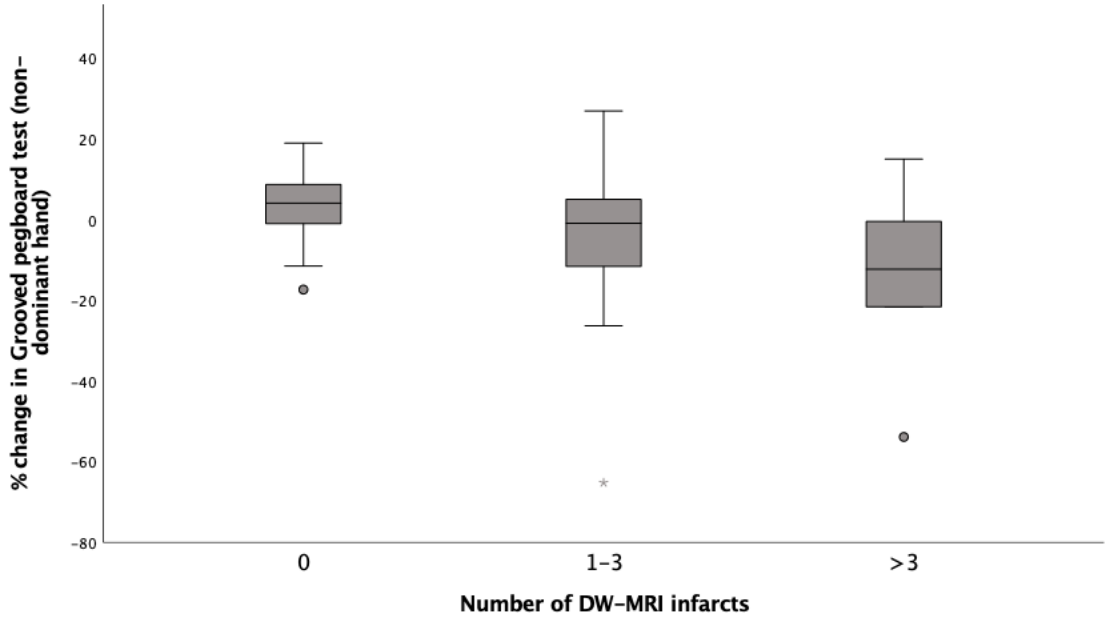
1-3 DW-MRI lesions: median % change in score -0.07 (IQR -9.07 – 2.90)

>3 DW-MRI lesions: median % change in score -8.93 (IQR -9.70 - 4.10)

Kruskal Wallis p = 0.158

Number of infarcts	Mann Whitney U test, p value
0 and >3 infarcts	0.085
0 and 1-3	0.095
1-3 and >3 infarcts	0.646

h. Percentage change in Grooved peg board (non-dominant hand) according to number of infarcts



0 DW-MRI-lesions: median% change in score 4.05 (IQR -1-8.70)

1-3 DW-MRI lesions: median % change in score -0.94 (IQR -9.08 – 3.93)

>3 DW-MRI lesions: median % change in score -12.3 (IQR -21.64 - 0.47)

Kruskal Wallis p = 0.107

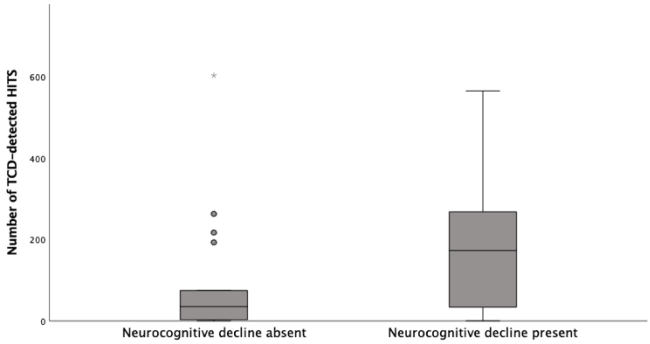
Number of infarcts	Mann Whitney U test, p value
0 and >3 infarcts	0.096
0 and 1-3	0.117
1-3 and >3 infarcts	0.574

4.2.9 Neurocognitive outcomes in relation to TCD data

A median of 173 HITS (34-152) were observed in patients with a 20% cognitive decline in at least one neurocognitive test compared to 35 HITS (3-75, p=0.093, figure 4.6a). Most HITS were gaseous in patients with and without neurocognitive decline (figure 4.6b). There was no significant difference in the median number of solid and gaseous HITS between patients with and without neurocognitive decline.

Figure 4.6

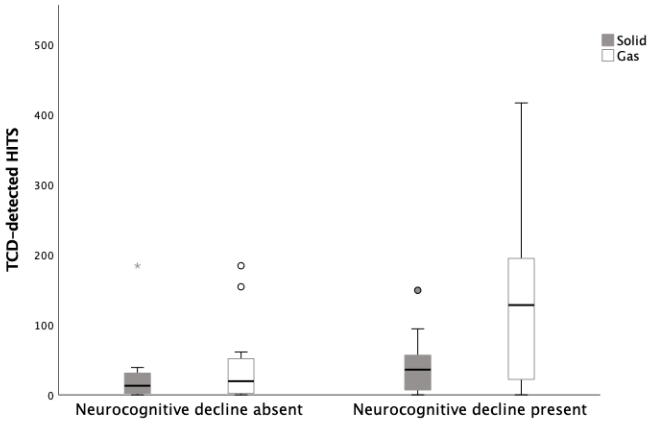
a. TCD-detected HITS in patients with and without a 20% decline in at least one neurocognitive test.



HITS	Neurocognitive decline absent	Neurocognitive decline present	P value
Median Total HITS (IQR)	35.0 (3-75)	173.0 (34.0-152)	0.093

Mann Whitney U test used for comparative analysis

b. Differentiated TCD-detected HITS in patients with and without a 20% decline in at least one neurocognitive test



HITS	Neurocognitive decline absent	Neurocognitive decline present	P value
Median Solid HITS (IQR)	13.0 (2.0-31.0)	36.0 (7-34.5)	0.061
Median Gas HITS (IQR	21.0 (2.0-61.0)	128.0 (22.0-113.0)	0.093

Mann Whitney U test used for comparative analysis

4.2.10 Predictors of neurocognitive outcomes

On univariate logistic regression, the presence of a DW-MRI infarct was associated with a 3.6-fold non-statistically significant increase in neurocognitive decline (OR 3.6, CI 1.01–14.4, p=0.189). The number of new DW-MRI infarcts was associated with a statistically significant 2-fold increase in neurocognitive impairment (OR 2.2, CI 1.04-4.37; p =0.039). The surface area was also found to be significantly predictive of neurocognitive decline (OR 1.07; CI 1.02–1.14; p = 0.037). None of these variables could be confirmed as independent predictors by multivariable analysis. Demographic, operative variables and TCD-detected HITS (including solid and gas) were also not predictors of neurocognitive decline.

4.3 Discussion

This pilot study has demonstrated that the rate of new DW-MRI infarction with CO_2 flushed TEVAR endografts was 43% (38% excluding patients who developed a stroke) and that patients who have fewer or no cerebral infarcts following TEVAR are less likely to experience neurocognitive decline during 6-week follow-up, compared to patients with procedure-related infarcts. Earlier studies have found rates of postoperative DW-MRI infarcts after TEVAR (without CO_2 flushing) ranging from 63% to 81%[51,52] and neurocognitive impairment in the post-operative period in 6 of 7 neurocognitive domains tested in up to 88% of patients with cerebral infarcts.[52] As such, the use of CO_2 flushing of endografts was associated with a 30-50% reduction in incident procedure-related infarcts, and the reduction in ischaemic load to the brain was associated with less neurocognitive impairment in the post-operative period.

The pattern of ischaemic injury (multiple, small infarcts dispersed in both hemispheres) identified on DW-MRI, the occurrence of TCD-detected HITS indicative of microemboli in the cerebral circulation, during specific procedural steps and the positive correlation between HITS and DW-MRI infarcts observed in this study confirms an embolic mechanism of injury related to the procedure.[41-43] Furthermore, the comparatively greater number of gaseous HITS at all phases of TEVAR is consistent with an air microembolic pathogenesis.

During TEVAR, there is a danger of air microembolism due to the entry of air through intravascular catheters, angiography and during endograft deployment. Previous TCD studies in TEVAR have identified endograft deployment as the highest risk phase for TCD-detected HITS,[25,52,74] and more recently gaseous HITS.[75] Endografts are manufactured and packaged in room air conditions and therefore entrap air. To prevent cerebral air embolism, the delivery device must be flushed with saline to purge out entrapped air, but this may not be effective at purging small pockets of air within the folds of the endograft fabric.

Benchtop experiments on phantom models have demonstrated the significant 'shower' of small and large bubbles that are released during endograft deployment, despite saline flushing with up to 0.7ml of gas collected.[92,93,95]

Contrary to popular belief, air microembolism is dangerous for the brain. Cerebral air microembolism results in focal ischaemia due to obstruction of blood flow, and/or vascular endothelial damage and an inflammatory response to the bubble that ultimately decreases cerebral blood flow to levels below those required for neuronal survival.[124,128] The arteriolar system in the brain ranges from 5 to 100 μm.[339] In animal models, as little as 5-25μl[124,126] of air and air bubbles of 45μm[123] in diameter have been shown to arrest cerebral blood flow and reduce cerebral activity on electrocorticographic (ECoG) monitoring with histological evidence of infarction.[340] Periods of hypotension prolong the duration of ischaemia.[126]

The practice of 'field flooding' the cardiac chambers with CO_2 to prevent neurological complications from cerebral air microemboli during cardiac surgery has been reported since the 1960's. CO_2 is 1.5 times denser than air and is 25 times more soluble in blood making it a valuable and safe neuroprotective agent that can displace air. It is also inexpensive and readily available. The use of CO_2 insufflation into the cardiac cavity has been associated with fewer bubbles on echocardiography.[156] Identical quantities of CO_2 injected into cerebral arteries of pigs were not associated with neurological symptoms with early reversibility of DW-MRI infarcts, in contrast to air injection that led to significant neurological sequele.[341]

Several clinical studies suggest a beneficial effect with CO_2 field flooding including an improvement on wave auditory evoked potentials as surrogate marker of brain damage with a (non-statistically significant) reduction in mortality, stroke, TIA,[153] improved myocardial function,[154] reduced S100B protein levels (marker of brain damage),[155] and a 0.30 (95%CI 0.14-0.63, p =0.001) relative risk reduction in

neurocognitive dysfunction compared to patients not exposed to CO_2 field flooding.[161] However, other studies suggest no benefit for its use.[154,342,343] The CO-Two study (Carbon dioxide insulation and brain protection during open heart surgery. A randomised controlled trial, currently recruiting)[344] should help address this important research question.

The only other study that has evaluated the incidence and cerebral distribution of procedural related cerebral infarction using DW-MRI is that by the Stroke in Thoracic Endovascular Procedures (STEP) collaborative. The authors report a 50% incidence of new DW-MRI infarcts in patients undergoing TEVAR in PLZ's 0-3 with tubular, fenestrated and branched arch devices with CO_2 flushed endografts.[165] While this study included significantly more 'higher' risk proximal zones and the use of endovascular arch repair techniques, CO_2 flushing was used in addition to sequential carotid clamping for zones 0 to 1 with some devices flushed for 2 minutes and others 3 minutes, making it difficult to determine whether the reduction in DW-MRI infarcts were the result of CO_2 flushing against cerebral air embolisation, or the result of carotid clamping that theoretically could protect against both solid and air cerebral embolism.

Furthermore, this study utilised a 1.5T MRI scanner with a magnet strength that is half the strength of a 3T scanner used in this study. This potentially reduces the diagnostic yield in the evaluation of new DW-MRI infarcts, particularly small (1-2mm^2) infarcts, despite the use of diffusion-weighted sequencing that highlight new and acute lesions as bright 'dots with 99% sensitivity and 92% specificity, respectively.[53] 3T MRI has been shown to yield a higher cerebral lesion load than 1.5T that missed many lesions in Multiple Sclerosis patients, a population in whom the identification of even a small lesion has significant clinical impact.[345]

The finding of a reduction in neurocognitive decline with reduced embolic load to the brain has also been observed in cardiac and non-cardiac surgery settings. Barber et al reported [66] neurocognitive decline in all patients with DW-MRI infarcts following cardiac surgery, compared to 35% of patients with no DW-MRI infarcts, with an association between number of abnormal cognitive tests and ischaemic load ($p<0.001$). Lund et al[346] observed that patients with new DW-MRI infarcts following left cardiac catheterisation performed well on neurocognitive tests assessing learning and attention in comparison to patients with no DW-MRI infarcts. Zhou et al[67] observed a correlation between higher infarct volume and worsening declarative memory. The Neurovision study[65] investigated 1114 participants undergoing elective non-cardiac surgery and found that those with new DW-MRI infarcts post-surgery were twice as likely to develop postoperative delirium, had a 4-fold increased risk of stroke or TIA at 1-year follow-up.

Elsewhere, large observational studies have also associated incident infarcts in the general population with cognitive decline. The AGES-Reykjavik Study (Age Gene/Environment Susceptibility-Reykjavik Study) of 2612 participants found that the presence of infarcts is associated with a steeper cognitive decline and almost doubles the risk of dementia.[347] Furthermore, this study also found that the number and cerebral distribution (subcortical/cortical/cerebellar) of infarcts contributes to cognitive impairment.[348] Lastly, a recent systematic review has found that MRI detected brain infarcts was doubles the risk of stroke (HR, 2.38; 95% CI, 1.87-3.04; $P < .001$), ischemic stroke (HR, 2.18; 95% CI, 1.67-2.85; $P < .001$), and increases the risk of death (HR, 1.64; 95% CI, 1.40-1.91; $P < .001$).[349]

The findings from these studies ultimately suggest that any intervention that can reduce the embolic load with respect to the brain is likely to be beneficial.

As a test of the ability to co-ordinate the fingers and manipulate objects (manual dexterity), upper-limb motor speed and hand-eye co-ordination, all of which are important in carrying out everyday life self-care, work and/or leisure activities, the improved neurocognitive scores in the grooved pegboard test in patients with no DW-MRI infarcts has important clinical implications for patients in the post-operative recovery period. Similarly, a reduction in the decline in change scores with patients with no infarcts compared to those with 1 to 3 and >3 infarcts for RAVLT (delayed memory) and FAS tests (verbal fluency and executive function) stresses the need to protect the brain from peri-procedural embolic damage. Univariate analysis demonstrated number of infarcts and infarct surface area as independent predictors of neurocognitive decline. This suggests that neuroprotective strategies should aim to reduce the embolic load to the brain and provides support for their use and study end-points in future neuroprotective trials.

The stroke rate in this study was 7% and all strokes occurred in zones 0 (40%) and 2 (20%). There were no strokes in zone 1. Interestingly, Melissano et al[43] observed a similar trend. The GREAT reported an overall stroke rate of 3.4%, however, stroke rate by PLZ revealed a stroke rate of 13.3% for zone 0, 2.9% for zone 1, 2.5% for zone 2, 0.6% for zone 3 and 0.4% for zone 4.[320] More proximal zones (0-2) were identified as significant predictors of DW-MRI infarcts and stroke in this study, which together with the aforementioned studies emphasises the importance of assessing stroke according to the PLZ of TEVAR.

The number and surface area of new DW-MRI infarcts were also predictors of post-procedural stroke. This provides further evidence that new DW-MRI infarcts are not harmless events, but that have important clinical implications. Longer term follow-up of the patients in this study will be important to determine the impact of procedure-related DW-MRI infarcts on the development of future stroke and/or neurocognitive decline.

While there is no comparator group in this study to compare the effect of CO_2 flushed endografts to standard saline flushing to reduce stroke, it is perhaps unlikely that CO_2 flushing alone can reduce clinical stroke, given that air emboli are more likely to be washed away under the force of cardiac pulsation than solid emboli. Indeed, TCD-detected solid HITS were identified as a predictor of new DW-MRI infarcts and stroke. The use of cerebral embolic protection devices clearly have a role here as a neuroprotective adjunct, and even more of a role for TEVAR in more proximal landing zones.

While this study was not powered to detect a reduction in clinical stroke, future studies exploring the use of neuroprotective adjuncts to reduce clinical stroke will need to consider the varying incidence of stroke according to PLZ.

As mentioned earlier, the highest number of TCD-detected HITS have been observed to occur during endograft deployment, followed by arch angiography.[52,74] These have been differentiated to be gas in nature.[75] However, in this current study this relationship was reversed whereby the highest number of TCD-detected gaseous HITS were observed to occur during arch angiography, followed by endograft deployment. This suggests that the use of CO_2 flushing of endografts reduced the gas released during deployment. This is in line with studies that have shown a reduction in the number of air emboli on transoesophageal echo following CO_2 insufflation of the cardiac chambers.[154,156,350,351]

While there is no way to attribute a DW-MRI infarct to a gas or solid embolus, the reduction in TCD-detected gaseous HITS at endograft deployment, together with the finding of a reduction in DW-MRI infarcts, compared to prior literature, the reduced incidence of neurocognitive decline and less decline in neurocognitive change scores in those with fewer TCD HITs and no DW-MRI infarcts demonstrates the

neuroprotective effect of CO_2 flushing in reducing the embolic injury to the brain by reducing cerebral air mircoembolisation.

With this in mind, intra-procedural TCD monitoring is a powerful tool that serves several purposes including (1) elucidating the mechanism(s) of cerebral injury thereby contributing to the development of neuroprotective adjuncts, (2) monitoring the success of any neuroprotective adjunct by way of TCD quantification, and the (3) identification of which patients are likely to benefit from neuroprotective adjuncts based on the associated between TCD HITS and patient and procedure related factors. For example, higher number of HITS were observed in patients with higher atheroma grade, grade III arch, greater deep white matter disease and with more proximal landing zones. TCD-detected HITS, both solid and gas were all found to be predictors of new DW-MRI infarcts and stroke making TCD-detected HITS a promising therapeutic target.

The recordings from TCD have also been used to determine the size distribution and volume of bubbles entering the brain, allowing an even better understanding of the impact of cerebral air embolisation and more accurate quantification of procedure-related air emboli, beyond a simple frequency count.[351]

There are several other embolic and nonembolic mechanisms that could have caused DW-MRI infarcts, stroke, and cognitive decline.

A significant number of TCD-detected emboli were differentiated as solid. TCD-detected solid HITS were also found to be predictors of new DW-MRI infarcts and stroke. This emphasises the important of solid embolisation as a separate mechanism of brain injury and may explain why the DW-MRI infarct rate was

not zero with the use of CO_2 flushing. Solid emboli may be generated from fragmentation of atherosclerotic plaques during wire and catheter, stiffwire manipulations and endograft deployment, and during arch angiography when contrast is injected at a high pressure into the aorta. This process may also generate 'gas' bubbles due to cavitation that may then shoot off into the brain under pulsatile flow. Bendszus et al [352] demonstrated a significant reduction in new DW-MRI infarcts after intra-arterial cerebral angiography with the use of an air filter with a significant reduction in TCD-detected HTS in this group compared to the control group. In the future, a similar air filter that can tolerate the pressures used for arch angiography could be designed to prevent cerebral embolisation of gas bubbles.

Cerebral hypoperfusion is a well-recognised cause of cerebral infarcts. However, this typically leads to infarcts at the borderzone or watershed areas of the brain. Unfortunately, intra-operative hypotension and its duration was not accurately collected in this study to determine its impact brain injury. However, only 7% of the total number of infarcts were found in these regions, suggesting that embolisation outweighed the effects of cerebral hypoperfusion. Importantly, cerebral hypoperfusion leads to a reduction in 'embolic washout' meaning that emboli persist for longer.[134]

The systemic inflammatory response following surgical trauma, type and dosage of anaesthesia, temperature and glucose management during surgery may also lead to neurocognitive impairment.[353]

4.4 Limitations

There are several limitations to this study that are acknowledged. Firstly, there was no comparator control group, limiting the conclusions of this study. Secondly, the same researcher (LH) was responsible for patient recruitment, TCD collection and analysis, and was not blinded to patient outcomes. Blinded analysis and a second assessor to determine inter-rater reliability would have been preferable but was not possible at this time. Thirdly, not every patient underwent TCD, MRI and cognitive function testing. A high proportion of patients were treated as an emergency, and this made it a challenge to place the headset and perform TCD. The inclusion of emergency patients also meant that was not practice or clinically appropriate for these patients to undergo cognitive testing and they were often the ones with co-morbidities and who could not undergo an MRI. This limits the generalisability of the results to mainly elective or 'semi-elective' patients only. Fourthly, the routine neurological assessment by a neurologist may have uncovered 'subtle' forms of stroke, however, for pragmatic reasons this was not possible. The researcher (LH) did however receive extensive training into conducting a thorough neurological examination. Routine collection of the National Institute of Stroke Severity (NIHSS) would have provided an objective measure of neurological deficits. Lastly, it is likely that the number of microemboli and new DW-MRI infarcts were underestimated. When showers of microemboli enter the Doppler sample volume as seen in arch angiography and endograft deployment, it is impossible for the machine and/or the researcher to count each single embolus. While the sensitivity of DW-MRI is high, it is not 100%. This may explain why some patients had neurocognitive decline in the absence of a lesion. Furthermore, not all gaseous emboli lead to a visible MRI infarct, Animal models of cerebral air embolisation have demonstrated neurological deficits even in the absence of overt infarcts on histological straining of cerebral tissue, which may be the result of endothelial damage rather than occlusive effects of a bubble.[125,340]

There are also limitations with respect to the population. Patients were recruited consecutively in an 'all comers' approach to limit any selection bias given the observational nature of this study. Nevertheless,

those patients who dropped out during the study or who were lost to follow-up or sadly died in hospital or during follow-up and could not complete all the testing of end-points of represents an inherent bias that may have impacted the results. Nevertheless, given the large incidence of DW-MRI infarcts and what we know about their impact on neurocognition, it is likely that the impact of missing data on the results of this study are underestimated. Missing data also presents challenges for more complex multivariate analyses. Nevertheless, this study provides the most robust data at this present time in this area of research, given the limitations already described in other published papers in this area namely the use of multiple neuroprotective adjuncts alongside CO_2, making interpretation of any impact of CO_2 flushing challenging.

4.5 Conclusion

This is the first study to assess the effect of CO_2 flushing of endografts to prevent cerebral air embolisation and subsequent brain injury with respect to new DW-MRI infarcts, stroke, and neurocognitive decline. CO_2 flushed endografts were associated with a reduction in gaseous HITS at endograft deployment and new DW-MRI infarcts that resulted in less neurocognitive decline in the post-operative period. CO_2 flushing did not reduce the incidence of stroke compared to published rates in the literature. This study also confirmed that procedure-related cerebral embolisation was a risk factor for new DW-MRI infarcts and stroke, and that new DW-MRI infarcts increase the risk of neurocognitive decline. Furthermore, this study has demonstrated that both solid and gaseous emboli are harmful to the brain. Every effort should therefore be made to reduce both solid and gas embolisation to the brain during TEVAR.

Chapter 5: Comparative analysis between CO_2 flushed endografts and standard saline flushed endografts: DW-MRI and stroke outcome

5.1 Aim

To compare the incidence and characteristics of new post-operative new DW-MRI infarcts and clinical stroke between CO_2 flushed endografts and standard saline flushed endografts and evaluate patient and procedural risk factors new DW-MRI infarcts and clinical stroke.

5.2 Results

5.2.1 Study population

A total of 112 patients underwent TEVAR with standard saline flushing between 2012 and 2021 and a total of 75 patients underwent TEVAR with CO_2 flushing between 2018 and 2021. Patient demographic characteristics are shown in Table 5.1. There was a greater prevalence of ischaemic heart disease and chronic obstructive pulmonary disease in the CO_2 group. However, the saline group had a greater prevalence of chronic kidney disease, previous thoracic surgery. Nevertheless, the VPOSSUM morbidity score was greater in the saline group. There were more zone 3 TEVAR's in the CO_2 group and more zone 2 TEVAR's in the saline group. However, a greater number of patients underwent left subclavian revascularisation (with either a carotid-subclavian bypass or LSA fenestration) in the saline group. More patients in the saline group had a spinal drain inserted, probably because there were more type II TAAA's that underwent single stage TEVAR and an abdominal procedure such as visceral hybrid repair, FEVAR or BEVAR than the CO_2 group, and because the saline group included patients as far back as 2012 when TEVAR practice was just starting when spinal drains were used more liberally than in contemporary practice. Procedural

characteristics are shown in Table 5.2. Due to the small numbers of varying permutations of TEVAR and arch and/or abdominal endovascular procedures, it was not possible to statistically analyse the types of procedures between the two groups.

Table 5.1 Demographic characteristics of the study population

Characteristics	**Saline group (n=112)**	**CO_2 group (n=75)**	**P-value**
Demographics			
Age (years)	66.8 ± 14	69.8 ± 12	0.188
Male	71 (63)	52 (69)	0.401
Co-morbidities			
Hypertension	85 (76)	67 (89)	0.021
Atrial fibrillation	10(9)	5 (7)	0.670
Ischaemic heart disease	22(20)	26 (35)	0.021
CABG/coronary stents	7 (6)	8 (11)	0.216
Valve procedures	7 (6)	3 (4)	0.572
Hypercholesterolaemia	55 (49)	47 (63)	0.068
Diabetes mellitus	11(10)	7 (9)	0.691
Chronic obstructive pulmonary disease	25(22)	29 (39)	0.016
Chronic kidney disease (eGFR < 60ml/min)	34(30)	13 (17)	0.044
Previous TIA/CVA	15 (13)	6 (8)	0.252
Previous thoracic surgery	31(28)	9 (12)	0.010
Previous abdominal surgery	6 (5)	4 (5)	0.994
Smoking history	64(58)	50 (67)	0.216
Medication			
Anticoagulation	11(10)	14 (19)	0.106
Antiplatelets	56 (51)	48 (64)	0.078
Statins	67 (60)	51 (68)	0.256
Fazekas scale: PVWM			
0-1	30† (41)	28** (43)	0.814
2-3	43† (59)	37** (57)	0.814
Fazekas scale: DWM			
0-1	35† (48)	34**(52)	0.609
2-3	38† (52)	31**(48)	0.609
***Arch atheroma grade**			
3-4	48(43)	22 (31)	0.112
***Arch grade**			
1	32 (29)	26 (37)	0.217
2	37 (4)	35 (50)	0.029
3	41(37)	9 (13)	0.0003

CABG, coronary artery bypass grafting; TIA, transient ischaemia attack; CVA, cerebrovascular incident; PVWM, periventricular white matter; DWM, deep white matter. *5 patients from BSWH could not be analysed due to suboptimal imaging.

**Denominator is 65 patients who underwent MRI. †Denominator is 73 patients who underwent MRI. Data are presented as n (%) or mean standard ± deviation

Table 5.2 Procedural characteristics of the study population

Characteristics	**Saline group (n=112)**	**CO_2 group(n=75)**	**P value**
Indication			
Chronic degenerative aneurysm *Atherosclerotic aneurysm* *Penetrating aortic ulcer* *Coarctation*	68 (61) 50 (45) 10 (9) 8 (7)	43 (57) 36 (48) 6(8) 1(1)	0.645
Chronic type b dissection aneurysm	17(15)	14 (19)	0.530
Acute type b dissection	15(13)	12 (16)	0.619
Other (mycotic aneurysm, trauma, endoleak relining)	12(11)	6(8)	0.537
Emergency	42 (38)	22 (29)	0.249
VPOSSUM mortality	6.9 ± 6.7	6.5 ± 12.5	0.807
VPOSSUM morbidity	56.4 ± 20.1	44.0 ± 24.5	0.001
Ishimaru Proximal landing Zone			
0	6 (5)	5 (7)	0.709
1	9 (8)	2 (3)	0.126
2	40 (36)	15 (20)	0.021
3	38(34)	42 (56)	0.003
4	19 (17)	11 (14)	0.675
Management of the LSA			
Uncovered	66(60)*	56 (75)	0.056
Covered	12 (11)	6 (8)	0.687
Revascularized	32 (29)	13 (17)	0.098
Spinal drain	52(46)	12 (16)	0.000017
Operative time (mins)	191.38 ± 162.0	160.1 ± 114.5	0.228

VPOSSUM, vascular-physiological and operative severity score for the enumeration of mortality and morbidity; TEVAR, thoracic endovascular aortic repair; FEVAR, fenestrated endovascular aortic repair; BEVAR, branched endovascular aortic repair. Data are presented as n (%) or mean standard ± deviation. * denominator is 110 as two patients did not have a LSA.

5.2.2 Clinical outcomes

The clinical outcomes of the patients are shown in Table 5.3. There were no significant differences in the in-hospital mortality or morbidity. There was a significant difference in the length of hospital stay, with patients in the saline group a mean of 5 days longer than the CO_2 group.

Table 5.3 Clinical outcomes of the study population

Characteristics	Saline group (n=112)	CO_2 group(n=75)	P value
[a]n-hospital death[a]	12 (11)	10(13)	0.586
Cause of death[a]			
Retrograde aortic dissection	1	1	
Aortic rupture	2	1	
Cardiac	3	3	
Respiratory failure	3	4	
Stroke	0	1	
Bowel ischaemia	2	0	
Sepsis	2	0	
In-hospital morbidity[a]	63 (56)	35 (47)	0.198
Cardiac[a]	4	3	
Respiratory [a]	14	9	
Stroke[a]	13	5	
Spinal cord ischaemia[a]	2*	2**	
Brachial plexopathy[a]	2	0	
Retrograde aortic dissection[a]	1	1	
Gastrointestinal[a]	3	0	
Haemofiltration/dialysis[a]	4	0	
Lower limb ischaemic complications[a]	2	2	
Wound related/pseudoaneurysm[a]	7	6	
Return to theatre/reintervention[a]	10	7	
Length of hospital stay [b]	14.3 ± 17.3	9.1 ± 9.4	0.013

*following FEVAR and visceral hybrid, respectively; **following TEVAR for acute dissection with malperfusion in both cases.
Data are presented as n (%) or mean standard ± deviation. [a] Chi-squared test; [b] Mann-Whitney U test.

5.2.3 DW-MRI outcomes

Seventy-seven patients in the saline group underwent cerebral neuroimaging; 73 patients underwent a DW-MRI, and 4 patients underwent a CT head. The latter four patients all had neurological symptoms, confirmed by a Neurologist, but were not medically fit to undergo a DW-MRI and had to undergo a CT head instead. Thirty-five patients did not undergo any form of imaging because of medical instability (n= 11), claustrophobia (n=8), significant post-operative morbidity or death (n= 8), contraindication to pacemaker (n=5), patient refusal (n=3). Post-operative scans were performed at a median of 6 days (IQR 2- 9) after TEVAR.

Sixty-five patients (87%) in the CO_2 group underwent a DW-MRI brain scan according to the protocol. Ten patients did not undergo an MRI due to post-operative death 0 (n = 2) claustrophobia/refusal (n=3), pacemaker insertion (n =1), medically unstable (n = 2), no scan time availability (n = 1) and penile implant (n=1). Post-operative scans were performed at a median of 4 days (IQR 3-6) following TEVAR.

The DW-MRI characteristics according to cerebrovascular territory and laterality are shown in Table 5.4. The incidence of new infarcts (proportion of patients with new infarcts) on any neuroimaging (CT or MRI) was 74% in the saline group and 43% in the CO_2 group, respectively ($p<0.001$). Excluding the 4 patients who had a CT head, the incidence of new DW-MRI infarcts was 73% in the saline group compared to 43% in the CO_2 group ($p<0.001$). There was no significant difference in the clinical stroke rate (13% saline vs. 7% CO_2; $p=0.196$).

There was a significant reduction in the median total number of new DW-MRI infarcts ($p<0.001$) and a significant reduction in the median total surface area of new DW-MRI infarcts ($p=0.007$) with CO_2 flushing compared to saline flushing. Furthermore, there was a significant reduction in the maximum diameter of new DW-MRI infarcts with CO_2 flushing compared to saline flushing ($p=0.03$).

When examining DW-MRI infarcts according to cerebrovascular territory, there was a significant reduction in the median number of new DW-MRI infarcts in the posterior circulation ($p=0.01$) and borderzone areas ($p=0.001$, respectively), but no significant difference in the number of DW-MRI infarcts in the anterior circulation ($p=0.26$). Likewise, there was a significant reduction in the median total surface area of the

posterior circulation (p=0.01) and borderzone areas (p=0.002, respectively), but not in the anterior circulation (p=0.33).

When examining the DW-MRI infarcts according to laterality, there was a significant reduction in the number (p<0.001) and surface area (p=0.001) of new DW-MRI infarcts in the left hemisphere, and a significant reduction in the surface area of new DW-MRI infarcts in the right hemisphere (p<0.001) only with CO_2 flushing. Paradoxically, there were more DW-MRI infarcts in the right hemisphere with CO_2 flushing (p=0.01).

Table 5.4 DW-MRI characteristics

Characteristic	**Saline group (n=112)**	**CO_2 group (n=75)**	**P-value**
Incidence of new infarction on any cerebral imaging[a]	57/77 (74)	28/65 (43)	0.0002
Clinical stroke[a]	14(13)	5(7)	0.196
Incidence of new infarction on DW-MRI[a]	53/73 (73)	28/65(43)	0.0004
Median total number of DW-MRI infarcts (range)[b]	2(0-25)	0(0-31)	0.0003
Median total number of DW-MRI infarcts: anterior circulation (range)[b]	0(0-8)	0(0-23)	0.209
Median total number of DW-MRI infarcts: posterior circulation (range)[b]	2(0-19)	0(0-7)	0.012
Median total number of DW-MRI infarcts: borderzones (range)[b]	0(0-11)	0 (0-3)	0.001
Median total surface area of lesions (range, mm^2)[b]	10 (0-2912)	0 (0-1679)	0.007
Median total surface area of DW-MRI infarcts (range, mm^2): anterior circulation[b]	0 (0-2520)	0 (0-336)	0.330

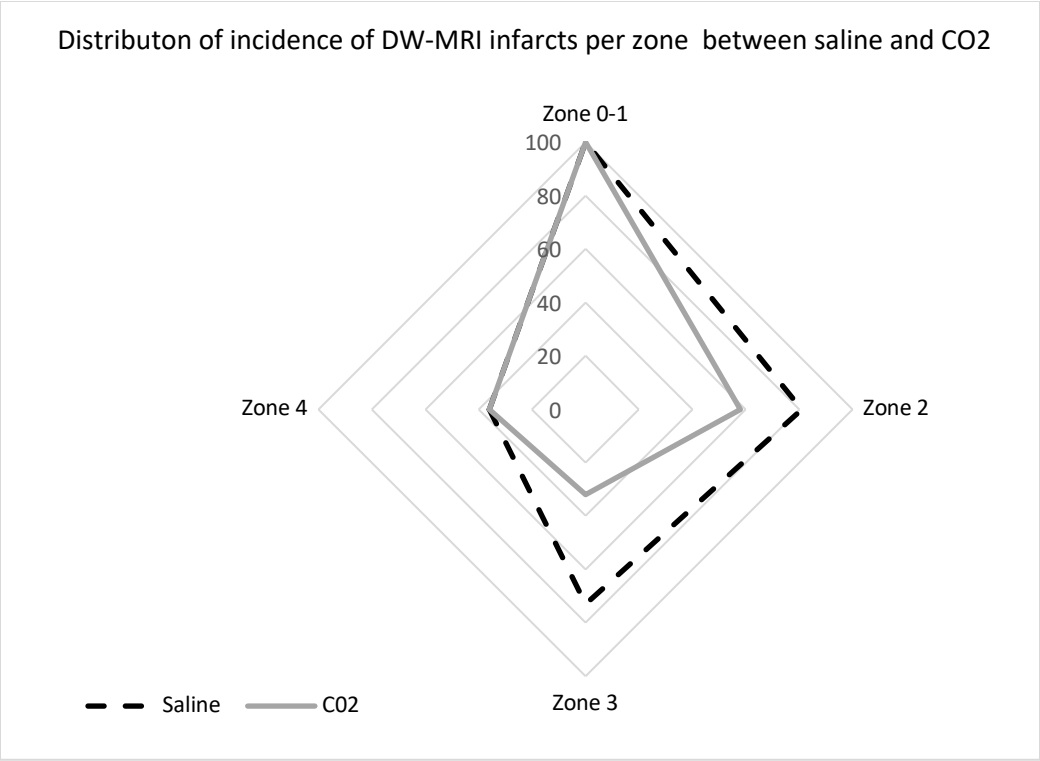
Median total surface area DW-MRI infarcts (range, mm^2): posterior circulation[b]	1(0-2844)	0(0-1671)	0.010
Median total surface area of DW-MRI infarcts(range, mm^2): borderzones[b]	0 (0-594)	0 (0-52)	0.002
Median maximum diameter of DW-MRI infarcts (range, mm)[b]	3(0-88)	0 (0-45)	0.028
Median number of left sided DW-MRI infarcts[b]	1(0-22)	0(0-9)	0.00009
Median surface area of left-sided DW-MRI infarcts (mm^2)[b]	6(0-2541)	0 (0-276)	0.001
Median number of right sided DW-MRI infarcts[b]	0(0-16)	0(0-26)	0.012
Median surface area of right-sided DW-MRI infarcts (mm^2)[b]	0(0-2776)	0 (0-1671)	0.0002

DW-MRI, diffusion-weighted magnetic resonance imaging. . [a] Chi-squared test; [b] Mann-Whitney U test.

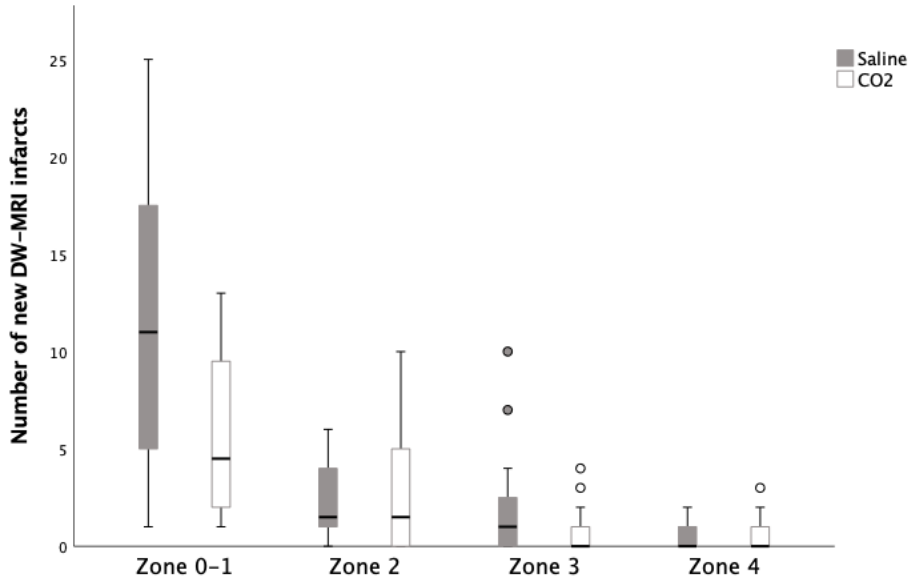
When examining DW-MRI infarcts according to PLZ, all patients in zone 0-1 had new DW-MRI infarcts. In PLZ 2, 81% of patients developed a new DW-MRI infarcts with saline flushing compared to 58%, however this was not statistically significant (p=0.14). As can be seen Figure 5.1 and table 5.5, there was a significant reduction in the number of patients who developed new DW-MRI infarcts (73% saline flushing vs 32% CO_2 flushing; p=0.003) in PLZ 3. There was no difference in the number of patients who developed infarcts in PLZ 4 (36% in each group; p=0.973). Similar findings were observed when analysing the number and surface area of new DW-MRI infarcts according to PLZ (Figures 5.1a- c, Table 5.5) CO_2 flushing was associated with a significant reduction in the number and surface area of new DW-MRI infarcts (p=0.005). Fewer lesions and smaller surface area of infarcted brain tissue was observed in the other zones, but this did not reach statistical significance.

Figure 5.1

a. Comparison of the proportion of patients (incidence) with new DW-MRI infarcts according to zone for saline and CO_2 group.



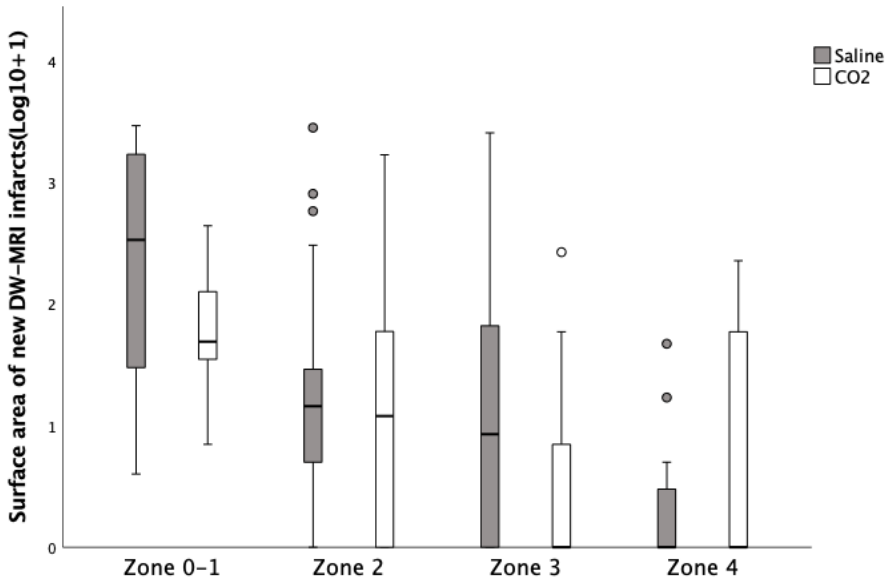
b. Number of new DW-MRI infarcts according to **proximal landing zone**



Saline group: n = 73; CO_2 group: n= 65

outliers removed from graph for scaling purposes but included in statistical analysis)

c. Surface area of new DW-MRI infarcts according to **proximal landing zone**



Saline group: n = 73; CO_2 group: n= 65

Log_{10}+1 transformation was used to normalise skewed data with lots of zeros

Table 5.5 Characteristics of DW-MRI infarcts according to proximal landing zone

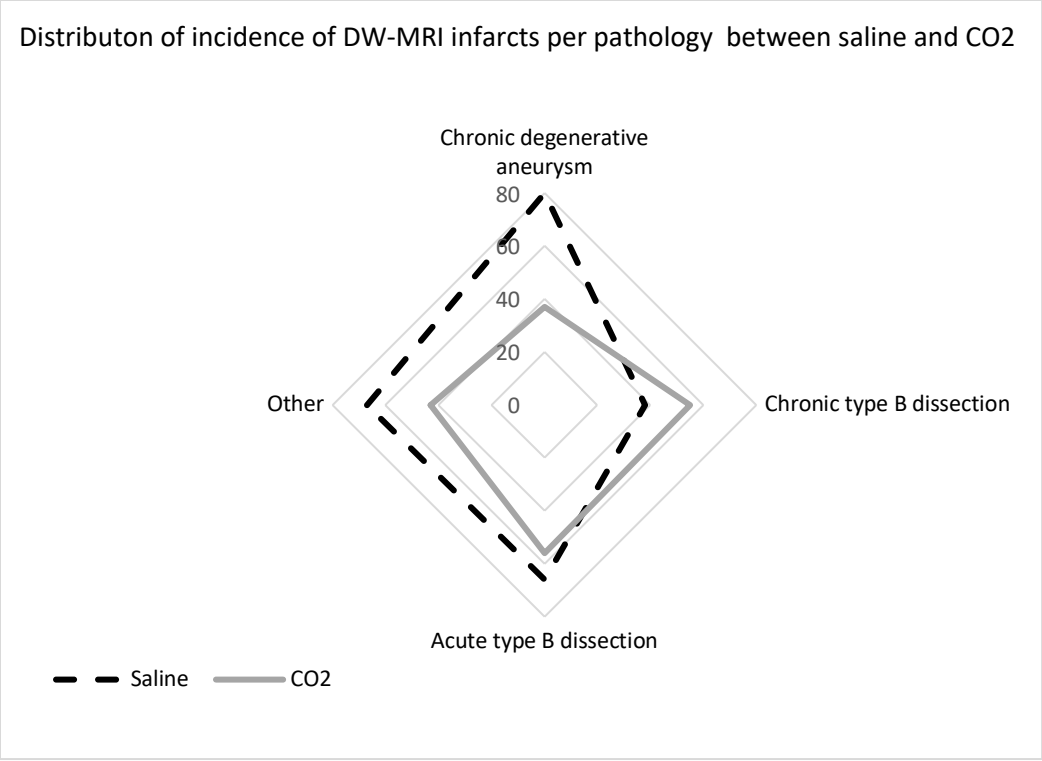
Zone	Saline group (n=73)	CO_2 group (n=65)	P-value
Incidence of DW-MRI infarcts[a]			
Zone 0-1	11/11 (100)	5/5 (100)	-
Zone 2	21/26 (81)	7/12 (58)	0.144
Zone 3	16/22 (73)	12/37 (32)	0.003
Zone 4	5/14 (36)	4/11 (36)	0.973
Median total number of DW-MRI infarcts[b]			
Zone 0-1	11(5-17.5)	6(3-13)	0.690
Zone 2	2(1-4)	1.5 (0-5)	0.823
Zone 3	1.5(0.25-3.75)	0(0-1)	0.001
Zone 4	0(0-1)	0(0-1)	0.974
Median surface area of DW-MRI infarcts (mm^2)[b]			
Zone 0-1	334(29-1716)	48(34-125)	0.396
Zone 2	13.5(4-27.5)	11(0-53.75)	0.788
Zone 3	7.5(0.57.75)	0(0-6)	0.005
Zone 4	0(0-1.75)	0(0-58)	0.503

DW-MRI infarcts, diffusion-weighted magnetic resonance imaging. [a] Chi-squared test; [b] Mann-Whitney U test.

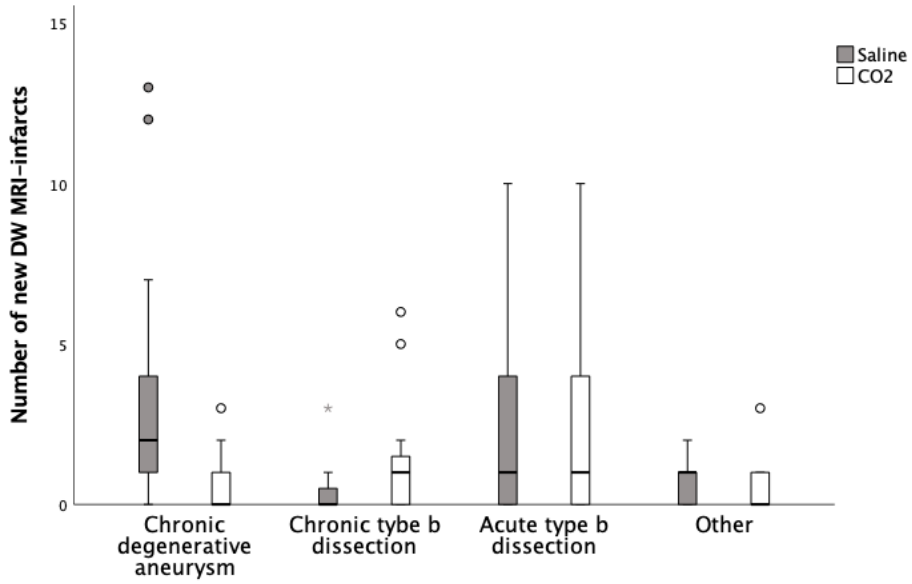
The proportion of patients with new DW-MRI infarcts was significantly reduced with CO_2 flushing in patients with chronic degenerative atherosclerotic aneurysmal disease only ($p<0.001$, Figure 5.2a). Similarly, a statistically significant reduction in the number ($p<0.001$) and surface area ($p=0.001$) of new DW-MRI infarcts was observed in patients with atherosclerotic aneurysm only (Figures 5.2b and c, and Table 5.6).

Figure 5.2

a. Comparison of the proportion of patients (incidence) with new DW-MRI infarcts according to pathology for saline and CO_2 group.

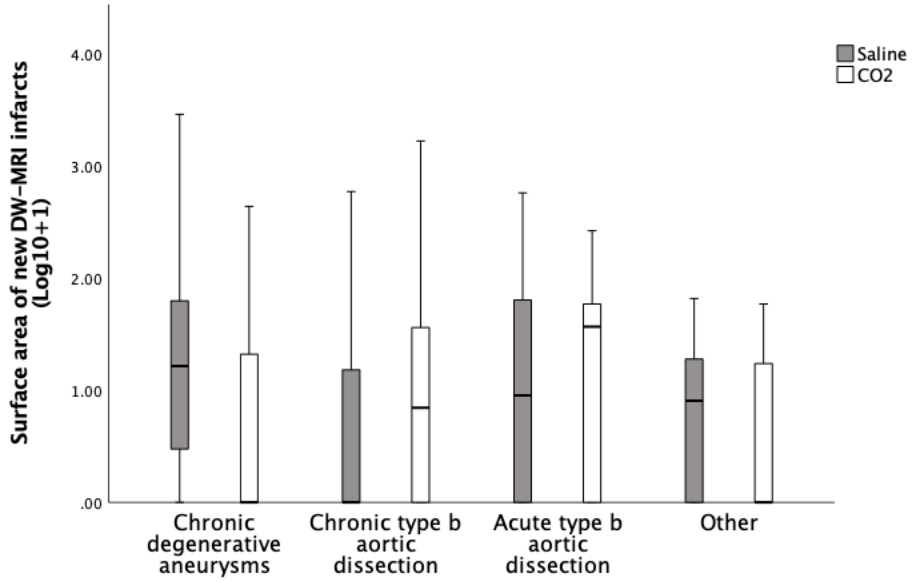


b. Number of new DW-MRI infarcts according to **pathology**



Saline group: n = 73; CO_2 group: n= 65

c. Surface area of new DW-MRI infarcts according to **pathology**



Saline group: n = 73; CO_2 group: n= 65

Log_{10}+1 transformation was used to normalise skewed data with lots of zeros.

Table 5.6 Characteristics of DW-MRI infarcts according to pathology

Pathology	**Saline group (n=73)**	**CO_2 group (n=65)**	**P-value**
Incidence of DW-MRI infarcts[a]			
Chronic degenerative aneurysm	40/50(80)	14/38 (37)	0.000038
Chronic Type B dissection	3/8(38)	6/11 (55)	0.462
Acute type B dissection	6/9 (66)	5/9 (56)	0.629
Other	4/6(67)	3/7(43)	0.390
Median total number of DW-MRI infarcts[b]			
Chronic degenerative aneurysm	2(1-4.75)	0(0-1)	0.000073
Chronic Type B dissection	0 (0-1.5)	1(0-1.5)	0.654
Acute type B dissection	1(0-4)	1(0-4)	0.855
Other	1(0.25-1.75)	0(0-1)	0.360
Median surface area of DW-MRI infarcts (mm^2)[b]			
Chronic degenerative aneurysm	15.5(2-58)	0(0-18)	0.001
Chronic Type B dissection	0 (0-12.5)	6(0-37)	0.503
Acute type B dissection	8(0-63)	36(0-58)	0.820
Other	8(1-16.5)	0(0-24)	0.548

DW-MRI, diffusion-weighted magnetic resonance imaging. [a] Chi-squared test; [b] Mann-Whitney U test.

5.2.4 Univariate and multivariate analyses for DWM-MRI and stroke outcomes

Univariate and multivariate analyses were conducted to determine independent predictors of DW-MRI infarcts and stroke (clinical and imaging), respectively. Variables entered into univariate analyses included age, co-morbidities, statins, antiplatelets, anticoagulants, smoking status, pathology, type of TEVAR operation including coverage of left subclavian artery, zone of TEVAR, arch grade, atheroma grade, operative time. Only CO_2 compared to saline (control) and those significant variables ($p<0.05$) from univariate analyses were entered into multivariable analyses.

On univariate analyses, using saline as the control group, there was a (non significant) trend towards a reduction in stroke incidence (OR 0.5 [CI 0.172-1.452], p=0.203). AF increased the incidence of stroke (OR 3.685 [CI 1.044-13.00]; p = 0.043) as did a higher atheroma grade (arch grade 4>1; OR 7 1.45-33.79; p = 0.015), arch grade (3 >1 (control) (OR 5.17 [CI 1.35-19.76]; p=0.016). Using zone 3-4 as control, zone 2 and zone 0/1 were independent predictors of stroke (OR 4.12 [CI 1.31- 12.94]; p=0.016 vs OR 6.18 [CI 1.62-23.62]; p=0.008, respectively). On multivariate analyses, again there was a non significant trend towards reduction in stroke incidence compared to saline (control) [OR 0.718 (0.111 - 4.648)]; p=0.728. Only atrial fibrillation was found to be a significant co-variate.

On univariate analyses for DW-MRI infarct incidence, CO_2 flush was found to cause a significant reduction compared to saline (control) (OR 0.27 [CI 0.13-0.54]; p= < 0.001). Statins (OR 0.46 [CI 0.22-0.96); p=0.04) and antiplatelets (OR 0.46 [CI 0.22-0.93]; p=0.03) were

associated with a significant reduction in DW-MRI infarct incidence. On multivariate analyses, there was a nonsignificant reduction in DW-MRI infarct incidence with CO2 flushing compared to saline (OR 0.60 [CI 0.19-1.78); p=0.34). None of the significant co-variates on univariate analysis were found to be significant in the multivariate analysis.

5.3 Discussion

This is the first study to compare DW-MRI outcomes and clinical stroke between CO_2 flushing and standard saline flushing of TEVAR endografts. The aim of this study was to determine whether CO_2 flushing could protect the brain from cerebral air embolisation compared to standard saline flushing.

From a global point of view, CO_2 flushing was associated with a significant reduction in the proportion of patients who developed new DW-MRI infarcts following TEVAR compared to standard saline flushing. CO_2 flushing was also associated with a significant reduction in the total number of new DW-MRI infarcts, the total surface area of infarcted cerebral tissue and the maximum diameter of an infarct.

CO_2 flushing of endografts is hypothesised to de-air endografts more efficiently than standard saline flushing because of the physical properties of CO_2 to displace and remove air from the endograft prior to deployment, thereby preventing the clinical and radiological sequelae of cerebral air embolisation.[93,341] The reduction in overall embolic load to the brain with CO_2 flushing compared to saline flushing supports this hypothesis.

However, these results must be interpreted with caution; DW-MRI outcomes clearly varied according to cerebrovascular territory, laterality, PLZ and pathology.

CO_2 flushing did not reduce significantly reduce the number of infarcts in the anterior circulation and maximum number of DW-MRI infarcts was greater in the CO_2 group. On closer inspection of the data, a reduction in the maximum number of DW-MRI infarcts was seen in all cerebrovascular territories for the left and right side of the brain with CO_2 flushing, except for the right anterior circulation. This part of the

brain is supplied predominantly by the right anterior and middle cerebral arteries that are branches of the right internal carotid artery, which in turn branches off the innominate artery.[354] Inspecting the data according to PLZ 0 where endograft placement directly involves the innominate artery, revealed that DW-MRI infarcts were seen in all patients in this zone. As such, it is reasonable to conclude that (1) CO_2 flushing alone is not effective at preventing DW-MRI infarcts in this zone as evidenced by the infarcts observed in its related cerebrovascular territory and (2) solid embolisation may play a larger contribution for zone 0 TEVAR. Endograft placement in this zone may generate a greater risk for solid embolisation for two reasons; (1) the proximity of endovascular instruments to the calcified aortic valve and/or (2) the need for endograft placement in zone 0 may indicate more severe disease atherosclerotic disease. Indeed, post-hoc analysis of TCD-detected HITS revealed that zone 0 TEVAR was associated with the greatest number of solid HITS compared to the other zones.

In contrast, CO_2 flushing appeared to be most efficacious for zone 3 TEVAR. While this zone may be considered a 'lower' risk zone with a lower embologenic potential for gas bubbles due to its distal location from the arch and the increased likelihood of gas bubbles washed away with antegrade flow, it is perhaps the most suitable zone to test the efficacy of CO_2 flushing. The procedural steps to deploy a TEVAR in zone 3 are devoid of other steps that may confound results for example stiffwire insertion near the aortic valve that may generate solid emboli, and the need for hypotension when deploying in more proximal zones.

The impact of CO_2 flushing on zone 0-2 TEVAR, and cerebral air embolisation as a mechanism of brain injury in these zones cannot be completely refuted because fewer DW-MRI infarcts and were observed in the CO_2 group, and the median surface area of new DW-MRI infarcts was reduced with CO_2 flushing in these zones, albeit without statistical significance.

Interestingly, CO_2 flushing did not appear to influence the DW-MRI outcomes of zone 4 TEVAR with a similar incidence of new DW-MRI infarcts in patients with saline flushing, and CO_2 flushing, and no reduction to the number of new DW-MRI infarcts. Paradoxically, a larger maximum surface area was found in the CO_2 group. These results could be due to the small sample size and hence a type II error, however, there are also several noteworthy points from these findings. The presence of DW-MRI infarcts in zone 4 highlight that this is not a 'low risk' zone and that the brain is not immune from being injured when endografts are displayed in at least 2cm distal to the left subclavian artery. While retrograde embolisation from the descending thoracic aorta is an infrequent event, [355,356] using 4D-flow MRI technology, several studies have demonstrated end diastolic retrograde flow at the site of atheromatous plaque > 4mm. This has been hypothesised to carry plaque material back to the aortic arch leading to embolisation. Thus, cerebral injury in zone 4 could be from retrograde flow of solid emboli and/or the retrograde transport of gas bubbles towards the proximal aortic arch.[357-359]

With respect to pathology, CO_2 endograft flushing reduced the number and surface area of new DW-MRI infarcts for atherosclerotic aneurysmal disease only. There was a trend towards a reduction in new DW-MRI infarcts for 'other' pathology such as mycotic aneurysms, trauma and endoleak relining. Conversely, CO_2 flushing did not appear to have an impact for dissecting disease, with a (non-significant) increase in the surface area of new DW-MRI infarcts observed.

The reduction new DW-MRI infarcts in the atherosclerotic aneurysmal group with CO_2 flushing, a neuroprotective method against air embolisation only is encouraging given the expectation that solid embolisation would be assumed to be the predominant mechanism of injury in this disease group.

The increase in infarcts in the dissecting group, the group in whom cerebral air embolisation would be most concerning given the relatively atheroma free aorta, and therefore would be expected to derive the most benefit from CO_2 flushing seems paradoxical. The mechanism of injury here may be the result of solid embolisation from artery-artery embolisation of newly formed thrombus on the thrombogenic and inflamed dissected intimal surface[360,361] and/or from newly formed thrombus on endovascular instruments.

CO_2 flushing did not reduce the incidence of clinical stroke. Experimental animal models demonstrate that the amount of air required to cause focal symptomatic neurological deficits is variable, [124,126,340] and is dependent on other factors such as temperature, blood pressure, and dissolution time all of which impact whether a bubble will be cleared from the circulation, coalesce to form larger bubbles, or fragment into small ones. This makes the relationship between cerebral air embolisation during TEVAR highly complex. The use of TCD data to try and size bubbles in the cerebral circulation and modelling the motion of gaseous emboli through the vascular tree with respect to these factors may hold the key to further our understanding.[135]

Based on the findings of this study it may be that solid emboli are more likely to cause a stroke than gaseous emboli given that relatively small gas bubbles are released during TEVAR deployment[92,93] that are likely to be washed away under the force of pulsatile blood flow, and based on our understanding of stroke due to vulnerable carotid plaques.[362]

Gaseous embolisation may be responsible for diffuse radiological and clinical injury to the brain as by showering the brain with new DW-MRI infarcts that disrupt the neuronal circuitry of the brain leading to impaired neurocognition, rather than focal neurological deficits (clinical stroke), akin to the development of microinfarcts and the cognitive impairment seen in Alzheimer's disease.[71] Nevertheless, the reduction

in embolic load to the brain with CO_2 flushing that can only prevent cerebral air embolisation cannot be ignored.

Univariate analysis revealed that CO_2 flushing was associated with a nonsignificant reduction in stroke and a significant reduction in DW-MRI infarcts. While multivariate analyses, did not demonstrate significant reductions in stroke or DW-MRI incidence with CO_2 flushing, the trend towards a lower odds ratio for both of these outcomes heralds a signal that deserves further investigation in a powered RCT.

5.4 Limitations

This study has some limitations that will be acknowledged. The saline control group was collected over a 9-year period, and although patients were recruited prospectively, this 9-year period is likely to be associated with a learning curve when TEVAR was still a relatively new technique in 2012, and the use of 1st and 2nd generation endografts that may have had a more embologenic profile than contemporary low-profile devices. There are also some differences in co-morbidities, and procedural characteristics between the two groups. To try and account for this, multivariate analyses were undertaken and although there was no significant difference between CO_2 and saline flushing to reduce stroke and DW-MRI infarcts, this is likely due to the study not being powered for a given end-point. Nevertheless, there would appear to be a signal in the data that CO_2 may be able to reduce adverse neurological complications and this deserves further study in an adequately powered RCT using this observational study.

Heterogeniety in reporting of MRI scans was also mitigated by standardised reporting of all MRI scans by the same consultant neurointerventionalist who has been involved in the project for the last 9-years. TCD data would have been helpful to correlate intra-operative HITS to DW-MRI infarcts, however, there was an upgrade of machines, and the purchase of gas-solid differentiation software towards the latter years of the study period, preventing amalgamation of this data. Neurocognitive data would have also been helpful, but again, a change in test battery towards the latter years meant that not all data could be included.

As mentioned in other chapters of this thesis, this study although retrospective and observational with many limitations, remains the only study of its kind to be published in the literature in a population that has undergone TEVAR under only CO_2 flushing or saline, and without any other neuroprotective adjunct that could bias any results.

5.5 Conclusion

This study has demonstrated the potential efficacy of CO_2 flushing to reduce the incidence, number, and surface area of new procedure-related DW-MRI infarcts. The reduction was determined by PLZ and aortic pathology. An adequately powered trial with relevant clinical endpoints in now required to definitively determine the efficacy of CO_2 flushing of endografts to prevent TEVAR induced brain injury.

Chapter 6: Benchtop experimental studies

6.1 Aim

These experiments were devised to determine the optimal time of CO_2 flushing needed to reach the end of the endograft, determine the composition of the gas bubbles released following CO_2 flushing and whether CO_2 flushing plus standard saline is better than standard saline flushing alone, and to determine the volume of gas bubble released with CO_2 flushing compared to standard saline flushing. Lastly, I aimed to determine the distribution of gas release in a realistic simulated thoracoabdominal model to better understand the pattern of cerebral injury following with respect to endograft placement in the arch following TEVAR.

6.2 Results

6.2.1 Time needed to flush endografts

This experiment determined that as CO_2 moves as a plug within the metal tube without the endograft, and through the endograft by the stepwise pattern on Figure 6.1. This indicates that CO_2 will replace another gas through displacement rather than by diffusion (curvilinear graph would be expected).

As can be seen from Table 6.2, it takes less than 2 seconds to fully purge the endograft and reach a steady CO_2 state at flow rates between 2 and 10 L/min. Higher flow rates are associated with a shorter purge time. For a minimum 1 second uncertainty, the effect of flowrate on the required purging time is negligible. While this is desirable, at 6-10L/min, leakage of CO_2 was observed from the connection between the tubing to the filter, and between the flush line on the endograft to the CO_2 tubing, despite changing the tubing. Therefore, it was decided that maximum flow rate to be tested would be 6L. Leakage was likely due to the fact that the increased flow rate increased the pressure within the endograft which was tolerated up until

the point of the endograft. Thereafter, the endograft created a point of resistance that resulted in back flow of CO_2 that led to CO_2 leaking through any connection points of the system.

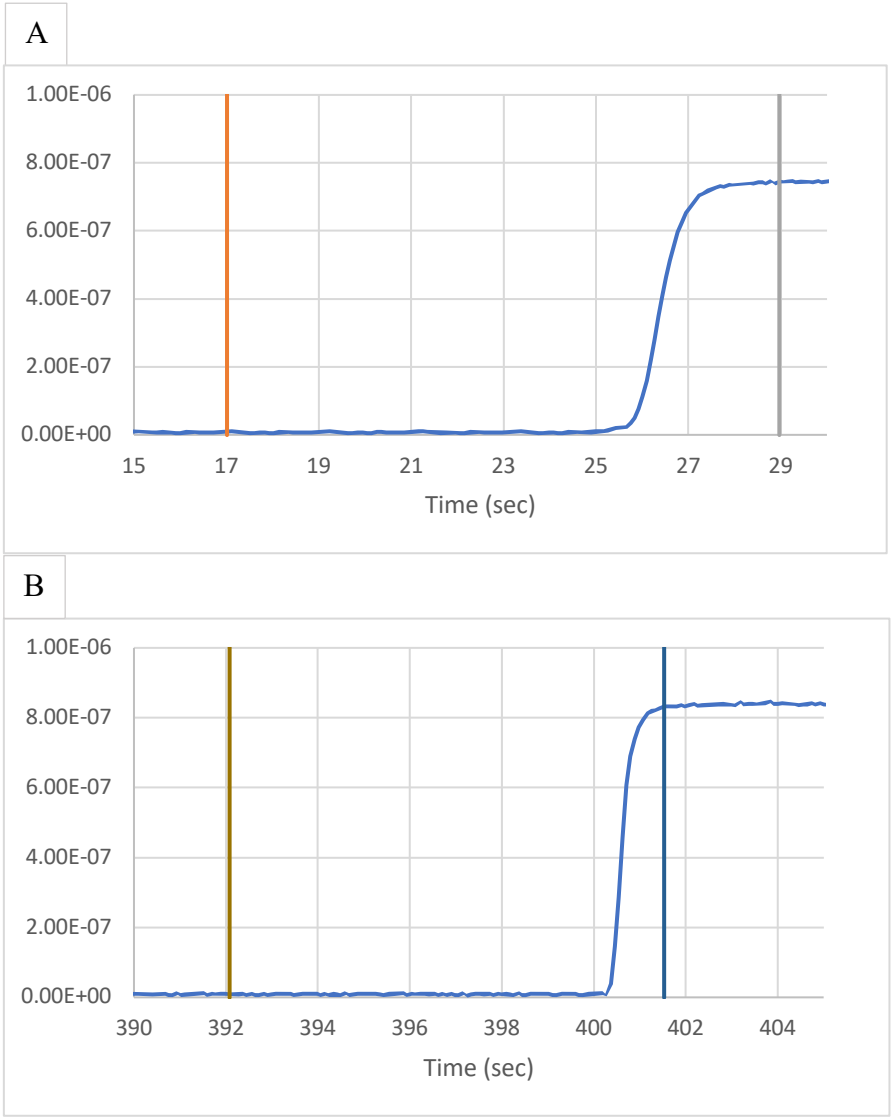


Figure 6.1 Mass spectrometry plot for CO_2 flushing through the metal tube (A) and through the endograft (B) showing stepwise pattern indicating plug flow through the tube and endograft

Table 6.1 Time taken for CO_2 to purge the endograft at various flow rates.

CO_2 flowrate (L/min)	**Breakthrough time (sec)**		**Endograft purging time (sec)**
	No endograft	With endograft	
2	12 ± 0.5	11.1 ± 0.8	-1 ± 1
4	10.3 ± 0.5	10.6 ± 1.1	0.3 ± 1
6	10 ± 0.4	10.3 ± 0.9	0.3 ± 1
8	9.5 ± 0.3	9.2 ± 0.6	-0.4 ± 0.7
10	9 ± 0.4	9.8 ± 0.5	0.8 ± 0.6

Data is shown as mean ± standard deviation

6.2.2 Gas volumetric analysis

The results of volume of gas released for a given intervention are shown in table 6.2. Saline flushing was associated with the greatest amount of gas release. There was a significant reduction in the amount of gas released with CO_2 flushing compared to saline at any given flow rate of CO_2. Interestingly, 2L/min flow rate was associated with the least amount of gas released compared to 4L and 6L. There was no difference in the amount of gas released between 4L and 6L of CO_2.

Table 6.2 Bubbles released under various flush techniques

Endograft number	Bubbles released with Saline flush(ml)	Bubbles released with 2L CO_2 flush (ml)	Bubbles released with 4L CO_2 flush (ml)	Bubbles released with 6L CO_2 flush (ml)
1	0.30	0.01	0.1	0.07
2	0.34	0.06	0.06	0.06
3	0.43	0.09	0.05	0.11
4	2.0	0.05	0.06	0.07
5	1.5	0.01	0.02	0.02
6	0.24	0.08	0.03	0.07
7	0.24	0.01	0.05	0.06
8	0.25	0.01	0.08	0.07
9	0.33	0.01	0.08	0.08
10	0.16	0.02	0.11	0.07
Mean	**0.579**	**0.035**	**0.064**	**0.08**
SD	**0.632**	**0.032**	**0.028**	**0.022**

Saline flush vs 2L CO_2 flush: p=0.024

Saline flush vs 4L CO_2 flush: p= 0.029

Saline flush vs 6L CO_2 flush: p= 0.031

2L vs 4L flush: p=0.047

4L vs 6L CO_2 flush: p= 0.756

2L vs 6L CO_2 flush: p= 0.021

6.2.3 Gas composition analysis

The results of the gas composition analysis are displayed in table 6.3. Due to a lack of endografts I decided to test the highest and lowest flow rate only. I therefore omitted testing the 4L flow rate testing in previous experiments.

The baseline level of CO_2 and O_2 signal are shown under the 'argon' group. Following injection air into the chamber and analysis of the gas bubbles (bubbles in argon) Analysis of gas released from the endograft following CO_2 flushed demonstrated more CO_2 than O_2, as would be expected (bubbles in CO_2 only). These experiments served to establish some baseline results to ensure the mass spectroscopy could detect any changes in composition between CO_2 and O_2 of gas bubbles under different conditions.

There was a significant reduction in the O_2 signal with 2L/min of CO_2 flushing compared to saline flushing alone (23± 17 vs. 50 ±18; p=0.04), and to 6L/min CO_2 (23± 17 vs 49 ± 19; p=0.96), respectively. There was no significant difference in the O_2 signal between 6L and saline flushing (49 ± 19 vs 50 ± 18; p=0.96). The proportion of O_2 to CO_2 was significantly reduced with both 2L and 6L of CO_2 flushing (p= 0.02 for both) compared to saline flushing along, and with 2L CO_2 compared to 6L CO_2 (p=0.01).

Table 6.3 Composition of gas release using mass spectroscopy

Sample		**Argon**	**Bubbles in Argon**	**Bubbles in Argon**	**Bubbles In Argon**	**Bubbles in Argon**	**Bubbles in Argon**
CO_2 flush		No	No	6 L/min	No	6 L/min	2 L/min
Saline flush		No	No	No	Yes	Yes	Yes
Volume (mL)		N/A	8.6 ± 0.3	6.4 ± 0.4	3.2 ± 0.4	2.2 ± 0.3	2.2 ± 0.2
Number of samples		5	5	6	5	5	6
Signal area	CO_2	7 ± 3	19 ± 3	2588 ± 411	3 ± 2	9 ± 3	8 ± 3
	O_2	12 ± 3	990 ± 103	52 ± 10	50 ± 18	49 ± 19	23 ± 17
	O_2/CO_2	2 ± 1	55 ± 9	0.021±0.006	24±12	5 ±2	3±2

Data is shown as mean ± standard deviation

6.2.4 Gas distribution

Prior to endograft deployment, the haemodynamic properties of the model were optimised to achieve physiological parameters. The stroke volume and heart rate were varied for a 30/70 systole/diastole ratio to achieve a physiological blood pressure (BP) and mean arterial pressure (MAP). Callipers were applied to the 'upper limbs' of the model and tightened to simulate resistance. The haemodynamic measures generated are displayed in Table 6.4.

Table 6.4 Haemodynamic measures from the model under various systolic/diastolic ratios (SD), stroke volume (SV), heart rate (HR), blood pressure (BP), mean arterial pressure (MAP)

SD	SV	HR	BP	
30/70	30	50	109/52	79
25/75	30	50	110/52	80
S/D	SV	HR	BP	MAP
50/60	30	60	116/52	89
45/55	30	60	119/65	92
40/60	30	60	121/66	94
35/65	30	60	121/66	94
30/70	30	60	122/65	93
25/75	30	60	123/65	93
SD				
S/D	SV	HR	BP	
50/60	30	70	140/89	116
45/55	30	70	148/94	121
40/60	30	70	143/86	113
35/65	30	70	146/88	115
30/70	30	70	147/89	116
25/75	30	70	150/91	118
S/D	SV	HR	BP	MAP
50/60	30	80	164/106	132

45/55	30	80	170/112	138
40/60	30	80	174/116	143
35/65	30	80	177/119	145
30/70	30	80	179/120	147
25/75	30	80	181/122	149
SD	SV	HR	BP	
50/50	40	50	114/47	80
45/55	40	50	117/48	81
40/60	40	50	119/48	83
35/65	40	50	119/48	82
30/70	40	50	119/48	83
25/75	40	50	120/48	83
S/D	SV	HR	BP	
50/60	40	60	130/67	99
45/55	40	60	132/69	101
40/60	40	60	131/71	103
35/65	40	60	140/72	105
30/70	40	60	142/73	106
25/75	40	60	145/74	107
SD	Sv	HR	BP	
50/50	50	50	132/56	93
45/55	50	50	137/59	97
40/60	50	50	139/60	99
35/65	50	50	141/62	101
30/70	50	50	142/62	102
25/75	50	50	143/65	103
S/D	SV	HR	BP	MAP
50/50	50	40	107/31	68
45/55	50	40	109/31	69
40/60	50	40	111/30	70
35/65	50	40	113/30	70
30/70	50	40	115/30	70
25/75	50	40	116/29	70
S/D	SV	HR	BP	MAP

50/50	60	40	130/45	88
45/55	60	40	136/47	91
40/60	60	40	139/47	91
35/65	60	40	141/47	92
30/70	60	40	145/47	93
25/75	60	40	148/47	94
SD	SV	HR	BP	
50/50	20	60	63/25	44
45/55	20	60	64/25	43
40/60	20	60	66/25	44
35/65	20	60	68/24	44
30/70	20	60	69/24	44
25/75	20	60	70/24	44
S/D	SV	HR	BP	MAP
50/50	20	70	77/35	55
45/55	20	70	81/38	58
40/60	20	70	84/39	60
35/65	20	70	86/40	61
30/70	20	70	88/41	62
25/75	20	70	90/42	63
S/D	SV	HR	BP	MAP
50/50	20	80	95/51	70
45/55	20	80	100/54	74
40/60	20	80	103/56	77
35/65	20	80	105/58	79
30/70	20	80	106/59	80
25/75	20	80	107/60	81
S/D	SV	HR	BP	MAP
50/50	20	90	110/67	86
45/55	20	90	114/70	89
40/60	20	90	115/71	90
35/65	20	90	119/75	94
30/70	20	90	120/76	95
25/75	20	90	121/78	96

S/D	SV	HR	BP	MAP
50/50	20	100	120/78	97
45/55	20	100	119/78	98
40/60	20	100	118/79	98
35/65	20	100	118/79	98
30/70	20	100	117/78	98
25/75	20	100	117/78	98

Based on these results, the final settings used for all deployments are highlighted in the red box in the above table. The corresponding arterial waveform at these haemodynamic measures is shown in Figure 6.2.

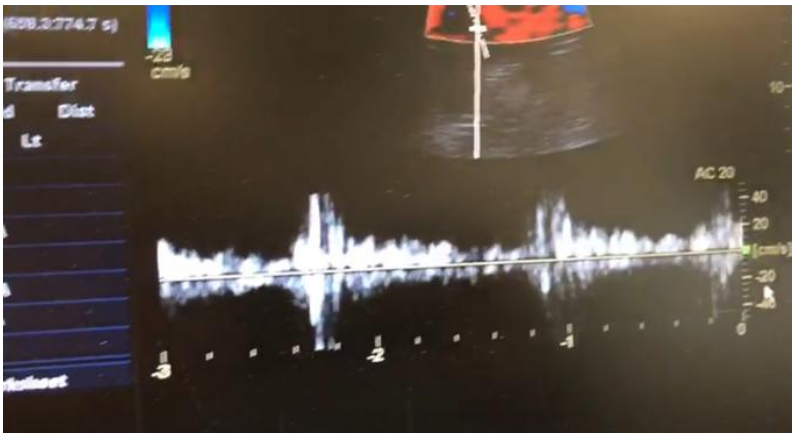


Figure 6.2 Arterial waveform using an ultrasound scan produced at the ascending aorta

All Endografts were deployed in zone 3. The results of the number of bubbles detected by the GAMPT detector and on aspiration are shown in Table 6.5. During endograft deployments, significant methodological issues were experienced with the model. In between endograft deployments, the GAMPT bubble detector would record bubble activity, despite no activity going on within the model. The 60ml syringe that was filled with 10mls saline would often be filled up with circulating fluid during deployments and no bubbles were aspirated. At other times, small bubbles would get stuck on the tubing and could not be aspirated. The results presented in Table 6.5 must therefore be interpreted with caution. No statistical

analysis has been conducted on the data due to concerns regarding the reliability of the model in detecting the number and volume of gas released during endograft deployments.

Table 6.5 Bubble detector results under various flushing conditions

Total volume of gas/sample	**IFU**			**Saline**			**CO_2**		
1	RCCA	LCCA	LVA	RCCA	LCAA	LVA	RCCA	LCCA	LVA
Number	0	2	4	1	3	2	0	0	0
Total volume(ml)	0.02			0.02			0.01		
2	RCCA	LCCA	LVA	RCCA	LCCA	LVA	RCCA	LCCA	LVA
Number	2	1	3	0	0	0	1	1	1
Total volume(ml)	0.03			0.05			0.04		
4	RCCA	LCCA	LVA	RCCA	LCCA	LVA	RCCA	LCCA	LVA
Number	1	3	2	0	0	0	2	3	1
Total volume(ml)	0			0			0.02		
5	RCCA	LCCA	LVA	RCCA	LCCA	LVA	RCCA	LCCA	LVA
Number	2	5	8	2	4	7	1	3	3
Total volume(ml)	0.2			0			0		

IFU, instructions for use; RCCA, right common carotid artery; LCCA, left common carotid artery; LVA, left vertebral artery.

6.3 Discussion

A series of experiments were conducted to determine (1) the optimal time and flow rate for CO_2 flushing to achieve a significant reduction in the volume of air bubbles released (2) cerebral distribution of air bubbles released to further understand the trajectory of released air bubbles.

Firstly, the 'time' experiment determined that CO_2 moves through the endograft as a plug. This is demonstrated from the stepwise mass spectroscopy plots. The method by which CO_2 purges or removes gas within the endograft is therefore through displacement (the replacement of one substance by another) and not through dilution (the replacement of one substance by another through appreciable mixing/diffusion). Some mixing/diffusion occurs early on as CO_2 fills up the endograft as the beginning of the graph displays a gradual incline just after 25 seconds (Figure 6.1B).

This finding is in keeping with the purging of industrial pipelines (of which an endograft is of a similar shape) whereby the area of contact between the purging gas and gas to be purged is small that very little mixing occurs.[363] CO_2 is 1.5x denser to air and therefore is likely to stratify and remain on the bottom/sink to the bottom of a chamber/pipe (such as an endograft). As the heavier gas it can then push out the lighter gas. To facilitate this process, it is important that the endograft is kept elevated as is done during standard saline purging.

This experiment also established that it takes about 2 seconds for CO_2 to reach the end of the endograft and reach a steady state. Therefore, the 2 minutes flushing that was used in the clinical experiments described in chapters 4 and 5 was an adequate time for CO_2 flushing. A short flush time (relative to the operation) is

important for the clinical translation of CO_2 given that during an emergency when the endograft needs to be urgently inserted into a patient to prevent death, longer flush times are not ideal.

Secondly, the 'volume' experiment demonstrated that CO_2 flushing (at any flow rate) is better than saline alone in reducing the volume of 'gas' released from the endograft. This experiment also demonstrated that a slow flow rate (2L/min) compared to higher flow rates (4L and 6L) was associated with the least volume of 'gas' released from the endograft, with no difference in the 'gas' released between 4L and 6L.

At 6L, significant leakage of CO_2 was observed from all connection points in the system. This may in part explain why greater volumes of 'gas' were observed at this high flow rate. These findings are again in keeping with industrial purging processes. In addition to using a gas with a higher density as the purging gas (eg. CO_2), displacement purging is reported to work efficiently at slow flow rates when the height to diameter ratio (as with an endograft) is high.[364] This is in contrast to dilution/mixing purging mentioned above that is the method of purging of the apparatus has a low height to diameter ratio and no dead space in the system (as in an endograft that has several pockets of air from the compressed fabric of the endograft).[364] Slower flow rates are also used to displace air in lab experiments for example during chromatography mobile phases, a slower and longer duration of purging is used to push air out of the liquid.

One theory as to why high flow rates (4L and 6L) weere not as effective as lower flow rates may be due to the way CO_2 flows within the endograft with different flow rates and the impact of resistance to flow within the endograft.

Laminar flow is observed when fluids/gases flow smoothly, with little friction within the system. Little mixing occurs during this type of flow. Conversely, turbulent flow occurs when the layers of a fluid/gas travel in a disordered pattern, creating eddies (swirling of fluid).[365] Turbulent flow increases the pressure in the system and ultimately the resistance, all of which are exacerbated by non-modifiable points of increased resistance within the system that the gas has to pass through (eg at the in-line filter and at the point of contact of the highly compressed endograft). The final endpoint of this is the system needing to give way and leaking at points of weakness (hence the CO_2 leaks observed with higher flow rates and the tubing breaking). Turbulent flow also leads to purge mixing, creating a sinusoidal graph plot.[366]

I was able to demonstrate this principle by observing the pattern of CO_2 flow under water as it flushes the endograft (figure 6.3) whereby 2L of flow was associated with an organised pattern of bubble release, whereas 6L of flow was associated with a chaotic and disorganised pattern of bubble release.

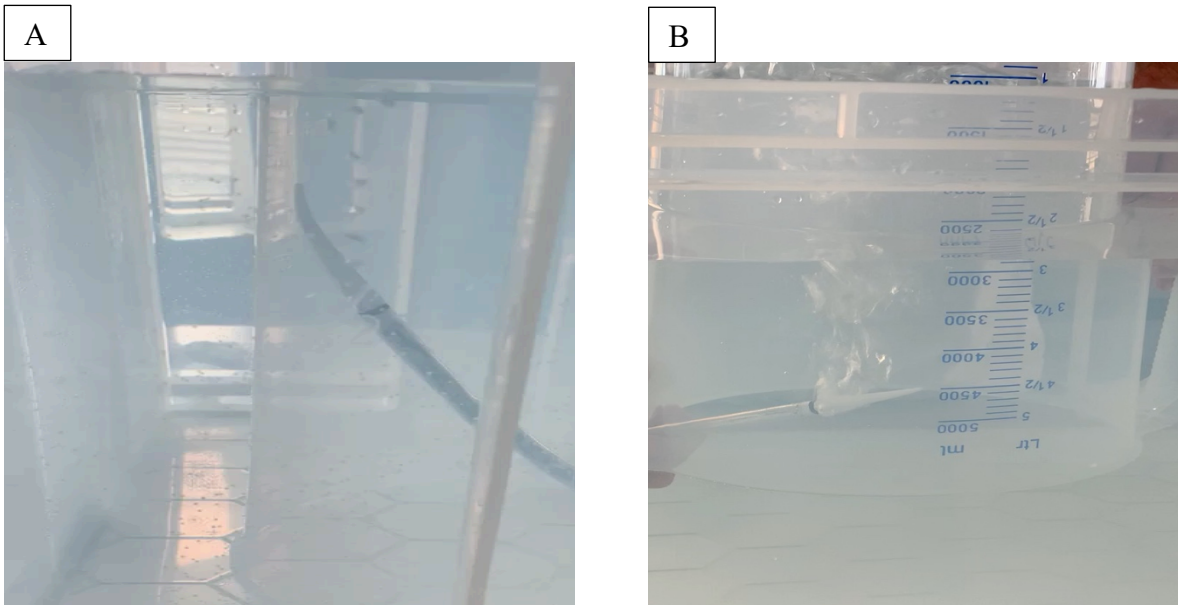


Figure 6.3 Neat and organised pattern of CO_2 bubbles released at 2L (A) compared to disorganised pattern of CO_2 bubbles released with 6L(B).

The findings of this experiment were also confirmed through bubble composition analysis using mass spectrometry. CO_2 at a slower (2L) flow rate was associated with a significant reduction in the O_2 signal compared to saline flushing, while the 6L flow rate made no significant reduction to the O_2. Furthermore, 2L flow rate was better than 6L flow rate at reducing the O_2 signal.

The final experiment unfortunately did not go according to plan due to several methodological flaws as explained in the results section. The complexity of the set-up did not allow for the accurate flow volume quantification and there were concerns regarding the detection of microbubbles within the setup by the GAMPT bubble detector.

Makaloski et al[96] are the only other group to attempt to set up a pulsatile thoracic phantom to quantify the volume of air bubbles according to zone of TEVAR. They concluded that zone 2 TEVAR was associated with more air bubbles collected from the right carotid artery, while more air bubbles were observed in the distal descending thoracic aorta for deployments in zone 3.

My set-up differed from this study with the use of the blood mimicking fluid. It is possible that the small orgasol particles interfered with the bubble GAMPT detector signal. This was fed back to the company, and a sample of the blood mimicking fluid has been sent to them to allow for calibration of the GAMPT bubble detector. Nevertheless, there was also a concern regarding the accuracy of the gas volumes that were being aspirated. This technique has been described before in other experimental models, and while this was accurate for the static chamber experiment, it was felt not to be accurate in the pulsatile flow model set-up.

As explained in the results, there were endograft deployments where bubbles were clearly seen to be released from the endograft but following aspiration, we did not find them in the syringes. Similarly, there were times when there were clearly no bubbles seen, yet air was collected in the syringes. I suspected that this may be coming from the leur lock connections, despite best efforts to prime all lines and connections to remove air from the model.

One possible solution to these issues was to use normal saline as the fluid medium for the model to and depend on the counts from the GAMPT bubble detector only for a given supra-aortic vessel. There were concerns, however that small air bubbles from leur lock connections would be circulated throughout the model with the Harvard pulsatile pump and further jeopardise the results of the GAMPT bubble detector. At this point, there was also not enough endografts to continue any further testing despite best efforts to acquire more from the companies. The remaining endografts had also started to break from repeated re-sheathing and were also not suitable for further use.

The model therefore requires further modification in order to ensure it is a valid way of quantifying the volume of gas released according to a zone of deployment and cerebral distribution.

6.4 Limitations

The series of benchtop experiments described in this study cannot fully simulate the in vivo environment of endograft deployment. Gas bubble physiology is complex and is influenced by the solubility of the gas in each fluid, the temperature and pressure of the environment. While all experiments were conducted at room temperature, the other variables were not controlled for. Small bubbles released during all deployments would often get stuck to the surface of the deployment chamber and this may influence the volume and composition experiments. The composition experiments do not provide a quantity or concentration of O_2 and CO_2. The re-sheathing of endografts is also not ideal as the gas environment may not fully replicate the manufacturing process. While I ensured there were no bubbles visible within the delivery system after deployment and before re-sheathing, and all endografts were purged with compressed heated air to dry out the endografts thoroughly and remove small bubbles, there is no guarantee that the inside of the delivery system was completely dry. The results in this series of studies are also on only one type of TEVAR endograft and should be validated for the other TEVAR endografts.

6.5 Conclusion

This series of experiments have demonstrated that it takes a minimum of 2 seconds for CO_2 to purge an endograft and reach a steady state. They have also demonstrated that CO_2 is better than saline at reducing the volume of gas released following endograft deployment. Slower flow rates of CO_2 flushing are better than higher flow rates and saline flushing alone at achieving a lower O_2 signal of the bubbles released following endograft deployment. These results need to be validated for other TEVAR endografts. More developmental work is required to optimise the pulsatile thoracoabdominal aortic model to ensure it is reliable and valid in determining the volume and number of gas bubbles released during endograft deployment under physiological conditions.

Chapter 7: Cerebral Embolic Filter Study

7.1 Aim

Determine the effect of the Sentinel CEPD to prevent peri-procedural cerebral embolisation, DW-MRI injury, clinical stroke, and neurocognitive impairment.

7.2 Results

7.2.1 Study population

Eighteen patients were recruited to undergo CEPD insertion, and 29 patients were recruited as controls. The demographic characteristics are described in Table 7.1. The procedural characteristics are described in Table 7.2. Eighteen proximal and 17 distal filters were deployed. CEPD success was 94% (17/18); the distal filter could not be deployed in one patient due to difficulty navigating complex anatomy. All filters were retrieved successfully. Use of the CEPD did not increase total operative time, fluoroscopy time or contrast volume.

Table 7.1 Demographic characteristics of the study population

	CEPD (N= 18)	**Controls (N= 29)**	**P=value**
Median Age, yrs (IQR, Range)	74 (16, 46-85)	73 (22, 28-86)	0.569
Male	28 (5/18)	69 (20/29)	0.064
Co-morbidities			
HTN	100 (18/18)	55 (16/29)	0.001
IHD	83 (15/18)	24 (7/29)	0.000
AF	11 (2/18)	14 (4/29)	0.789
COPD	44 (8/18)	38 (11/29)	0.658
DM	17 (3/18)	10 (3/29)	0.732
Previous history of stroke/TIA	11 (2/18)	10 (3/29)	0.934
Smoker	33 (6/18)	34 (10/29)	0.934

Renal failure (eGFR < 60ml/min) Previous thoracic aorta surgery Previous abdominal surgery	11 (2/18) 44 (4/18) 6 (1/18)	31 (9/29) 21 (6/29) 3 (1/29)	0.117 0.901 0.728
Pathology Acute dissection/aortic syndrome Aneurysmal disease (chronic type B, post-coarctation)	 28 (5/18) 72 (13/18)	 14 (4/29) 86 (25/29)	 0.236
Median VPOSSUM morbidity, % (IQR, Range) **Median VPOSSUM mortality, % (IQR, Range)**	61.8 (40, 12-96) 6.1 (7.3, 0.8-27)	58.9 (35,1.2-84) 5.3 (4, 0.7, 46)	0.125 0.518
Arch Atheroma 1-2 3-4	 61 (11/18) 39 (7/18)	 55 (16/29) 45 (13/29)	 0.689
Fazekas grade Periventricular white matter 0-1 2-3 **Deep white matter** 0-1 2-3	 71 (12/17) 29 (5/17) 100 (17/17) 0 (0/17)	 72 (21/29) 28 (8/29) 83 (24/29) 17 (5/29)	 0.894
Medication Statins Antiplatelet Anticoagulant	 78 (14/18) 17 (3/18) 17 (3/18)	 76 (20/29) 86 (25/29) 7 (2/29)	 0.927 0.000 0.291

Values are reported as percentages and whole numbers in parentheses.

7.2.2 Clinical outcomes

Clinical outcomes are reported in Table 7.3. One patient in the CEPD arm experienced TEVAR stent-graft migration into zone 1 resulting in partial coverage of the left common carotid artery and underwent an unplanned right to left common carotid artery bypass to preserve antegrade flow into the left common carotid artery. This patient did not suffer a neurological event. Three patients in the CEPD arm died during the hospital admission. None of the patients suffered a transient ischaemic attack. There were no peri-operative strokes in the CEPD arm; one patient in the control arm developed a left sided middle cerebral artery territory stroke confirmed on post procedural MRI and resulting in weakness in the right hand (mRS 3) that improved (mRS 1) at 6-week follow-up (CEPD arm, 0% vs control arm 6% stroke rate; p=0.49).

Table 7.2 Procedural characteristics of the study population

	CEPD (N= 18)	**Controls (N= 29)**	**P=value**
Sentinel device Right Brachial artery access Both filters deployed	 100(18/18) 94 (17/18)	 NA NA	
Emergency	39 (7/18)	24 (7/29)	0.282
TEVAR procedure TEVAR TEVAR + CS TEVAR + CC-CS	 72 (13/18) 22 (4/18) 6 (1/18)	 72 (21/29) 27 (8/29) 0 (0/29)	0.420
Zone 1 2 3 4	 6 (1/18) 22 (4/18) 56 (10/18) 17 (3/18)	 0 (0/29) 45 (13/29) 34 (10/29) 21 (6/29)	0.218
LSA management Uncovered Covered Revascularised	 72 (13/18) 0 (0/18) 28% (5/18)	 55 (16/29) 10 (3/29) 34 (10/29)	0.281
Spinal drain	56 (10/18)	45 (13/29)	0.474
Median Operative time, mins (IQR, Range)	135 (63, 95-750)	240 (102, 52-439)	0.437
Median Fluoroscopy time, mins (IQR, Range)	11 (4, 4-17)	0.18 (0.31, 0.01-0.25)	0.135
Median DAP, mGy.cm2 (IQR, Range)	64208 (137514, 10200-434569)	44000 (133535, 129-454945)	0.341
Median Total contrast omnipaque, mls (IQR, Range)	90 (42, 50-180)	80 (63, 30-260)	0.594
Intra-operative transfusion	33 (6/18)	21 (6/29)	0.334

TEVAR, thoracic endovascular aortic repair, CC, carotid-carotid; CS, carotid-subclavian, LSA, left subclavian artery; CEPD, cerebral embolic protection device; DAP, dose area products, IQR, interquartile range. Values are reported as percentages and whole numbers in parentheses.

Table 7.3 Clinical outcomes

	CEPD (N= 18)	Controls (N= 29)	P=value
Any MACCE*	28 (5/18)	17 (5/29)	0.473
Clinical stroke within 30 days	0 (0/18)	3 (1/29, disabling)	1.000
Clinical stroke > 30 days	6 (1/18)	7 (2/29)	1.000
In-hospital death	17 (3/18) (retrograde dissection, spinal sepsis, ischaemic gut)	0 (0/29)	0.05
In-hospital complications			
Retrograde dissection	1		
Cardiac	1		
Respiratory	1	3	
GI	1		
Neurological	1 (spinal sepsis)		
Wound related	1	1	
Return to theatre	1	1	
CEPD complications			
brachial pseudoaneurysm	4	NA	
Major vascular complications			
Brachial	1	0	
Femoral	0	0	
Median Length of hospital stay, days (IQR, Range)	12 (5-18)	7 (5 -9)	0.089

MACCE, major cerebrovascular and cardiovascular events (defined as all deaths, strokes, AKI stage 3, within 30 days); CEPD, cerebral embolic protection device, GI, gastrointestinal. Values are reported as percentages and whole numbers in parentheses.

7.2.3 DW-MRI outcomes

MRI outcomes are shown in Table 7.4. New DW-MRI infarcts were observed in 71% of patients in the CEPD arm and 65% of patients in the control arm (p=0.71). The median total infarct surface area in the CEPD arm was 5mm^2 (0-16mm^2) versus 15mm^2 (0-36mm^2) in the control arm (p=0.42), representing a 67% reduction. The median total infarct surface area for the left hemisphere was 4mm^2 (0-15mm^2) versus 6mm^2 (0-28mm^2; p=0.53), representing a 33% reduction. This was mainly driven by a 45% reduction in the number of infarcts to the left anterior circulation between the two arms (26% reduction in infarcts for the left posterior circulation). The median total number of infarcts was 2 in both arms (CEPD range 0-3mm^2 vs. control arm range 0-4mm^2; p= 0.69). There were no significant differences in the number of infarcts when analysed by cerebrovascular territory.

Table 7.4 DW-MRI infarcts according to cerebrovascular territory

	CEPD (N= 18)	**Control (N= 29)**	**P=value**
Number of patients with new infarcts	71 (12/17)*	59 (17/29)	0.417
Number of patients with			
Bi-hemispherical infarcts	35 (6/17)	38 (11/29)	0.858
>1 infarct left hemisphere	35 (6/17)	31 (9/29)	0.766
>1 infarct right hemisphere	24 (4/17)	28 (8/29)	1.00
Number of Patients with infarcts by territory			
Left hemisphere	65 (11/17)	55 (16/29)	0.526
Right hemisphere	41 (7/17)	45 (13/29)	0.809
Left ACA	29 (5/17)	28 (8/29)	1.00
Right ACA	12 (2/17)	17 (5/29)	1.00
Left PCA	41 (7/17)	34 (10/29)	0.650
Right PCA	29 (5/17)	24 (7/29)	0.737
Left borderzone	29 (5/17)	19 (3/29)	0.125
Right borderzone	6 (1/17)	7 (2/29)	1.00
Total number of new infarcts (median, range)	40 (2, 0-12)	84 (2, 0-20)	0.972
Total number of infarcts by territory (median, range)			
Left hemisphere	26 (1,0-7)	58 (1, 0-17)	0.711
Right hemisphere	14 (0,0-5)	26 (0,0-6)	0.781
Left ACA	5(0, 0-1)	16(0,0-5)	0.818
Right ACA	3(0, 0-2)	8 (0,0-2)	0.61
Left PCA	16 (0, 0-6)	38 (0,0-15)	0.481
Right PCA	10 (0, 0-5)	16 (0,0-6)	0.802
Left borderzone	5 (0, 0-1)	4 (0,0-2)	0.124
Right borderzone	1 (0,0-1)	2 (0,0-1)	0.894
Total Infarct surface area, mm^2 (median, range)	455 (5, 0-302)	2046 (4, 0-804)	0.981
Total surface area of infarcts by territory, mm^2 (median, range)			
Left hemisphere	291 (4, 0-184)	1708 (4, 0-792)	0.897
Right hemisphere	164 (0, 0-118)	338 (0, 0-221)	0.890
Left ACA	36 (0, 0-15)	215 (0,0-142)	0.897
Right ACA	18 (0,0-10)	37 (0,0-19)	0.689
Left PCA	219 (0,0-169)	1323 (0,0-784)	0.509
Right PCA	144 (0,0-118)	288 (0,0-221)	0.735
Left borderzone	36 (0,0-18)	170 (0,0-160)	0.130
Right borderzone	2 (0,0-2)	13 (0,0-9)	0.852

Values are reported as percentages and whole numbers in parentheses. Non-parametric data are presented as median + interquartile range. DW-MRI, diffusion-weighted magnetic resonance imaging; ACA, anterior circulation, PCA, posterior circulation. *Outcomes for 17 patients as 1 patient did not undergo MRI.

7.2.4 Neurocognitive outcomes

Neurocognitive outcomes are detailed in Table 7.5. Post-operative neurocognitive impairment on the composite score was observed in 47% (7/15) of patients in the CEPD arm and 50% (7/14) of patients in the control arm (p=0.86). At 6-week follow-up, 10% (1/10) patients in the CEPD arm experienced neurocognitive impairment on the composite score compared to 33% (4/12) in the control arm (p=0.32).

Table 7.5 Neurocognitive outcomes

	CEPD (18)	**Controls (29)**	**P-value**
***'Composite' neurocognitive impairment**			
Baseline to post-operatively	47 (7/15)	56 (14/25)	0.567
Baseline to 6-weeks	10 (1/10)	42 (8/19)	0.076
Baseline to 6-months	18 (2/11)	29 (4/14)	0.661
****Executive function**			
Baseline to post-operatively	13 (2/15)	28 (7/25)	0.440
Baseline to 6-weeks	20 (2/10)	42 (8/19)	0.414
Baseline to 6-months	18 (2/11)	7 (1/14)	0.565
****Verbal Learning**			
Baseline to post-operatively	7 (1/15)	38 (9/24)	0.057
Baseline to 6-weeks	0 (0/10)	21 (4/19)	0.268
Baseline to 6-months	8 (1/12)	0 (0/14)	0.462
****Verbal memory**			
Baseline to post-operatively	13 (2/15)	42 (10/24)	0.147
Baseline to 6-weeks	10 (1/10)	21 (4/19)	0.633
Baseline to 6-months	8 (1/12)	21 (3/14)	0.598
****Visual search and motor skills**			
Baseline to post-operatively	36 (5/14)	50 (11/22)	0.4
Baseline to 6-weeks	10 (1/10)	33 (6/18)	0.364
Baseline to 6-months	8 (1/12)	36 (5/14)	0.170
****Mental flexibility and switching**			
Baseline to post-operatively	57 (8/14)	35 (8/23)	0.183
Baseline to 6-weeks	20 (2/10)	28 (5/18)	1.000
Baseline to 6-months	17 (2/12)	21 (3/14)	1.000
****Manual dexterity**			
Dominant hand			
Baseline to post-operatively	25 (3/12)	33 (7/21)	0.710
Baseline to 6-weeks	0 (0/9)	0 (0/18)	-
Baseline to 6-months	0 (0/10)	0 (0/12)	-
Non-dominant hand			
Baseline to post-operatively	17 (2/12)	10 (2/21))	0.610
Baseline to 6-weeks	20 (2/10)	24 (4/17)	1.000

Baseline to 6-months	10 (1/10)	8 (1/12)	1.000

Values are reported as percentages and whole numbers in parentheses. *Cognitive decline >20% decline on 2 or more of the tests (total of 7 tests). ** Cognitive decline > 20% on a respective test.

7.2.5 Histological analysis

A total of 35 filters were analysed (Figure 7.1); 17/18 (94%) proximal and 15/17 (89%) distal filters contained debris composed mainly of acute platelet-rich thrombi associated with tissue or foreign material (80%). The median total number of particles captured per patient was 939 (range: 102-13,602). The median total particle area per patient was 2.6mm^2 (0.13mm^2 -51.8mm^2), with the distal filters containing more tissue than the proximal filters (total median area 1.42mm^2 [0-14.2mm^2] vs 0.99mm^2 [0.12-5.2mm^2]). The distal filters also captured larger tissue fragments than the proximal filters (5975.1 µm^2 vs 4322.5 µm^2). The median number of particles captured per patient measuring at least 150 µm in maximum diameter was 47.5, with distal filters showing a greater incidence than the proximal filters (33 vs 20.5). The average minimum, median, and maximum particle diameters were 26.1 µm, 44.5 µm, and 77.5 µm, respectively, with the distal filters having a greater value for each category compared to proximal filters (23.4 µm vs 14.7 µm, 39.2 µm vs 25.2 µm, and 66.0 µm vs 45.8 µm, respectively).

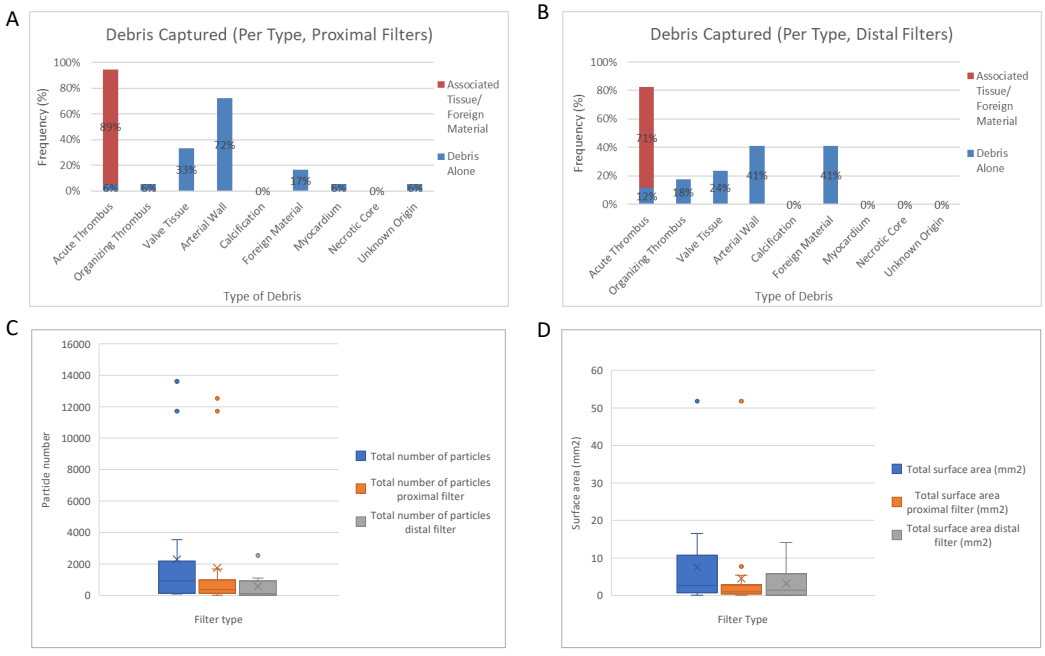


Figure 7.1 Histological analysis of debris caught from the filters.

7.3 Discussion

This is the first study to explore the clinical efficacy of the Sentinel^{TM} dual-filter to reduce the effects of peri-procedural embolization during TEVAR. Patients undergoing TEVAR with a CEPD demonstrated a 67% reduction in total surface area of infarcted brain tissue that was mainly driven by a reduction in the total surface area of infarcted cerebral tissue in the left hemisphere (anterior circulation > posterior circulation). There were no clinical neurological events and there was a (non-statistically significant) trend towards improved neurocognitive function during follow-up compared to patients undergoing TEVAR without CEPD protection.

The incidence of new peri-procedural DW-MRI infarcts following TEVAR is reported to be in the order of 63-81%.[5,6] The use of a CEPD in this study did not reduce this (71% DW-MRI infarct rate). The imaging results of this study are, broadly in-line with several of the randomised controlled trials of commercially available CEPDs in TAVR that demonstrate a reduction in the volume of infarcts mainly in filter protected regions of the brain and to some extent for unprotected regions.[12-14, 17,18] The 67% reduction in the median total surface area of infarcted tissue is in line with the 42% reduction in median total new lesion volume observed in the SENTINEL trial,[14] the largest published RCT of any CEPD in TAVR to date. Two recent meta-analyses comparing CEPD versus no CEPD in TAVR have demonstrated a reduction in single lesion and total lesion volumes in favour of CEPD but did not find a difference in the incidence or in the number of DW-MRI infarcts per patient.[7,25]

The greater reduction in the surface area of infarcted tissue in the left hemisphere compared to the right is unsurprising. Including only zones 2-4 cases meant that navigation, manipulation, and stent-graft deployments were near the left common carotid artery that supplies most of the left hemisphere and is

protected by the distal filter. Accordingly, the distal filter captured a greater larger sized particles in comparison to the proximal filter that protects the right hemisphere.

Proportionally, the greatest number and largest amount of infarcted cerebral tissue in both arms was in the left posterior circulation that is supplied by the posterior inferior cerebellar artery and that remains unprotected by the Sentinel^{TM} CEPD. The Sentinel^{TM} CEPD is reported to provide protection to 74% of the brain through protection of the innominate and left common carotid artery.[20] While this may be adequate cover for TAVR where high risk embologenic manoeuvres (valve deployment) mainly occur proximal to these (protected) vessels, the 26% of cerebral tissue that is partially/not protected with a filter (posterior inferior cerebellar territory) is a particularly significant issue for TEVAR.

Ischaemic damage following TEVAR has a predilection for the left hemisphere with up to 66.7% of ischaemic strokes occurring in the posterior circulation.[3,6] This is most likely due to (1) the retrograde nature of the procedure whereby instruments and stent-grafts are typically manipulated close to or past the left subclavian artery (that branches into the posterior inferior cerebellar artery), irrespective of the zone, and (2) because a complete Circle of Willis may allow emboli to impact either hemisphere, irrespective of whether passage into the cerebral circulation occurred through the left or right supra-aortic vessel. This, together with the partial protection afforded to the right posterior circulation may also explain the proportionately high number of infarcts observed in this region (25% of infarcts in CEPD group). The temporary loss of antegrade flow from large delivery sheaths, and vortical/helical flow patterns within the aorta may also increase the likelihood of emboli travelling upwards into the unprotected left subclavian artery.

Van Gils *et al*[26] describe the use of the Wirion filter into the left vertebral artery, in addition to the Sentinel CEPD during TAVR and found comparable amounts of debris between the two CEPDs with a median of 0.33mm diameter particles captured by the Wirion, suggesting a benefit to the additional use of a filter for the left subclavian artery. Protection of all three supra-aortic trunks to provide complete brain protection during TEVAR may also be important and requires further investigation.

The neurological and neurocognitive trends observed in this study are also in-keeping with the CEPD TAVR trials. The SENTINEL trial,[14] observed fewer strokes (5.6% vs 9.1%, p= 0.25) and while neurocognitive testing showed no difference in overall composites scores at all follow-up time-points, there was a correlation between median infarct volume and cognitive change scores from baseline to 30-day follow-up. The CSI-Ulm TAVR that used the Sentinel™ CEPD[27] is the only study to demonstrate a significant reduction in clinical stroke (1.4% vs 4.2%, unpublished data and still undergoing follow-up), and the MISTRAL-C trial[13] is the only study to date that has demonstrated less cognitive deterioration with CEPD protection (4% vs 27%, p=0.017). Meta-analysis of all of the published CEPD RCTs has not demonstrated a protective effect against stroke, or death with the use of a CEPD.[28] Analysis of 10,985 patients from the U.S. Vizient administrative database also found no statistically significant differences in stroke or TIA, even after propensity score matching.[29] Interestingly, a meta-analysis using robust cognitive change definitions found that the use of CEPDs was one of the factors associated with decreased prevalence of cognitive decline following TAVR.[30]

Putative explanations for the lack of statistically significant reductions in clinically relevant outcomes despite the reported high (>80%) capture rate of embolic debris by CEPDs and the concomitant reduction in new DW-MRI infarcts, may in part be due to the lack of protection of the left subclavian artery, the small and transient effects of infarcts (>80% of infarcts from TAVR disappear by 3-months),[31] the use of 3T or

1.5 T MRI that may lead to over or underreporting of infarcts, heterogeneity in neurocognitive testing with respect to the specific tests and timing of these tests, and the definition of clinically significant neurocognitive impairment. The standardisation of the conduct and reporting of the neurological endpoints for cardiovascular clinical trials including TEVAR and TAVR by the Neurological Academic Research Consortium Initiative (NeuroARC) may circumvent these limitations.[32]

7.4 Limitations

The data in this study evidenced significant skew and dispersion which together with the small sample size and high drop-out rate from neurocognitive testing precluded regression analysis to determine predictors of DW-MRI infarcts and neurocognitive impairment The occurrence of cerebral microemboli and DW-MRI infarcts may have been generated by the CEPD itself. The reduction in protected territories, however, does not support this notion. Nevertheless, there is no TEVAR-specific CEPD and as a first-in-kind study, we have demonstrated the feasibility and safety of the use of CEPD as a potential neuroprotective adjunct in TEVAR workflow. Its strengths lie in the use of 3T DW-MRI, blinded analysis, and extensive neurocognitive testing, and as such this study should be considered hypothesis generating. The reduction in destructive ischaemic damage to the brain on neuroimaging from the capture of embolic debris by CEPDs and the potential benefit this may have in reducing procedure-related stroke and neurocognitive impairment, both of which have a negative impact on quality of life for patients, warrants further investigation in large trials powered to clinically relevant end points.

7.5 Conclusion

Use of the Sentinel^{TM} CEPD in TEVAR was associated with a reduction in the total surface area of infarcted cerebral tissue on neuroimaging, and a high degree of embolic debris capture. An adequately powered study is required to definitively determine the efficacy of using CEPD during TEVAR.

Chapter 8: Conclusions and future work

8.1 General discussion and conclusion

A wide range of pathologies develop in the thoracic aorta. At present, there is no medical treatment to prevent their development and/or progression. The main stay of treatment remains surgical intervention. As discussed in **Chapter 1**, Thoracic endovascular aortic repair (TEVAR) has revolutionised the management of a wide range of aortic pathologies that affect the thoracic aorta. As a minimally invasive endovascular procedure. It has significantly reduced the mortality and morbidity from open surgical repair by obviating the need for thoracotomy and aortic cross-clamping.

However, peri-procedural stroke remains a principal concern. The systematic review and meta-analysis conducted in **Chapter 2** has demonstrated no change in the stroke rate over the last 31 years for any pathology, despite reported improvements in patient selection, anaesthesia, new generation low-profile devices, and the configuration of vascular services. This study also demonstrated that the evaluation, definition and reporting of stroke and neurological brain injury following TEVAR is poor, resulting in significant heterogeneity between studies and very low quality of evidence according to GRADE criteria. Very few studies used a standardised stroke definition, and the assessment of stroke was unclear. Thus, it is likely that the incidence of TEVAR-related stroke is underestimated and remains largely unknown.

Several neuroimaging studies have demonstrated that the aetiology and predominant mechanism of injury is embolic.[41,42,45,74,250] Transcranial doppler (TCD) monitoring studies of the cerebral arteries have confirmed the embolic theory and have allowed us to understand that both solid and gaseous emboli may contribute to peri-procedural brain injury following TEVAR.[45,52,75,77]

In addition to clinical stroke, there is increasing recognition that high burden (81%) of procedure-related embolic injury to the brain as evident on DW-MRI is not 'silent' but can lead to neurocognitive decline.[52] The occurrence of a new infarct can disrupt highly complex and interconnected neuronal networks which may lead to neurocognitive decline.[71]

In recent years, two neuroprotective adjuncts have been proposed for TEVAR that have been driven by the findings of TCD monitoring. The overwhelming proportion of gaseous HITS on TCD monitoring compared to solid HITS throughout all phases of TEVAR, and in particular at the point of endograft deployment, and the positive correlation to new DW-MRI infarcts[75] has led to the hypothesis that endografts may release air during deployment and cerebral air embolisation is a mechanism of brain injury, despite standard saline flushing to purge out air from the devices and endografts. However, the presence of solid HITS also demonstrates that neuroprotective adjuncts against solid embolisation of atherosclerotic and thrombotic debris are required.

Armed with these findings, and as detailed in the methodology in **Chapter 3**, this thesis explored the effect of CO_2 flushing of endografts to prevent cerebral air embolisation during endograft deployment and reduce clinical and radiological TEVAR related brain injury. It also aimed to refine the CO_2 flushing technique for clinical practice and for possible further evaluation in a larger and well powered randomised trial through a series of benchtop experiments. This thesis also explored the effect of embolic filters during TEVAR to prevent solid cerebral embolisation.

As detailed in **Chapter 4**, CO_2 flushing of TEVAR endografts was associated with a 43% incidence of new DW-MRI infarcts. The recent STEP study also demonstrated a new DW-MRI infarct rate of 50%.[165] These are the only two studies that have evaluated the effect of CO_2 flushing to prevent cerebral air embolisation

and DW-MRI infarcts. The findings in both studies compare favourably to the neuroimaging studies that describe a DW-MRI infarction rate of 63-81%.[51,52]

This is the second study to differentiate TCD HITs into solid and gas. In line with the previous study by Grover et al.[75] both solid and gas HITS were detected at all procedural phases. However, in this study presented within this thesis, the proportion of gas was either the same or outweighed solid HITS for all procedural phases, except for endograft deployment, when fewer gaseous TCD HITS were observed. This further points to a potential neuroprotective effect of CO_2 flushing.

This study also confirmed the association between cerebral embolisation as the mechanism of brain injury related to the development of DW-MRI infarction and stroke. Furthermore, this is the first study to demonstrate that DW-MRI infarcts are not a silent event following TEVAR; the presence of DW-MRI infarcts increased the risk of neurocognitive decline two-fold. This provides further support to develop neuroprotective adjuncts that can reduce procedure-related DW-MRI infarcts.

As discussed in **Chapter 1**, several patient-related and procedure-related risk factors for TEVAR related stroke have been described such as higher atheroma grade and higher arch grade.[329] The study in **Chapter 4** identified that many of these risk factors are associated with greater TCD HITS, providing further support for the embolic theory. It may also explain why the clinical stroke rate was unaffected by CO_2 flushing; a higher atheroma grade and a higher arch grade indicate an increased atheroma burden and increase procedural complexity from an angulated arch, making it more likely that endovascular instruments contact the aortic wall more frequently, leading to solid embolisation which may have a greater propensity to cause stroke, than cerebral air embolisation of small bubbles, which may be associated with global brain injury in the form of cognitive decline.

In **Chapter 5**, I aimed to compare the DW-MRI infarcts and clinical stroke rate in patients undergoing TEVAR with CO_2 flushing versus standard saline flushing. Unfortunately, no TCD data or neurocognitive data were available, limiting comparative analysis to these two endpoints only. This study demonstrated significant reductions in the incidence, number, and surface area of new DW-MRI infarcts with CO_2 compared to saline flushing. However, as discussed in chapter 5, the neuroprotective effect was not observed for all cerebrovascular territories of the brain and was dependent upon the zone of TEVAR. The stroke rate was also not significantly different between the two groups, suggesting that CO_2 alone cannot prevent clinical stroke.

In **Chapter 6** I confirmed that commercially available endografts release a gas that could theoretically embolise to the brain. I sought to refine the CO_2 flushing technique to make it suitable and pragmatic for clinical use. I concluded that CO_2 flushing was a better technique to de-air stent-grafts than traditional saline flushing.

In **Chapter 7** I explored the impact of cerebral embolic filters to protect the brain against peri-procedural solid embolisation. This study demonstrated that while the proportion (incidence) of people with new DW-MRI infarcts was not different between the two groups, patients who underwent TEVAR with an embolic filter had fewer and smaller infarcts. While the results were not statistically significant, there was a trend to suggest that less neurocognitive decline was observed in patients who had the filters.

In conclusion, this body of work has confirmed that the aetiology of brain injury from TEVAR is embolic with both solid and gaseous emboli contributing to the mechanism of injury. There was evidence to suggest

that reducing the solid and gaseous embolic burden to the brain during the procedure was associated with fewer DW-MRI infarcts and cognitive impairment. However, the incidence of clinically overt stroke as a hard clinical endpoint, was not reduced by either neuroprotective adjunct.

8.2 Future work

The limitations of each study have been discussed at length under each respective chapter. Future work should attempt to address these in addition to investigating the research questions that have resulted from these studies.

8.2.1 Gaseous embolisation

The research regarding gaseous embolisation represents an important step in understanding the role of gaseous embolisation during TEVAR to cerebral injury. Future work should centre around repeating the work described herein for both reliability and validity.

This would involve several phases as follows:

Phase 1. Benchtop/experimental

I strongly believe that the benchtop work using mass spectrometry should be repeated to include all commercially available endografts. The largest diameter endograft should be used from all the companies to determine the optimal flush time for a particular endograft. This would involve a series of experiments and 'buy in' from companies to provide their endografts for testing with/without their engineers. A minimum of 10 endografts per 'flush protocol' should be tested and these should either be new or sent back to the company for re-packaging in the same way they would be when needed to be used for clinical use.

This would avoid having to recycle the endograft which we were forced to do and may have led to spurious results. To determine the flow rate through the endograft, a flow meter could be designed to be carefully inserted into the endograft. Testing with varying volumes of pressurised saline to determine whether this also provides a more effective purging technique could also be conducted

Phase 2. INTERCEPTevar^{CO_2}: INTERVention with Cerebral Embolic Protection in TEVAR: A feasibility randomised controlled trial

Armed with the optimal flush it is imperative that the efficacy of the CO_2 flush technique is tested clinically in a in a well-designed multi-centre randomised controlled trial with appropriate end-points. I was fortunate enough to submit a grant proposal to test the efficacy of CO_2 compared to standard saine flushing to Heart Research UK and JP Moulton who are jointly funding this randomised controlled trial (RCT) titled INTERCEPTevar^{CO_2} (clinicaltrials.gov identifier NCT03886675). The protocol be viewed in Appendix 9. This RCT was designed as a feasibility study to determine recruitment and retention (primary outcomes), with clinical secondary end-points. I am grateful to Mr Steve Crockett for taking up this study as his doctoral thesis. An interim statistical analysis will take place to allow a sample size calculation for the full-scale RCT.

Phase 3. Full scale randomised controlled trial

Once certain milestones have been achieved, this trial can then progress to a full-scale randomised trial. The power calculation will be derived from the secondary clinical endpoints derived from the feasibility study in phase 2.

8.2.2 Solid embolisation

Expanding on the work with the Sentinel^{TM} CEPD would involve mitigating the risk of leaving the left subclavian artery unprotected by the use of an additional filter. While a substantial amendment was granted for this study the COVID-19 pandemic halted recruitment and only one patient was recruited. Figure 8.1

demonstrates the use of two Sentinel^{TM} CEPD devices. Access was via the right and left brachial arteries, respectively. The proximal and distal filters of one device (access via right brachial artery) were deployed in the brachiocephalic and left common carotid arteries, and the proximal filter of a second device (access via the left brachial artery) was deployed in the left subclavian artery. While this provides an elegant solution to cerebral solid embolisation, its instructions for use alongside TEVAR need to be developed as unlike TAVI, there will be many permutations of TEVAR that need to be considered to ensure CEPD compatibility, including arch debranching and eventually the use of arch branch devices.

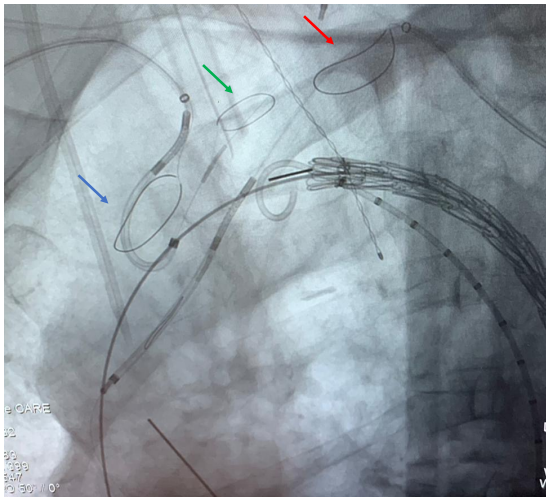


Figure 8.1 Fluoroscopy image showing three vessel filter protection using two Sentinel^{TM} CEPDs. The proximal and distal filters in the brachiocephalic (blue arrow) and left common carotid (green arrow), respectively, and the proximal filter in the left subclavian (red arrow)

Future research in this area should include the following phases:

Phase 1. Benchtop-testing involving a few centres expert in endovascular surgery

Phase 2. Feasibility/pilot study involving a few centres expert in endovascular surgery to establish safety and feasibility

Phase 3. Randomised controlled trial randomising patients to three vessel filter protection versus standard saline flushing in a similar study as INTERCEPTevar^{CO_2}.

8.2.3 Complete embolic protection in TEVAR

The aforementioned studies provide an important steppingstone to further understanding the impact of solid and gaseous embolisation and the efficacy of the neuroprotective adjuncts in isolation, removing confounding factors. However, from the evidence generated in this thesis, it is plausible that both solid and gaseous emboli contribute harmful effects to the brain. The ultimate study would involve using both CO_2 and CEPDs together in patients undergoing TEVAR and comparing such 'complete embolic protection' against standard saline. CO_2 is relatively safe and cheap and could therefore be used in every patient if found to be better than saline flush. However, inserting CEPDs carries risk, including that of vessel dissection and other access related complications, as well as solid embolisation and further stroke. Thus, we now need to determine which patients will get an additive benefit with the use of both CO_2 flushing and CEPD. For example, it may be that patients in zone 0-1 would gain most benefit with CEPD compared to patients undergoing TEVAR in zone 4 in whom a CO_2 flush may be adequate.

The radiological (MRI and TCD), clinical data (patient characteristics, operative characteristics, stroke and cognitive decline, quality of life) generated in these studies would help greatly in refining patient selection for both or either neuroprotective adjunct.

Appendix list

1 CO_2/embolic filter NIAS study participant information sheet

2 CO_2/embolic filter Patient consent form

3 DW-MRI reporting protocol

4 Modified rankin scale

5 REY auditor verbal learning test

6 Trail Making test part A and B

7 Grooved pegboard test

8 Controlled oral word association test (COWAT)

9 Protocol for INTERCEPTevar^{CO_2}

Appendix 1 CO_2/embolic filter NIAS study participant information sheet

Imperial College London

Participant Information Sheet

Neurological Injury in Aortic Stenting (NIAS study)

Chief Investigator: Mr Richard Gibbs MD FRCS, Consultant Vascular Surgeon and Honorary Senior Lecturer

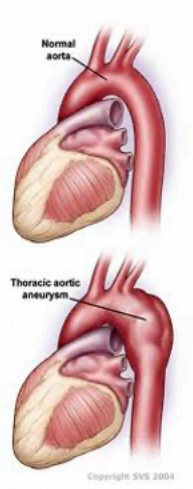
Funder: J.P. Moulton Charitable Foundation

Introduction

You are being invited to take part in the above research study. Before you decide it is important for you to understand why the research is being done and what it will involve. Please take time to read the following information carefully and discuss it with others if you wish. Please do not hesitate to ask us if anything is unclear or if you require any further information.

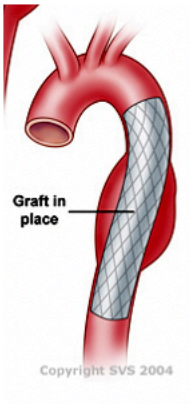
What is the purpose of the study?

The aorta (the body's main artery) can be affected by diseases such as an aneurysm (swelling) or a dissection (splitting of the layers of the artery). Traditionally this was treated with a major operation through a large incision in the chest or abdomen. It is now common for these diseases to be treated with an endovascular (minimally invasive) procedure where a stent (specially designed plastic tube) is introduced into the aorta through a small incision in the groin. This is known as an 'TEVAR' which stands for **T**horacic **E**ndovascular **A**ortic **R**epair.



REC Ref. 147211
Version 11 14/04/2019

In this study we are looking at patients such as yourself who are undergoing TEVAR. These patients have a shorter hospital stay and fewer post-operative problems than patients who have the open operation. However the procedure is not without any risk. If you are having a TEVAR (Thoracic Endovascular Aneurysm Repair) as the area of your aorta that is affected is in the chest, there are some particular risks. There is a small risk of stroke (about 3 in 100 cases) which is a devastating complication. In addition there may be tiny areas of damage to the brain due to poor blood supply called **vascular brain infarcts**. These can lead to 'silent stroke'. While this form of stroke does not affect a persons ability to speak or move as a 'stroke' would, the areas of brain damage lead to problems with **memory, mood and emotions** that can affect your quality of life and independent living. **We have detected these problems in affects 8 out of 10 patients undergoing this procedure.**



http://www.vascularweb.org/vascularhealth/pages/ thoracic-aortic-aneurysm.aspx)

This research is about trying to reduce stroke AND silent stroke so that you can have a good outcome from this procedure without it affecting any aspect of your life.

Why does Stroke and 'silent stroke' happen in TEVAR?

Solid Debris

There have been studies that have shown that whilst the stent (TEVAR) is being positioned and opened in the area of affected aorta in the chest, small emboli (small solid particles of disease from the aorta), can travel up the blood vessels supplying the brain, to cause tiny areas of damage.

Gas bubbles

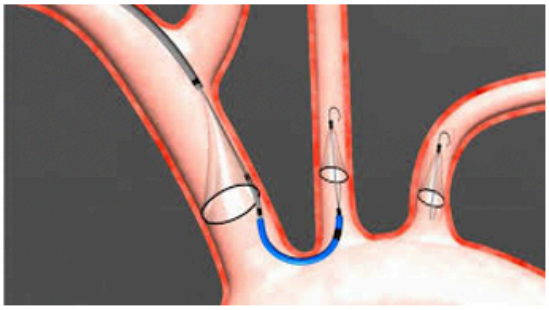
There have been other studies in addition to our ongoing study, that have shown that as the stent is released from its enclosing delivery system, air is released that we think has come from the conditions that the stent-graft was manufactured in. We think that this air may travel into the blood vessels supplying the brain, to also cause tiny areas of damage.

We think that solid debris and/or gas bubbles may be responsible for causing damage to the brain that can cause stroke, 'silent stroke' and increase risk of future stoke or dementia.

What can be done about this?

1)SOLID PROTECTION: Cerebral Embolic Filter Devices (CEPD)

We plan to introduce two unique devices to filter, capture and remove these embolic debris to reduce the risk of stroke and small areas of brain damage. This has been used safely and effectively before in replacement of heart valves where there is manipulation and intervention through this area of the aorta and we have also used these devices in TEVAR patients. The filters are inserted into the blood vessels to protect the brain through a key-hole procedure. A small needle is introduced into the right and left artery at the elbow crease allowing the filters to protect the right and left sides of the brain. These arteries are often also used to place your TEVAR accurately.



2) GAS PROTECTION: Carbon-dioxide Flushing

To reduce the air from inside the stents, we want to flush the stent with carbon-dioxide, a gas that is found in the air and that we breathe out. Carbon-dioxide flushing has been used in open heart surgery before to remove air from the heart and stop it getting to the brain to cause damage. Studies have shown that this can help protect against memory problems and stroke.

Why have I been chosen?

We are inviting you to take part in this study because you are going to have a TEVAR. We are asking all patients undergoing TEVAR to take part in this study. You will either have solid protection or gas protection as a treatment. Patients will be chosen to have this depending on what the surgical team feel is best for you.

Do I have to take part?

It is up to you to decide whether or not to take part. If you do decide to take part you will be asked to sign a consent form. If you decide to take part you are still free to withdraw at any time and without giving a reason. A decision not to take part or to withdraw at any time will not affect the standard of care you receive.

What will happen to me if I take part?

- Participation in the study will not interfere with or result in any change to your planned treatment. There will be no extra hospital visits or personal costs incurred as a result of study participation. There is no lifestyle or dietary restriction and you will not have to commence or discontinue any form of medication as part of this study.

- Each patient will be randomly chosen to have either saline or carbon-dioxide to flush the stent with. You will not know which group you have been allocated to. Only the researcher and your operating team will which group you belong to.
- As part of your standard care a clinical history and examination including neurological examination will be performed by a doctor.
- The following steps will be carried out the day before your operation after you are admitted to the vascular ward and will be repeated after your operation the day before you are discharged.

1) We request that you attend the Radiology Department at the hospital where you will have your TEVAR to undergo an MRI scan of your brain.
2) You will be asked to complete a series of paper-based tests of mental function at your bedside and post-operatively at 6 weeks and 6 months follow-up when you are seen in a vascular clinic to check on you after TEVAR in the outpatient clinics of the hospital where you have your TEVAR.

-MRI scanning (http://www.howstuffworks.com/mri.htm)



MRI stands for Magnetic Resonance Imaging and is a way of creating pictures of your body that does not use X-rays or radiation. During the scan you will be lying inside a large tubular machine. The inside of the scanner is well lit, and has a fan to blow fresh air gently over you. The machine is noisy and you will be given earplugs to wear if you wish. The MRI scan will take approximately 15 minutes. The Radiographers will talk to you through an intercom system. MRI scanning will not be undertaken on any patients with contraindications to MRI such as pacemaker, metallic heart valves or metallic foreign bodies. If you have experienced claustrophobia, or have trouble in enclosed spaces, talk about it with the MRI staff before your appointment date. It is very important not to bring any metal into the scan room without letting the Radiographer know, as metal objects can be damaged by the strong magnet of the MRI scanner, or might cause distortions in the MRI pictures.

-Transcranial Doppler Monitoring





http://www.jcirc.or.jp/english/sessions/reports/69th/sym03.htm, http://www.medcat.nl/dopfixatie.htm

This is a type of ultrasound that shows the blood flow to the brain, and it will be performed during the operation. It is measured using probes which will be placed on your head attached to a headset. This is usually performed on patients who are awake and is painless and harmless. The headset can occasionally cause a bit of discomfort. For your procedure you will be under a general anaesthetic or sedated and you therefore should not notice it.

- Neurocognitive Testing

In order to help us detect any brain infarcts which have not resulted in an obvious stroke, you will undergo paper-based tests of mental function (neurocognitive testing) before and after your operation. The tests have been specially designed to measure several aspects including: visual memory, attention and decision-making.

You will be asked to complete the tests on 3 occasions -

1. On admission, the day prior to your operation
2. Following your operation, prior to your discharge home
3. When you attend your routine follow up outpatient appointments(6 week and 6 months)

What are the possible benefits of me taking part?

We want to be able to offer TEVAR, a life saving therapy whilst minimalizing brain injury and this study is already helping us understand brain injury during TEVAR. The flushing techniques described in this study are already being used routinely in many European centres around the world, however, this is the first study that is extensively studying the protective effects of these flushing techniques in patients. We are recruiting patients from all across London to make sure our results are reliable. By taking part, you will allow us to make significant advances towards protecting the brain from injury during TEVAR and information about you from this study will contribute greatly to this research which you have a chance to be a part of and help others in the future who will need this operation.

What are the possible harms of me taking part?

The risks of participating in the study are the same as the risks of undergoing a standard TEVAR. The risks associated with TEVAR will be explained to you in detail during your clinic appointment and also on your admission to hospital prior to your surgery. You will be asked to sign a consent form to undergo the operation at that time.

The filters have a risk of causing stroke but this is rare and in our experience the risk of stroke with the filters is 1 out of 100 people. The risk of having a stroke with TEVAR is 3-10 out of 100 people. Sometimes people can experience some bruising at the elbow that is not permanent and will settle.

MRI, Duplex, transcranial Doppler and the neurocognitive tests have been chosen to obtain the measurements because they are safe, effective and painless. They are not known to have any adverse health implications as they are non-invasive and do not involve x-rays or radiation.

During the MRI scan of your brain if any new information is found which may require further investigation or management, this information will be passed onto the consultant in charge of your care and your GP or you will be referred to the appropriate services, following discussion with you.

What if something goes wrong?

We do not believe that you would be harmed as a result of your participation in this study. Your operation and treatment pathway will remain the same if you wish to participate in the study or not. Imperial College London holds insurance policies which apply to this study. If you lose capacity at any point during the study, you would be withdrawn from the study. Identifiable data collected with consent would be retained and used in the study. No further data or tissue would be collected or any other research procedures carried out on or in relation to the participant.

If you experience harm or injury as a result of taking part in this study you will be eligible to claim compensation without having to prove that Imperial College is at fault. This does not affect your legal rights to seek compensation. If you are harmed due to someone's negligence you may have grounds for a legal action. If you wish to complain, or have any concerns about the way you have been treated during the course of this study then you should immediately inform the Consultant Vascular Surgeon in charge of your care who will immediately contact the investigator *(Mr Richard Gibbs. Address: Vascular Surgery Office, 2nd floor, Waller Cardiac Unit, St Mary's Hospital, Imperial College Healthcare NHS Trust, London W21NY. Tel: +44 207 886 7918 Fax: +44 207 886 2216)*. If you wish to contact Mr Richard Gibbs directly, please do so.

The Standard NHS Complaints procedures is also available to you including The Patient Advice and Liaison Service (PALS) who can offer you support, information and assistance on 020 3312 7777 Ground floor of the Queen Elizabeth the Queen Mother (QEQM) building, St Mary's Hospital, South Wharf Road, London W2 1NY. If you are still not satisfied with the response, you may contact Ruth Nicholson, Research Governance Manager Room 221, Level 2, Medical School Building, Norfolk Place, W21PG 02075941862 r.nicholson@imperial.ac.uk.

Will my taking part in this study be kept confidential?

All information which is collected about you during the course of the research will be kept strictly confidential in accordance with the Data Protection Act 2018; Imperial College is the sponsor for this study based in the United Kingdom. We will be using information from you and your medical records in order to undertake this study and will act as the data controller for this study. This means that we are responsible for looking after your information and using it properly. Imperial College will keep identifiable information about you for 10 year until the study has finished. Your rights to access, change or move your information are limited, as we need to manage your information in specific ways in order for the research to be reliable and accurate. If you withdraw from the study, we will keep the information about you that we have already obtained. To safeguard your rights, we will use the minimum personally-identifiable information possible.

Imperial College Healthcare NHS Trust will use your name, NHS number and contact number to contact you about the research study, and make sure that relevant information about the study is recorded for your care, and to oversee the quality of the study. Individuals from Imperial College and

regulatory organisations may look at your medical and research records to check the accuracy of the research study. The only people in Imperial College London who will have access to information that identifies you will be people who need to contact you to if further information is required for the research or audit the data collection process. The people who analyse the information will not be able to identify you and will not be able to find out your name, NHS number or contact details.

Imperial College Healthcare NHS Trust will keep identifiable information about you from this study for 10 years after the study has finished.

LEGAL BASIS

As a university we use personally-identifiable information to conduct research to improve health, care and services. As a publicly-funded organisation, we have to ensure that it is in the public interest when we use personally-identifiable information from people who have agreed to take part in research. This means that when you agree to take part in a research study, we will use your data in the ways needed to conduct and analyse the research study.

Health and care research should serve the public interest, which means that we have to demonstrate that our research serves the interests of society as a whole. We do this by following the UK Policy Framework for Health and Social Care Research.

INTERNATIONAL TRANSFERS

There may be a requirement to transfer information to countries outside the European Economic Area (for example, to a research partner). Where this information contains your personal data, Imperial College London will ensure that it is transferred in accordance with data protection legislation. If the data is transferred to a country which is not subject to a European Commission (**EC**) adequacy decision in respect of its data protection standards, Imperial College London will enter into a data sharing agreement with the recipient organisation that incorporates EC approved standard contractual clauses that safeguard how your personal data is processed.

CONTACT US

If you wish to raise a complaint on how we have handled your personal data or if you want to find out more about how we use your information, please contact Imperial College London's Data Protection Officer via email at dpo@imperial.ac.uk, via telephone on 020 7594 3502 and via post at Imperial College London, Data Protection Officer, Faculty Building Level 4, London SW7 2AZ.

If you are not satisfied with our response or believe we are processing your personal data in a way that is not lawful you can complain to the Information Commissioner's Office (ICO). The ICO does recommend that you seek to resolve matters with the data controller (us) first before involving the regulator.

What will happen to the results of the research study?

The results of the study will be published in scientific journals and presented at scientific meetings so that we can show our findings to other hospitals within the UK, Europe and more globally so that others can benefit from our findings to help other patients that need this operation. No patient identifiable information will be used.

Who is organising and funding the research?

J.P Moulton Charitable Foundation is funding the study. Imperial College London and the Department of Vascular Surgery is organising the study.

Who has reviewed the study?

The Fulham London NHS Research Ethics Committee has reviewed and approved the study.

Contact for Further Information

For further information, or any other enquiry please contact:

Miss Lydia Hanna MRCS, Vascular Clinical Research Fellow

Imperial Vascular Unit, 8th floor, Zachary Cope Ward, St Mary's Hospital W2 1NY, Imperial College London. Email: l.hanna@imperial.ac.uk

We would like to thank you for your time and for considering participation in this study If you do decide to take part, you will be given this Patient Information Leaflet along with a copy of your consent form to keep.

Appendix 2 CO_2/embolic filter Patient consent form

NHS
Imperial College Healthcare
NHS Trust

Patient Identification Number for this trial:

CONSENT FORM

Title of Project: **NIAS Study**

Name of Principal Investigators at St Mary's Hospital: **Mr Richard Gibbs**

Chief Investigator at St Mary's Hospital: **Mr Richard Gibbs**

Please initial all boxes

1. I confirm that I have read and understand the information sheet dated **14/04/2019 version 11** for the above study. I have had the opportunity to consider the information, ask questions and have had these answered satisfactorily. ☐

2. I understand that my participation is voluntary and that I am free to withdraw at any time without giving any reason, without my medical care or legal rights being affected. ☐

3. I understand that relevant sections of my medical notes and data collected during the study, may be looked at by individuals from **Imperial College London** from regulatory authorities or from the NHS Trust, where it is relevant to my taking part in this research. I give permission for these individuals to have access to my records. ☐

4. I agree to my GP being informed of my participation in the study. ☐

5. I agree to take part in the above study. ☐

Name of Participant	Date	Signature
Name of Person taking consent.	Date	Signature

Consent form date of issue: 14/04/2019
Consent form version number: 10

Page 1 of 1

Appendix 3 DW-MRI reporting protocol

Name	
Absolute no lesions	
Total surface area mm2 region of interest	

Max diameter (mm)	≤ 5mm	6-10mm	11-20mm	≥20mm
No of lesions				

Anterior circulation	LEFT		RIGHT	
	Frontal		Frontal	
	Parietal		Parietal	
	Temporal		Temporal	
	Basal ganglia		Basal ganglia	

Posterior circulation	LEFT		RIGHT	
	midbrain/pons/ medulla (brainstem)		midbrain/pons/ medulla (brainstem)	
	thalamus		thalamus	
	cerebellum/ occipital		cerebellum/ occipital	
	medial temporal		medial temporal	

Borderzone	LEFT		RIGHT	
	Fronto/parietal ACA/MCA		Fronto/parietal ACA/MCA	
	Frontal ACA/ MCA		Frontal ACA/ MCA	
	Parietal/occipital MCA/PCA		Parietal/occipital MCA/PCA	
	Tempor/occipital MCA/PCA		Tempor/occipital MCA/PCA	

Pre-op MRI Fazekas Scale (ARWMC)

Periventricular lesions		**White matter lesions**	
0 - No lesions		0 - No lesions	
1 - Caps or thin line		1 - Punctate foci	
2 - Smooth halo		2 - Beginning confluence of foci	
3 - Extension into the white matter		3 - Large confluent areas	

Appendix 4 Modified Rankin scale

Level	Description
0	No symptoms
1	No significant disability, despite symptoms; able to perform all usual duties and activities
2	Slight disability; unable to perform all previous activities but able to look after own affairs without assistance
3	Moderate disability; requires some help, but able to walk without assistance
4	Moderately severe disability; unable to walk without assistance and unable to attend to own bodily needs without assistance
5	Severe disability; bedridden, incontinent and requires nursing care and attention

Adapted from Rankin, 1957[71] and van Swieten et al., 1988[72]

Appendix 5 REY auditory verbal learning test

Trial 1: *'I am going to read you a list of words and then ask you to remember as many words as possible in any order. When I stop reading, I want you to tell me all the words you remember straight away. Ok?'* If no response when finished reading, prompt with: *'What do you remember?'*

Trials 2-5: *'I am going to read you the list again and I would like you to tell me as many words as you remember as soon as I stop reading'*

Trial 6 (interference): *'Now I am going to read you a **different** list of words and as before, I would like you to tell me all the words you remember as soon as I have stopped reading'*

Trial 7: *'Now I would like you to tell me all the words you remember from the **first** list of words I read to you'*

Trial A		1	2	3	4	5		7		Trial B	6
Drum	/						/		/	Desk	
Curtain	/						/		/	Ranger	
Bell	/						/		/	Bird	
Coffee	/						/		/	Shoe	
School	/						/		/	Stove	
Parent	/						/		/	Mountain	
Moon	/						/		/	Glasses	
Garden	/						/		/	Towel	
Hat	/						/		/	Cloud	
Farmer	/						/		/	Boat	
Nose	/						/		/	Lamb	
Turkey	/						/		/	Gun	
Colour	/						/		/	Pencil	
House	/						/		/	Church	
River	/						/		/	Fish	
Total	/						/		/		
Persev.	/						/		/		

Average =_____

Trial 1: *'I am going to read you a list of words and then ask you to remember as many words as possible in any order. When I stop reading, I want you to tell me all the words you remember straight away. Ok?'* If no response when finished reading, prompt with: *'What do you remember?'*

Trials 2-5: *'I am going to read you the list again and I would like you to tell me as many words as you remember as soon as I stop reading'*

Trial 6 (interference): *'Now I am going to read you a **different** list of words and as before, I would like you to tell me all the words you remember as soon as I have stopped reading'*

Trial 7: *'Now I would like you to tell me all the words you remember from the **first** list of words I read to you'*

Trial AC[2]		1	2	3	4	5		7		Trial BC[2]	6
Doll	/						/		/	Dish	
Mirror	/						/		/	Jester	
Nail	/						/		/	Hill	
Sailor	/						/		/	Coat	
Heart	/						/		/	Tool	
Desert	/						/		/	Forest	
Face	/						/		/	Water	
Letter	/						/		/	Ladder	
Bed	/						/		/	Girl	
Machine	/						/		/	Foot	
Milk	/						/		/	Shield	
Helmet	/						/		/	Pie	
Music	/						/		/	Insect	
Horse	/						/		/	Ball	
Road	/						/		/	Car	
TOTAL	/						/		/		
Persev.	/						/		/		

Average =_____

Appendix 6 Trail Making test part A & B

Trail Making Test (TMT) Parts A & B

Both parts of the Trail Making Test consist of 25 circles distributed over a sheet of paper. In PartA, the circles are numbered 1 – 25, and the patient should draw lines to connect the numbers inascending order. In Part B, the circles include both numbers (1 – 13) and letters (A – L); as in Part A, the patient draws lines to connect the circles in an ascending pattern, but with the addedtask of alternating between the numbers and letters (i.e., 1-A-2-B-3-C, etc.). The patient should be instructed to connect the circles as quickly as possible, without lifting the pen or pencil from the paper. Time the patient as he or she connects the "trail." If the patient makes an error, point it out immediately and allow the patient to correct it. Errors affect the patient's score only in that the correction of errors is included in the completion time for the task. It is unnecessary to continue the test if the patient has not completed both parts after five minutes have elapsed.

Step 1: Give the patient a copy of the Trail Making Test Part A worksheet and a pen orpencil.

Step 2: Demonstrate the test to the patient using the sample sheet (Trail Making Part A – *SAMPLE*).

Step 3: Time the patient as he or she follows the “trail” made by the numbers on the test.Step 4: Record the time.

Step 5: Repeat the procedure for Trail Making Test Part B.

Results for both TMT A and B are reported as the number of seconds required to complete the task; therefore, higher scores reveal greater impairment.

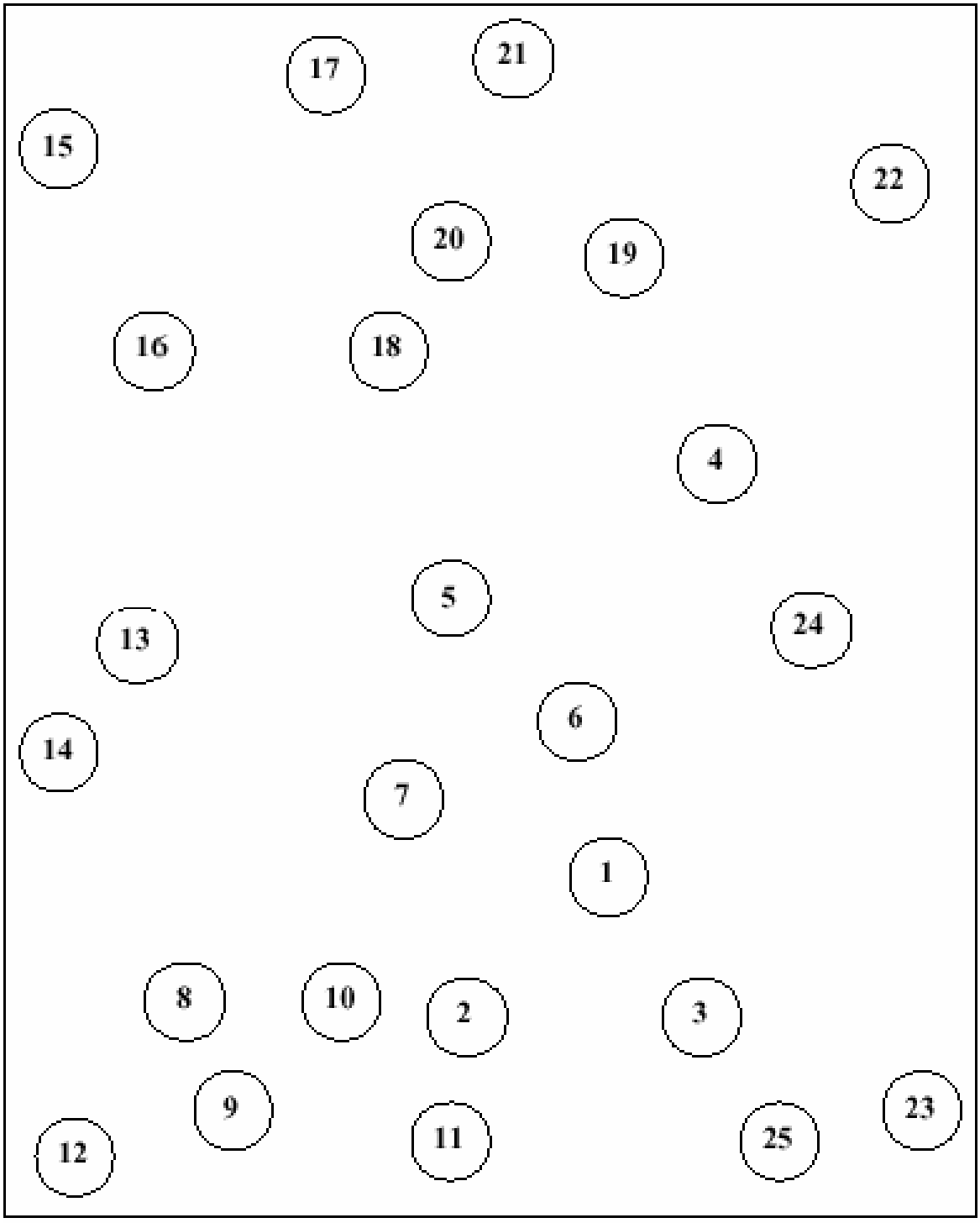
	Average	**Deficient**	**Rule of Thumb**
Trail A	29 seconds	> 78 seconds	Most in 90 seconds
Trail B	75 seconds	> 273 seconds	Most in 3 minutes

Sources:

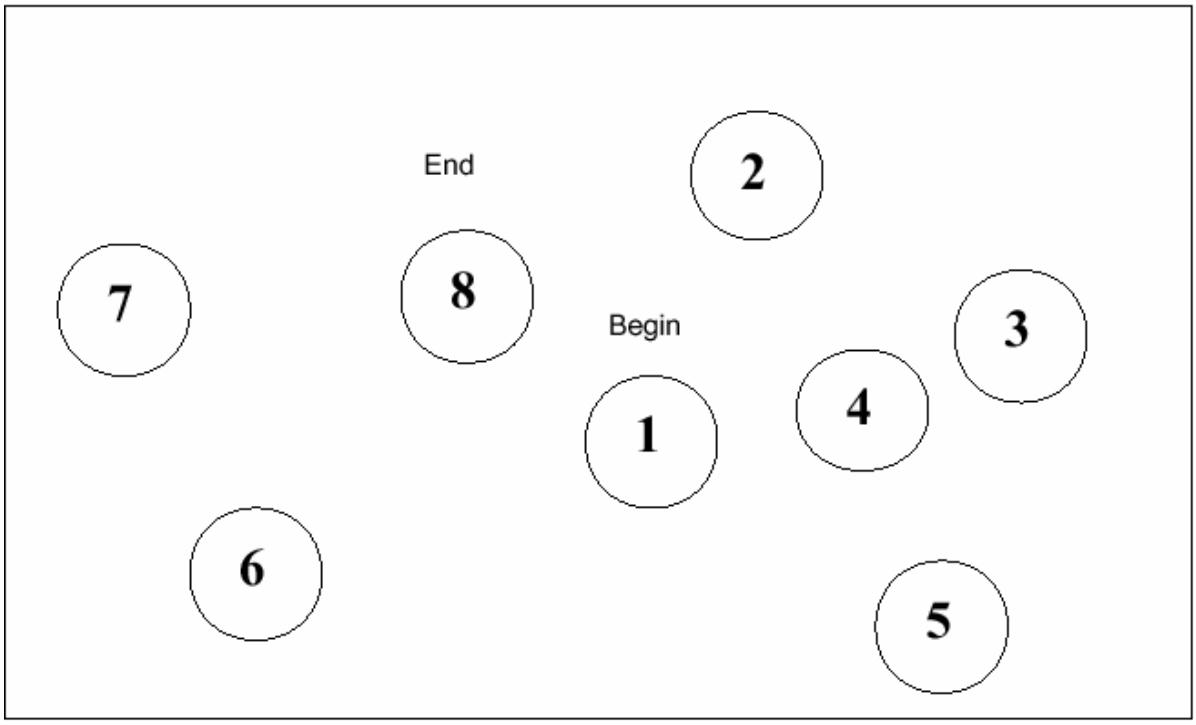
- Corrigan JD, Hinkeldey MS. Relationships between parts A and B of the Trail Making Test. *JClin Psychol*. 1987;43(4):402–409.
- Gaudino EA, Geisler MW, Squires NK. Construct validity in the Trail Making Test: whatmakes Part B harder? *J Clin Exp Neuropsychol*. 1995;17(4):529-535.
- Lezak MD, Howieson DB, Loring DW. *Neuropsychological Assessment*. 4th ed. New York:Oxford University Press; 2004.
- Reitan RM. Validity of the Trail Making test as an indicator of organic brain damage. *PerceptMot Skills*. 1958;8:271-276.

Trail Making Test Part A

Patient's Name:_____ Date: _____

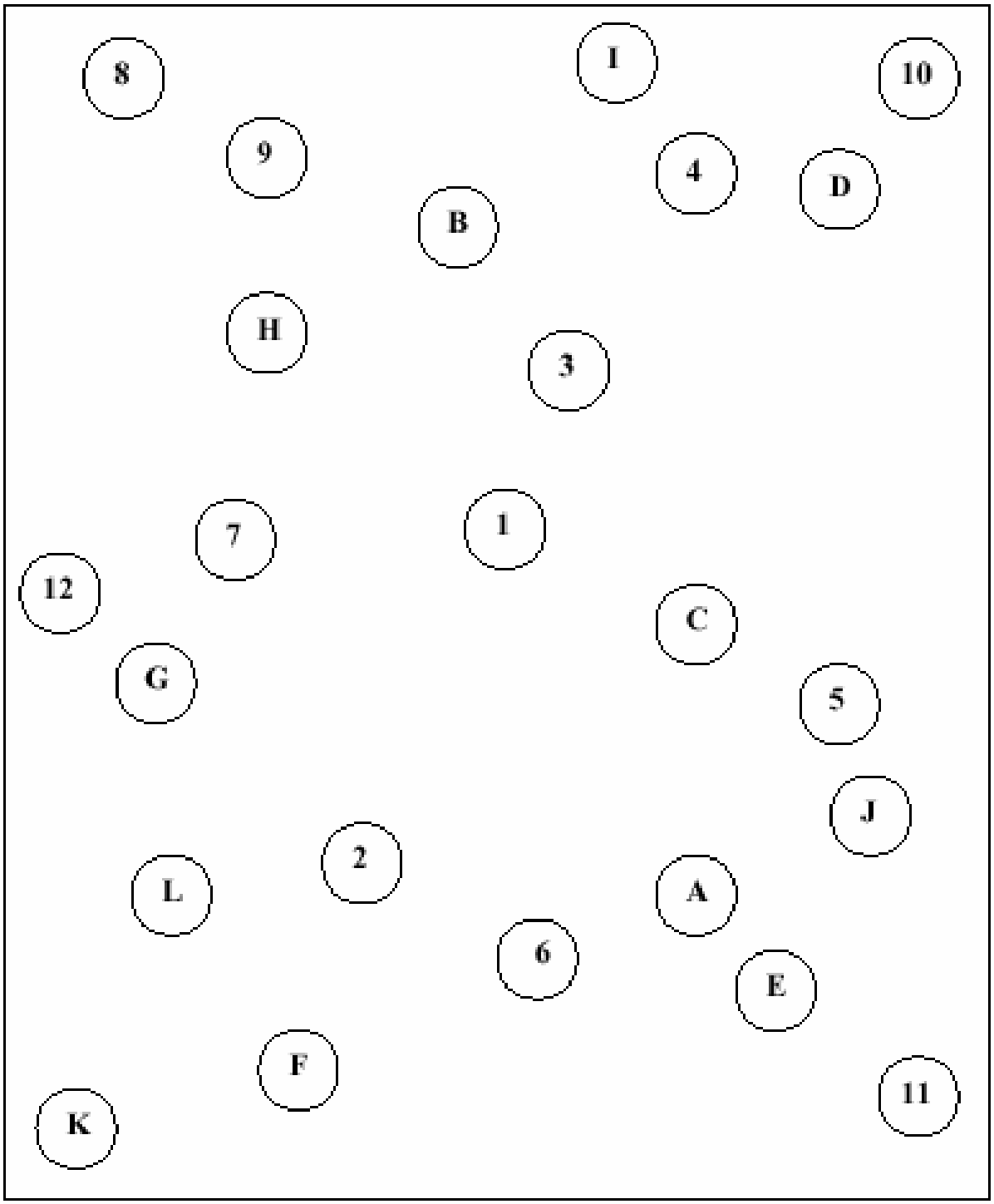


Trail Making Test Part A – *SAMPLE*

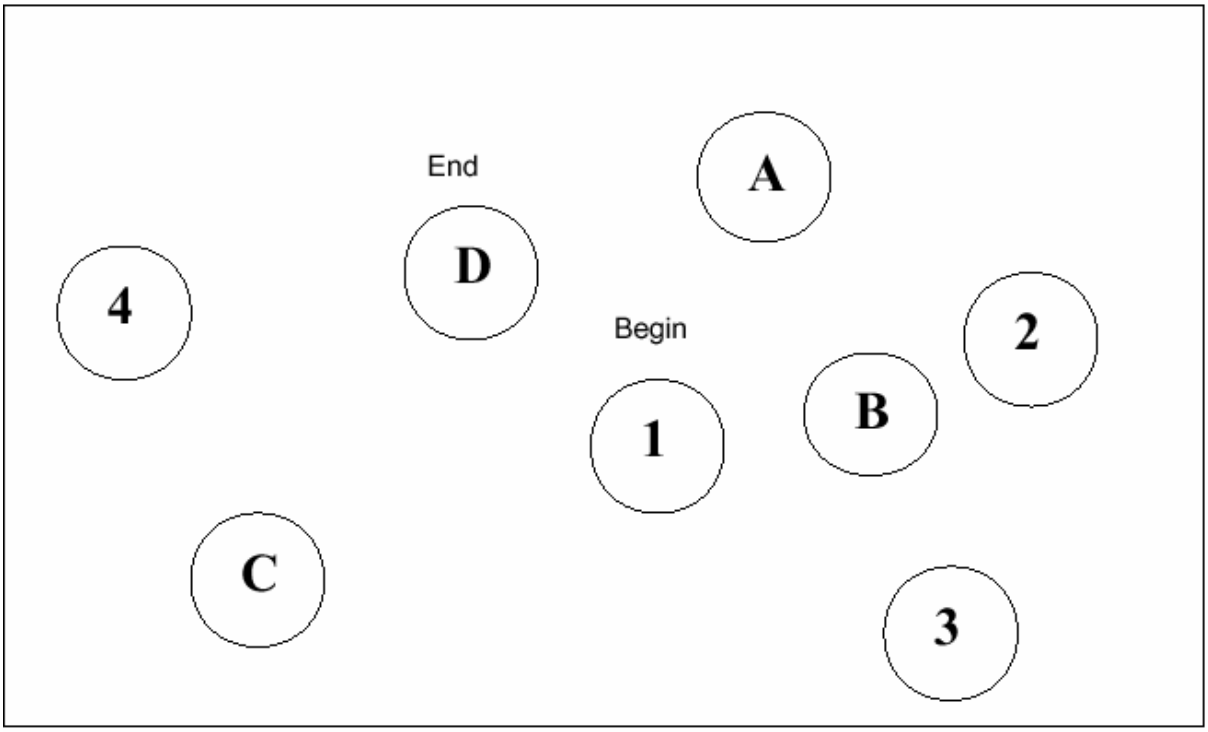


Trail Making Test Part B

Patient's Name:_____ Date: _____



Trail Making Test Part B – *SAMPLE*



Grooved pegboard scores

Dominant hand:

1. Total time (in seconds) =
2. Total number of drops =
3. Total number of pegs correctly placed =

Total score =

Non-dominant hand:

1. Total time (in seconds) =
2. Total number of drops =
3. Total number of pegs correctly placed =

Total score =

Appendix 8 Controlled oral word association test (COWAT)

Word fluency: FAS

I am going to say a letter of the alphabet, and I would like you to give me as many words that you can think of that begin with that letter as quickly as you can. You can say any English word with two letters or more, except for proper names. For example, if I say 'B' you might give me 'bad' or 'bed'. But don't say proper names like 'Bob' or 'Bedford'. And also don't give me the same word with a different ending, like 'beat' or 'beating'. Any questions? Please begin when I say the letter.



Allow one minute for each letter

F.....

.....

.....

Total_____

A.....

.....

.....

Total_____

S.....

.....

.....

Total_____

Overall Total_____

References

1. Komutrattananont P, Mahakkanukrauh P, Das S. Morphology of the human aorta and age-related changes: anatomical facts. *Anat Cell Biol*. Jun 2019;52(2):109-114. doi:10.5115/acb.2019.52.2.109
2. Mitchell RS, Ishimaru S, Ehrlich MP, et al. First International Summit on Thoracic Aortic Endografting: roundtable on thoracic aortic dissection as an indication for endografting. *J Endovasc Ther*. Jun 2002;9 Suppl 2:II98-105.
3. Dagenais F. Anatomy of the thoracic aorta and of its branches. *Thorac Surg Clin*. May 2011;21(2):219-27, viii. doi:10.1016/j.thorsurg.2010.12.004
4. Natsis KI, Tsitouridis IA, Didagelos MV, Fillipidis AA, Vlasis KG, Tsikaras PD. Anatomical variations in the branches of the human aortic arch in 633 angiographies: clinical significance and literature review. *Surg Radiol Anat*. Jun 2009;31(5):319-23. doi:10.1007/s00276-008-0442-2
5. Kalsch H, Lehmann N, Mohlenkamp S, et al. Body-surface adjusted aortic reference diameters for improved identification of patients with thoracic aortic aneurysms: results from the population-based Heinz Nixdorf Recall study. *Int J Cardiol*. Feb 10 2013;163(1):72-8. doi:10.1016/j.ijcard.2011.05.039
6. Hager A, Kaemmerer H, Rapp-Bernhardt U, et al. Diameters of the thoracic aorta throughout life as measured with helical computed tomography. *J Thorac Cardiovasc Surg*. Jun 2002;123(6):1060-6.
7. Isselbacher EM. Thoracic and abdominal aortic aneurysms. *Circulation*. Feb 15 2005;111(6):816-28. doi:10.1161/01.CIR.0000154569.08857.7A
8. Fowkes FG, Macintyre CC, Ruckley CV. Increasing incidence of aortic aneurysms in England and Wales. *BMJ*. Jan 7 1989;298(6665):33-5. doi:10.1136/bmj.298.6665.33
9. Howard DP, Sideso E, Handa A, Rothwell PM. Incidence, risk factors, outcome and projected future burden of acute aortic dissection. *Ann Cardiothorac Surg*. May 2014;3(3):278-84. doi:10.3978/j.issn.2225-319X.2014.05.14
10. Nienaber CA, Sievers HH. Intramural hematoma in acute aortic syndrome: more than one variant of dissection? *Circulation*. Jul 16 2002;106(3):284-5. doi:10.1161/01.cir.0000023453.90533.82
11. Vilacosta I, Aragoncillo P, Canadas V, San Roman JA, Ferreiros J, Rodriguez E. Acute aortic syndrome: a new look at an old conundrum. *Postgrad Med J*. Jan 2010;86(1011):52-61. doi:10.1136/hrt.2008.153650
12. Collins JS, Evangelista A, Nienaber CA, et al. Differences in clinical presentation, management, and outcomes of acute type a aortic dissection in patients with and without previous cardiac surgery. *Circulation*. Sep 14 2004;110(11 Suppl 1):II237-42. doi:10.1161/01.CIR.0000138219.67028.2a

13. Bonderman D, Gharehbaghi-Schnell E, Wollenek G, Maurer G, Baumgartner H, Lang IM. Mechanisms underlying aortic dilatation in congenital aortic valve malformation. *Circulation*. Apr 27 1999;99(16):2138-43. doi:10.1161/01.cir.99.16.2138
14. Eagle KA, Isselbacher EM, DeSanctis RW, International Registry for Aortic Dissection I. Cocaine-related aortic dissection in perspective. *Circulation*. Apr 2 2002;105(13):1529-30. doi:10.1161/01.cir.105.13.1529
15. Suzuki T, Mehta RH, Ince H, et al. Clinical profiles and outcomes of acute type B aortic dissection in the current era: lessons from the International Registry of Aortic Dissection (IRAD). *Circulation*. Sep 9 2003;108 Suppl 1:II312-7. doi:10.1161/01.cir.0000087386.07204.09
16. Hatzaras IS, Bible JE, Koullias GJ, Tranquilli M, Singh M, Elefteriades JA. Role of exertion or emotion as inciting events for acute aortic dissection. *Am J Cardiol*. Nov 1 2007;100(9):1470-2. doi:10.1016/j.amjcard.2007.06.039
17. Daily PO, Trueblood HW, Stinson EB, Wuerflein RD, Shumway NE. Management of acute aortic dissections. *Ann Thorac Surg*. Sep 1970;10(3):237-47. doi:10.1016/s0003-4975(10)65594-4
18. Debakey ME, Henly WS, Cooley DA, Morris GC, Jr., Crawford ES, Beall AC, Jr. Surgical Management of Dissecting Aneurysms of the Aorta. *J Thorac Cardiovasc Surg*. Jan 1965;49:130-49.
19. Czerny M, Schmidli J, Adler S, et al. Editor's Choice - Current Options and Recommendations for the Treatment of Thoracic Aortic Pathologies Involving the Aortic Arch: An Expert Consensus Document of the European Association for Cardio-Thoracic Surgery (EACTS) & the European Society for Vascular Surgery (ESVS). *Eur J Vasc Endovasc Surg*. Feb 2019;57(2):165-198. doi:10.1016/j.ejvs.2018.09.016
20. Rylski B, Perez M, Beyersdorf F, et al. Acute non-A non-B aortic dissection: incidence, treatment and outcome. *Eur J Cardiothorac Surg*. Dec 1 2017;52(6):1111-1117. doi:10.1093/ejcts/ezx142
21. Evangelista A, Czerny M, Nienaber C, et al. Interdisciplinary expert consensus on management of type B intramural haematoma and penetrating aortic ulcer. *Eur J Cardiothorac Surg*. Feb 2015;47(2):209-17. doi:10.1093/ejcts/ezu386
22. Smith RS, Chang FC. Traumatic rupture of the aorta: still a lethal injury. *Am J Surg*. Dec 1986;152(6):660-3. doi:10.1016/0002-9610(86)90444-7
23. Davies RR, Goldstein LJ, Coady MA, et al. Yearly rupture or dissection rates for thoracic aortic aneurysms: simple prediction based on size. *Ann Thorac Surg*. Jan 2002;73(1):17-27; discussion 27-8. doi:10.1016/s0003-4975(01)03236-2
24. Coselli JS, LeMaire SA, Preventza O, et al. Outcomes of 3309 thoracoabdominal aortic aneurysm repairs. *J Thorac Cardiovasc Surg*. May 2016;151(5):1323-37. doi:10.1016/j.jtcvs.2015.12.050
25. Chiesa R, Tshomba Y, Civilini E, et al. Open repair of descending thoracic aneurysms. *HSR Proc Intensive Care Cardiovasc Anesth*. 2010;2(3):177-90.

26. Svensson LG, Crawford ES, Hess KR, Coselli JS, Safi HJ. Experience with 1509 patients undergoing thoracoabdominal aortic operations. *J Vasc Surg*. Feb 1993;17(2):357-68; discussion 368-70.
27. Estrera AL, Miller CC, 3rd, Chen EP, et al. Descending thoracic aortic aneurysm repair: 12-year experience using distal aortic perfusion and cerebrospinal fluid drainage. *Ann Thorac Surg*. Oct 2005;80(4):1290-6; discussion 1296. doi:10.1016/j.athoracsur.2005.02.021
28. Patel HJ, Shillingford MS, Mihalik S, Proctor MC, Deeb GM. Resection of the descending thoracic aorta: outcomes after use of hypothermic circulatory arrest. *Ann Thorac Surg*. Jul 2006;82(1):90-5; discussion 95-6. doi:10.1016/j.athoracsur.2006.02.055
29. Goldstein LJ, Davies RR, Rizzo JA, et al. Stroke in surgery of the thoracic aorta: incidence, impact, etiology, and prevention. *J Thorac Cardiovasc Surg*. Nov 2001;122(5):935-45. doi:10.1067/mtc.2001.117276
30. Anwar MA, Hamady M. Various Endoluminal Approaches Available for Treating Pathologies of the Aortic Arch. *Cardiovasc Intervent Radiol*. Dec 2020;43(12):1756-1769. doi:10.1007/s00270-020-02561-y
31. Matsumura JS, Melissano G, Cambria RP, et al. Five-year results of thoracic endovascular aortic repair with the Zenith TX2. *J Vasc Surg*. Jul 2014;60(1):1-10. doi:10.1016/j.jvs.2014.01.043
32. Conrad MF, Tuchek J, Freezor R, Bavaria J, White R, Fairman R. Results of the VALOR II trial of the Medtronic Valiant Thoracic Stent Graft. *J Vasc Surg*. Aug 2017;66(2):335-342. doi:10.1016/j.jvs.2016.12.136
33. Jordan WD, Jr., Rovin J, Moainie S, et al. Results of a prospective multicenter trial of CTAG thoracic endograft. *J Vasc Surg*. Mar 2015;61(3):589-95. doi:10.1016/j.jvs.2014.09.033
34. Harky A, Kai Chan JS, Ming Wong CH, Bashir M. Open versus Endovascular Repair of Descending Thoracic Aortic Aneurysm Disease: A Systematic Review and Meta-analysis. *Ann Vasc Surg*. Jan 2019;54:304-315 e5. doi:10.1016/j.avsg.2018.05.043
35. Harky A, Chan JSK, Wong CHM, Francis N, Grafton-Clarke C, Bashir M. Systematic review and meta-analysis of acute type B thoracic aortic dissection, open, or endovascular repair. *J Vasc Surg*. May 2019;69(5):1599-1609 e2. doi:10.1016/j.jvs.2018.08.187
36. Harky A, Bleetman D, Chan JSK, et al. A systematic review and meta-analysis of endovascular versus open surgical repair for the traumatic ruptured thoracic aorta. *J Vasc Surg*. Jan 2020;71(1):270-282. doi:10.1016/j.jvs.2019.05.011
37. Chiu P, Goldstone AB, Schaffer JM, et al. Endovascular Versus Open Repair of Intact Descending Thoracic Aortic Aneurysms. *J Am Coll Cardiol*. Feb 19 2019;73(6):643-651. doi:10.1016/j.jacc.2018.10.086
38. Geisbusch S, Kuehnl A, Salvermoser M, Reutersberg B, Trenner M, Eckstein HH. Increasing Incidence of Thoracic Aortic Aneurysm Repair in Germany in the Endovascular Era: Secondary Data Analysis of the Nationwide German DRG Microdata. *Eur J Vasc Endovasc Surg*. Apr 2019;57(4):499-509. doi:10.1016/j.ejvs.2018.08.013

39. Hellgren T, Beck AW, Behrendt CA, et al. Thoracic endovascular aortic repair practice in 13 countries: A report from VASCUNET and the International Consortium of Vascular Registries. *Ann Surg*. Nov 17 2020;doi:10.1097/SLA.0000000000004561
40. Buth J, Harris PL, Hobo R, et al. Neurologic complications associated with endovascular repair of thoracic aortic pathology: Incidence and risk factors. a study from the European Collaborators on Stent/Graft Techniques for Aortic Aneurysm Repair (EUROSTAR) registry. *J Vasc Surg*. Dec 2007;46(6):1103-1110; discussion 1110-1. doi:10.1016/j.jvs.2007.08.020
41. Feezor RJ, Martin TD, Hess PJ, et al. Risk factors for perioperative stroke during thoracic endovascular aortic repairs (TEVAR). *J Endovasc Ther*. Aug 2007;14(4):568-73. doi:10.1177/152660280701400420
42. Gutsche JT, Cheung AT, McGarvey ML, et al. Risk factors for perioperative stroke after thoracic endovascular aortic repair. *Ann Thorac Surg*. Oct 2007;84(4):1195-200; discussion 1200. doi:10.1016/j.athoracsur.2007.04.128
43. Melissano G, Tshomba Y, Bertoglio L, Rinaldi E, Chiesa R. Analysis of stroke after TEVAR involving the aortic arch. *Eur J Vasc Endovasc Surg*. Mar 2012;43(3):269-75. doi:10.1016/j.ejvs.2011.12.009
44. Haulon S, Greenberg RK, Spear R, et al. Global experience with an inner branched arch endograft. *J Thorac Cardiovasc Surg*. Oct 2014;148(4):1709-16. doi:10.1016/j.jtcvs.2014.02.072
45. Ullery BW, McGarvey M, Cheung AT, et al. Vascular distribution of stroke and its relationship to perioperative mortality and neurologic outcome after thoracic endovascular aortic repair. *J Vasc Surg*. Dec 2012;56(6):1510-7. doi:10.1016/j.jvs.2012.05.086
46. Jonker FH, Verhagen HJ, Heijmen RH, et al. Endovascular repair of ruptured thoracic aortic aneurysms: predictors of procedure-related stroke. *Ann Vasc Surg*. Jan 2011;25(1):3-8. doi:10.1016/j.avsg.2010.05.001
47. Clough RE, Modarai B, Topple JA, et al. Predictors of stroke and paraplegia in thoracic aortic endovascular intervention. *Eur J Vasc Endovasc Surg*. Mar 2011;41(3):303-10. doi:10.1016/j.ejvs.2010.12.005
48. Waterford SD, Chou D, Bombien R, Uzun I, Shah A, Khoynezhad A. Left Subclavian Arterial Coverage and Stroke During Thoracic Aortic Endografting: A Systematic Review. *Ann Thorac Surg*. Jan 2016;101(1):381-9. doi:10.1016/j.athoracsur.2015.05.138
49. Mariscalco G, Piffaretti G, Tozzi M, et al. Predictive factors for cerebrovascular accidents after thoracic endovascular aortic repair. *Ann Thorac Surg*. Dec 2009;88(6):1877-81. doi:10.1016/j.athoracsur.2009.08.020
50. Huang Q, Chen XM, Yang H, Lin QN, Qin X. Effect of Left Subclavian Artery Revascularisation in Thoracic Endovascular Aortic Repair: A Systematic Review and Meta-analysis. *Eur J Vasc Endovasc Surg*. Nov 2018;56(5):644-651. doi:10.1016/j.ejvs.2018.07.018
51. Kahlert P, Eggebrecht H, Janosi RA, et al. Silent cerebral ischemia after thoracic endovascular aortic repair: a neuroimaging study. *Ann Thorac Surg*. Jul 2014;98(1):53-8. doi:10.1016/j.athoracsur.2014.03.037

52. Perera AH, Rudarakanchana N, Monzon L, et al. Cerebral embolization, silent cerebral infarction and neurocognitive decline after thoracic endovascular aortic repair. *Br J Surg*. Mar 2018;105(4):366-378. doi:10.1002/bjs.10718
53. Brazzelli M, Sandercock PA, Chappell FM, et al. Magnetic resonance imaging versus computed tomography for detection of acute vascular lesions in patients presenting with stroke symptoms. *Cochrane Database Syst Rev*. Oct 7 2009;(4):CD007424. doi:10.1002/14651858.CD007424.pub2
54. Augustin M, Bammer R, Simbrunner J, Stollberger R, Hartung HP, Fazekas F. Diffusion-weighted imaging of patients with subacute cerebral ischemia: comparison with conventional and contrast-enhanced MR imaging. *AJNR Am J Neuroradiol*. Oct 2000;21(9):1596-602.
55. Smith EE, Schneider JA, Wardlaw JM, Greenberg SM. Cerebral microinfarcts: the invisible lesions. *Lancet Neurol*. Mar 2012;11(3):272-82. doi:10.1016/S1474-4422(11)70307-6
56. Bendszus M, Stoll G. Silent cerebral ischaemia: hidden fingerprints of invasive medical procedures. *Lancet Neurol*. Apr 2006;5(4):364-72. doi:10.1016/S1474-4422(06)70412-4
57. Albach FN, Brunecker P, Usnich T, et al. Complete early reversal of diffusion-weighted imaging hyperintensities after ischemic stroke is mainly limited to small embolic lesions. *Stroke*. Apr 2013;44(4):1043-8. doi:10.1161/STROKEAHA.111.676346
58. Li F, Liu KF, Silva MD, et al. Transient and permanent resolution of ischemic lesions on diffusion-weighted imaging after brief periods of focal ischemia in rats : correlation with histopathology. *Stroke*. Apr 2000;31(4):946-54. doi:10.1161/01.str.31.4.946
59. Ghanem A, Dorner J, Schulze-Hagen L, et al. Subacute Subclinical Brain Infarctions after Transcatheter Aortic Valve Implantation Negatively Impact Cognitive Function in Long-Term Follow-Up. *PLoS One*. 2017;12(1):e0168852. doi:10.1371/journal.pone.0168852
60. Kahlert P, Knipp SC, Schlamann M, et al. Silent and apparent cerebral ischemia after percutaneous transfemoral aortic valve implantation: a diffusion-weighted magnetic resonance imaging study. *Circulation*. Feb 23 2010;121(7):870-8. doi:10.1161/CIRCULATIONAHA.109.855866
61. Ringer TM, Neumann-Haefelin T, Sobel RA, Moseley ME, Yenari MA. Reversal of early diffusion-weighted magnetic resonance imaging abnormalities does not necessarily reflect tissue salvage in experimental cerebral ischemia. *Stroke*. Oct 2001;32(10):2362-9. doi:10.1161/hs1001.096058
62. Beaulieu C, de Crespigny A, Tong DC, Moseley ME, Albers GW, Marks MP. Longitudinal magnetic resonance imaging study of perfusion and diffusion in stroke: evolution of lesion volume and correlation with clinical outcome. *Ann Neurol*. Oct 1999;46(4):568-78. doi:10.1002/1531-8249(199910)46:4<568::aid-ana4>3.0.co;2-r
63. Fairbairn TA, Mather AN, Bijsterveld P, et al. Diffusion-weighted MRI determined cerebral embolic infarction following transcatheter aortic valve implantation: assessment of predictive risk factors and the relationship to subsequent health status. *Heart*. Jan 2012;98(1):18-23. doi:10.1136/heartjnl-2011-300065

64. Messe SR, Acker MA, Kasner SE, et al. Stroke after aortic valve surgery: results from a prospective cohort. *Circulation*. Jun 3 2014;129(22):2253-61. doi:10.1161/CIRCULATIONAHA.113.005084
65. Neuro VI. Perioperative covert stroke in patients undergoing non-cardiac surgery (NeuroVISION): a prospective cohort study. *Lancet*. Sep 21 2019;394(10203):1022-1029. doi:10.1016/S0140-6736(19)31795-7
66. Barber PA, Hach S, Tippett LJ, Ross L, Merry AF, Milsom P. Cerebral ischemic lesions on diffusion-weighted imaging are associated with neurocognitive decline after cardiac surgery. *Stroke*. May 2008;39(5):1427-33. doi:10.1161/STROKEAHA.107.502989
67. Zhou W, Baughman BD, Soman S, et al. Volume of subclinical embolic infarct correlates to long-term cognitive changes after carotid revascularization. *J Vasc Surg*. Mar 2017;65(3):686-694. doi:10.1016/j.jvs.2016.09.057
68. Gupta A, Giambrone AE, Gialdini G, et al. Silent Brain Infarction and Risk of Future Stroke: A Systematic Review and Meta-Analysis. *Stroke*. Mar 2016;47(3):719-25. doi:10.1161/STROKEAHA.115.011889
69. Wu RH, Li Q, Tan Y, Liu XY, Huang J. Depression in silent lacunar infarction: a cross-sectional study of its association with location of silent lacunar infarction and vascular risk factors. *Neurol Sci*. Oct 2014;35(10):1553-9. doi:10.1007/s10072-014-1794-5
70. Vermeer SE, Prins ND, den Heijer T, Hofman A, Koudstaal PJ, Breteler MM. Silent brain infarcts and the risk of dementia and cognitive decline. *N Engl J Med*. Mar 27 2003;348(13):1215-22. doi:10.1056/NEJMoa022066
71. Suter OC, Sunthorn T, Kraftsik R, et al. Cerebral hypoperfusion generates cortical watershed microinfarcts in Alzheimer disease. *Stroke*. Aug 2002;33(8):1986-92. doi:10.1161/01.str.0000024523.82311.77
72. Markus HS. Stroke genetics: prospects for personalized medicine. *BMC Med*. Sep 27 2012;10:113. doi:10.1186/1741-7015-10-113
73. Ringelstein EB, Droste DW, Babikian VL, et al. Consensus on microembolus detection by TCD. International Consensus Group on Microembolus Detection. *Stroke*. Mar 1998;29(3):725-9. doi:10.1161/01.str.29.3.725
74. Bismuth J, Garami Z, Anaya-Ayala JE, et al. Transcranial Doppler findings during thoracic endovascular aortic repair. *J Vasc Surg*. Aug 2011;54(2):364-9. doi:10.1016/j.jvs.2010.12.063
75. Grover G, Perera AH, Hamady M, et al. Cerebral embolic protection in thoracic endovascular aortic repair. *J Vasc Surg*. Dec 2018;68(6):1656-1666. doi:10.1016/j.jvs.2017.11.098
76. Benson RA, Matthews D, Loftus V, Nicholson G, Tropman D, Loftus IM. Cerebral embolization during endovascular infrarenal, juxtarenal, and suprarenal aortic aneurysm repair, high-risk maneuvers, and associated neurologic outcomes. *J Vasc Surg*. Nov 2018;68(5):1374-1381. doi:10.1016/j.jvs.2018.01.041
77. Kim K RT, Khoynezhad A, Donayre C, Kruse M, Chauvapun J, Kopchock G, Walot I, White Rodney. Transcranial Doppler Assessment of Embolic Events During Thoracic

Endovascular Aortic Repair. *Journal of Vascular Surgery*. 01/08/2010 2010;52(2):531. doi:https://doi.org/10.1016/j.jvs.2010.05.047
78. Wolf O, Heider P, Heinz M, et al. Microembolic signals detected by transcranial Doppler sonography during carotid endarterectomy and correlation with serial diffusion-weighted imaging. *Stroke*. Nov 2004;35(11):e373-5. doi:10.1161/01.STR.0000143184.69343.ec
79. Skjelland M, Krohg-Sorensen K, Tennoe B, Bakke SJ, Brucher R, Russell D. Cerebral microemboli and brain injury during carotid artery endarterectomy and stenting. *Stroke*. Jan 2009;40(1):230-4. doi:10.1161/STROKEAHA.107.513341
80. Nakajima M, Kimura K, Shimode A, et al. Microembolic signals within 24 hours of stroke onset and diffusion-weighted MRI abnormalities. *Cerebrovasc Dis*. 2007;23(4):282-8. doi:10.1159/000098328
81. Kimura K, Minematsu K, Koga M, et al. Microembolic signals and diffusion-weighted MR imaging abnormalities in acute ischemic stroke. *AJNR Am J Neuroradiol*. Jun-Jul 2001;22(6):1037-42.
82. Higuchi E, Toi S, Shirai Y, et al. Prevalence of Microembolic Signals in Embolic Stroke of Undetermined Source and Other Subtypes of Ischemic Stroke. *Stroke*. Feb 2020;51(2):655-658. doi:10.1161/STROKEAHA.119.027008
83. Fearn SJ, Pole R, Wesnes K, Faragher EB, Hooper TL, McCollum CN. Cerebral injury during cardiopulmonary bypass: emboli impair memory. *J Thorac Cardiovasc Surg*. Jun 2001;121(6):1150-60. doi:10.1067/mtc.2001.114099
84. Braekken SK, Reinvang I, Russell D, Brucher R, Svennevig JL. Association between intraoperative cerebral microembolic signals and postoperative neuropsychological deficit: comparison between patients with cardiac valve replacement and patients with coronary artery bypass grafting. *J Neurol Neurosurg Psychiatry*. 1998;65(4):573-6.
85. Lloyd AJ, Hayes PD, London NJM, Bell PRF, Naylor AR. Does carotid endarterectomy lead to a decline in cognitive function or health related quality of life? *J Clin Exp Neuropsychol*. 2004;26(6):817-25.
86. Gaunt ME, Martin PJ, Smith JL, et al. Clinical relevance of intraoperative embolization detected by transcranial Doppler ultrasonography during carotid endarterectomy: a prospective study of 100 patients. *Br J Surg*. 1994;81(10):1435-9.
87. Drews T, Pasic M, Buz S, et al. Transcranial Doppler sound detection of cerebral microembolism during transapical aortic valve implantation. *Thorac Cardiovasc Surg*. Jun 2011;59(4):237-42. doi:10.1055/s-0030-1250495
88. Katz ES, Tunick PA, Rusinek H, Ribakove G, Spencer FC, Kronzon I. Protruding aortic atheromas predict stroke in elderly patients undergoing cardiopulmonary bypass: experience with intraoperative transesophageal echocardiography. *J Am Coll Cardiol*. Jul 1992;20(1):70-7. doi:10.1016/0735-1097(92)90139-e
89. Autar A, Taha A, van Duin R, et al. Endovascular procedures cause transient endothelial injury but do not disrupt mature neointima in Drug Eluting Stents. *Sci Rep*. Feb 7 2020;10(1):2173. doi:10.1038/s41598-020-58938-z

90. Rodriguez RA, Nathan HJ, Ruel M, Rubens F, Dafoe D, Mesana T. A method to distinguish between gaseous and solid cerebral emboli in patients with prosthetic heart valves. *European journal of cardio-thoracic surgery : official journal of the European Association for Cardio-thoracic Surgery*. 2009;35(1):89-95.
91. Markus HS, Punter M. Can transcranial Doppler discriminate between solid and gaseous microemboli? Assessment of a dual-frequency transducer system. *Stroke*. 2005;36(8):1731-4.
92. Inci K, Koutouzi G, Chernoray V, Jeppsson A, Nilsson H, Falkenberg M. Air bubbles are released by thoracic endograft deployment: An in vitro experimental study. *SAGE Open Med*. 2016;4:2050312116682130. doi:10.1177/2050312116682130
93. Rohlffs F, Tsilimparis N, Saleptsis V, Diener H, Debus ES, Kolbel T. Air Embolism During TEVAR: Carbon Dioxide Flushing Decreases the Amount of Gas Released from Thoracic Stent-Grafts During Deployment. *J Endovasc Ther*. Feb 2017;24(1):84-88. doi:10.1177/1526602816675621
94. Gagnon J T, J, Misskey, J. Analysis and Quantification of Retained Air in Thoracic Aortic Endografts. *Journal of Vascular Surgery*. 2017;65(6):73S.
95. Rylski B, Mayer F, Beyersdorf F, et al. How to minimize air embolisms during thoracic endovascular aortic repair with Relay Pro? *Interact Cardiovasc Thorac Surg*. 2020;30(2):293-295.
96. Makaloski V, Rohlffs F, Trepte C, et al. Distribution of Air Embolization During TEVAR Depends on Landing Zone: Insights From a Pulsatile Flow Model. *J Endovasc Ther*. Aug 2019;26(4):448-455. doi:10.1177/1526602819849931
97. Spencer MP CS. Development of bubbles in venous and arterial blood during hyperbaric decompression. *Bull Mason Clinic*. 1968;22:26-32.
98. Rodriguez HE PW, Yao JST. *Ischemic Extremities, New Findings & Treatment (Modern Trends in Vascular Surgery)* 1st ed. People's Medical Publishing House-USA, Shelton, CT.
99. Tsetsou S, Eeckhout E, Qanadli SD, Lachenal Y, Vingerhoets F, Michel P. Nonaccidental arterial cerebral air embolism: a ten-year stroke center experience. *Cerebrovasc Dis*. 2013;35(4):392-5. doi:10.1159/000348656
100. Muth CM, Shank ES. Gas embolism. *N Engl J Med*. Feb 17 2000;342(7):476-82. doi:10.1056/NEJM200002173420706
101. Gerriets T, Schwarz N, Sammer G, et al. Protecting the brain from gaseous and solid micro-emboli during coronary artery bypass grafting: a randomized controlled trial. *Eur Heart J*. Feb 2010;31(3):360-8. doi:10.1093/eurheartj/ehp178
102. Mitchell SJ, Merry AF. Perspective on Cerebral Microemboli in Cardiac Surgery: Significant Problem or Much Ado About Nothing? *J Extra Corpor Technol*. Mar 2015;47(1):10-5.
103. Mitchell SJ WT, McDougall C, Gorman DF. Emboli generation by the Medtronic Maxima hardshell adult venous reservoir in cardio-pulmonary bypass circuits: A preliminary report. *Perfusion*. 1996;11:145-155.

104. Willcox TW, Mitchell SJ, Gorman DF. Venous air in the bypass circuit: a source of arterial line emboli exacerbated by vacuum-assisted drainage. *Ann Thorac Surg*. Oct 1999;68(4):1285-9. doi:10.1016/s0003-4975(99)00721-3
105. Taylor RL, Borger MA, Weisel RD, Fedorko L, Feindel CM. Cerebral microemboli during cardiopulmonary bypass: increased emboli during perfusionist interventions. *Ann Thorac Surg*. Jul 1999;68(1):89-93. doi:10.1016/s0003-4975(99)00475-0
106. Milsom FP MS. A novel dual vent heart de-airing technique markedly reduces carotid artery microemboli. *Ann Thorac Surg*. 1998;66:785-791.
107. Soderman M, Bystam J. Cerebral air emboli from angiography in a patient with stroke. A case report. *Acta Radiol*. Mar 2001;42(2):140-3. doi:10.1034/j.1600-0455.2001.042002140.x
108. Chuang DY, Sundararajan S, Sundararajan VA, Feldman DI, Xiong W. Accidental Air Embolism. *Stroke*. Jul 2019;50(7):e183-e186. doi:10.1161/STROKEAHA.119.025340
109. Deklunder G, Roussel M, Lecroart JL, Prat A, Gautier C. Microemboli in cerebral circulation and alteration of cognitive abilities in patients with mechanical prosthetic heart valves. *Stroke*. Sep 1998;29(9):1821-6. doi:10.1161/01.str.29.9.1821
110. Gorman DF, Browning DM. Cerebral vasoreactivity and arterial gas embolism. *Undersea Biomed Res*. Sep 1986;13(3):317-35.
111. Gorman DF BD, Parsons DW, Traugott FM. The distribution of arterial gas emboli in the pial circulation *SPUMS J*. 1987;17:101-16.
112. Urenjak J, Obrenovitch TP. Pharmacological modulation of voltage-gated Na+ channels: a rational and effective strategy against ischemic brain damage. *Pharmacol Rev*. Mar 1996;48(1):21-67.
113. Dexter F HB. Computer simulation of microscopic cerebral air emboli during cardiac surgery. . *Undersea and Hyperbaric Med* 1998;25:43-50.
114. Feinstein SB SP, Bing RJ et al Microbubble dynamics visualized in the intact capillary circulation. *J Am Coll Cardiol*. 1984;4:595–600.
115. Branger AB, Eckmann DM. Theoretical and experimental intravascular gas embolism absorption dynamics. *J Appl Physiol (1985)*. Oct 1999;87(4):1287-95. doi:10.1152/jappl.1999.87.4.1287
116. Francis TJR GD. *Pathogenesis of the decompression disorders in: The Physiology and Medicine of Diving*. 4 ed. Bennett PB, Elliott DH, eds. London: W.B. Saunders; 1993.
117. J D. The corticoangioarchitecture of the human brain. *Acta Neurol Belg*. 1972;72:323-9.
118. Dutka AJ KP, Hallenbeck JM, Storey JR Air embolism may cause unrecognized ischemia of the grey–white matter junction. *Undersea Biomed Res*. 1988;15:99–106.
119. Barak M, Nakhoul F, Katz Y. Pathophysiology and clinical implications of microbubbles during hemodialysis. *Semin Dial*. May-Jun 2008;21(3):232-8. doi:10.1111/j.1525-139X.2008.00424.x
120. Butler BD, Morris WP. Transesophageal echocardiographic study of decompression-induced venous gas emboli. *Undersea Hyperb Med*. Jun 1995;22(2):117-28.

121. Mitchell S, Gorman D. The pathophysiology of cerebral arterial gas embolism. *J Extra Corpor Technol*. Mar 2002;34(1):18-23.
122. Weenink RP, Hollmann MW, van Hulst RA. Animal models of cerebral arterial gas embolism. *J Neurosci Methods*. Apr 15 2012;205(2):233-45. doi:10.1016/j.jneumeth.2011.12.025
123. Juenemann M, Yeniguen M, Schleicher N, et al. Impact of bubble size in a rat model of cerebral air microembolization. *J Cardiothorac Surg*. Oct 18 2013;8:198. doi:10.1186/1749-8090-8-198
124. Helps SC, Meyer-Witting M, Reilly PL, Gorman DF. Increasing doses of intracarotid air and cerebral blood flow in rabbits. *Stroke*. Sep 1990;21(9):1340-5. doi:10.1161/01.str.21.9.1340
125. Hindman BJ, Dexter F, Subieta A, Smith T, Cutkomp J. Brain injury after cerebral arterial air embolism in the rabbit as determined by triphenyltetrazolium staining. *Anesthesiology*. May 1999;90(5):1462-73. doi:10.1097/00000542-199905000-00032
126. Furlow TW, Jr. Experimental air embolism of the brain: an analysis of the technique in the rat. *Stroke*. Nov-Dec 1982;13(6):847-52. doi:10.1161/01.str.13.6.847
127. Feinstein SB, Shah PM, Bing RJ, et al. Microbubble dynamics visualized in the intact capillary circulation. *J Am Coll Cardiol*. Sep 1984;4(3):595-600. doi:10.1016/s0735-1097(84)80107-2
128. Helps SC, Parsons DW, Reilly PL, Gorman DF. The effect of gas emboli on rabbit cerebral blood flow. *Stroke*. Jan 1990;21(1):94-9. doi:10.1161/01.str.21.1.94
129. Hills BA, James PB. Microbubble damage to the blood-brain barrier: relevance to decompression sickness. *Undersea Biomed Res*. Mar 1991;18(2):111-6.
130. Warren BA, Philp RB, Inwood MJ. The ultrastructural morphology of air embolism: platelet adhesion to the interface and endothelial damage. *Br J Exp Pathol*. Apr 1973;54(2):163-72.
131. Boyle EM, Jr., Pohlman TH, Johnson MC, Verrier ED. Endothelial cell injury in cardiovascular surgery: the systemic inflammatory response. *Ann Thorac Surg*. Jan 1997;63(1):277-84. doi:10.1016/s0003-4975(96)01061-2
132. Geiser T, Sturzenegger M, Genewein U, Haeberli A, Beer JH. Mechanisms of cerebrovascular events as assessed by procoagulant activity, cerebral microemboli, and platelet microparticles in patients with prosthetic heart valves. *Stroke*. Sep 1998;29(9):1770-7. doi:10.1161/01.str.29.9.1770
133. Skjelland M, Michelsen A, Brosstad F, Svennevig JL, Brucher R, Russell D. Solid cerebral microemboli and cerebrovascular symptoms in patients with prosthetic heart valves. *Stroke*. Apr 2008;39(4):1159-64. doi:10.1161/STROKEAHA.107.493031
134. Caplan LR, Hennerici M. Impaired clearance of emboli (washout) is an important link between hypoperfusion, embolism, and ischemic stroke. *Arch Neurol*. Nov 1998;55(11):1475-82. doi:10.1001/archneur.55.11.1475

135. Hague JP, Banahan C, Chung EM. Modelling of impaired cerebral blood flow due to gaseous emboli. *Phys Med Biol*. Jul 7 2013;58(13):4381-94. doi:10.1088/0031-9155/58/13/4381
136. Gray WA, Mehta M, Alani F, et al. Use of a novel embolic filter in carotid artery stenting: 30-Day results from the EMBOLDEN Clinical Study. *Catheter Cardiovasc Interv*. Nov 15 2018;92(6):1128-1135. doi:10.1002/ccd.27474
137. Haussig S, Mangner N, Dwyer MG, et al. Effect of a Cerebral Protection Device on Brain Lesions Following Transcatheter Aortic Valve Implantation in Patients With Severe Aortic Stenosis: The CLEAN-TAVI Randomized Clinical Trial. *JAMA*. Aug 9 2016;316(6):592-601. doi:10.1001/jama.2016.10302
138. Van Mieghem NM, van Gils L, Ahmad H, et al. Filter-based cerebral embolic protection with transcatheter aortic valve implantation: the randomised MISTRAL-C trial. *EuroIntervention*. Jul 20 2016;12(4):499-507. doi:10.4244/EIJV12I4A84
139. Lansky AJ SJ, Tchetche D, Stella P, Pietras CG, Parise H, Abrams K, Forrest JK, Cleman M, Reinoehl J, Cuisset T. A prospective randomized evaluation of the TriGuard™ HDH embolic DEFLECTion device during transcatheter aortic valve implantation: results from the DEFLECT III trial. *European Heart Journal*. 2015;14:2070-8.
140. Rodes-Cabau J, Kahlert P, Neumann FJ, et al. Feasibility and exploratory efficacy evaluation of the Embrella Embolic Deflector system for the prevention of cerebral emboli in patients undergoing transcatheter aortic valve replacement: the PROTAVI-C pilot study. *JACC Cardiovasc Interv*. Oct 2014;7(10):1146-55. doi:10.1016/j.jcin.2014.04.019
141. J W. Coronary and Structural Interventions Ulm Transcatheter Aortic Valve Replacement (CSI-Ulm-TAVR) University of Ulm. *German Society for Cardiology (DGK)*. 2017;in press
142. Kapadia SR, Kodali S, Makkar R, et al. Protection Against Cerebral Embolism During Transcatheter Aortic Valve Replacement. *J Am Coll Cardiol*. Jan 31 2017;69(4):367-377. doi:10.1016/j.jacc.2016.10.023
143. RA J. Cerebral Protection against Embolization during Thoracic EndoVascular Aortic Repair. LINC. 2016. Accessed 28th March 2020, http://claretmedical.com/pdf/studies/LINC_2016_Claret_Janosi_TEVAR.pdf. http://claretmedical.com/pdf/studies/LINC_2016_Claret_
144. Shah AS, Akhmerov A, Gupta N, Chakravarty T, Makkar RR, Azizzadeh A. Use of a Dual-Filter Cerebral Embolic Protection Device in Thoracic Endovascular Aortic Repair. *Ann Vasc Surg*. May 2020;65:54 e1-54 e4. doi:10.1016/j.avsg.2020.01.077
145. Van Gils L, Kroon H, Daemen J, et al. Complete filter-based cerebral embolic protection with transcatheter aortic valve replacement. *Catheter Cardiovasc Interv*. Mar 1 2018;91(4):790-797. doi:10.1002/ccd.27323
146. Shimamura K, Kuratani T, Kin K, Shijo T, Masada K, Sawa Y. Effectiveness of embolic protection filter devices in stroke prevention during endovascular aortic arch repair in significant aortic atheroma patients. *Interact Cardiovasc Thorac Surg*. Jun 1 2019;28(6):974-980. doi:10.1093/icvts/ivz004

147. Tsutsumi M, Kazekawa K, Onizuka M, et al. Cerebral protection during retrograde carotid artery stenting for proximal carotid artery stenosis: technical note. *Neurol Med Chir (Tokyo)*. Jun 2007;47(6):285-7; discussion 287-8. doi:10.2176/nmc.47.285
148. Masada K, Kuratani T, Shimamura K, et al. Silent cerebral infarction after thoracic endovascular aortic repair: a magnetic resonance imaging study. *Eur J Cardiothorac Surg*. Jun 1 2019;55(6):1071-1078. doi:10.1093/ejcts/ezy449
149. Ribo M, Molina CA, Alvarez B, Rubiera M, Alvarez-Sabin J, Matas M. Transcranial Doppler monitoring of transcervical carotid stenting with flow reversal protection: a novel carotid revascularization technique. *Stroke*. Nov 2006;37(11):2846-9. doi:10.1161/01.STR.0000244781.68371.59
150. Luk Y, Chan YC, Cheng SW. Transcarotid Artery Revascularization as a New Modality of Treatment for Carotid Stenosis. *Ann Vasc Surg*. Apr 2020;64:397-404. doi:10.1016/j.avsg.2019.11.001
151. Rippel RA, Rolls AE, Riga CV, Hamady M, Cheshire NJ, Bicknell CD. The use of robotic endovascular catheters in the facilitation of transcatheter aortic valve implantation. *Eur J Cardiothorac Surg*. May 2014;45(5):836-41. doi:10.1093/ejcts/ezt524
152. Perera AH, Riga CV, Monzon L, Gibbs RG, Bicknell CD, Hamady M. Robotic Arch Catheter Placement Reduces Cerebral Embolization During Thoracic Endovascular Aortic Repair (TEVAR). *Eur J Vasc Endovasc Surg*. Mar 2017;53(3):362-369. doi:10.1016/j.ejvs.2016.10.017
153. Martens S, Neumann K, Sodemann C, Deschka H, Wimmer-Greinecker G, Moritz A. Carbon dioxide field flooding reduces neurologic impairment after open heart surgery. *Ann Thorac Surg*. Feb 2008;85(2):543-7. doi:10.1016/j.athoracsur.2007.08.047
154. Skidmore KL, Jones C, DeWet C. Flooding the surgical field with carbon dioxide during open heart surgery improves segmental wall motion. *J Extra Corpor Technol*. Jun 2006;38(2):123-7.
155. Listewnik M, Kotfis K, Slozowski P, Mokrzycki K, Brykczynski M. The influence of carbon dioxide field flooding in mitral valve operations with cardiopulmonary bypass on S100ss level in blood plasma in the aging brain. *Clin Interv Aging*. 2018;13:1837-1845. doi:10.2147/CIA.S177356
156. Webb WR, Harrison LH, Jr., Helmcke FR, et al. Carbon dioxide field flooding minimizes residual intracardiac air after open heart operations. *Ann Thorac Surg*. Nov 1997;64(5):1489-91. doi:10.1016/S0003-4975(97)00945-4
157. Nichols HT MD, Hirose T. Coronary and other air embolixation occurring during open cardiac surgery. . *Surgery*. 1958;43:236-44.
158. Stehouwer MC, de Vroege R, Hoohenkerk GJF, et al. Carbon Dioxide Flush of an Integrated Minimized Perfusion Circuit Prior to Priming Prevents Spontaneous Air Release Into the Arterial Line During Clinical Use. *Artif Organs*. Nov 2017;41(11):997-1003. doi:10.1111/aor.12909

159. Nyman J, Rundby C, Svenarud P, van der Linden J. Does CO(2) flushing of the empty CPB circuit decrease the number of gaseous emboli in the prime? *Perfusion*. Jul 2009;24(4):249-55. doi:10.1177/0267659109350241
160. Hargrove M MA, Fitzpatrick G. Carbon dioxide flushing prior to priming the bypass circuit. An experimental derivation of the optimal flow rate and duration of the flushing process. *Perfusion*. 1987;2:177-179.
161. Ganguly G, Dixit V, Patrikar S, Venkatraman R, Gorthi SP, Tiwari N. Carbon dioxide insufflation and neurocognitive outcome of open heart surgery. *Asian Cardiovasc Thorac Ann*. Sep 2015;23(7):774-80. doi:10.1177/0218492315583562
162. Beckman RR, Gisner C, Evans E. An in vitro study of the effectiveness of carbon dioxide flushing of arterial line filters. *J Extra Corpor Technol*. Sep 2009;41(3):161-5.
163. Benedetto U, Caputo M, Guida G, et al. Carbon Dioxide Insufflation During Cardiac Surgery: A Meta-analysis of Randomized Controlled Trials. *Semin Thorac Cardiovasc Surg*. Autumn 2017;29(3):301-310. doi:10.1053/j.semtcvs.2017.05.002
164. Kolbel T, Rohlffs F, Wipper S, Carpenter SW, Debus ES, Tsilimparis N. Carbon Dioxide Flushing Technique to Prevent Cerebral Arterial Air Embolism and Stroke During TEVAR. *J Endovasc Ther*. Apr 2016;23(2):393-5. doi:10.1177/1526602816633705
165. Charbonneau P, Kolbel T, Rohlffs F, et al. Silent Brain Infarction After Endovascular Arch Procedures: Preliminary Results from the STEP Registry. *Eur J Vasc Endovasc Surg*. Feb 2021;61(2):239-245. doi:10.1016/j.ejvs.2020.11.021
166. Rohlffs F, Tsilimparis N, Trepte C, et al. Air Embolism During TEVAR: An Additional Flush Port on the Delivery System Pusher Significantly Reduces the Amount of Air Released During Deployment of a Thoracic Stent-Graft in an Experimental Setting. *J Endovasc Ther*. Aug 2018;25(4):435-439. doi:10.1177/1526602818780951
167. Rohlffs F, Trepte C, Ivancev K, et al. Air Embolism During TEVAR: Liquid Perfluorocarbon Absorbs Carbon Dioxide in a Combined Flushing Technique and Decreases the Amount of Gas Released From Thoracic Stent-Grafts During Deployment in an Experimental Setting. *J Endovasc Ther*. Feb 2019;26(1):76-80. doi:10.1177/1526602818819501
168. Schonburg M, Ziegelhoeffer T, Kraus B, et al. Reduction of gaseous microembolism during aortic valve replacement using a dynamic bubble trap. *Gen Physiol Biophys*. Jun 2006;25(2):207-14.
169. Motallebzadeh R, Jahangiri M. The effect of the dynamic air bubble trap on cerebral microemboli and S100 beta. *J Thorac Cardiovasc Surg*. Jul 2004;128(1):154. doi:10.1016/j.jtcvs.2004.02.024
170. Perthel M, Kseibi S, Bendisch A, Laas J. Use of a dynamic bubble trap in the arterial line reduces microbubbles during cardiopulmonary bypass and microembolic signals in the middle cerebral artery. *Perfusion*. May 2005;20(3):151-6. doi:10.1191/0267659105pf813oa
171. Haiman G, Nazif T, Moses JW, Ashkenazi A, Margolis P, Lansky AJ. Reduction of Cerebral Emboli: In vitro Study with a Novel Cerebral Embolic Protection Device. *Med Devices (Auckl)*. 2020;13:67-73. doi:10.2147/MDER.S234961

172. RDocumentation. metaprop: Meta-analysis of single proportions. Accessed 10th June 2021, https://www.rdocumentation.org/packages/meta/versions/4.9-6/topics/metaprop.
173. W V. Conducting meta-analyses in R with the metafor package. *Journal of Statistical Software* 2010;36(3):1-48.
174. Freeman MF TJ. Transformations Related to the Angular and the Square Root. *The Annals of Mathematical Statistics*. 1950;21(4):607-11,5.
175. DerSimonian R, Laird N. Meta-analysis in clinical trials. *Control Clin Trials*. Sep 1986;7(3):177-88. doi:10.1016/0197-2456(86)90046-2
176. Higgins JP, Thompson SG, Deeks JJ, Altman DG. Measuring inconsistency in meta-analyses. *BMJ*. Sep 6 2003;327(7414):557-60. doi:10.1136/bmj.327.7414.557
177. Duval S, Tweedie R. Trim and fill: A simple funnel-plot-based method of testing and adjusting for publication bias in meta-analysis. *Biometrics*. Jun 2000;56(2):455-63. doi:10.1111/j.0006-341x.2000.00455.x
178. National Institute of Health Quality Assessment Tool Accessed 11th May 2021, https://www.nhlbi.nih.gov/health-topics/study-quality-assessment-tools
179. The Newcastle-Ottawa Scale (NOS) for assessing the quality of nonrandomised studies in meta-analyses. Accessed 15th May 2021, http://www.ohri.ca/programs/clinical_epidemiology/oxford.asp
180. GRADEpro. Accessed 20th May 2022, https://www.gradepro.org/
181. Makaroun MS, Dillavou ED, Kee ST, et al. Endovascular treatment of thoracic aortic aneurysms: results of the phase II multicenter trial of the GORE TAG thoracic endoprosthesis. *J Vasc Surg*. Jan 2005;41(1):1-9. doi:10.1016/j.jvs.2004.10.046
182. Azizzadeh A, Desai N, Arko FR, 3rd, et al. Pivotal results for the Valiant Navion stent graft system in the Valiant EVO global clinical trial. *J Vasc Surg*. Nov 2019;70(5):1399-1408 e1. doi:10.1016/j.jvs.2019.01.067
183. Heijmen RH, Thompson MM, Fattori R, Goktay Y, Teebken OE, Orend KH. Valiant thoracic stent-graft deployed with the new captivia delivery system: procedural and 30-day results of the Valiant Captivia registry. *J Endovasc Ther*. Apr 2012;19(2):213-25. doi:10.1583/11-3652MR.1
184. Fairman RM, Criado F, Farber M, et al. Pivotal results of the Medtronic Vascular Talent Thoracic Stent Graft System: the VALOR trial. *J Vasc Surg*. Sep 2008;48(3):546-54. doi:10.1016/j.jvs.2008.03.061
185. Matsumura JS, Cambria RP, Dake MD, et al. International controlled clinical trial of thoracic endovascular aneurysm repair with the Zenith TX2 endovascular graft: 1-year results. *J Vasc Surg*. Feb 2008;47(2):247-257; discussion 257. doi:10.1016/j.jvs.2007.10.032
186. Fairman RM, Tuchek JM, Lee WA, et al. Pivotal results for the Medtronic Valiant Thoracic Stent Graft System in the VALOR II trial. *J Vasc Surg*. Nov 2012;56(5):1222-31 e1. doi:10.1016/j.jvs.2012.04.062
187. Kasirajan K, Morasch MD, Makaroun MS. Sex-based outcomes after endovascular repair of thoracic aortic aneurysms. *J Vasc Surg*. Sep 2011;54(3):669-75; discussion 675-6. doi:10.1016/j.jvs.2011.03.010

188. Patel HJ, Dake MD, Bavaria JE, et al. Branched Endovascular Therapy of the Distal Aortic Arch: Preliminary Results of the Feasibility Multicenter Trial of the Gore Thoracic Branch Endoprosthesis. *Ann Thorac Surg*. Oct 2016;102(4):1190-8. doi:10.1016/j.athoracsur.2016.03.091
189. Farber MA, Lee WA, Szeto WY, Panneton JM, Kwolek CJ. Initial and midterm results of the Bolton Relay Thoracic Aortic Endovascular Pivotal Trial. *J Vasc Surg*. Jun 2017;65(6):1556-1566 e1. doi:10.1016/j.jvs.2016.11.061
190. Malas M, Locham S, Hughes C, et al. Midterm outcomes in patients undergoing endovascular repair of thoracic aortic aneurysms and penetrating atherosclerotic ulcers using the RelayPlus stent graft. *Journal of Vascular Surgery*. 2021/02/01/ 2021;73(2):459-465. doi:https://doi.org/10.1016/j.jvs.2020.05.059
191. Maldonado TS, Dexter D, Rockman CB, et al. Left subclavian artery coverage during thoracic endovascular aortic aneurysm repair does not mandate revascularization. *J Vasc Surg*. Jan 2013;57(1):116-24. doi:10.1016/j.jvs.2012.06.101
192. Mezzetto L, Scorsone L, Silingardi R, et al. Early and Long-term Results of ePTFE (Gore TAG®) versus Dacron (Relay Plus® Bolton) Grafts in Thoracic Endovascular Aneurysm Repair. *Annals of Vascular Surgery*. 2021/02/01/ 2021;71:419-427. doi:https://doi.org/10.1016/j.avsg.2020.07.054
193. Schlosser FJ, Verhagen HJ, Lin PH, et al. TEVAR following prior abdominal aortic aneurysm surgery: increased risk of neurological deficit. *J Vasc Surg*. Feb 2009;49(2):308-14; discussion 314. doi:10.1016/j.jvs.2008.07.093
194. Varkevisser RRB, Swerdlow NJ, de Guerre L, et al. Thoracic Endovascular Aortic Repair With Left Subclavian Artery Coverage Is Associated With a High 30-Day Stroke Incidence With or Without Concomitant Revascularization. *J Endovasc Ther*. Oct 2020;27(5):769-776. doi:10.1177/1526602820923044
195. Shimizu H, Hirahara N, Motomura N, Miyata H, Takamoto S. Current status of cardiovascular surgery in Japan, 2015 and 2016: analysis of data from Japan Cardiovascular Surgery Database. 4-Thoracic aortic surgery. *Gen Thorac Cardiovasc Surg*. Sep 2019;67(9):751-757. doi:10.1007/s11748-019-01163-x
196. Neuhauser B, Perkmann R, Greiner A, et al. Mid-term results after endovascular repair of the atherosclerotic descending thoracic aortic aneurysm. *Eur J Vasc Endovasc Surg*. Aug 2004;28(2):146-53. doi:10.1016/j.ejvs.2004.04.006
197. Glade GJ, Vahl AC, Wisselink W, Linsen MA, Balm R. Mid-term survival and costs of treatment of patients with descending thoracic aortic aneurysms; endovascular vs. open repair: a case-control study. *Eur J Vasc Endovasc Surg*. Jan 2005;29(1):28-34. doi:10.1016/j.ejvs.2004.10.003
198. Marcheix B, Dambrin C, Bolduc JP, et al. Midterm results of endovascular treatment of atherosclerotic aneurysms of the descending thoracic aorta. *J Thorac Cardiovasc Surg*. Nov 2006;132(5):1030-6. doi:10.1016/j.jtcvs.2006.07.006

199. Appoo JJ, Moser WG, Fairman RM, et al. Thoracic aortic stent grafting: improving results with newer generation investigational devices. *J Thorac Cardiovasc Surg*. May 2006;131(5):1087-94. doi:10.1016/j.jtcvs.2005.12.058
200. Saratzis N, Saratzis A, Melas N, et al. Endovascular treatment of descending thoracic aortic aneurysms with the EndoFit stent-graft. *Cardiovasc Intervent Radiol*. Mar-Apr 2007;30(2):177-81. doi:10.1007/s00270-006-0168-7
201. Yunoki J, Kuratani T, Shirakawa Y, et al. Mid-term results of endovascular treatment with the Gore TAG device for degenerative descending thoracic aortic aneurysms. *Gen Thorac Cardiovasc Surg*. Jan 2015;63(1):38-42. doi:10.1007/s11748-014-0436-4
202. Ranney DN, Cox ML, Yerokun BA, Benrashid E, McCann RL, Hughes GC. Long-term results of endovascular repair for descending thoracic aortic aneurysms. *J Vasc Surg*. Feb 2018;67(2):363-368. doi:10.1016/j.jvs.2017.06.094
203. Matsuyama M, Nakamura K, Nagahama H, et al. Long-term results of endovascular repair for distal arch and descending thoracic aortic aneurysms treated by custom-made endografts: usefulness of fenestrated endografts. *Ann Vasc Dis*. 2014;7(4):383-92. doi:10.3400/avd.oa.14-00057
204. Hughes GC, Lee SM, Daneshmand MA, et al. Endovascular repair of descending thoracic aneurysms: results with "on-label" application in the post Food and Drug Administration approval era. *Ann Thorac Surg*. Jul 2010;90(1):83-9. doi:10.1016/j.athoracsur.2010.03.052
205. Andrassy J, Weidenhagen R, Meimarakis G, Rentsch M, Jauch KW, Kopp R. Endovascular versus open treatment of degenerative aneurysms of the descending thoracic aorta: a single center experience. *Vascular*. Feb 2011;19(1):8-14. doi:10.1258/vasc.2010.oa0256
206. Zamor KC, Eskandari MK, Rodriguez HE, Ho KJ, Morasch MD, Hoel AW. Outcomes of Thoracic Endovascular Aortic Repair and Subclavian Revascularization Techniques. *J Am Coll Surg*. Jul 2015;221(1):93-100. doi:10.1016/j.jamcollsurg.2015.02.028
207. Kratimenos T, Antonopoulos CN, Tomais D, et al. Repair of descending thoracic aortic aneurysms with Ankura Thoracic Stent Graft. *J Vasc Surg*. Apr 2019;69(4):996-1002 e3. doi:10.1016/j.jvs.2018.07.065
208. Ziza V, Canaud L, Molinari N, Branchereau P, Marty-Ane C, Alric P. Thoracic endovascular aortic repair: A single center's 15-year experience. *J Thorac Cardiovasc Surg*. Jun 2016;151(6):1595-1603 e7. doi:10.1016/j.jtcvs.2015.12.030
209. Tanious A, Boitano L, Canha L, et al. Thoracic aortic remodeling with endografting after a decade of thoracic endovascular aortic repair experience. *J Vasc Surg*. Mar 2021;73(3):844-849. doi:10.1016/j.jvs.2020.06.120
210. Torsello GF, Inchingolo M, Austermann M, Torsello GB, Panuccio G, Bisdas T. Durability of a low-profile stent graft for thoracic endovascular aneurysm repair. *J Vasc Surg*. Dec 2017;66(6):1638-1643. doi:10.1016/j.jvs.2017.04.042

211. Lombardi JV, Gleason TG, Panneton JM, et al. STABLE II clinical trial on endovascular treatment of acute, complicated type B aortic dissection with a composite device design. *J Vasc Surg*. Apr 2020;71(4):1077-1087 e2. doi:10.1016/j.jvs.2019.06.189
212. Cambria RP, Conrad MF, Matsumoto AH, et al. Multicenter clinical trial of the conformable stent graft for the treatment of acute, complicated type B dissection. *J Vasc Surg*. Aug 2015;62(2):271-8. doi:10.1016/j.jvs.2015.03.026
213. Bavaria JE, Brinkman WT, Hughes GC, et al. Outcomes of Thoracic Endovascular Aortic Repair in Acute Type B Aortic Dissection: Results From the Valiant United States Investigational Device Exemption Study. *Ann Thorac Surg*. Sep 2015;100(3):802-8; discussion 808-9. doi:10.1016/j.athoracsur.2015.03.108
214. Ehrlich MP, Rousseau H, Heijmen R, et al. Midterm results after endovascular treatment of acute, complicated type B aortic dissection: the Talent Thoracic Registry. *J Thorac Cardiovasc Surg*. Jan 2013;145(1):159-65. doi:10.1016/j.jtcvs.2011.10.093
215. Torsello GB, Torsello GF, Osada N, Teebken OE, Ratusinski CM, Nienaber CA. Midterm results from the TRAVIATA registry: treatment of thoracic aortic disease with the valiant stent graft. *J Endovasc Ther*. Apr 2010;17(2):137-50. doi:10.1583/09-2905.1
216. Torrent DJ, McFarland GE, Wang G, et al. Timing of thoracic endovascular aortic repair for uncomplicated acute type B aortic dissection and the association with complications. *J Vasc Surg*. Mar 2021;73(3):826-835. doi:10.1016/j.jvs.2020.05.073
217. Zhang H, Qiao T. Aortic remodeling in Type B aortic dissection after thoracic endovascular aortic repair with an aortic extender cuff implantation. *Clin Interv Aging*. 2018;13:2359-2366. doi:10.2147/CIA.S179526
218. Steuer J, Bjorck M, Mayer D, Wanhainen A, Pfammatter T, Lachat M. Distinction between acute and chronic type B aortic dissection: is there a sub-acute phase? *Eur J Vasc Endovasc Surg*. Jun 2013;45(6):627-31. doi:10.1016/j.ejvs.2013.03.013
219. Sobocinski J, Dias NV, Hongku K, et al. Thoracic endovascular aortic repair with stent grafts alone or with a composite device design in patients with acute type B aortic dissection in the setting of malperfusion. *J Vasc Surg*. Feb 2020;71(2):400-407 e2. doi:10.1016/j.jvs.2019.04.478
220. Khoynezhad A, Donayre CE, Omari BO, Kopchok GE, Walot I, White RA. Midterm results of endovascular treatment of complicated acute type B aortic dissection. *J Thorac Cardiovasc Surg*. Sep 2009;138(3):625-31. doi:10.1016/j.jtcvs.2009.04.044
221. Qin YL, Wang F, Li TX, et al. Endovascular Repair Compared With Medical Management of Patients With Uncomplicated Type B Acute Aortic Dissection. *J Am Coll Cardiol*. Jun 21 2016;67(24):2835-42. doi:10.1016/j.jacc.2016.03.578
222. Zhang MH, Du X, Guo W, Liu XP, Jia X, Ge YY. Early and midterm outcomes of thoracic endovascular aortic repair (TEVAR) for acute and chronic complicated type B aortic dissection. *Medicine (Baltimore)*. Jul 2017;96(28):e7183. doi:10.1097/MD.0000000000007183
223. Gao HQ, Xu SD, Ren CW, et al. Analysis of perioperative outcome and long-term survival rate of thoracic endovascular aortic repair in uncomplicated type B dissection: single-

centre experience with 751 patients. *Eur J Cardiothorac Surg*. Dec 1 2019;56(6):1090-1096. doi:10.1093/ejcts/ezz131
224. Zha B, Qiu P, Xie W, et al. Surgical Outcomes And Postoperative Descending Aorta Morphologic Remodeling After Thoracic Endovascular Aortic Repair For Acute And Chronic Type B Aortic Dissection. *Clin Interv Aging*. 2019;14:1925-1935. doi:10.2147/CIA.S225305
225. Shu C, He H, Li QM, Li M, Jiang XH, Luo MY. Endovascular repair of complicated acute type-B aortic dissection with stentgraft: early and mid-term results. *Eur J Vasc Endovasc Surg*. Oct 2011;42(4):448-53. doi:10.1016/j.ejvs.2011.05.013
226. Du Y, Aizezi M, Lin H, et al. Left ventricular remodeling in patients with acute type B aortic dissection after thoracic endovascular aortic repair: Short- and mid-term outcomes. *Int J Cardiol*. Jan 1 2019;274:283-289. doi:10.1016/j.ijcard.2018.09.008
227. Du ZK, Wang Y, Wang XZ, Jing QM, Han YL. Influence of distal extension of false lumen on adverse aortic events after TEVAR in patients with acute type B aortic dissection. *Catheter Cardiovasc Interv*. Mar 2016;87 Suppl 1:599-607. doi:10.1002/ccd.26427
228. He H, Yao K, Nie WP, et al. Modified Petticoat Technique with Pre-placement of a Distal Bare Stent Improves Early Aortic Remodeling after Complicated Acute Stanford Type B Aortic Dissection. *Eur J Vasc Endovasc Surg*. Oct 2015;50(4):450-9. doi:10.1016/j.ejvs.2015.04.035
229. Ruan ZB, Zhu L, Yin YG, Chen GC. Risk factors of early and late mortality after thoracic endovascular aortic repair for complicated stanford B acute aortic dissection. *J Card Surg*. Jul 2014;29(4):501-6. doi:10.1111/jocs.12377
230. Zhu C, Huang B, Zhao J, et al. Influence of distal entry tears in acute type B aortic dissection after thoracic endovascular aortic repair. *J Vasc Surg*. Aug 2017;66(2):375-385. doi:10.1016/j.jvs.2016.12.142
231. Huang W, Yang F, Luo J, et al. Outcomes and morphologic changes of immediate type Ia endoleak following endovascular repair of acute type B aortic dissection. *Ann Vasc Surg*. Feb 2015;29(2):174-82. doi:10.1016/j.avsg.2014.10.015
232. Stelzmueller ME, Nolz R, Mahr S, et al. Thoracic endovascular repair for acute complicated type B aortic dissections. *J Vasc Surg*. Feb 2019;69(2):318-326. doi:10.1016/j.jvs.2018.05.234
233. Parsa CJ, Schroder JN, Daneshmand MA, McCann RL, Hughes GC. Midterm results for endovascular repair of complicated acute and chronic type B aortic dissection. *Ann Thorac Surg*. Jan 2010;89(1):97-102; discussion 102-4. doi:10.1016/j.athoracsur.2009.09.029
234. Szeto WY, McGarvey M, Pochettino A, et al. Results of a new surgical paradigm: endovascular repair for acute complicated type B aortic dissection. *Ann Thorac Surg*. Jul 2008;86(1):87-93; discussion 93-4. doi:10.1016/j.athoracsur.2008.04.003
235. Zeeshan A, Woo EY, Bavaria JE, et al. Thoracic endovascular aortic repair for acute complicated type B aortic dissection: superiority relative to conventional open surgical and medical therapy. *J Thorac Cardiovasc Surg*. Dec 2010;140(6 Suppl):S109-15; discussion S142-S146. doi:10.1016/j.jtcvs.2010.06.024

236. Desai ND, Gottret JP, Szeto WY, et al. Impact of timing on major complications after thoracic endovascular aortic repair for acute type B aortic dissection. *J Thorac Cardiovasc Surg*. Feb 2015;149(2 Suppl):S151-6. doi:10.1016/j.jtcvs.2014.10.105
237. Lou X, Duwayri YM, Jordan WD, Jr., Chen EP, Veeraswamy RK, Leshnower BG. The Safety and Efficacy of Extended TEVAR in Acute Type B Aortic Dissection. *Ann Thorac Surg*. Sep 2020;110(3):799-806. doi:10.1016/j.athoracsur.2019.12.036
238. Afifi RO, Sandhu HK, Leake SS, et al. Outcomes of Patients With Acute Type B (DeBakey III) Aortic Dissection: A 13-Year, Single-Center Experience. *Circulation*. Aug 25 2015;132(8):748-54. doi:10.1161/CIRCULATIONAHA.115.015302
239. Pearce BJ, Passman MA, Patterson MA, et al. Early outcomes of thoracic endovascular stent-graft repair for acute complicated type B dissection using the Gore TAG endoprosthesis. *Ann Vasc Surg*. Nov 2008;22(6):742-9. doi:10.1016/j.avsg.2008.08.035
240. Pruitt EY, Scali ST, Arnaoutakis DJ, et al. Complicated acute type B aortic dissection: update on management and results. *J Cardiovasc Surg (Torino)*. Dec 2020;61(6):697-707. doi:10.23736/S0021-9509.20.11555-6
241. Mastroroberto P, Onorati F, Zofrea S, Renzulli A, Indolfi C. Outcome of open and endovascular repair in acute type B aortic dissection: a retrospective and observational study. *J Cardiothorac Surg*. Apr 9 2010;5:23. doi:10.1186/1749-8090-5-23
242. Faure EM, El Batti S, Abou Rjeili M, Julia P, Alsac JM. Mid-term Outcomes of Stent Assisted Balloon Induced Intimal Disruption and Relamination in Aortic Dissection Repair (STABILISE) in Acute Type B Aortic Dissection. *Eur J Vasc Endovasc Surg*. Aug 2018;56(2):209-215. doi:10.1016/j.ejvs.2018.04.008
243. Guangqi C, Xiaoxi L, Wei C, et al. Endovascular repair of Stanford type B aortic dissection: early and mid-term outcomes of 121 cases. *Eur J Vasc Endovasc Surg*. Oct 2009;38(4):422-6. doi:10.1016/j.ejvs.2009.04.015
244. Jing QM, Han YL, Wang XZ, et al. Endovascular stent-grafts for acute and chronic type B aortic dissection: comparison of clinical outcomes. *Chin Med J (Engl)*. Nov 20 2008;121(22):2213-7.
245. Eggebrecht H, Herold U, Kuhnt O, et al. Endovascular stent-graft treatment of aortic dissection: determinants of post-interventional outcome. *Eur Heart J*. Mar 2005;26(5):489-97. doi:10.1093/eurheartj/ehi099
246. Kato N, Shimono T, Hirano T, et al. Midterm results of stent-graft repair of acute and chronic aortic dissection with descending tear: the complication-specific approach. *J Thorac Cardiovasc Surg*. Aug 2002;124(2):306-12. doi:10.1067/mtc.2002.122302
247. Palma JH, de Souza JA, Rodrigues Alves CM, Carvalho AC, Buffolo E. Self-expandable aortic stent-grafts for treatment of descending aortic dissections. *Ann Thorac Surg*. Apr 2002;73(4):1138-41; discussion 1141-2. doi:10.1016/s0003-4975(02)03397-0
248. Rodriguez JA, Olsen DM, Lucas L, Wheatley G, Ramaiah V, Diethrich EB. Aortic remodeling after endografting of thoracoabdominal aortic dissection. *J Vasc Surg*. Jun 2008;47(6):1188-94. doi:10.1016/j.jvs.2008.01.022

249. Chen S, Yei F, Zhou L, et al. Endovascular stent-grafts treatment in acute aortic dissection (type B): clinical outcomes during early, late, or chronic phases. *Catheter Cardiovasc Interv*. Aug 2006;68(2):319-25. doi:10.1002/ccd.20821
250. Chemelli-Steingruber I, Chemelli A, Strasak A, et al. Endovascular repair or medical treatment of acute type B aortic dissection? A comparison. *Eur J Radiol*. Jan 2010;73(1):175-80. doi:10.1016/j.ejrad.2008.09.031
251. Sze DY, van den Bosch MA, Dake MD, et al. Factors portending endoleak formation after thoracic aortic stent-graft repair of complicated aortic dissection. *Circ Cardiovasc Interv*. Apr 2009;2(2):105-12. doi:10.1161/CIRCINTERVENTIONS.108.819722
252. Brunkwall J, Kasprzak P, Verhoeven E, et al. Endovascular repair of acute uncomplicated aortic type B dissection promotes aortic remodelling: 1 year results of the ADSORB trial. *Eur J Vasc Endovasc Surg*. Sep 2014;48(3):285-91. doi:10.1016/j.ejvs.2014.05.012
253. Nienaber CA, Rousseau H, Eggebrecht H, et al. Randomized comparison of strategies for type B aortic dissection: the INvestigation of STEnt Grafts in Aortic Dissection (INSTEAD) trial. *Circulation*. Dec 22 2009;120(25):2519-28. doi:10.1161/CIRCULATIONAHA.109.886408
254. Nienaber CA, Fattori R, Lund G, et al. Nonsurgical reconstruction of thoracic aortic dissection by stent-graft placement. *N Engl J Med*. May 20 1999;340(20):1539-45. doi:10.1056/NEJM199905203402003
255. Lee SJ, Kang WC, Ko YG, et al. Aortic Remodeling and Clinical Outcomes in Type B Aortic Dissection According to the Timing of Thoracic Endovascular Aortic Repair. *Ann Vasc Surg*. Aug 2020;67:322-331. doi:10.1016/j.avsg.2020.03.022
256. Kazimierczak A, Rynio P, Jedrzejczak T, et al. Expanded Petticoat technique to promote the reduction of contrasted false lumen volume in patients with chronic type B aortic dissection. *J Vasc Surg*. Dec 2019;70(6):1782-1791. doi:10.1016/j.jvs.2019.01.073
257. Nozdrzykowski M, Etz CD, Luehr M, et al. Optimal treatment for patients with chronic Stanford type B aortic dissection: endovascularly, surgically or both? *Eur J Cardiothorac Surg*. Sep 2013;44(3):e165-74; discussion e174. doi:10.1093/ejcts/ezt291
258. Lee M, Lee DY, Kim MD, et al. Outcomes of endovascular management for complicated chronic type B aortic dissection: effect of the extent of stent graft coverage and anatomic properties of aortic dissection. *J Vasc Interv Radiol*. Oct 2013;24(10):1451-60. doi:10.1016/j.jvir.2013.06.007
259. Gao F, Jing Y, Zang P, et al. Vascular Cognitive Impairment Caused by Cerebral Small Vessel Disease Is Associated with the TLR4 in the Hippocampus. *J Alzheimers Dis*. Jun 24 2019;doi:10.3233/JAD-190240
260. Xu SD, Huang FJ, Yang JF, et al. Early and midterm results of thoracic endovascular aortic repair of chronic type B aortic dissection. *J Thorac Cardiovasc Surg*. Jun 2010;139(6):1548-53. doi:10.1016/j.jtcvs.2009.08.051
261. Kitamura T, Torii S, Oka N, et al. Key success factors for thoracic endovascular aortic repair for non-acute Stanford type B aortic dissection. *Eur J Cardiothorac Surg*. Sep 2014;46(3):432-7; discussion 437. doi:10.1093/ejcts/ezu012

262. Mizoguchi T, Zempo N, Kaneda Y. Early and Mid-Term Outcomes Following TEVAR for Chronic Type B Aortic Dissection. *Ann Vasc Dis*. Dec 25 2017;10(4):345-350. doi:10.3400/avd.oa.17-00078
263. Andersen ND, Keenan JE, Ganapathi AM, Gaca JG, McCann RL, Hughes GC. Current management and outcome of chronic type B aortic dissection: results with open and endovascular repair since the advent of thoracic endografting. *Ann Cardiothorac Surg*. May 2014;3(3):264-74. doi:10.3978/j.issn.2225-319X.2014.05.07
264. Dohle DS, Laverne T, Bavaria J, et al. Aortic remodelling after thoracic endovascular aortic repair in acute and chronic type B aortic dissections. *Eur J Cardiothorac Surg*. Oct 1 2020;58(4):730-737. doi:10.1093/ejcts/ezaa118
265. Andacheh ID, Donayre C, Othman F, Walot I, Kopchok G, White R. Patient outcomes and thoracic aortic volume and morphologic changes following thoracic endovascular aortic repair in patients with complicated chronic type B aortic dissection. *J Vasc Surg*. Sep 2012;56(3):644-50; discussion 650. doi:10.1016/j.jvs.2012.02.050
266. Lou X, Chen EP, Duwayri YM, et al. The Impact of Thoracic Endovascular Aortic Repair on Long-Term Survival in Type B Aortic Dissection. *Ann Thorac Surg*. Jan 2018;105(1):31-38. doi:10.1016/j.athoracsur.2017.06.016
267. Kang WC, Greenberg RK, Mastracci TM, et al. Endovascular repair of complicated chronic distal aortic dissections: intermediate outcomes and complications. *J Thorac Cardiovasc Surg*. Nov 2011;142(5):1074-83. doi:10.1016/j.jtcvs.2011.03.008
268. Massara M, Alberti A, Volpe P. Early and mid-term results of endovascular treatment of thoracic aorta diseases: a single-center experience. *Semin Vasc Surg*. Mar 2020;32(3-4):111-116. doi:10.1053/j.semvascsurg.2020.03.002
269. Pamler RS, Kotsis T, Gorich J, Kapfer X, Orend KH, Sunder-Plassmann L. Complications after endovascular repair of type B aortic dissection. *J Endovasc Ther*. Dec 2002;9(6):822-8. doi:10.1177/152660280200900616
270. Manning BJ, Dias N, Ohrlander T, et al. Endovascular treatment for chronic type B dissection: limitations of short stent-grafts revealed at midterm follow-up. *J Endovasc Ther*. Oct 2009;16(5):590-7. doi:10.1583/09-2717.1
271. Starnes BW, Dwivedi AJ, Giglia JS, Woo K, Yeh C, Investigators TS. Endovascular repair for blunt thoracic aortic injury using the Zenith Alpha low-profile device. *J Vasc Surg*. Dec 2015;62(6):1495-503 e1. doi:10.1016/j.jvs.2015.07.098
272. Farber MA, Giglia JS, Starnes BW, et al. Evaluation of the redesigned conformable GORE TAG thoracic endoprosthesis for traumatic aortic transection. *J Vasc Surg*. Sep 2013;58(3):651-8. doi:10.1016/j.jvs.2013.02.015
273. Khoynezhad A, Azizzadeh A, Donayre CE, et al. Results of a multicenter, prospective trial of thoracic endovascular aortic repair for blunt thoracic aortic injury (RESCUE trial). *J Vasc Surg*. Apr 2013;57(4):899-905 e1. doi:10.1016/j.jvs.2012.10.099
274. Shackford SR, Dunne CE, Karmy-Jones R, et al. The evolution of care improves outcome in blunt thoracic aortic injury: A Western Trauma Association multicenter study. *J Trauma Acute Care Surg*. Dec 2017;83(6):1006-1013. doi:10.1097/TA.0000000000001555

275. DuBose JJ, Leake SS, Brenner M, et al. Contemporary management and outcomes of blunt thoracic aortic injury: a multicenter retrospective study. *J Trauma Acute Care Surg*. Feb 2015;78(2):360-9. doi:10.1097/TA.0000000000000521
276. Kim HM, Cho YK, Kim JH, et al. Clinical Outcomes of the Seal(R) Thoracic Stent Graft for Traumatic Aortic Injury in a Korean Multicenter Retrospective Study. *Ann Vasc Surg*. Nov 2019;61:400-409. doi:10.1016/j.avsg.2019.06.006
277. Dunham MB, Zygun D, Petrasek P, Kortbeek JB, Karmy-Jones R, Moore RD. Endovascular stent grafts for acute blunt aortic injury. *J Trauma*. Jun 2004;56(6):1173-8. doi:10.1097/01.ta.0000123039.92225.e5
278. Hoornweg LL, Dinkelman MK, Goslings JC, et al. Endovascular management of traumatic ruptures of the thoracic aorta: a retrospective multicenter analysis of 28 cases in The Netherlands. *J Vasc Surg*. Jun 2006;43(6):1096-102; discussion 1102. doi:10.1016/j.jvs.2006.01.034
279. Demetriades D, Velmahos GC, Scalea TM, et al. Operative repair or endovascular stent graft in blunt traumatic thoracic aortic injuries: results of an American Association for the Surgery of Trauma Multicenter Study. *J Trauma*. Mar 2008;64(3):561-70; discussion 570-1. doi:10.1097/TA.0b013e3181641bb3
280. Dake MD, White RA, Diethrich EB, et al. Report on endograft management of traumatic thoracic aortic transections at 30 days and 1 year from a multidisciplinary subcommittee of the Society for Vascular Surgery Outcomes Committee. *J Vasc Surg*. Apr 2011;53(4):1091-6. doi:10.1016/j.jvs.2010.11.126
281. Tehrani HY, Peterson BG, Katariya K, et al. Endovascular repair of thoracic aortic tears. *Ann Thorac Surg*. Sep 2006;82(3):873-7; discussion 877-8. doi:10.1016/j.athoracsur.2006.04.012
282. Pacini D, Angeli E, Fattori R, et al. Traumatic rupture of the thoracic aorta: ten years of delayed management. *J Thorac Cardiovasc Surg*. Apr 2005;129(4):880-4. doi:10.1016/j.jtcvs.2004.10.012
283. Antonello M, Menegolo M, Maturi C, et al. Intentional coverage of the left subclavian artery during endovascular repair of traumatic descending thoracic aortic transection. *J Vasc Surg*. Mar 2013;57(3):684-690 e1. doi:10.1016/j.jvs.2012.08.119
284. Martinelli O, Malaj A, Gossetti B, Bertoletti G, Bresadola L, Irace L. Outcomes in the emergency endovascular repair of blunt thoracic aortic injuries. *J Vasc Surg*. Sep 2013;58(3):832-5. doi:10.1016/j.jvs.2013.02.243
285. Di Eusanio M, Folesani G, Berretta P, et al. Delayed management of blunt traumatic aortic injury: open surgical versus endovascular repair. *Ann Thorac Surg*. May 2013;95(5):1591-7. doi:10.1016/j.athoracsur.2013.02.033
286. Rousseau H, Dambrin C, Marcheix B, et al. Acute traumatic aortic rupture: a comparison of surgical and stent-graft repair. *J Thorac Cardiovasc Surg*. May 2005;129(5):1050-5. doi:10.1016/j.jtcvs.2004.12.023
287. Andrassy J, Weidenhagen R, Meimarakis G, Lauterjung L, Jauch KW, Kopp R. Stent versus open surgery for acute and chronic traumatic injury of the thoracic aorta: a single-

center experience. *J Trauma*. Apr 2006;60(4):765-71; discussion 771-2. doi:10.1097/01.ta.0000210275.58266.24
288. Buz S, Zipfel B, Mulahasanovic S, Pasic M, Weng Y, Hetzer R. Conventional surgical repair and endovascular treatment of acute traumatic aortic rupture. *Eur J Cardiothorac Surg*. Feb 2008;33(2):143-9. doi:10.1016/j.ejcts.2007.10.017
289. Scheinert D, Krankenberg H, Schmidt A, et al. Endoluminal stent-graft placement for acute rupture of the descending thoracic aorta. *Eur Heart J*. Apr 2004;25(8):694-700. doi:10.1016/j.ehj.2004.02.022
290. Geisbusch P, Leszczynsky M, Kotelis D, Hyhlik-Durr A, Weber TF, Bockler D. Open versus endovascular repair of acute aortic transections--a non-randomized single-center analysis. *Langenbecks Arch Surg*. Nov 2009;394(6):1101-7. doi:10.1007/s00423-009-0468-x
291. Garcia Reyes ME, Goncalves Martins G, Fernandez Valenzuela V, Dominguez Gonzalez JM, Maeso Lebrun J, Bellmunt Montoya S. Long-Term Outcomes of Thoracic Endovascular Aortic Repair Focused on Bird Beak and Oversizing in Blunt Traumatic Thoracic Aortic Injury. *Ann Vasc Surg*. Jul 2018;50:140-147. doi:10.1016/j.avsg.2018.02.001
292. Mosquera VX, Gonzalez-Barbeito M, Marini M, et al. Evolution of conservative treatment of acute traumatic aortic injuries: lights and shadows. *Eur J Cardiothorac Surg*. Oct 1 2018;54(4):689-695. doi:10.1093/ejcts/ezy109
293. Fernandez V, Mestres G, Maeso J, Dominguez JM, Aloy MC, Matas M. Endovascular treatment of traumatic thoracic aortic injuries: short- and medium-term Follow-up. *Ann Vasc Surg*. Feb 2010;24(2):160-6. doi:10.1016/j.avsg.2009.05.013
294. Skripochnik E, Novikov D, Bilfinger TJ, Loh SA. Short-term results of left subclavian artery salvage in blunt thoracic aortic injury with short proximal landing zones. *J Vasc Surg*. Oct 2018;68(4):985-990. doi:10.1016/j.jvs.2018.01.046
295. Patel HJ, Hemmila MR, Williams DM, Diener AC, Deeb GM. Late outcomes following open and endovascular repair of blunt thoracic aortic injury. *J Vasc Surg*. Mar 2011;53(3):615-20; discussion 621. doi:10.1016/j.jvs.2010.09.058
296. Go MR, Barbato JE, Dillavou ED, et al. Thoracic endovascular aortic repair for traumatic aortic transection. *J Vasc Surg*. Nov 2007;46(5):928-33. doi:10.1016/j.jvs.2007.06.049
297. Garcia-Toca M, Naughton PA, Matsumura JS, et al. Endovascular repair of blunt traumatic thoracic aortic injuries: seven-year single-center experience. *Arch Surg*. Jul 2010;145(7):679-83. doi:10.1001/archsurg.2010.114
298. Estrera AL, Miller CC, 3rd, Guajardo-Salinas G, et al. Update on blunt thoracic aortic injury: fifteen-year single-institution experience. *J Thorac Cardiovasc Surg*. Mar 2013;145(3 Suppl):S154-8. doi:10.1016/j.jtcvs.2012.11.074
299. Mansour MA, Kirk JS, Cuff RF, et al. Endovascular repair of traumatic thoracic aortic tears. *Am J Surg*. Mar 2012;203(3):401-4; discussion 404. doi:10.1016/j.amjsurg.2011.10.008
300. Azizzadeh A, Ray HM, Dubose JJ, et al. Outcomes of endovascular repair for patients with blunt traumatic aortic injury. *J Trauma Acute Care Surg*. Feb 2014;76(2):510-6. doi:10.1097/TA.0b013e3182aafe8c

301. Riesenman PJ, Brooks JD, Farber MA. Acute blunt traumatic injury to the descending thoracic aorta. *J Vasc Surg*. Nov 2012;56(5):1274-80. doi:10.1016/j.jvs.2012.04.035
302. Kenel-Pierre S, Ramos Duran E, Abi-Chaker A, et al. The role of heparin in endovascular repair of blunt thoracic aortic injury. *J Vasc Surg*. Dec 2019;70(6):1809-1815. doi:10.1016/j.jvs.2019.01.065
303. Li S, Cai W, Li X, Qiu J, Li Q, Shu C. Thoracic endovascular aortic repair for traumatic type B aortic dissection: a 5-year experience from a single center. *Int Angiol*. Aug 2017;36(4):316-321. doi:10.23736/S0392-9590.17.03782-8
304. Shan JG, Zhai XM, Liu JD, Yang WG, Xue S. Thoracic Endovascular Aortic Repair for Traumatic Thoracic Aortic Injury: A Single-Center Initial Experience. *Ann Vasc Surg*. Apr 2016;32:104-10. doi:10.1016/j.avsg.2015.09.023
305. Tigkiropoulos K, Sigala F, Tsilimigras DI, et al. Endovascular Repair of Blunt Thoracic Aortic Trauma: Is Postimplant Hypertension an Incidental Finding? *Ann Vasc Surg*. Jul 2018;50:160-166 e1. doi:10.1016/j.avsg.2018.01.100
306. Spiliotopoulos K, Kokotsakis J, Argiriou M, et al. Endovascular repair for blunt thoracic aortic injury: 11-year outcomes and postoperative surveillance experience. *J Thorac Cardiovasc Surg*. Dec 2014;148(6):2956-61. doi:10.1016/j.jtcvs.2014.08.019
307. Cindy M, Sabrina H, Kim D, Geert M, Inge F. Traumatic aortic rupture: 30 years of experience. *Ann Vasc Surg*. May 2011;25(4):474-80. doi:10.1016/j.avsg.2010.12.019
308. Steuer J, Wanhainen A, Thelin S, Nyman R, Eriksson MO, Bjorck M. Outcome of endovascular treatment of traumatic aortic transection. *J Vasc Surg*. Oct 2012;56(4):973-8. doi:10.1016/j.jvs.2012.03.259
309. Agostinelli A, Saccani S, Borrello B, Nicolini F, Larini P, Gherli T. Immediate endovascular treatment of blunt aortic injury: our therapeutic strategy. *J Thorac Cardiovasc Surg*. May 2006;131(5):1053-7. doi:10.1016/j.jtcvs.2005.12.015
310. Broux C, Thony F, Chavanon O, et al. Emergency endovascular stent graft repair for acute blunt thoracic aortic injury: a retrospective case control study. *Intensive Care Med*. May 2006;32(5):770-4. doi:10.1007/s00134-006-0115-8
311. Fattori R, Napoli G, Lovato L, et al. Indications for, timing of, and results of catheter-based treatment of traumatic injury to the aorta. *AJR Am J Roentgenol*. Sep 2002;179(3):603-9. doi:10.2214/ajr.179.3.1790603
312. Pratesi C, Dorigo W, Troisi N, et al. Acute traumatic rupture of the descending thoracic aorta: endovascular treatment. *Am J Surg*. Sep 2006;192(3):291-5. doi:10.1016/j.amjsurg.2006.01.048
313. Orend KH, Pamler R, Kapfer X, Liewald F, Gorich J, Sunder-Plassmann L. Endovascular repair of traumatic descending aortic transection. *J Endovasc Ther*. Oct 2002;9(5):573-8. doi:10.1177/152660280200900503
314. Lachat M, Pfammatter T, Witzke H, et al. Acute traumatic aortic rupture: early stent-graft repair. *Eur J Cardiothorac Surg*. Jun 2002;21(6):959-63. doi:10.1016/s1010-7940(02)00062-3

315. Melnitchouk S, Pfammatter T, Kadner A, et al. Emergency stent-graft placement for hemorrhage control in acute thoracic aortic rupture. *Eur J Cardiothorac Surg*. Jun 2004;25(6):1032-8. doi:10.1016/j.ejcts.2004.03.005
316. Kaneyuki D, Asakura T, Iguchi A, et al. Early- and long-term results of thoracic endovascular aortic repair for blunt traumatic thoracic aortic injury: a single-centre experience. *Eur J Cardiothorac Surg*. Feb 7 2019;doi:10.1093/ejcts/ezz023
317. Steingruber IE, Czermak BV, Chemelli A, et al. Placement of endovascular stent-grafts for emergency repair of acute traumatic aortic rupture: a single-centre experience. *Eur Radiol*. Jul 2007;17(7):1727-37. doi:10.1007/s00330-006-0451-7
318. Hanna L, Sounderajah V, Abdullah AA, et al. Trends in thoracic aortic aneurysm hospital admissions, interventions and mortality in England between 1998 to 2020: An observational study. *Eur J Vasc Endovasc Surg*. Jul 13 2022;doi:10.1016/j.ejvs.2022.07.003
319. Patterson B, Holt P, Nienaber C, Cambria R, Fairman R, Thompson M. Aortic pathology determines midterm outcome after endovascular repair of the thoracic aorta: report from the Medtronic Thoracic Endovascular Registry (MOTHER) database. *Circulation*. Jan 1 2013;127(1):24-32. doi:10.1161/CIRCULATIONAHA.112.110056
320. Piazza M, Squizzato F, Milan L, et al. Incidence and Predictors of Neurological Complications Following Thoracic Endovascular Aneurysm Repair in the Global Registry for Endovascular Aortic Treatment. *Eur J Vasc Endovasc Surg*. Oct 2019;58(4):512-519. doi:10.1016/j.ejvs.2019.05.011
321. Biancari F, Mariscalco G, Mariani S, Saari P, Satta J, Juvonen T. Endovascular Treatment of Degenerative Aneurysms Involving Only the Descending Thoracic Aorta: Systematic Review and Meta-analysis. *J Endovasc Ther*. Apr 2016;23(2):387-92. doi:10.1177/1526602815626560
322. von Allmen RS, Gahl B, Powell JT. Editor's Choice - Incidence of Stroke Following Thoracic Endovascular Aortic Repair for Descending Aortic Aneurysm: A Systematic Review of the Literature with Meta-analysis. *Eur J Vasc Endovasc Surg*. Feb 2017;53(2):176-184. doi:10.1016/j.ejvs.2016.10.025
323. Fillinger MF, Greenberg RK, McKinsey JF, Chaikof EL, Society for Vascular Surgery Ad Hoc Committee on TRS. Reporting standards for thoracic endovascular aortic repair (TEVAR). *J Vasc Surg*. Oct 2010;52(4):1022-33, 1033 e15. doi:10.1016/j.jvs.2010.07.008
324. Lansky AJ, Messe SR, Brickman AM, et al. Proposed Standardized Neurological Endpoints for Cardiovascular Clinical Trials: An Academic Research Consortium Initiative. *Eur Heart J*. May 14 2018;39(19):1687-1697. doi:10.1093/eurheartj/ehx037
325. Riambau V, Bockler D, Brunkwall J, et al. Editor's Choice - Management of Descending Thoracic Aorta Diseases: Clinical Practice Guidelines of the European Society for Vascular Surgery (ESVS). *Eur J Vasc Endovasc Surg*. Jan 2017;53(1):4-52. doi:10.1016/j.ejvs.2016.06.005
326. Hanna L, Abdullah A, Kashef E, et al. 4-Year Results of the Bolton Relay Proximal Scallop Endograft in the Management of Thoracic and Thoraco-Abdominal Aortic Pathology with Unfavourable Proximal Landing Zone. *J Vasc Surg*. Apr 30 2021;doi:10.1016/j.jvs.2021.04.027

327. Konstantinou N, Kolbel T, Debus ES, Rohlffs F, Tsilimparis N. Fenestrated versus debranching thoracic endovascular aortic repair for endovascular treatment of distal aortic arch and descending aortic lesions. *J Vasc Surg*. Jun 2021;73(6):1915-1924. doi:10.1016/j.jvs.2020.10.078
328. Li X, Zhang L, Song C, et al. Long-Term Outcomes of Thoracic Endovascular Repair for Aortic Arch Dissection Using Customized Single-Branched Fenestrated Stent-Graft. *Vasc Endovascular Surg*. Aug 2021;55(6):577-585. doi:10.1177/15385744211010446
329. Kotelis D, Bischoff MS, Jobst B, et al. Morphological risk factors of stroke during thoracic endovascular aortic repair. *Langenbecks Arch Surg*. Dec 2012;397(8):1267-73. doi:10.1007/s00423-012-0997-6
330. Fazekas F, Chawluk JB, Alavi A, Hurtig HI, Zimmerman RA. MR signal abnormalities at 1.5 T in Alzheimer's dementia and normal aging. *AJR Am J Roentgenol*. Aug 1987;149(2):351-6. doi:10.2214/ajr.149.2.351
331. Sacco RL, Kasner SE, Broderick JP, et al. An updated definition of stroke for the 21st century: a statement for healthcare professionals from the American Heart Association/American Stroke Association. *Stroke*. Jul 2013;44(7):2064-89. doi:10.1161/STR.0b013e318296aeca
332. Murkin JM, Newman SP, Stump DA, Blumenthal JA. Statement of consensus on assessment of neurobehavioral outcomes after cardiac surgery. *Ann Thorac Surg*. May 1995;59(5):1289-95. doi:10.1016/0003-4975(95)00106-u
333. Moore CG, Carter RE, Nietert PJ, Stewart PW. Recommendations for planning pilot studies in clinical and translational research. *Clin Transl Sci*. Oct 2011;4(5):332-7. doi:10.1111/j.1752-8062.2011.00347.x
334. Raymond PD H-BA, Radel M, Ray MJ, Marsh NA. Assessment of statistical change criteria used to define significant change in neuropsychological test performance following cardiac surgery. *European journal of cardio-thoracic surgery*. 2006;21:82-8.
335. Hiden Analytics. Gas Analysis Systems | Mass Spectrometer | Manufacturer | HPR-20 R&D Accessed 10th July 2021, https://www.hidenanalytical.com/products/gas-analysis/hpr-20-rd/
336. Hiden Analytics. Quadrupole Mass Spectroscopy Concepts. Accessed 15th July 2021, https://www.hidenanalytical.com/wp-content/uploads/2016/09/Mass_spec_concepts.ppsx
337. Munson BR YD, Okiishi TH, Huebsch WW. *Fundamentals of fluid mechanics*. 7th ed. N.J: John Wiley & Sons; 2013.
338. McCarthy CJ, Behravesh S, Naidu SG, Oklu R. Air Embolism: Practical Tips for Prevention and Treatment. *J Clin Med*. Oct 31 2016;5(11)doi:10.3390/jcm5110093
339. Pappano AJ, Gil Wier W. 8 - The Microcirculation and Lymphatics. In: Pappano AJ, Gil Wier W, eds. *Cardiovascular Physiology (Tenth Edition)*. Elsevier; 2013:153-170.
340. Gerriets T, Walberer M, Nedelmann M, et al. A rat model for cerebral air microembolisation. *J Neurosci Methods*. Jun 30 2010;190(1):10-3. doi:10.1016/j.jneumeth.2010.04.016

341. Martens S, Theisen A, Balzer JO, et al. Improved cerebral protection through replacement of residual intracavital air by carbon dioxide: a porcine model using diffusion-weighted magnetic resonance imaging. *J Thorac Cardiovasc Surg*. Jan 2004;127(1):51-6. doi:10.1016/s0022-5223(03)01329-1
342. Martens S, Dietrich M, Wals S, Steffen S, Wimmer-Greinecker G, Moritz A. Conventional carbon dioxide application does not reduce cerebral or myocardial damage in open heart surgery. *Ann Thorac Surg*. Dec 2001;72(6):1940-4. doi:10.1016/s0003-4975(01)03224-6
343. Giordano S, Biancari F. Does the use of carbon dioxide field flooding during heart valve surgery prevent postoperative cerebrovascular complications? *Interact Cardiovasc Thorac Surg*. Aug 2009;9(2):323-6. doi:10.1510/icvts.2009.206177
344. Carbon Dioxide Insufflation and Brain Protection During Open Heart Surgery. A Randomized Controlled Trial (CO-Two). Accessed 12th July 2021, https://www.fundingawards.nihr.ac.uk/award/17/145/40
345. Stankiewicz JM, Glanz BI, Healy BC, et al. Brain MRI lesion load at 1.5T and 3T versus clinical status in multiple sclerosis. *J Neuroimaging*. Apr 2011;21(2):e50-6. doi:10.1111/j.1552-6569.2009.00449.x
346. Lund C, Nes RB, Ugelstad TP, et al. Cerebral emboli during left heart catheterization may cause acute brain injury. *Eur Heart J*. Jul 2005;26(13):1269-75. doi:10.1093/eurheartj/ehi148
347. Sigurdsson S, Aspelund T, Kjartansson O, et al. Incidence of Brain Infarcts, Cognitive Change, and Risk of Dementia in the General Population: The AGES-Reykjavik Study (Age Gene/Environment Susceptibility-Reykjavik Study). *Stroke*. Sep 2017;48(9):2353-2360. doi:10.1161/STROKEAHA.117.017357
348. Saczynski JS, Sigurdsson S, Jonsdottir MK, et al. Cerebral infarcts and cognitive performance: importance of location and number of infarcts. *Stroke*. Mar 2009;40(3):677-82. doi:10.1161/STROKEAHA.108.530212
349. Debette S, Schilling S, Duperron MG, Larsson SC, Markus HS. Clinical Significance of Magnetic Resonance Imaging Markers of Vascular Brain Injury: A Systematic Review and Meta-analysis. *JAMA Neurol*. Jan 1 2019;76(1):81-94. doi:10.1001/jamaneurol.2018.3122
350. Kalpokas MV, Nixon IK, Kluger R, Beilby DS, Silbert BS. Carbon dioxide field flooding versus mechanical de-airing during open-heart surgery: a prospective randomized controlled trial. *Perfusion*. Sep 2003;18(5):291-4. doi:10.1191/0267659103pf671oa
351. Svenarud P, Persson M, van der Linden J. Effect of CO2 insufflation on the number and behavior of air microemboli in open-heart surgery: a randomized clinical trial. *Circulation*. Mar 9 2004;109(9):1127-32. doi:10.1161/01.CIR.0000118501.44474.83
352. Bendszus M, Koltzenburg M, Bartsch AJ, et al. Heparin and air filters reduce embolic events caused by intra-arterial cerebral angiography: a prospective, randomized trial. *Circulation*. Oct 12 2004;110(15):2210-5. doi:10.1161/01.CIR.0000144301.82391.85

353. Berger M, Terrando N, Smith SK, Browndyke JN, Newman MF, Mathew JP. Neurocognitive Function after Cardiac Surgery: From Phenotypes to Mechanisms. *Anesthesiology*. Oct 2018;129(4):829-851. doi:10.1097/ALN.0000000000002194
354. Chandra A, Li WA, Stone CR, Geng X, Ding Y. The cerebral circulation and cerebrovascular disease I: Anatomy. *Brain Circ*. Apr-Jun 2017;3(2):45-56. doi:10.4103/bc.bc_10_17
355. Cohen A, Tzourio C, Bertrand B, Chauvel C, Bousser MG, Amarenco P. Aortic plaque morphology and vascular events: a follow-up study in patients with ischemic stroke. FAPS Investigators. French Study of Aortic Plaques in Stroke. *Circulation*. Dec 2 1997;96(11):3838-41. doi:10.1161/01.cir.96.11.3838
356. Kronzon I, Tunick PA. Aortic atherosclerotic disease and stroke. *Circulation*. Jul 4 2006;114(1):63-75. doi:10.1161/CIRCULATIONAHA.105.593418
357. Wehrum T, Dragonu I, Strecker C, et al. Aortic atheroma as a source of stroke - assessment of embolization risk using 3D CMR in stroke patients and controls. *J Cardiovasc Magn Reson*. Sep 6 2017;19(1):67. doi:10.1186/s12968-017-0379-x
358. Harloff A, Hagenlocher P, Lodemann T, et al. Retrograde aortic blood flow as a mechanism of stroke: MR evaluation of the prevalence in a population-based study. *Eur Radiol*. Oct 2019;29(10):5172-5179. doi:10.1007/s00330-019-06104-z
359. Wehrum T, Kams M, Strecker C, et al. Prevalence of potential retrograde embolization pathways in the proximal descending aorta in stroke patients and controls. *Cerebrovasc Dis*. 2014;38(6):410-7. doi:10.1159/000369001
360. Veyssier-Belot C, Cohen A, Rougemont D, Levy C, Amarenco P, Bousser MG. Cerebral infarction due to painless thoracic aortic and common carotid artery dissections. *Stroke*. Dec 1993;24(12):2111-3. doi:10.1161/01.str.24.12.2111
361. Fernandez E, Nadig R, Mathew T, Sarma GR. Aortic dissection causing embolic stroke. *Neurol India*. Sep-Oct 2009;57(5):689. doi:10.4103/0028-3886.57784
362. Saba L, Saam T, Jager HR, et al. Imaging biomarkers of vulnerable carotid plaques for stroke risk prediction and their potential clinical implications. *Lancet Neurol*. Jun 2019;18(6):559-572. doi:10.1016/S1474-4422(19)30035-3
363. Association AG. *Purging principles and practice* 3rd ed.
364. BOC. Inerting in the chemical industry. Accessed 6th March 2021, https://www.boconline.co.uk/en/images/Inerting-in-the-chemical-industry_tcm410-166975.pdf
365. De Pauw R, Choikhet K, Desmet G, Broeckhoven K. Occurrence of turbulent flow conditions in supercritical fluid chromatography. *J Chromatogr A*. Sep 26 2014;1361:277-85. doi:10.1016/j.chroma.2014.07.088
366. Johnson JE SS, Kuhl CA. Pipeline puring principles and practice 1996:765-755.